SCIENTIFIC RESEARCH OF THE SCO COUNTRIES: SYNERGY AND INTEGRATION

上合组织国家的科学研究：协同和一体化

Proceedings of the International Conference

Date: February 10

Beijing, China 2023

上合组织国家的科学研究：协同和一体化国际会议

参与者的英文报告

International Conference “Scientific research of the SCO countries: synergy and integration”

Part 2

2023 年 2 月 10 日，中国北京
February 10, 2023. Beijing, PRC

Proceedings of the International Conference
“Scientific research of the SCO countries: synergy and integration” - Reports in English

(February 10, 2023. Beijing, PRC)

ISBN 978-5-905695-82-7

这些会议文集结合了会议的材料 – 研究论文和科学工作者的论文报告。 它考察了职业化人格的技术和社会学问题。一些文章涉及人格职业化研究问题的理论和方法论方法和原则。
作者对所引用的出版物，事实，数字，引用，统计数据，专有名称和其他信息的准确性负责

These Conference Proceedings combine materials of the conference – research papers and thesis reports of scientific workers. They examine technical, juridical and sociological aspects of research issues. Some articles deal with theoretical and methodological approaches and principles of research questions of personality professionalization.

Authors are responsible for the accuracy of cited publications, facts, figures, quotations, statistics, proper names and other information.

ISBN 978-5-905695-82-7

CONTENTS

MEDICAL SCIENCES

PHYSICAL AND MATHEMATICAL SCIENCES

TECHNICAL SCIENCES

DOI 10.34660/INF.2023.29.46.051

婴幼儿急性肾功能衰竭的体温昼夜节律
CIRCADIAN RHYTHM OF BODY TEMPERATURE IN ACUTE RENAL FAILURE IN INFANTS

Muhitdinova Hura Nuritdinovna
Doctor of Medical Sciences, Full Professor
Center for the Development of Professional Qualifications of Medical Workers

抽象的。 对10名3岁以下儿童每小时体温监测数据的研究显示，第1天，预后良好组和不良结局组体温昼夜节律指标均在正常值范围内。 发现体温昼夜节律的振幅与炎症反应的严重程度、进展或中毒程度的降低相关联。 尽管肾脏的排泄活动逐渐恢复，但在后来的第 2 组治疗的背景下温度升高，对应于负面动态，即幼儿一般状况的恶化。

关键词：昼夜节律、体温、急性肾功能衰竭、婴儿。

Abstract. *The study of the data of hourly monitoring of body temperature in 10 children under the age of 3 years revealed that on day 1, the indicators of the mesor of the circadian rhythm of body temperature in groups with favorable and unfavorable outcomes were within normal values. Correspondence of the amplitude of the circadian rhythm of body temperature with the severity of the inflammatory reaction, progression or decrease in the degree of intoxication was found. The temperature increase against the background of the therapy in group 2 at a later date, despite the gradual recovery of the excretory activity of the kidneys, corresponded to the negative dynamics, the deterioration of the general condition in young children.*

Keywords: *circadian rhythm, body temperature, acute renal failure, infants.*

Relevance. Acute renal failure (ARF) is a sudden impairment of kidney function with a decrease in filtration and reabsorption processes, leading to a breakdown in water, electrolyte, nitrogen and other types of metabolism. ARF is a potentially reversible event. Acute renal failure (ARF) is a non-specific clinical and laboratory syndrome that occurs due to the acute loss of all homeostatic functions of the kidneys. This process, with timely diagnosis and proper treatment, is reversible. ARF significantly worsens the child's condition, and mortality ranges from 3-5% in hemolytic-uremic syndrome, up to 30-70% in sepsis and multiple

organ failure. Even with successful treatment and restoration of urinary function, long-term consequences are possible - 10-25% of children develop chronic kidney disease. ARF is dangerous electrolyte disorders (hyperkalemia, hypocalcemia, hyperphosphatemia).

Depending on the causes of development, pathological processes in acute renal failure are caused by different mechanisms: ischemia of the renal parenchyma, activation of shunts in the juxtamedullary zone, toxic damage to the glomeruli and tubular epithelium, and acute obstruction of the urinary tract. The changes that occur are initially reversible, and when the provoking factors are eliminated, the functions of the nephrons are completely restored. However, there is not enough information in the literature on the characteristics of the inflammatory response in acute renal failure, which developed against the background of an acute bacterial pulmonary infection in children under the age of 3 years [1-4].

Objective. To study and give a comparative assessment of the temperature response with a favorable and unfavorable outcome in acute renal failure in infancy, which developed against the background of an acute infection.

Material and research methods. When correcting infusion therapy, the dynamics of the child's weight, the ratio between the injected and excreted fluid, and the serum concentration of Na + were taken into account. The daily fluid requirement in a child with ARF was calculated by adding the amount of urine excreted per day and extrarenal water losses (hidden losses and losses through the gastrointestinal tract). Indications for dialysis (renal replacement therapy (RRT)) were: anuria for more than 24 hours with a progressively worsening condition of the patient; an increase in the level of urea more than 25 mmol/l. The data of hourly monitoring of body temperature in 10 children with acute renal failure admitted to the ICU of the RSCEM with anuria from 1 up to 4 days at the age of 10 months to 3 years 4 months from the ICU of regional children's hospitals and branches of RSCEM. Before admission to the clinic, all patients received anti-inflammatory therapy aimed at the treatment of ARD-2, pneumonia 7, AII-1 patient due to severe progressive respiratory failure, patients received invasive mechanical respiratory support on the first day. All patients underwent hemodialysis, plasmapheresis under the control of hemodynamics, acid-base balance, respiratory system, supportive, antibacterial, anti-inflammatory, syndromic corrective intensive therapy. Favorable outcome with the restoration of full functional activity of the kidneys and discharge from the hospital was observed in 7 children (Group 1), an unfavorable outcome - in 3 children (Group 2). Pathological diagnosis: 1 patient - the main disease: bilateral total viral-bacterial pneumonia. Complications of the underlying disease: toxic dystrophy of internal organs, multiple punctate hemorrhages in the serous and mucous membranes, uremia (urea 29.8 mmol/l, creatinine 0.65 mmol/l, potassium 5.4 mmol/l), anasarca, bilateral hydrothorax, hydropericardium, hemo-

dialysis sessions No. 6, acute stomach ulcers, acute pulmonary heart failure. 2 - Bilateral interstitial pneumonia. Complications of the underlying disease: Toxic dystrophy of internal organs, uremia (urea 40.1 mmol/l, creatinine 0.7 mmol/l, potassium 7.1 mmol/l), acute stomach ulcers, hemodialysis sessions No. 4, acute pulmonary heart failure. 3- bilateral interstitial pneumonia. Toxic dystrophy of internal organs, uremia (urea 15.2 mmol/l, creatinine 0.482 mmol/l, potassium 5.6 mmol/l), acute stomach ulcers, hemodialysis sessions No. 7, acute pulmonary heart failure.

Results and its discussion.

The average daily values for 30 days averaged 36.9±0.1°C in group 1 and 36.9±0.1°C in group 2. On day 1, the circadian rhythm mesor indices in groups 1 and 2 were within normal values limits. In group 1, the dynamics revealed an increase in temperature by 0.5°C on days 2,5,6,8-13, again on days 16,25 within subfebrile numbers. The tendency to increase the temperature against the background of ongoing therapy was noted in group 2 at a later date (Table 1) despite the appearance of excretory activity of the kidneys. The studied indicators in group 2 indicated a more significant hyperthermic reaction, which corresponded to a general deterioration in the condition due to an increase in the inflammatory reaction, intoxication at a later date (27-30 days) (Table 3). The average values of body temperature in the circadian rhythm did not reveal any features in the daytime and at night (Table 2).

Table 1.

Dynamics of the circadian mesor
Body temperature rhythm

Days	1 group	2 group
1	36,5±0,3	36,6±0,1
2	37,0±0,1‴	36,8±0,1
3	36,8±0,1	36,8±0,1
4	36,8±0,1	36,8±0,1
5	37,0±0,02‴	36,8±0,1
6	37,0±0,1‴	36,9±0,1
7	36,9±0,1	37,0±0,1
8	37,0±0,1‴	36,9±0,1
9	37,0±0,1‴	37,0±0,1
10	37,0±0,1‴	37,0±0,1
11	37,0±0,1‴	37,0±0,1
12	37,0±0,1‴	36,9±0,1
13	37,0±0,1‴	36,9±0,1
14	36,9±0,1	37,1±0,1

15	36,9±0,01	36,9±0,1
16	37,0±0,01‴	36,8±0,1
17	36,8±0,1	36,9±0,1
18	36,9±0,1	36,9±0,1
19	36,8±0,1	36,8±0,2
20	36,9±0,1	37,0±0,1
21	36,9±0,1	36,9±0,1
22	36,9±0,1	37,0±0,1
23	36,8±0,01	36,8±0,1
24	36,8±0,1	36,8±0,2
25	37,0±0,1‴	37,1±0,01
26	36,9±0,1	36,9±0,1
27	36,7±0,1	37,1±0,1*
28	36,8±0,1	37,4±0,1*
29	36,8±0,1	37,2±0,2*
30	36,7±0,1	37,1±0,1*

Table 2.

Circadian rhythm of body temperature in infancy with ARF

Hours	**1 group**	**2 group**
8	36,8±0,1	37,0±0,2
9	36,9±0,1	36,9±0,2
10	36,9±0,1	36,9±0,1
11	36,9±0,1	36,9±0,2
12	37,0±0,1	37,0±0,2
13	36,9±0,2	37,0±0,2
14	36,9±0,1	36,9±0,2
15	36,9±0,1	37,0±0,2
16	36,9±0,1	37,0±0,1
17	36,8±0,1	36,9±0,2
18	36,9±0,1	37,0±0,2
19	36,8±0,1	37,0±0,2
20	36,9±0,1	36,9±0,2
21	36,9±0,1	36,9±0,2
22	36,9±0,1	36,9±0,2
23	36,9±0,1	36,9±0,2
24	36,9±0,1	36,9±0,1
1	36,9±0,1	36,9±0,1
2	36,9±0,1	36,9±0,2

3	36,9±0,1	36,9±0,1
4	36,9±0,1	36,9±0,2
5	36,9±0,1	36,9±0,1
6	36,9±0,1	37,0±0,1
7	36,9±0,1	37,0±0,1

‴ - the dynamics is reliable relative to the indicator in 1 day

*- the difference is significant relative to the indicator in group 1

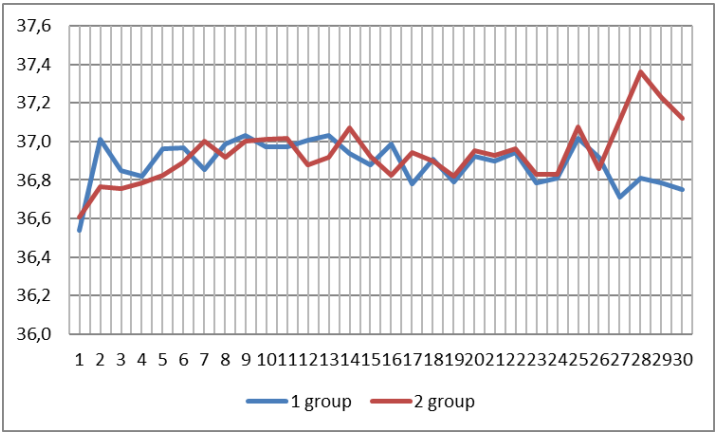

Figure 1. *Inflammatory reaction in ARF up to 3 years on the background of hemodialysis*

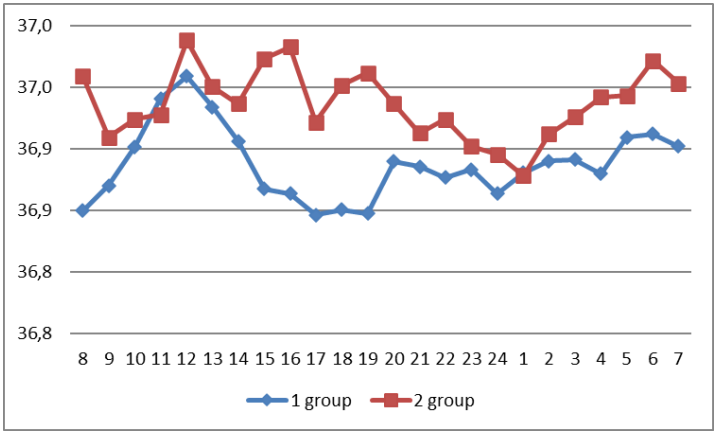

Figure 2. *Comparative assessment of circadian rhythms*

From 12 to 23 hours and in the dark (at 2-7 hours), there was a tendency to a more significant hyperthermic reaction in patients of group 2, which characterized a more pronounced inflammatory reaction, intoxication, which led to an unfavorable outcome.

Hourly monitoring of the temperature response made it possible to identify the correspondence between the amplitude of the circadian rhythm of body temperature, the severity of the inflammatory reaction, the progression of intoxication, which led to an unfavorable outcome in children of the 2nd group (Fig. 3).

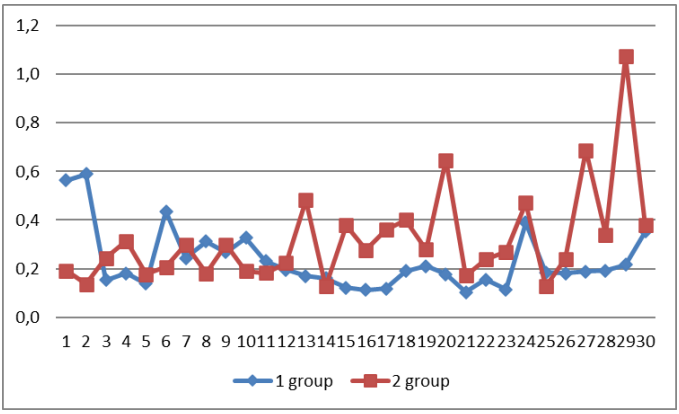

Figure 3. *The amplitude of the circadian rhythm of body temperature up to 3 years*

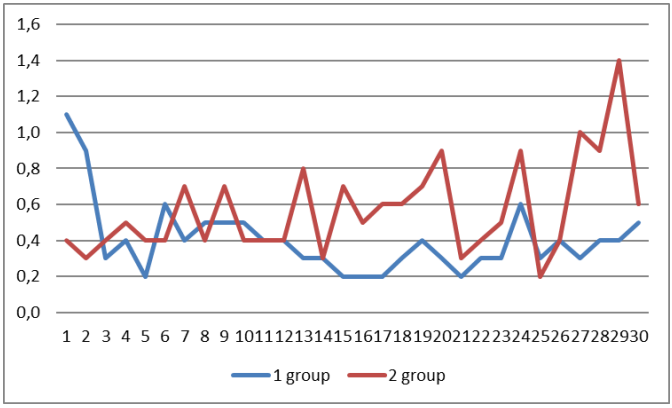

Figure 4. *Daily fluctuations in body temperature in ARF in children under 3 years of age*

More pronounced changes in body temperature during the day, despite the ongoing intensive therapy in group 2, indicated a more pronounced intoxication, a more severe degree of thermoregulation dysfunction in group 2 (Table 3).

Table 3

	Amplitude in degrees	**Daily range in degrees**
1 group	0,2± 0,1	0,4±0,1
2 group	0,3±0,1	0,6±0,2

The duration of the shift in the acrophase of the circadian rhythm of body temperature in ARF in infants.

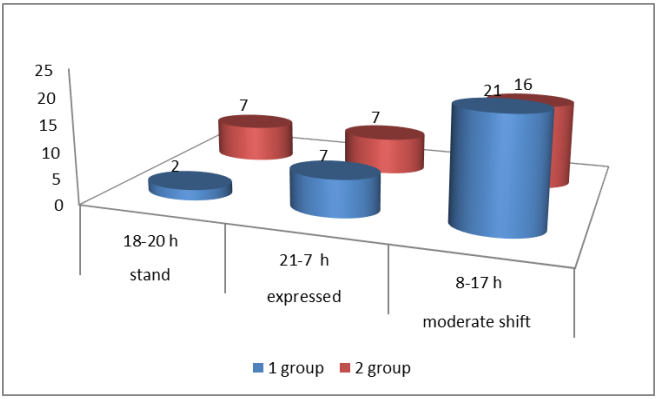

Figure 5. *The duration of the shift in the acrophase of the circadian rhythm of body temperature in ARF in children under 3 years of age.*

The predominance of a moderate shift in the projection of the acrophase within the daytime hours was revealed (Fig. 5), which is regarded as the effect of intensive therapy on the severity of the systemic inflammatory response in children with severe pneumonia complicated by ARF.

Conclusion. On day 1, the mesor values of the circadian rhythm of body temperature in groups with favorable and unfavorable outcomes were within normal values. Hourly monitoring of the temperature response made it possible to identify the correspondence between the amplitude of the circadian rhythm of body temperature and the severity of the inflammatory reaction, progression or decrease in the degree of intoxication. An increase in temperature during therapy in group 2 at a later date against the background of a gradual recovery of the excretory activity of the kidneys corresponded to negative dynamics, a deterioration in the general condition in young children.

References

1. *https://www.krasotaimedicina.ru/diseases/children/renal-failure*
2. *https://www.bsmu.by/downloads/kafedri/k_2_child/lohpn.pdf*
3. *https://ru.wikipedia.org/wiki/%D0%9E%*
4. *https://meduniver.com/Medical/nefrologia/lechenie_opn_u_detei.html*

DOI 10.34660/INF.2023.98.38.052

宫颈外翻的综合治疗方法

AN INTEGRATED APPROACH TO THE TREATMENT OF CERVICAL ECTROPION

Khvorostukhina Natalia Fedorovna
Doctor of Medical Sciences, Professor, Head of the Department
Saratov State Medical University named after V.I. Razumovsky

Zmeeva Marina Anatolyevna
Candidate of Medical Sciences, Assistant of the Department
Saratov State Medical University named after V.I. Razumovsky

Chebonyan Victoria Eduardovna
Resident of the Department
Saratov State Medical University named after V.I. Razumovsky

概括。 介绍了 133 名宫颈外翻妇女的检查和治疗结果。 第1组（n=83）采用我们开发的宫颈糜烂治疗方法，包括两个阶段：I期-清除微生物和病毒病原体结合免疫调节治疗，II期-电外科治疗（Leep-biopsy） 用溶解在 5 ml Miramistin 中的 Galavit（100 mg 干物质）治疗子宫颈（发明专利 RU 2568768 C1）。 在第 2 组 (n=50) 中，宫颈外翻的手术治疗之前是阴道卫生、经验性抗菌和抗病毒治疗。 对照组 3 由 56 名健康女性组成。 除标准外，诊断措施还包括：宫颈管中白细胞介素 IL-1ß、IL-6、IL-8、IL-10 的测定，宫颈中央区血管的多普勒超声诊断。 结果发现，第 1 组 Leep 活检后的修复过程在 65.6% 的患者中于 3 周结束时结束，第 2 组 - 25.5%，5 周后 - 分别为 100% 和 57.4%，8 周后 - 在第 2 组中为 91.5%。 第 1 组宫颈伤口上皮化的平均持续时间为 27.4±4.3 天，第 2 组为 39.5±5.6 天 (p=0.01)。 事实证明，使用已开发的宫颈外翻二阶段复合治疗方法可提高治疗效果，预防 Leep 活检后的并发症，加速上皮化 30.6% 并避免疾病复发。

关键词：宫颈外翻； 宫颈内膜炎； 泌尿生殖系统感染； 局部免疫状态； 宫颈血管化； 复杂的处理

Summary. *The results of examination and treatment of 133 women with cervical ectropion are presented. In group 1 (n=83), a method of cervical ectropion treatment developed by us was used, including two stages: stage I – elimination of microbial and viral pathogens in combination with immunomodulatory therapy, stage II – electrosurgical treatment (Leep-biopsy) and treatment of the cervix with Galavit (100 mg of dry matter) dissolved in 5 ml Miramistin (Patent for invention*

RU 2568768 C1). In group 2 (n=50), surgical treatment of cervical ectropion was preceded by vaginal sanitation, empirical antibacterial and antiviral therapy. Control group 3 consisted of 56 healthy women. Diagnostic measures, in addition to standards, included: determination of interleukins IL-1ß, IL-6, IL-8, IL-10 in the cervical canal, ultrasound diagnostics with dopplerometry in the vessels of the central zone of the cervix. It was found that the reparative process after a Leep biopsy in group 1 ended by the end of 3 weeks in 65.6% of patients, in the 2nd – in 25.5%, after 5 weeks - respectively, in 100% and 57.4%, after 8 – in group 2 in 91.5%. The average duration of cervical wound epithelization in group 1 was 27.4±4.3 days, in group 2 – 39.5±5.6 days (p=0.01). It is proved that the use of the developed method of two-stage complex therapy of cervical ectropion increases the effectiveness of treatment, prevents complications after a Leep biopsy, accelerates epithelialization by 30.6% and avoids relapse of the disease.

Keywords: *cervical ectropion; endocervicitis; urogenital infections; local immune status; cervical vascularization; complex treatment*

Ectropion or eversion of the cervix is a benign disease that can be safely attributed to the category of poorly studied. Despite the widespread introduction of new terms, classifications and modern diagnostic methods into the practice of obstetricians and gynecologists, in relation to pathological conditions of the cervix, the problem of managing patients with cervical pathology does not lose its relevance [1, 2].

As is known, ectropion is a combination of scarring of the cervix (as a result of traumatic injuries) with visualization of the ectopic portion of the cylindrical epithelium on its vaginal part. It should be emphasized that currently ectopia is attributed to a variant of the normal histophysiological state of the cervix and is more common in adolescence and during pregnancy [3], but a large number of domestic and foreign publications are devoted to this nosology [4, 5, 6]. There is a point of view that the cylindrical epithelium of the ectocervix with its crypts is an ideal place for the introduction of pathogens of urogenital infections [7], and the long association of ectopia with cervicitis can cause epithelial proliferation disorders, the development of dysplasia and cervical cancer [8, 9].

Unfortunately, to date, some experts continue to mistakenly combine the concepts of erosion, ectopia and ectropion, considering cervical ectropion a variant of the norm that does not require any intervention [10]. According to the existing recommendations, in the absence of complaints and a normal cytological picture, ectropion treatment is not recommended, and in case of cervical ruptures of II-III degree, reconstructive plastic surgery is indicated [11]. At the same time, in recent years, more and more studies have begun to appear indicating an increasing frequency of complicated ectropion, which negatively affects both the parameters

of women's quality of life [8, 12, 13] and creates problems with the realization of reproductive function, increasing the risks of miscarriage and premature birth [7, 14]. In our work, we drew attention to the category of patients in whom ectropion was diagnosed after using various methods of destruction of cervical pathology in the anamnesis.

The aim of the study: to evaluate the effectiveness of a new method of complex treatment of cervical ectropion.

Materials and methods. To achieve this goal, an open prospective study was conducted in the period from 2011 to 2019 at the Department of Obstetrics and Gynecology of the Pediatric Faculty of Saratov State Medical University named after V.I. Razumovsky, after the approval of the ethics committee and obtaining the voluntary informed consent of women for examination and treatment. A total of 189 patients took part in this work, 133 of them with cervical ectropion (cervical ectropion – groups 1 and 2) and 56 practically healthy women (group 3). The inclusion criteria were: the age of the participants from 25 to 40 years; in groups 1 and 2 – the presence of ectropion after coagulation of cervical pathology in the anamnesis. The exclusion criteria from the study were: gross ruptures of the cervix (II-III degree); inflammatory diseases of the internal genitals in the acute stage; tumors and neoplasms of the internal genitals, pregnancy and lactation; dysplasia (II-III degree) and cervical cancer; concomitant somatic pathology in the decompensation stage.

Depending on the variant and stages of treatment, patients with cervical ectropion were divided into 4 groups. In group 1A (n=22), only the first stage of the method developed by us was carried out. In group 1B (n=61), both stages were used, including electrosurgical treatment of the cervix (Leep biopsy), with repeated detection of abnormal patterns of cytological and colposcopic studies. Our new method of complex treatment of cervical ectropion consists of two stages [15]. At the first stage, in the first phase of the menstrual cycle (day 3), a course of immunotherapy with Pyrogenal was prescribed (intramuscularly, with an initial dose of 25 mcg, after 48 hours, with a gradual and sequential increase in the dose by 25 mcg) until the pyrogenic effect appeared - an increase in body temperature not lower than 38°C, but no more than the maximum dose the drug is 150 mcg. From the moment hyperthermia was fixed or a dose of Pyrogenal 150 mcg was administered, vaginal sanitation, combined antibacterial, antimycotic, antiprotozoal and antiviral therapy in combination with the immunomodulatory and anti-inflammatory drug Galavit (100 mg, in the form of rectal candles) was started for 10 days. The second stage of complex treatment included a Leep biopsy of the cervix and its treatment on the 3rd, 5th and 7th days after surgery with Galavit (100 mg of dry matter) dissolved in 5 ml of Miramistin, followed by a tampon soaked in this solution for 5 hours.

In group 2 (n=50), cervical ectropion treatment was performed according to generally accepted standard methods. At the first stage, when diagnosing vulvovaginitis and cervicitis, all patients of this group (group 2A: n=3 + group 2B: n=47) were prescribed vaginal sanitation, empirical antibacterial and antiviral therapy for 10 days. The second stage is electrosurgical treatment of the cervix (group 2B). In groups 1B and 2B, a cervical biopsy was performed on the second day after the completion of the next menstruation using a VESALIUS LX 80 molecular resonance surgical device.

The examination of all women met the standards. Additionally, the state of the local immune status was studied in dynamics by the content of pro- and anti-inflammatory cytokines (interleukins IL-1β, IL-6, IL-8, IL-10 in the cervical canal being separated) by solid-phase enzyme immunoassay (ELISA) with Vector-BEST reagent kits (Novosibirsk). The results were evaluated using an enzyme immunoassay "Stat Fax-2100" (USA), cytokine concentrations were expressed in pg/ml. Ultrasound diagnostics with Dopplerography was performed on a Logiq S8 device (GE Healthcare, USA), the parameters of maximum arterial velocity (Vmax) and resistance index (RI) were measured in subendocervical and intraendocervical vessels of the central zone of the cervix. Cervical vascularization was determined by the method of M.N. Bulanov (2004) [16]. Histological examination was performed by the standard method. The effectiveness of therapeutic measures was evaluated with dynamic control of laboratory and instrumental diagnostic methods after 1 and 2 months from the start of treatment, the timing of epithelialization, the frequency of complications and recurrence of cervical pathology were also taken into account

For statistical processing, the packages Statistica 7.0, SPSS 17 and statistical functions of MS Excel 2003 were used. Using the Kolmogorov-Smirnov criterion, the hypothesis was tested for the normality of the initial data. The results obtained were presented in the form of an average value and a standard deviation – M (SD). When comparing qualitative indicators, the absolute and relative frequencies of observations (n, %) were calculated. To establish differences between the two average values of the parameters, the Student's t-criterion was used, the Fisher's $\chi 2$ criterion was used as qualitative (differences were considered significant at $p<0.05$). The relationship between the individual indicators was established using correlation analysis for nonparametric methods, the significance was assessed by the Spearman coefficient (R).

Results and discussion. All women included in the study were comparable in age (Table 1). Despite the fact that all groups had a history of childbirth, problems with the full realization of reproductive function were noted only by patients with cervical ectropion: premature birth occurred in every fourth observation (group 1 – n=15 (24.6%); 2nd – n=9 (26.5%), p=0.84), and the frequency of abortions and

spontaneous miscarriages in groups 1 and 2 was 22 times higher than in control group 3.

Table 1

General characteristics of women in groups

Parameters	**1-st (n=83)**		**2-nd (n=50)**		**3-rd (n=56)**		**p^{1-2}**	**p^{2-3}**	**p^{1-3}**
	28,4 (6,2)		**27,8 (7,5)**		**27,5 (5,1)**		**0,95**	**0,97**	**0,91**
Features of obstetric and gynecological anamnesis									
Age, years - M (SD)	n	%	n	%	n	%			
Labour	61	73,5	34	68,0	38	67,9	0,50	0,99	0,47
Abortion/ spontaneous miscarriage	67	80,7	39	78,0	2	3,6	0,71	<0,001	<0,001
Chronic salpingoophoritis	76	91,6	43	86,0	0	0,0	0,31	<0,001	<0,001
Vulvovaginitis	77	92,8	47	94,0	1	1,8	0,79	<0,001	<0,001
Menstrual cycle disorders	49	59,0	26	52,0	0	0,0	0,43	<0,001	<0,001
Concomitant extragenital diseases									
Tonsillitis	28	33,7	19	38,0	0	0,0	0,62	<0,001	<0,001
Pyelonephritis	52	62,7	26	52,0	0	0,0	0,23	<0,001	<0,001
Gastritis	38	45,8	20	40,0	4	7,1	0,52	<0,001	<0,001
Pancreatitis	11	13,3	8	16,0	0	0,0	0,66	0,002	0,005
Enlargement of the thyroid gland	32	38,6	18	36,0	8	14,3	0,77	0,01	0,002
Fatness	43	51,8	25	50,0	2	3,6	0,84	<0,001	<0,001

In addition, the proportion of concomitant genital and somatic diseases, with the prevalence of foci of chronic infection, in patients with cervical ectropion (in the absence of a statistical difference in values between groups 1 and 2) significantly exceeded similar parameters of group 3 (Table 1).

The duration of the existence of cervical pathology in the examined groups 1 and 2, before their inclusion in the study, varied from 2 to 5 years. The frequency of using various methods of destruction of the cervix in the past was comparable: diathermocoagulation was performed more often (group 1 – 26.5%; group 2 – 26.0%), cryo- (respectively: 24.1% and 26.0%) and radio wave destruction (21.7% and 20.0%), less often - laser (12.0% and 10.0%) and chemical coagulation (15.7% and 18.0%). The timing of the recurrence of cervical pathology in groups 1 and 2 ranged from 6 months to 1.5 years after the treatment.

In the initial examination of women, according to the results of bacterioscopic smear examination, normocenosis was established in all cases only in group 3 (100%) and only in isolated cases – with cervical ectropion (group 1 – 9.7%; 2nd – 10.0%, p=0.95). At the same time, bacterial vaginosis according to microscopy and pH-metry was diagnosed in more than half of patients with cervical ectropion

(group 1 – 55.4%; group 2 – 58.0%, p=0.77), and in a third – nonspecific vaginitis (respectively: 34.9 and 32.0%; p=0.73). When studying the features of the bacteriological landscape of the discharge from the cervical canal in cervical ectropion, attention was drawn to the diversity of the microbial spectrum of pathogens with a sufficiently high contamination of pathogens (10^4-10^6 CFU/ml): *Gardnerella vaginalis, Corynebacterium sp prevailed*. and *Proteus* (in almost 50% of cases), *Candida sp., Escherichia coli, Staphylococcus aureus* (25%), *Streptococcus sp.* and *Micoplasma hominis* (20%). In addition, infection screening by polymerase chain reaction (PCR) revealed various types and combinations of *Human papillomavirus* of high oncogenic risk (types 16, 18, 31, 33, 39, 52, 58) every 2nd patient with cervical ectropion (group 1 – 57.8%; 2nd – 54.0%, p=0.67), *Chlamydia trachomatis* (respectively: 18.1 and 20.0%, p=0.78), *Ureaplasma urealyticum* (16.9 and 18.0%, p=0.87), *Micoplasma hominis* (34.9 and 32.0%, p=0.73). With additional use of ELISA, IgG to *Ureaplasma urealyticum* and *Human herpesvirus* were detected in the blood serum of all participants of groups 1 and 2, IgG to *Chlamydia trachomatis* (81.9 and 80.0%, p=0.78) and almost 90% to *Trichomonas vaginalis* (91.6 and 92.0%, p=0.93) in 80%. And the specific weight of determination of serum IgM concentrations to pathogens of urogenital infections in ELISA coincided with the results of PCR testing.

The data of the primary cytological examination from the cervix testified to the predominance in patients with cervical ectropion of conclusions corresponding to ASCUS (atypical squamous cells undertermined significance or type III Pap smear: Group 1– n=56 (67.5%); group 2 – n=33 (66.0%), p=0.86) and NILM (negative for intraepithelial lesion or malignancy or type II: n=22 (26.5%) and n=14 (28.0%), p=0.85). A normal cytological picture (type I smear) with cervical ectropion was found only in 6.0% of women (in group 1: n=5; in group 2: n=3; p=0.99), which had significant differences (p<0.001) in comparison with the data of 3 control groups (n=56; 100%). With extended colposcopy before the start of treatment, signs of cervicitis were recorded in all patients with cervical ectropion, acetobelic epithelium and iodine negative zone were determined in 42.2% in group 1 (n=35) and 44.0% in group 2 (n=22), nabotov cysts – in 73.5 and 72.0%, open ducts of glands – in 33.7 and 32.0%, punctuation – in 22.9 and 24.0%, mosaic – in 25.3 and 26.0%, atypical vascularization and leukoplakia – in 16.7 and 14.0%, respectively, in the absence of significant intergroup differences. At the same time, every second patient with cervical ectropion initially had a combination of two or more abnormal colposcopic signs.

Control of laboratory tests after 1 month from the start of therapeutic measures showed positive dynamics in both the 1st and 2nd groups. According to microscopy data, normocytosis was achieved in all women with cervical ectropion, during bacteriological examination, no high contamination of pathogens in the cervical

canal was found in any observation. And screening for urogenital infections by PCR diagnostics gave a negative result. When analyzing the findings of cytology from the cervix in dynamics after the 1st stage of treatment, a more pronounced decrease in the frequency of diagnosis of type III smear reaction (ASCUS) was noted in group 1 – by 2 times, up to 33.7% (n=28; p<0.001), than in the 2nd – by 1.2 times, up to 56.0% (n=28; p=0.02). Dynamic colposcopy made it possible to trace the complete relief of endocervicitis in cervical ectropion in both groups, and the proportion of detection of abnormal colposcopic signs in total significantly decreased only in group 1 – by 1.4 times (from 100 to 73.5%; n=61; p<0.001), while in group 2, the frequency of visualization of such manifestations as atypical vascularization, acetobelic epithelium, mosaic and punctuation practically did not change (from 100 to 94.0%; n=47; p=0.08). The need to perform a Leep biopsy of the cervix, while maintaining abnormal cyto- and/or colposcopic conclusions after the 1st stage of treatment, statistically significantly increased in patients after empirical antibacterial therapy and vaginal sanitation (94.0% – in group 2 versus 73.5% – in group 1; p=0.004).

The results of ultrasound examination of the cervix with Dopplerometry in dynamics are presented in Table 2.

Table 2

Dynamics of the results of ultrasound and dopplerometry of the cervix in groups

Parameters	Terms of the study	1-st (n=83) M (SD)	2-nd (n=50) M (SD)	3-rd (n=56) M (SD)	p^{1-2}	p^{2-3}	p^{1-3}
The average volume of the cervix, cm^3	initially	64,7 (2,2)	65,9 (2,1)	41,6 (1,3)	0,69	<0,001	<0,001
	after 1 month	54,4 (1,5) * p<0,001	61,3 (1,8) p=0,10		0,004	<0,001	<0,001
	after 2 months	40,1 (1,2) * p<0,001	44,5 (1,8) * p<0,001		0,04	0,19	0,40
Endocervix thickness, mm	initially	6,93 (0,5)	6,87 (0,4)	5,42 (0,1)	0,89	<0,001	0,004
	after 1 month	5,51 (0,2) * p=0,009	5,59 (0,1) * p=0,002		0,72	0,23	0,69
	after 2 months	5,48 (0,2) * p=0,008	6,13 (0,2) p=0,10		0,02	0,002	0,79
Vmax in the arteries of the central zone, cm/s	initially	7,67 (0,17)	7,65 (0,15)	4,28 (0,2)	0,93	<0,001	<0,001
	after 1 month	5,68 (0,09) * p<0,001	6,32 (0,71) p=0,07		0,37	0,007	<0,001
	after 2 months	4,75 (0,30) * p<0,001	6,91 (0,58) p=0,22		0,001	<0,001	0,19

RI in the arteries of the central zone	initially	0,77 (0,06)	0,77 (0,04)	0,59 (0,03)	1,00	<0,001	0,008
	after 1 month	0,60 (0,02) * p=0,008	0,62 (0,07) p=0,07		0,78	0,69	0,78
	after 2 months	0,59 (0,01) * p=0,004	0,67 (0,03) p=0,05		0,01	0,06	1,00
Number of vascularization loci	initially	8,24 (0,3)	8,15 (0,5)	4,34 (0,4)	0,88	<0,001	<0,001
	after 1 month	5,12 (0,1) * p<0,001	6,34 (0,1) * p<0,001		<0,001	<0,001	0,06
	after 2 months	4,18 (0,06) * p<0,001	7,34 (0,15) p=0,12		<0,001	<0,001	0,69

Notes: * – statistical significance of indicators in comparison with the initial data.

At the initial examination, the heterogeneity of the cervical structure was recorded in 100% of women with cervical ectropion, the frequency of visualization of echonegative inclusions in the stroma reached 81.9% in group 1 (n=68), 80.0% in group 2 (n=40), (p=0.78), and cysts – 51.8 and 54.0%, accordingly, (p=0.81). The average volume of the cervix in cervical ectropion exceeded the same indicator of the 3 groups of healthy participants by 1.5 times (p<0.001), the thickness of the endocervix by 1.3 times, in the absence of a statistical difference between the parameters of groups 1 and 2 (Table 2). When studying hemodynamics in the vessels of the cervix in patients of groups 1 and 2 before the start of treatment, a significant increase in Vmax (1.5 times) and RI (1.3 times) in the arteries of the central zone was found in relation to the normative data of group 3. And the average number of vascularization loci according to energy Dopplerography data in cervical ectropion increased almost 2 times in comparison with the indicator of group 3 (Table 2).

After the 1st stage of treatment, more pronounced positive changes in sonography parameters were found in group 1 patients with a clear tendency to restore cervical hemodynamics (Table 2). While in group 2 patients, significant changes were achieved only when measuring the thickness of the endocervix and the degree of vascularization, which can be explained by the relief of the inflammatory process of the cervix.

A comparative assessment of the features of the local immune status in the examined groups (Table 3) demonstrated pronounced changes in the production of all studied cytokines in the cervical canal in cervical ectropion before treatment (p<0.001).

Table 3

Features of local immune status and dynamics of cytokine determination in groups

Indicator pg/ml	Terms of the study	1-st (n=83)	2-nd (n=50)	3-rd (n=56)	p^{1-2}	p^{2-3}	p^{1-3}
		M (SD)	M (SD)	M (SD)			
IL-10	initially	12,4 (0,8)	11,5 (1,1)	7,1 (0,9)	0,51	0,003	<0,001
	after 1 month	8,3 (0,6) * p<0,001	9,7 (0,8) p=0,19		0,16	0,03	0,27
	after 2 months	7,7 (0,3) * p<0,001	10,5 (0,9) p=0,48		0,004	0,009	0,53
IL-1β	initially	108,7 (13,3)	105,6 (11,9)	8,3 (1,1)	0,86	<0,001	<0,001
	after 1 month	33,3 (4,8) * p<0,001	72,1 (6,2) * p=0,01		<0,001	<0,001	<0,001
	after 2 months	9,9 (1,4) * p<0,001	91,3 (9,5) p=0,35		<0,001	<0,001	0,37
IL-6	initially	334,5 (26,6)	329,4 (30,3)	15,6 (2,1)	0,90	<0,001	<0,001
	after 1 month	35,8 (4,5) * p<0,001	76,9 (8,1) * p<0,001		<0,001	<0,001	<0,001
	after 2 months	19,4 (1,3) * p<0,001	160,7 (13,6) * p<0,001		<0,001	<0,001	0,13
IL-8	initially	292,1 (20,2)	267,2 (19,4)	102,9 (13,7)	0,38	<0,001	<0,001
	after 1 month	116,4 (14,4) * p<0,001	205,2 (15,7) * p=0,01		<0,001	<0,001	0,50
	after 2 months	95,6 (9,0) * p<0,001	252,8 (17,2) p=0,58		<0,001	<0,001	0,66

Notes: * – statistical significance of indicators in comparison with the initial data.

The content of anti-inflammatory IL-10 in patients with cervical ectropion increased in relation to the control values of group 3 by 1.7 times, a more significant increase in interleukin concentrations was revealed at the initial determination of pro–inflammatory cytokines: IL-8 – by 2.6 times; IL-1ß – by 13 times; IL-6 – by 20 times. Correlation analysis in groups 1 and 2 proved the existence of a direct dependence of the mean strength between the Vmax Doppler parameter in subendocervical and intraendocervical arteries and IL-10 ($r = 0.420$; $p<0.02$), IL-1ß ($r = 0.498$; $p<0.02$) and IL-8 ($r = 0.570$; $p<0.05$).An increase in the correlation coefficient was observed between Vmax and IL-6 ($r = 0.623$; $p<0.01$). In group 3, we did not find strong and average correlative relationships between the studied parameters (correlation coefficients did not exceed 0.254).

With dynamic control after 1 month from the start of cervical ectropion treatment, a decrease in the levels of all studied local interleukins was observed in both groups, but more significant changes in the studied parameters were observed in

group 1 (Table 3). Completely opposite results of laboratory and instrumental control were recorded 2 months after the start of treatment (Table 2-3). Performing a Leep biopsy of the cervix in women in group 2 a month later led to an increase in the production of both pro- and anti-inflammatory cytokines in comparison with previous data in this group after a course of empirical antimicrobial therapy and vaginal sanitation, while the obtained average values of IL-10, IL-8 and IL-1β did not significantly they differed from the initial parameters and retained significant differences with the control indicators of group 3. At the same time, in group 1 patients, a month after the Leep biopsy (2 months after the start of treatment), there was a further decrease in the concentrations of all detectable local cytokines to the control values of group 3, which had a statistical difference, both with the initial data and with similar results of interleukins in the same study period in 2 group (table 3).

Analysis of ultrasound results after 2 months indicated a significant decrease in the volume of the cervix after surgery in both groups (Table 2). At the same time, in group 1, the positive dynamics of the parameters of sonography and Dopplerometry, achieved after the 1st stage of complex treatment, remained. And in group 2, a month after the Leep biopsy, a slight increase in the number of color spots on the cervix, thickening of the endocervix and an increase in Vmax and RI in the central arteries were found, almost to the initial values, with significant differences with similar indicators of groups 1 and 3 (Table 2).

In addition, only in group 2, a month after the Leep biopsy, 10 women (21.3%) showed signs of nonspecific vaginitis (microscopy) and a cytological picture of NILM. When monitoring the conclusions of bacteriological studies of cervical canal crops in group 2 patients, various resident representatives of the microflora (*Candida sp., Escherichia coli, Ureaplasma urealyticum, Micoplasma hominis*) were sown 10 times more often (n=46 (92%) vs. n=7 (8.4%), $p<0.001$) with low contamination pathogens (no more than 10^3 CFU/ml).

When studying the features of the course of the period after the surgical treatment of cervical ectropion on the 7th-12th day, 42 patients of group 2B (89.4%) were diagnosed with clinical and laboratory signs of vaginitis and endocervicitis, and 9 (19.1%) – exacerbations of the chronic inflammatory process of the internal genitals. The reparative process after the Leep biopsy was monitored using a simple colposcopy in dynamics after three, five and eight weeks. Attention was drawn to the lengthening of the epithelization time of the wound on the cervix in group 2B to 39.5±5.6 days versus 27.4±4.3 days in group 1B ($p=0.01$). In group 1B, in most cases (n=40; 65.6%), the reparative process ended by the end of the third week, and the full effect of 100% was achieved in the fifth week after the Leep biopsy. In group 2B, the full effect was observed after three weeks in only 12 women (25.5%), after five – in 27 (57.4%), after eight – in 43 (91.5%). And

in 4 patients of this group (8.5%), 2 months after surgical treatment of cervical ectropion, only a partial effect was achieved: colposcopy around the cervical canal determined a portion of the mucosa with a cylindrical epithelium, >5-6 mm in size, against the background of unchanged multilayer flat epithelium (MFE) of the vaginal part of the cervix.

After 3 months from the start of treatment, during extended colposcopy, a normal colposcopic picture, with visualization on the vaginal part of the cervix of the uterus, was recorded in 72.3% of the subjects of group 1, while in the 2nd - only in 46.0% (p=0.003). Ectopia of the cylindrical epithelium (ECE) without abnormal manifestations was detected in 27.7% of cases in group 1, in group 2 – in 26.0%, and ECE in combination with cervicitis – in 28.0%.

Based on the results of histological examination of the cervical material removed with a Leep biopsy, a combination of cervical ectropion with chronic cervicitis (100% in both groups), stationary endocervicosis (group 1B – n=36 (59.0%); group 2B – n=30 (63.8%), p=0.61), nabotovye cysts was established (respectively, in 72.1 and 76.6% of observations, p=0.60). Parakeratosis was morphologically determined in each 3rd preparation (n=20 (32.8%) and n=16 (34.0%), p=0.89), and acanthosis and coilocytosis (24.6 and 25.5%, p=0.91) in each 4th preparation. Hyperkeratosis (1.5 times), leukoplakia (1.3 times) and vascular proliferation (2 times) were recorded somewhat more often when describing histopreparations in group 2B, but in the absence of significant intergroup differences. However, the specific weight of verification of cervical intraepithelial neoplasia of the I degree (CIN I) according to the results of histoanalysis in patients of group 2B (n=29; 61.7%) significantly exceeded (by 2 times) the data of group 1B (n=19; 31.1%, p=0.002).

Dynamic observation of the study participants over the next 2 years allowed us to state the absence of recurrence of cervical pathology in group 1, and in group 2 – the frequency of recurrence of cervical diseases was 34.0% (n=17).

As is known, the treatment of any disease will be effective if it is justified from the standpoint of etiopathogenesis. The results of our study once again clearly demonstrated the close relationship of cervical ectropion with foci of chronic inflammatory process, pathogens of urogenital infections, including *Human papillomavirus*, and dysbiotic disorders of the vaginal microbiota, which directly affects the quality of life of women, creating problems with the realization of reproductive function [12, 13, 14, 17]. It should be noted that it is with prolonged exposure to microbial or viral effects that stimulate the processes of cellular atypism in benign diseases of the cervix, some scientists associate the appearance of abnormal cyto- and colposcopic pictures [18, 19], which were found in our work in almost all patients with cervical ectropion.

No less important is the fact that we have identified violations of the local

immune status and increased cervical vascularization in patients with ectropion. According to existing publications, an increase in the production of proinflammatory cytokines in the mucus of the cervical canal is more associated with cervicitis [20, 21, 22]. At the same time, the increase in peripheral resistance indices in the uterine arteries and the acceleration of cervical perfusion are attributed by most researchers to markers of malignant neoplasm [23].

Based on the obtained data of correlation analysis, we concluded that an increase in the blood flow rate in the vessels of the cervix will entail a further increase in local interleukins, contributing to the progression of the inflammatory process, increasing the risk of dysplasia and cervical cancer. At the same time, it was suggested that with the elimination of an infectious pathogen and the correction of general and local immune disorders, one can count on the restoration of vascularization and cervical perfusion, providing favorable conditions for cervical epithelialization after the use of surgical methods of treatment.

It should be recognized that in recent years, many additional methods of treating benign diseases of the cervix have been proposed, including those that contribute to accelerating the process of epithelialization of the wound surface after using various methods of destruction [24, 25]. A distinctive feature of our method is a clear sequence of combined therapeutic measures to influence the etiopathogenetic factors of cervical ectropion occurrence [26].

Conclusions. 1. Ectropion is combined with cervicitis (100%), cytological picture of ASCUS type (more than 60%) and NILM (more than 25%), the appearance of abnormal colposcopic signs (100%), an imbalance of the local immune system with a predominance of Th1 cytokines against the background of increased vascularization and cervical perfusion, which dictates the need for a detailed examination and complex treatment.

2. The application of the developed method of two-stage complex therapy of cervical ectropion increases the effectiveness of treatment, due to the consistent and adequate impact on the cause and effect of pathological changes in the cervix, prevents complications after a Leep biopsy, accelerates epithelialization processes by 30.6% and avoids recurrence of cervical pathology.

References

1. Bayandina N.N., Slavnova E.N. Possibilities of using digital technologies in the cytological diagnosis of cervical pathology // P.A. Herzen Journal of oncology. – 2021. – Vol. 10(3). P. 11–18. https://www.elibrary.ru/item.asp?id=46146241

2. Computer-Aided Diagnosis of Label-Free 3-D Optical Coherence Microscopy Images of Human Cervical Tissue / Y. Ma, T. Xu, X. Huang [et al.] // IEEE Trans. Biomed. Eng. – 2019. – Vol. 66(9). – P. 2447–2456. doi: 10.1109/TBME.2018.2890167.

3. Rogovskaya S.I. The cervix, vagina, vulva. Physiology, pathology, colposcopy, aesthetic correction. 2nd ed., reprint. and updated. Moscow: Status Praesens, 2016. – 832 p..

4. Analisis of causes of relapse of cervix ectopia after coagulation / N.F. Khvorostukhina, Y.V. Mikheeva, D.A. Novichkov [et al.] // Fundamental research. – 2014. – № 10-3. – P. 562–566. https://www.elibrary.ru/item.asp?id=22270960

5. Mikheeva Y.V., Khvorostukhina N.F., Novichkov D.A. A modern approach to the treatment of complicated ectopia of the cervix // Obstetrics, Gynecology, and Reproduction. – 2016. – Vol. 10(2). – P. 24–31. https://www.elibrary.ru/item.asp?id=26535833

6. Uterine cervical ectopy during reproductive age: cytological and microbiological findings / J.E. Junior, P.C. Giraldo, A.K. Gonçalves [et al.] // Diagn. Cytopathol. – 2014. – Vol. 42(5). – P. 401–4. doi: 10.1002/dc.23053.

7. Koblosh N.D. Features microecology genital tract in women of reproductive age with benign cervical pathology // Lik. Sprava. – 2015. – Vol. (7-8). – P. 98–104. https://pubmed.ncbi.nlm.nih.gov/27491159/

8. Age and HPV type as risk factors for HPV persistence after loop excision in patients with high grade cervical lesions: an observational study / L. Pirtea, D. Grigoraş, P. Matusz [et al.] // BMC Surg. – 2016. – Vol. 16(1). – P. 70. doi: 10.1186/s12893-016-0185-7.

9. Risk factors of cervical cancer after a negative cytological diagnosis in Polish cervical cancer screening programme / A. Macios, J. Didkowska, U. Wojciechowska [et al.] // Cancer Med. – 2021. – Vol. 10(10). – P. 3449-3460. doi: 10.1002/cam4.3857.

10. Aggarwal P., Ben Amor A. Cervical Ectropion. 2020. In: StatPearls [Internet]. Treasure Island (FL): StatPearls. Publishing, 2021. –PMID: 32809544.

11. Ugly cervix. what to do? (Colposcopic pattern with no signs of HPV-associated lesions) / S.V. Firichenko, I.B. Manoukhin, G.N. Minkina [et al.] // Ginecology. – 2013. – Vol. 15(4). – P. 39–44. https://www.elibrary.ru/item.asp?id=20291887

12. The impact of cryotherapy for symptomatic cervical ectropion on female sexual function and quality of life / S. Yildiz, I. Alay, E. Eren [et al.] // J. Obstet. Gynaecol. – 2021. – Vol. 41(5). – P. 815-820. doi: 10.1080/01443615.2020.1803243.

13. Cervical Ectropion May Be a Cause of Desquamative Inflammatory Vaginitis / L. Mitchell, M. King, H. Brillhart, A. Goldstein // Sex. Med. – 2017. – Vol. 5(3). – P. e212-e214. doi: 10.1016/j.esxm.2017.03.001.

14. Khvorostukhina N.F., Novichkov D.A., Mikheeva Y.V. Ectropion of the cervix. Saratov: Publishing Center of Saratov State Medical University, 2020. – 144 p. https://www.elibrary.ru/item.asp?id=44646340

15. Khvorostukhina N.F., Novichkov D.A., Mikheeva Ju.V., Stoljarova U.V., Stepanova N.N. Method of treating cervical ectopia. Patent for the invention RU 2568768 C1, 20.11.2015. Application no. 2014145405/14 of 11.11.2014; Bjul. 32:11.https://www.elibrary.ru/item.asp?id=37459138

16. Bulanov M.N. Ultrasound diagnostics of cervical pathology: abstract of the dissertation of the Doctor of Medical Sciences: 14.00.19. Moscow, 2004. https://viewer.rusneb.ru/ru/rsl01002734451?page=1&rotate=0&theme=white

17. Galieva G.D., Kokareva V.V., Abilova N. A. The role of infections in the development of cervical pathology in patients of reproductive age // Rostov Scientific Journal. – 2018. – №11. – P. 222–227. https://www.elibrary.ru/item.asp?id=36511440

18. Pap smear for mass screening: Results of an African experiment / O.R. Somé, N. Zongo, S. Ka [et al.] // Gynecol. Obstet. Fertil. – 2016. – Vol. 44(6). – P. 336–40. doi: 10.1016/j.gyobfe.2016.04.006.

19. Paunovic V., Konevic S., Paunovic T. Association of human papillomavirus infection with cytology, colposcopy, histopathology, and risk factors in the development of low and high-grade lesions of the cervix // J. BUON. – 2016. – Vol. 21(3). – P. 659–65.

20. The state of the local immune system cervix uteri with chronic nonspecific cervicitis in women of reproductive age / S.N. Gribova, N.B. Zakharova, N.F. Khvorostukhina, Yu.V. Mikheeva // Modern problems of science and education. – 2015. – № 4. – P. 362. https://www.elibrary.ru/item.asp?id=23940196.

21. Features of cytokine synthesis in various forms of cervical cancer / Ju.V. Mikheeva, N.F. Khvorostukhina, N.B. Zakharova [et al.] // International journal of experimental education. – 2016. –№ 9-1. – P. 73–74. https://www.elibrary.ru/item.asp?id=26561502.

22. Pathogenesis and clinical significance of interleukin-8 and tumor necrosis factor-alpha in cervicitis / Y.M. Ning, Y. Wang, L. Lü [et al.] // Zhonghua Yi Xue Za Zhi. – 2009. – Vol. 89(24). – P. 1684–6.

23. Discriminating Performance of Early Uterine and Cervical Artery Pulsatility and Resistivity In Pre-Invasive Cervical Lesions / O. Doğan, Ç. Pulatoğlu, A. Başbuğ [et al.] // Sisli Etfal. Hastan. Tip. Bul. – 2018. – Vol. 52(3). – P. 206–211. doi: 10.14744/SEMB.2018.07769.

24. Davydov A.I., Shakhlamova M.N., Lebedev V.A. Surgical and post-operative treatment of cervical pathology associated with human papillomavirus // Gynecology, obstetrics and perinatology. 2019. – Vol. 18(1). – P. 11–19. doi: 10.20953/1726-1678-2019-1-11-19.

25. Effectiveness of various types of cryosurgical treatment in patients with benign uterine cervix pathology / L.A. Kaunov, A.M. Gerasimov, A.I. Malyshkina [et al.] // Bulletin of the Ivanovo state medical academy. – 2020. – Vol. 25(3-4). – P. 87-90. https://www.elibrary.ru/item.asp?id=46129588.

26. Khvorostukhina N.F., Novichkov D.A., Stepanova N.N. New possibilities of complex ttreatment of cervical ectropion // Medical Council. – 2021. – № 13. – P. 12-22. https://doi.org/10.21518/2079-701X-2021-13-12-22.

DOI 10.34660/INF.2023.90.83.053

将脐带缠绕在胎儿颈部的围产期结果，取决于分娩方式

PERINATAL OUTCOMES OF WRAPPING THE UMBILICAL CORD AROUND THE FETAL NECK, DEPENDING ON METHOD OF DELIVERY

Khvorostukhina Natalia Fedorovna
Doctor of Medical Sciences, Professor, Head of the Department
Saratov State Medical University named after V.I. Razumovsky

Simonova Antonina Nikolaevna
Candidate of Medical Sciences, Assistant of the Department
Saratov State Medical University named after V.I. Razumovsky

Belyaeva Irina Olegovna
Resident of the Department
Saratov State Medical University named after V.I. Razumovsky

概括。 介绍了对 109 例脐带缠绕在胎儿颈部的出生史的回顾性分析结果。主要群体由 73 名妇女组成，她们的妊娠以通过自然产道分娩而告终。 在对照组 (n=36) 中，剖宫产分娩。 考试是按照标准进行的。 为了评估胎儿在怀孕和分娩期间的状况，使用了超声波、心电图研究、胎儿头部血液中乳酸的测定。 结果发现，在 20.5% 的病例中，脐带缠绕在胎儿颈部使保守治疗的分娩过程复杂化，38.4% 的病例是新生儿缺氧缺血性脑损伤的原因。 脐带缠绕与真淋巴结的结合会增加不良结果的风险，并可能导致产前胎儿死亡，从而对围产期死亡率产生负面影响。 事实证明，脐带缠绕胎儿颈部时分娩方式的选择对新生儿的发病率没有显着影响。

关键词：脐带缠绕； 怀孕; 分娩; 围产期结局； 新生儿的发病率。

Summary. *The results of a retrospective analysis of 109 birth histories in which the umbilical cord was entwined around the fetal neck are presented. The main group consisted of 73 women whose pregnancy ended with childbirth through the natural birth canal. In the comparison group (n=36), delivery was performed by cesarean section. The examination was carried out in accordance with the standards. To assess the condition of the fetus during pregnancy and childbirth, ultrasound, cardiotocographic studies, determination of lactate in the blood from the fetal head were used. It was found that the entanglement of the umbilical cord around the fetal neck in 20.5% of cases complicates the course of labor with conservative management and in 38.4% is the cause of hypoxic–ischemic brain*

damage of the newborn. The combination of umbilical cord entanglement with a true node increases the risk of an unfavorable outcome and can lead to antenatal fetal death, which negatively affects perinatal mortality rates. It is proved that the choice of the delivery method when the umbilical cord is wrapped around the fetal neck does not significantly affect the morbidity rates of newborns.

Keywords: *umbilical cord entanglement; pregnancy; childbirth; perinatal outcomes; morbidity of newborns.*

One of the priorities of modern healthcare is to improve the quality of obstetric care in order to reduce perinatal morbidity and mortality. Among the causes of neonatal mortality, the proportion of fetal hypoxia and asphyxia at birth varies from 51.6% to 84.9% [1, 2]. Currently, it has been established that the occurrence of a critical condition of the fetus during pregnancy is most often due to decompensated placental insufficiency [3-6]. At the same time, in recent years, various umbilical cord abnormalities have been assigned no less important importance in the development of fetal distress [6-11]. This term refers to violations of the development of the umbilical cord throughout the gestation period, as well as its position relative to the fetus. According to the literature, the frequency of umbilical cord pathology ranges from 15 to 38%. At the same time, in 7.7-21.4% of cases, it can lead to asphyxia of the newborn, in 1.7-4.3% – stillbirth and in 1.5-1.6% – postnatal mortality [2, 12]. In the work of E.P. Belozertseva et al. (2015) showed a 3.2-fold increase in the risk of antenatal fetal death in umbilical cord pathology [13]. Previous studies have also proved that anomalies in the length and attachment of the umbilical cord are the cause of acute fetal distress in childbirth in 71.2% of cases, increasing the frequency of emergency surgical aids to 95.4% [6].

Among the variants of umbilical cord anomalies, pathology of its length (short, long), violations of the attachment site (marginal, shell), true and false nodes, vascular spiralization and the syndrome of a single umbilical artery are more often distinguished. However, the most common pathology is considered to be the entanglement of the umbilical cord around the neck (IVF) or parts of the fetus (from 9.23 to 33.72%), which can be easily diagnosed with ultrasound [2, 8, 14]. It is known that the proportion of unfavorable perinatal outcomes can reach 1,9-10% [8, 15]. Ya.E. Kogan (2016) in his publication noted an increase in the frequency of detection of signs of chronic hypoxia by 2 times, and acute hypoxia by 11 times in children born with tight OPV [2].

The high prevalence of hypoxic-ischemic brain injuries resulting from ante- and intranatal hypoxia in fetal OPV, the lack of clear criteria for choosing obstetric tactics indicate the urgency of the problem [1, 7, 14, 16].

The aim of the study: to investigate perinatal outcomes when the umbilical cord is wrapped around the fetal neck, depending on the method of delivery.

Material and methods. A retrospective analysis of 109 birth histories was carried out, in which the umbilical cord was entwined around the fetal neck according to the data of the Perinatal Center of the Saratov City Clinical Hospital No. 8. The main group consisted of 73 women whose pregnancy ended with childbirth through the natural birth canal. In the comparison group (n=36), delivery was performed by cesarean section. The examination was carried out in accordance with the standards. To assess the condition of the fetus during pregnancy and childbirth, ultrasound (ultrasound), cardiotocographic examination (CTG), determination of lactate in the blood from the adjacent fetal head were used. Statistical data processing was carried out using the application software package "MS Office Excel Professional" and "Statistic 6.0".

Results and discussion. The age of pregnant women ranged from 18 to 30 years, the average age in the comparison group slightly exceeded the same indicator of the main group, in the absence of significant differences (Table 1). The study of obstetric and gynecological anamnesis showed that pre-pregnant women prevailed in both groups, while genital pathology was more common in the group with an operative delivery plan. According to the Russian literature, the combination of young age (20-25 years) and the first pregnancy should be attributed to risk factors for the development of umbilical cord pathology [2]. At the same time, according to foreign researchers, umbilical cord anomalies are more common in women over 30 years of age [10, 17].

A detailed analysis of the anamnesis allowed us to note a decrease in the somatic health index of pregnant women with wrapping of the umbilical cord around the neck of fetus (WUCN) (Table 1).

Table 1

General characteristics of the groups

Studied indicators	**Main group (n=73)**		**Comparison group (n=36)**		**p**
	25,8 (2,1)		27,2 (3,6)		0,74
Obstetric and gynecological anamnesis					
Average age	n	%	n	%	
First-time pregnant	44	60,3	26	72,2	0,26
Benign diseases of the cervix	15	20,5	17	47,2	0,01
Infertility	4	5,5	6	16,7	0,06
Chronic inflammatory diseases of the pelvic organs	7	9,6	12	33,3	0,003
Extragenital diseases					
Endocrinopathy	26	35,6	8	22,2	0,16
Diseases of the urinary system	15	20,5	13	36,1	0,08

Diseases of the gastrointestinal tract	13	17,8	7	19,4	0,84
Respiratory diseases	8	11,0	3	8,3	0,67
Exogenous-constitutional obesity	8	11,0	3	8,3	0,67

Endocrinopathy (diffuse enlargement of the thyroid gland, diabetes mellitus) were detected in every third patient of the main group and in every fifth in the comparison group. Diseases of the urinary system with WUCN were somewhat more often traced in the group of women delivered by cesarean section. Chronic gastritis, cholecystitis and pancreatitis were noted in the anamnesis in pregnant women with WUCN with almost the same frequency – in every 5-6 cases. Respiratory diseases and exogenous-constitutional obesity were registered less frequently in both groups, in the absence of significant intergroup differences (Table 1).

The course of a real pregnancy with WUCN in patients of the main group was almost 2 times more often complicated by the development of placental insufficiency with disorders of uteroplacental blood flow in the II and III trimesters: the main group - 20.5% (n=15) versus 11.1% – in the comparison group (n=4,), in the absence of statistically significant intergroup differences (p=0.22). Polyhydramnios were found in 5.5% of pregnant women in the main group and 2.7% in the comparison group; lack of water – respectively, in 2.7% and 8.3%. In 2 women of the main group, when admitted to the hospital at 36-37 weeks gestation, antenatal fetal death occurred, which was the result of a combination of WUCN with a true umbilical cord node. According to the publications of domestic and foreign scientists, the frequency of occurrence of the true umbilical cord node ranges from 0.2 to 2,1% [2, 8, 17, 18]. At the same time, according to the authors, this anomaly increases the risk of antenatal fetal death by 4-5 times and acute fetal distress in childbirth by 10 times. At the same time, R.E. BohîlțEa et al. (2016) showed that ultrasound imaging of umbilical cord nodes is possible only in 0.08% of observations [17].

It should be noted that, according to our data, before delivery, fetal OPV was significantly more often established by ultrasound in the comparison group: 55.6% versus 21.9% in the main group ($p<0.001$), and the true umbilical cord node was diagnosed in isolated cases in both groups – 2.8 and 1.4%, respectively (p=0.61). In the remaining observations, the fact of the umbilical cord entanglement or the discovery of the true umbilical cord node was an accidental finding at the birth of the fetus or its extraction during operative delivery. Thus, the informative value of ultrasound in the diagnosis of umbilical cord entanglement and its anomalies in both groups did not exceed 33.0% in total.

In the majority of women included in the study, pregnancy ended with an urgent delivery: the main group – n=69; 94.5%; the comparison group – n=31; 86.1% (p=0.13). At the same time, the proportion of premature births in the range

from 28 to 37 weeks of gestation in the comparison group (13.9%) exceeded 2.5 times the indicator of the main group (5.5%), but we did not find statistical significance when comparing this parameter (p=0.13).

When analyzing the peculiarities of the course of labor, it was found that the presence of WUCN caused the development of acute fetal distress in 7 women of the main group (9.6%) in the second period of labor and in 10 (27.8%) of the comparison group in the first period. The onset of acute fetal asphyxia in the first period of labor, recorded according to CTG data (tachycardia with variable or late decelerations) and the results of determining the level of lactate in the blood of the fetal head (from 4.8 to 5.2 mmol/L), became an indication for emergency termination of labor by cesarean section. As is known, at the present stage, constant fetal monitoring and determination of lactate in the blood are considered more informative and accessible methods for assessing the condition of the fetus in childbirth, which allow timely diagnosis of intranatal fetal hypoxia [19, 20]. In the second period, the KIWI vacuum system was used for fast and gentle fetal extraction [21-23].

According to the results of our study, a total of 20.5% of WUCN complicated the course of labor with the appearance of signs of acute fetal distress during conservative management in the I or II periods of labor (81 observations out of 109), which was accompanied by indications for the use of delivery operations (vacuum extraction of the fetus and cesarean section) and is consistent with the opinion of many scientists [1, 2, 6, 7, 9, 11, 14, 23].

Among newborns in the main group, 75.3% had an Apgar score of 8-9 points, and 21.9% were born in a state of mild asphyxia (Table 2).

Table 2

General characteristics and morbidity of newborns, depending on the method of delivery

Studied indicators	**Main group (n=73)**		**Comparison group (n=36)**		**p**
	n	**%**	**n**	**%**	
Premature newborns	69	94,5	31	86,1	0,73
Full-term newborns	4	5,5	5	13,9	0,73
Assessment of newborns on the Apgar scale					
8-9 points	55	75,3	26	72,2	0,73
6-7 points (mild asphyxia)	16	21,9	7	19,5	0,77
4-5 points (moderate asphyxia)	0	0,0	2	5,5	0,04
3-4 points (severe asphyxia)	0	0,0	1	2,8	0,15
0 points	2	2,7	0	0,0	0,32

Morbidity of newborns					
Cerebral ischemia of the 1st degree	26	35,6	18	50,0	0,15
Cerebral ischemia of the 2nd degree	2	2,7	0	0,0	0,32
Kefalogematoma	4	5,5	0	0,0	0,15
Natal cervical injury	2	2,7	0	0,0	0,32
Respiratory distress syndrome	2	2,7	0	0,0	0,32

In the comparison group, a mild degree of asphyxia during the initial assessment of children was recorded in 7 observations, and in 3 observations, moderate and severe asphyxia was detected in newborns. The majority of infants in this group also had a high score on the Apgar scale (72.2%). It should be emphasized that despite the excess of the specific weight of premature infants in the comparison group (2.5 times), statistically significant differences were revealed only when comparing the frequency of occurrence of children born in a state of moderate asphyxia. At the same time, stillbirths, due to the antenatal death of fetuses that entered the delivery group through the natural birth canal, did not receive a significant difference when comparing the indicators in the groups (Table 2).

It should also be noted that in the main group, 79.5% of observations (n=58) had a tight WUCN at birth, in the comparison group – 69.4% (n=25), (p=0.25). As a rule, single umbilical cord entanglement prevailed in both groups (Table 3). However, one of the indications for planned operative delivery in the comparison group was, established by ultrasound, 3, 4, 5-fold fetal WUCN. The combination of APS with a true umbilical cord node was found in three cases in the main and two in the comparison group (p=0.74). At the same time, the combination of the umbilical cord node with a tight single entanglement in the main group in one case led to the birth of a child in a state of mild asphyxia, and in two cases was the main cause of antenatal fetal death. At the same time, in the comparison group, non-tight WUCN, even in the presence of a true node, did not have any effect on the perinatal outcome.

Table 3

Frequency of different variants of umbilical cord entanglement in groups

Studied indicators	**Main group (n=73)**		**Comparison group (n=36)**		**p**
	n	**%**	**n**	**%**	
1-fold entwining of the umbilical cord	62	84,9	22	61,1	0,01
2-fold entwining of the umbilical cord	7	9,6	9	25,0	0,03
3-fold entwining of the umbilical cord	1	1,4	1	2,8	0,61
4-fold entwining of the umbilical cord	0	0,0	1	2,8	0,15
5-fold entwining of the umbilical cord	0	0,0	1	2,8	0,15

The combination of the umbilical cord entwining around the fetal neck with a true umbilical cord knot	3	4,1	2	5,5	0,74

After birth, most of the newborns of the main group (n=68; 93.2%) and the comparison group (n=30; 83.3%) were in the neonatal unit. Intensive care in the intensive care unit required 3 children after conservative childbirth (4.1%) and 6 children after cesarean section (16.7%), (p=0.03).

The assessment of the health status of newborns indicated a slight increase in the morbidity of children of the main group (Figure 1). However, we did not find statistically significant differences when comparing the morbidity parameters of newborns in the groups (Table 2).

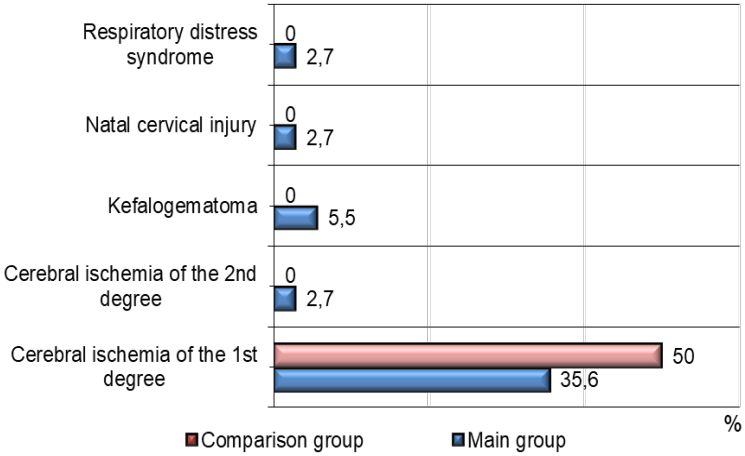

Figure 1. *Morbidity of newborns depending on the method of delivery*

In the structure of perinatal pathology in the main group, cerebral ischemia (38.4% in total), cephalohematoma (5.5%) and natal cervical trauma prevailed in isolated cases (2.7%). At the same time, in the newborns of the comparison group, the proportion of diagnosis of cerebral ischemia of the first degree was 1.4 times higher than the same indicator of the main group (p=0.15), which, in our opinion, may be associated with both the development of acute fetal distress in the presence of WUCN with the onset of labor, and with multiple entanglement of the umbilical cord, especially, in combination with the true node.

Conclusions. 1. The entanglement of the umbilical cord around the fetal neck in 20.5% of cases complicates the course of labor with conservative management, and in 38.4% is the cause of hypoxic–ischemic brain damage of the newborn.

2. The combination of umbilical cord entanglement with a true node increases the risk of an unfavorable outcome and can lead to antenatal fetal death, which negatively affects perinatal mortality rates.

3. The choice of the delivery method when the umbilical cord is wrapped around the fetal neck does not significantly affect the morbidity rates of newborns.

The inclusion of mandatory umbilical cord imaging in the protocol of ultrasound examination in pregnant women can increase the effectiveness of diagnosing its various anomalies for predicting possible obstetric complications and timely changes in the tactics of childbirth, which will become a reserve for reducing perinatal morbidity and mortality in umbilical cord pathology.

References

1. Asphyxia in full-term newborn infants: combination therapy using craniocerebral hypothermia / G.M. Savelyeva, R.I. Shalina, A.A. Smirnova [et al.] // Obstetrics and Gynecology. – 2015. – № 4. – P. 19-24. https://www.elibrary.ru/twefch

2. Kogan Ya.E. Umbilical cord pathology and its role in perinatal complications // Practical medicine. – 2016. – № 1 (93). – P. 22-25. https://www.elibrary.ru/vkwzct

3. Pathogenesis, diagnosis, perinatal outcomes in critical fetal condition/ I.V. Ignatko, M.A. Kardanova, M.M. Miryushchenko, Shch.Sh. Bajbulatova // V.F.Snegirev Archives of Obstetrics and Gynecology. – 2015. – Vol. 2, № 4. – P. 43-44. https://www.elibrary.ru/vaxqpj

4. Strizhakov A.N., Ignatko I.V., Kardanova M.A. A critical state of the foetus: definition, diagnostic criteria, obstetric tactics, perinatal outcomes // Gynecology, Obstetrics and Perinatology. – 2015. – Vol. 14, № 4. – P. 5-14. https://www.elibrary.ru/umodhd

5. Unterscheider J., O'Donoghue K., Malone F.D. Guidelines on fetal growth restriction: a comparison of recent national publications // Am. J. Perinatol. – 2015. – Vol. 32(4). – P. 307-16. doi: 10.1055/s-0034-1387927.

6. Analysis of risk factors threatening asphyxia of the fetus during pregnancy and childbirth / S.A. Kamalyan, N.F. Khvorostukhina, O.I. Bebeshko [et al.] // Postgraduate Doctor. – 2017. – Vol. 82, № 3.1. – P. 144-151. https://www.elibrary.ru/ypltzf

7. The reasons for the critical status of the fetus during labor / N.F. Khvorostukhina, S.A. Kamalyan, O.I. Bebeshko, K.V. Artemenko // Mezhdunarodnyj zhurnal eksperimental'nogo obrazovaniya. – 2016. – № 9-1. – P. 77-78. https://www.elibrary.ru/wjgjrl

8. Gagaev Ch.G.. Radzinskij V.E., red. Pathology of the umbilical cord. M.: GEOTAR-Media; 2011. 96 p.

9. The effects of umbilical cord entanglement upon labor management and fetal health: retrospective case control study / N. Buyukkayaci Duman, S. Topuz, M.O. Bostanci [et al.] // J. Matern. Fetal. Neonatal. Med. – 2018. – Vol. 31(5). – P. 656-660. doi: 10.1080/14767058.2017.1293033.

10. Nkwabong E., Ndoumbe Mballo J., Dohbit J.S. Risk factors for nuchal cord entanglement at delivery // Int. J. Gynaecol. Obstet. – 2018. – Vol. 141(1). – P. 108-112. doi: 10.1002/ijgo.12421.

11. Umbilical cord entanglement's frequency and its impact on the newborn / T. Walla, M.A. Rothschild, J.C. Schmolling, S. Banaschak // Int. J. Legal. Med. – 2018. – Vol. 132(3). – P. 747-752. doi: 10.1007/s00414-017-1746-8.

12. Clinical case of the fetus antenatal death due to the umbilical cord vein aneurysm rupture / N.S. Sozonova, I.P. Lazarev, A.L. Chernova [et al.] // Medical Science and Education of Ural. – 2017. – Vol. 18, № 4 (92). – P. 102-105. https://www.elibrary.ru/taiepn

13. Risk-factors of the antepartum fetal death: retrospective cohort study / T.E. Belokrinitskaya, E.P. Belozertceva, S.A. Iozefson [et al.] // Mother and Baby in Kuzbass. – 2015. – № 2. – P. 86-90. https://www.elibrary.ru/vdeyhz

14. Peesay M. Nuchal cord and its implications // Matern. Health Neonatol. Perinatol. – 2017. – Vol. 3. – P. 28. doi: 10.1186/s40748-017-0068-7.

15. Umbilical cord diameter percentile curves and their correlation to birth weight and placental pathology / L.K. Proctor, B. Fitzgerald, W.L. Whittle [et al.] // Placenta. – 2013. – Vol. 34(1). – P. 62-6.

16. Cord entanglement and perinatal outcomes depending on the mode of delivery / N.F. Khvorostukhina, S.A. Kamalyan, D.A. Novichkov, E.V. Naumova // The Bulletin of Contemporary Clinical Medicine. – 2018. – Vol. 11, № 6. – P. 46-52. https://doi.org/10.20969/VSKM.2018.11(6).46-52

17. Bohîlțea R.E., Turcan N., Cîrstoiu M. Prenatal ultrasound diagnosis and pregnancy outcome of umbilical cord knot - debate regarding ethical aspects of a series of cases // J. Med. Life. – 2016. – Vol. 9(3). – P. 297-301.

18. Veropotvelyan N.P., Rusak N.S. Prenatal diagnosis of umbilical cord true knot using volume ultrasound // Prenatal diagnosis. – 2014. – Vol. 13, № 2. – P. 149-153. https://www.elibrary.ru/tbetkv

19. Intrapartum fetal scalp lactate sam-pling for fetal assessment in the presence of a non-reassuring fetal heart rate trace / C.E. East, L.R. Leader, P. Sheehan [et al.] // Cochrane Database Syst. Rev. – 2010. – Vol. 17(3). – CD006174. doi: 10.1002/14651858.CD006174.pub2.

20. Gunin A.G., Milovanov M.M., Denisova T.G. Methods of fetal assessment in labors // HealthCare of Chuvashia. – 2014. – № 3 (39). – P. 39-48. https://www.elibrary.ru/tvvyyp

21. Fetal vacuum extraction in modern obstetrics / V.A. Petruhin, K.N. Ahvlediani, L.S. Logutova // Russian Bulletin of Obstetrician-Gynecologist. – 2013. – Vol. 13, № 6. – P. 53-59. https://www.elibrary.ru/rthwib

22. Analysis of effectiveness and safety of assisted / N.F. Khvorostukhina, T.U. Kozlova, D.A. Novichkov, O.I. Bebeshko // Saratov Journal of Medical Scientific Research. – 2014. – Vol. 10, № 2. – P. 346-349. https://www.elibrary.ru/slrhsd

23. Extreme umbilical cord lengths, cord knot and entanglement: Risk factors and risk of adverse outcomes, a population-based study / L.E. Linde, S. Rasmussen, J. Kessler, C. Ebbing // PLoS One. – 2018. – Vol. 13(3). – P. e0194814. doi: 10.1371/journal.pone.0194814.

DOI 10.34660/INF.2023.77.15.054

婴儿急性肾功能衰竭收缩压昼夜节律的动态变化
DYNAMICS OF THE CIRCADIAN RHYTHM OF SYSTOLIC BLOOD PRESSURE IN ACUTE RENAL FAILURE IN INFANTS

Muhitdinova Hura Nuritdinovna
Doctor of Medical Sciences, Full Professor
Center for the Development of Professional Qualifications of Medical Workers

Hamrayeva Gulchehra Shahobovna
Doctor of Medical Sciences, Head of Department
Center for the Development of Professional Qualifications of Medical Workers

Alauatdinova Gulhan Inyatdinovna
Assistant Professor
Center for the Development of Professional Qualifications of Medical Workers

抽象的。 对 15 名幼儿（10 个月至 3 岁）在急性肺炎背景下发生的急性肾功能衰竭收缩压（SBP）的昼夜节律研究揭示了一些特征。 根据急性肾功能衰竭病情的严重程度，整个强化治疗期间的 SBP 平均水平比年龄标准高 15-20 mmHg，各组之间没有显着差异。 相位结构变形最显着，SBP 昼夜节律反转，振幅增加，前 5 天指标的日波动范围，与 SBP 水平直接相关的趋势 体温 (0.48) 在不良结果组中被记录下来。 每日 SBP 指标的振幅和范围动态的振荡性质证实了在幼儿严重急性肾功能衰竭中构成 SBP 的功能机制的节律活动得以保留。

关键词：昼夜节律，收缩压，急性肾功能衰竭，幼儿。

Abstract. *The study of the circadian rhythm of systolic blood pressure (SBP) in acute renal failure that developed against the background of acute pneumonia in 15 young children (from 10 months to 3 years) revealed some features. The average level of SBP for the entire period of intensive therapy, depending on the severity of the condition in acute renal failure, was higher than the age norm by 15-20 mmHg, did not differ significantly by groups. The most significant degree of deformation of the phase structure with an inversion of the circadian rhythm of SBP, an increase in amplitude, a daily range of fluctuations in the indicator in the first 5 days, a tendency for a direct correlation between the level of SBP and body temperature (0.48) was noted in the group with an unfavorable outcome.*

The oscillatory nature of the dynamics of the amplitude and range of daily SBP indicators confirms the preservation of the rhythmic activity of the functional mechanisms that make up SBP in severe acute renal failure in young children.

Keywords: *circadian rhythm, systolic blood pressure, acute renal failure, young children.*

Relevance. Acute renal failure (ARF) is a non-specific clinical and laboratory syndrome that occurs due to the acute loss of all homeostatic functions of the kidneys. This process, with timely diagnosis and proper treatment, is reversible. On average, the incidence of acute renal failure ranges from 3 to 8 cases per 1,000,000 children (according to Russian authors), of which 1/3 occurs in infancy. AKI significantly worsens the child's condition, and mortality ranges from 3-5% with hemolytic-uremic syndrome, up to 30-70% with sepsis and multiple organ failure. Even with successful treatment and restoration of urinary function, long-term consequences are possible - 10-25% of children develop chronic kidney disease. ARF is dangerous electrolyte disorders (hyperkalemia, hypocalcemia, hyperphosphatemia). An increase in blood pressure that occurs against the background of pathologies of the heart, kidneys or disorders of the endocrine system, as a result of heart damage and disorders of the nervous system, is commonly called secondary hypertension. Children often suffer from such pathologies, which is why they register both spasmodic and constant increases in pressure. Such hypertension can be recorded from the neonatal period and disappear only after the elimination of the triggering factor - the true cause that leads to vasospasm and increased systemic pressure. However, there is not enough information in the literature on the specifics of the response of systolic blood pressure (SBP) in acute renal failure, which developed against the background of an acute bacterial pulmonary infection in children under the age of 3 years [1-7].

Goal of the work. To study and give a comparative assessment of the reaction of systolic blood pressure in acute renal failure in infancy, which developed against the background of an acute infection.

Material and research methods. When correcting infusion therapy, the dynamics of the child's weight, the ratio between the injected and excreted fluid, and the serum concentration of Na + were taken into account. The daily fluid requirement in a child with acute renal failure was calculated by adding the amount of urine excreted per day and extrarenal water losses (hidden losses and losses through the gastrointestinal tract). Indications for dialysis (renal replacement therapy (RRT) were: anuria for more than 24 hours with a progressively worsening condition of the patient; an increase in the level of urea more than 25 mmol/l. The data of hourly monitoring of body temperature in 10 children with acute renal failure admitted to the ICU of the RCCEMS with anuria from 1 up to 4 days at the age

of 10 months to 3 years 4 months from the ICU of regional children's hospitals and branches of RCCEMS. Prior to admission to the clinic, all patients received anti-inflammatory therapy aimed at the treatment of pneumonia 14, AII-1 patient. According to the indications, due to severe progressive respiratory failure, patients were provided with invasive mechanical respiratory support on the first day according to indications. All patients underwent hemodialysis, 3 - in combination with plasmophoresis under the control of hemodynamics, acid-base balance, respiratory system, maintenance, antibacterial, anti-inflammatory, syndromic corrective intensive therapy according to the recommendations in the literature. A favorable outcome with the restoration of full functional activity of the kidneys and discharge from the hospital was observed in 11 children (groups 1 and 2), an unfavorable outcome in 4 children (group 3). The first group consisted of patients who received intensive care in the ICU for up to 10 days, the second - children with a favorable outcome after intensive care for 11-45 days.

Results and its discussion. As shown in Table 1, male patients predominated in all studied groups of children. The duration of intensive care in children of groups 2 and 3 significantly exceeded the duration of treatment in the ICU in group 1 by 20 and 23 days ($p<0.05$, respectively). In group 1, mechanical ventilation was performed in 1 patient due to the severity of acute respiratory failure caused by severe acute pneumonia. In group 2, the duration of mechanical respiratory support (MRS) was 18.6 ± 8 days, in group 3, a 7-day longer MRS, unfortunately, did not improve the outcome of the disease.

Table 1.

Characteristics of patients

Groups	Age, months	gender, m/f	Start of mechanical ventilation, days	Duration of MRS, days	In ICU, days
1	29±2,8	3/2.	1больной в 1	9	7,8±1,9
2	19±9,7	5/1.	4,3±3,1	18,6±8	27,8±5,8*
3	30,5±6,5	3/1.	5,5±0,5	25,5±6,7	30,7±6,8*

* - the difference is significant relative to the indicator in group 1.

The average level of SBP for the entire period of study, depending on the severity of the condition with ARF, was higher than the age norm, did not differ significantly by groups, amounting to 113.2±2.1 mmHg in group 1, 112±2 mmHg in group 2, 1 mm Hg, in 3 - 112.4 ± 3 mm Hg.

Table 2.

Dynamics of SBP in ARF from 10 months to 3 years

Days	1 group	2 group	3 group
1	114,6±4,3	107,8±3,2	102,3±6,2
2	111,1±2,1	107,0±2,0	104,0±2,7
3	113,0±2,3	109,6±2,6	109,8±2,3
4	119,2±3,5	112,6±3,9	110,5±3,6
5	112,4±3,4	111,9±3,9	118,3±3,4
6	111,6±3,2	110,8±2,4	117,6±3,8
7	114,4±3,4	110,6±1,7	115,3±4,9
8	114,8±2,7	110,1±2,1	114,2±4,0
9	111,9±2,3	113,3±3,1	120,1±4,1
10	108,7±3,7	107,3±4,1	116,8±3,2
11		112,3±3,7	117,0±3,5
12		117,5±2,2	112,4±4,6
13		111,9±2,3	113,1±4,7
14		114,0±2,6	115,9±2,2
15		112,8±3,2	114,1±3,6
16		111,9±3,5	113,0±2,7
17		113,2±3,0	114,1±2,6
18		112,8±1,9	112,2±3,0
19		112,1±3,5	111,8±3,2
20		114,5±3,3	111,2±3,8
21		113,3±4,2	108,1±4,1
22		116,0±2,4	107,7±2,3
23		111,5±2,3	107,7±3,4
24		106,2±2,6	111,5±2,2
25		107,9±5,0	113,5±2,9
26		112,3±3,9	109,5±2,7
27		116,5±5,4	112,3±4,5
28		111,4±5,5	116,0±4,7
29		113,1±3,6	111,9±3,0
30		117,6±4,3	111,1±3,0

Table 3.

Mean SBP values in the circadian rhythm

Hours	1 group	2 group	3 group
8	113,7±3,5	111,7±5,0	113,7±4,2
9	113,7±3,3	111,7±5,1	113,8±3,6
10	112,7±4,2	112,5±4,2	114,0±4,7
11	110,7±3,2	111,5±4,9	112,9±3,7
12	113,2±6,9	111,2±4,0	110,7±6,0
13	112,5±3,9	110,4±4,9	112,8±5,5
14	110,9±3,7	111,6±3,8	115,0±5,2
15	110,0±5,8	111,9±3,7	113,3±4,4
16	111,7±3,7	111,9±4,2	113,6±5,9
17	112,3±3,0	111,8±4,1	112,8±4,7
18	111,3±2,5	113,9±4,0	111,4±5,6
19	112,5±4,1	113,5±4,0	113,1±5,5
20	115,1±2,2	113,0±3,5	112,1±5,1
21	115,4±2,5	113,2±3,7	112,6±4,0
22	115,3±3,4	112,1±4,7	112,2±3,8
23	113,2±4,2	112,0±3,4	112,8±4,3
24	114,6±3,5	111,4±3,7	112,2±4,7
1	114,9±3,7	111,3±3,4	110,5±4,6
2	113,5±3,1	111,4±3,0	110,8±5,2
3	114,6±3,2	111,7±3,5	111,1±3,7
4	113,6±2,7	112,3±4,0	112,4±4,5
5	112,5±4,4	111,7±4,3	112,0±3,8
6	113,5±3,5	112,9±3,8	111,9±4,4
7	113,7±4,3	111,3±3,2	112,4±4,2

Throughout the entire observation in the ICU, elevated SBP levels persisted in all subjects on the background of antihypertensive therapy, methods of extracorporeal blood purification (Table 2). In children of the 1st group, a tendency to a decrease in the peri-weekly rhythm to 6 days was revealed, with a more severe condition in the 2nd group, an increase in the period of fluctuations to 10, 9.8 days was noted, while in the 3rd group of patients, a tendency to the appearance of a 22-day fluctuation with stratified on it with shorter waves, consisting of 8, 4,10 day periods of oscillations characterized by instability of the structure, such as the wavelength, the amplitude of the phase characteristics (Fig. 1).

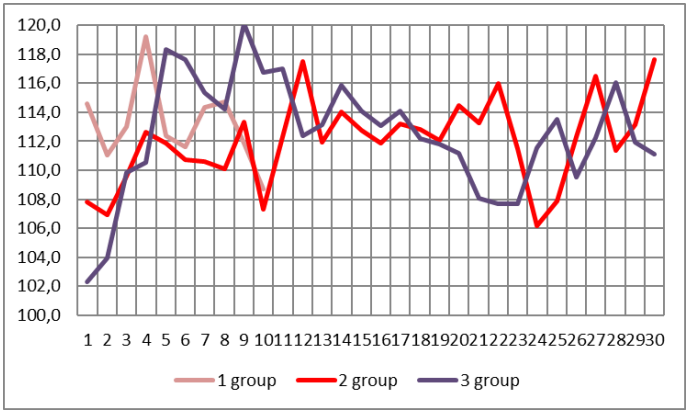

Figure 1. *Dynamics of the mesor of the circadian rhythm of SBP in acute renal failure in infancy, mm Hg*

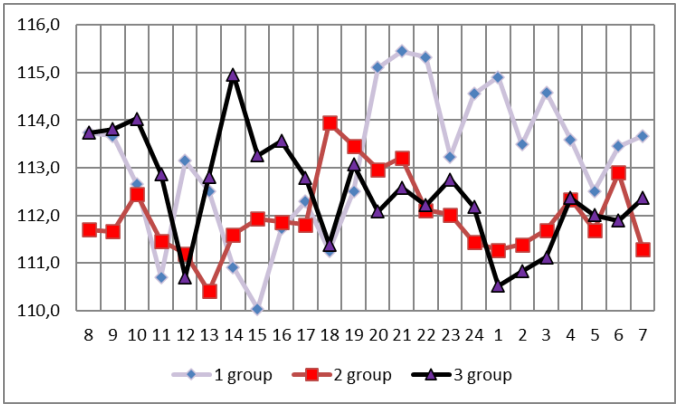

Figure 2. *Mean SBP values in circadian rhythm, mmHg*

A significant deformation of the structural characteristics of the circadian rhythm of SBP was revealed. Thus, in group 1, a shift in the peak of the acrophase of the circadian rhythm of SBP by 11 hours (inversion) was found. In group 2, there was a shift in the acrophase of the circadian rhythm of SBP by 8 hours clockwise. In patients of group 3, the maximum value of SBP was found at 14:00, and the projection of the bathyphase at 12:00 and at 1:00 am. That is, the most significant degree of deformation of phase structures with inversion of the circadian rhythm of SBP was noted in the group with an unfavorable outcome (Fig. 2).

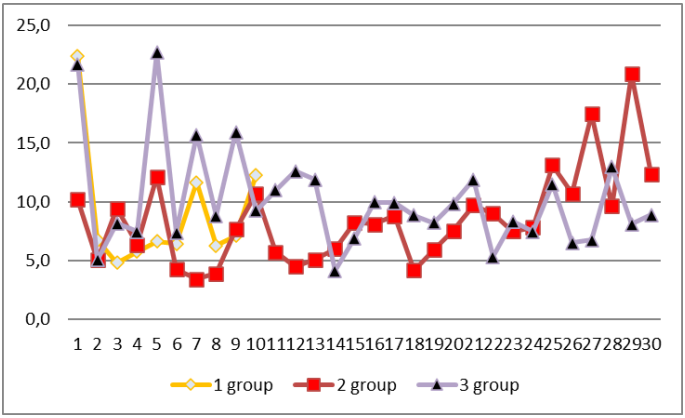

Figure 3. *Dynamics of the amplitude of the circadian rhythm SBP up to 3 years, mm Hg*

It is noteworthy that there were no significant differences in the severity of the condition of the amplitude of daily fluctuations in SBP, which amounted to 9 ± 3 mm Hg in group 1, 8.5 ± 2.9 mm Hg in group 2, and 10 in group 3. .1±3.1 mmHg. However, in group 2, the most significant instability of SBP on days 27.29 was manifested by an increase in the indicator to 10 mm Hg, and in group 3, on days 1-2, 4-5, changes in the amplitude of the daily fluctuations in SBP amounted to 17-18 mm. Hg Apparently, the increase in the amplitude of the circadian rhythm of SBP in the first 5 days by more than 10 mm Hg can be considered an indicator of the impossibility of restoring impaired perfusion characteristics of the kidneys due to various mechanisms: ischemia of the renal parenchyma, activation of shunts in the juxtamedullary zone, toxic damage to the glomeruli and tubular epithelium, acute obstruction of the urinary tract. These changes were initially reversible, and when the provoking factors were eliminated, the functions of the nephrons were completely restored. However, in patients of the 3rd group, a complete restoration of renal blood flow was impossible, an indicator of which was a pronounced instability of elevated SBP in the first 5 days of intensive care. In this regard, the identified feature can be interpreted as an objective sign of ineffective restoration of capillary blood flow, failure to correct ischemia of the renal parenchyma, causing the failure of the excretory function of the kidneys.

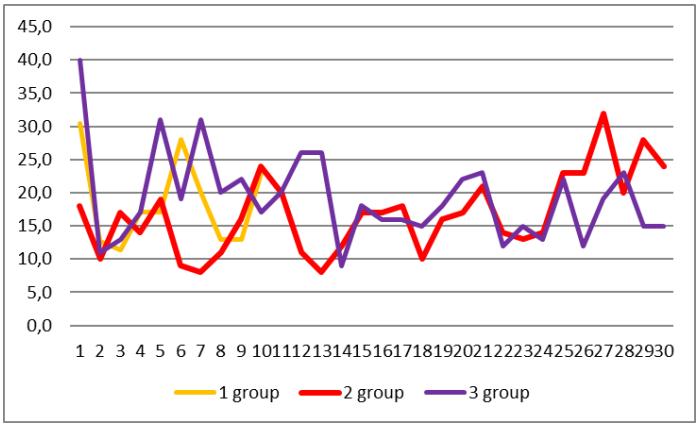

Figure 4. *Daily range of SBP up to 3 years, mm Hg*

Confirmation is the highest values of daily fluctuations in the increased rate of SBP up to 40 mm Hg. in 1 day, up to 32 mm Hg in group 2 on day 27 (Fig. 4). Attention is drawn to the oscillatory nature of the dynamics of the amplitude and range of daily SBP indicators, which confirms the preservation of the rhythmic activity of the functional mechanisms that make up the SBP. A trend of direct correlation between the level of SBP and body temperature (0.48) in the 3rd group was revealed. Analysis and assessment of the duration of the SBP acrophase shift depending on the severity of the condition with acute renal failure up to 3 years made it possible to state the longest (in % of the total duration of intensive care) inversion of the circadian rhythm in group 1. And in terms of the number of days, the longest shift of the acrophase peak to night hours was observed in children of the 2nd group (14 days) and in the 3rd group (8 days).

Table 4.

The duration of the SBP acrophase shift depending on the severity of the condition in acute renal failure is up to 3 years

	Norm	**moderate deviation**	**inversion**
	9-11 hour	**12-21 hour**	**22-7 hour**
1 group	0	30% (3)	70% (7)
2 group	16% (5)	36% (11)	48% (14)
3 group	13% (4)	60% (18)	27% (8)

The revealed feature of the adaptive restructuring of the circadian rhythm of SBP, apparently, is due to less pronounced stress-limiting therapy, sedative drug load than in groups 2 and 3.

Conclusion. The average level of SBP for the entire period of intensive therapy, depending on the severity of the condition in acute renal failure, was higher than the age norm by 15-20 mmHg, did not differ significantly by groups. The most significant degree of deformation of the phase structure with an inversion of the circadian rhythm of SBP, an increase in amplitude, a daily range of fluctuations in the indicator in the first 5 days, a tendency for a direct correlation between the level of SBP and body temperature (0.48) was noted in the group with an unfavorable outcome. The oscillatory nature of the dynamics of the amplitude and range of daily SBP indicators confirms the preservation of the rhythmic activity of the functional mechanisms that make up SBP in severe acute renal failure in young children.

References

1. Papayan, A.V. Clinical pediatric nephrology: a guide for physicians / A.V. Papayan, N.D. Savenkova. St. Petersburg: Levsha. St. Petersburg, 2008, pp. 508–548.

2. Shabalov, N.P. Children's diseases: textbook. : in 2 volumes / N. P. Shabalov. 5th ed. St. Petersburg: Piter, 2004, vol. 2, pp. 228–237.

3. Children's diseases: a practical guide for doctors and students / ed. A. M. Chichko, M. V. Chichko. Minsk: FUA inform, 2013, pp. 466–472.

4. Erman, M. V. Pediatric nephrology: a guide for physicians / M. V. Erman. 2nd ed., revis. and corr. St. Petersburg: SpetsLit, 2010, pp. 562–587.

5. https://angioclinic.ru/zabolevaniya/ostraya-pochechnaya-nedostatochnost/

6. https://meduniver.com/Medical/profilaktika/opn_u_detei.html

7. https://medaboutme.ru/articles/simptomaticheskie_gipertenzii_u_detey_problemy_pochek_serdtsa/

DOI 10.34660/INF.2023.48.97.055

从现代医学应用经验的棱镜看脱氧核糖核酸钠在产科的应用

ON THE USE OF SODIUM DEOXYRIBONUCLEATE IN OBSTETRICS THROUGH THE PRISM OF THE EXPERIENCE OF ITS APPLICATION IN MODERN MEDICINE

Khavansky Anton Yurievich
Head of Department
City Mariinsky Hospital, St. Petersburg c., Russia

Linde Victor Anatolievich
Doctor of Medical Sciences, Full Professor, Doctor
City Mariinsky Hospital, St. Petersburg c., Russia

Gurtsieva Diana Konstantinovna
Doctor
City Mariinsky Hospital, St. Petersburg c., Russia

抽象的。 免疫介导的疾病构成了传染性和非传染性全身性疾病的主要群体。免疫调节剂应在其治疗中发挥重要作用。 产科不禁忌的免疫调节剂是脱氧核糖核酸钠。 它作为一种具有免疫调节、抗炎、再生和修复作用的药物已在许多医学领域显示出其有效性。 这为其成功用于产后子宫内膜炎的复杂治疗创造了先决条件。

关键词：脱氧核糖核酸钠，免疫紊乱，免疫调节剂，修复过程。

Abstract. *Immune-mediated diseases constitute the main cohort of infectious and non-communicable systemic diseases. Immunomodulators should play an important role in their treatment. An immunomodulator not contraindicated in obstetrics is sodium deoxyribonucleate. It has shown its effectiveness as a drug with immunomodulatory, anti-inflammatory, regenerating and reparative effects in many areas of medicine. This creates the prerequisites for its successful use in the complex treatment of postpartum endometritis.*

Keywords: *sodium deoxyribonucleate, immune disorders, immunomodulators, reparative processes.*

The immunological component of most infectious and non-infectious systemic diseases is beyond doubt [1]. In their treatment, drugs are needed, in the mechanism of action of which immunomodulation plays a significant role [2]. The use of immunomodulators should be based on knowledge of their mechanisms of action,

as well as evidence of their efficacy and safety [3]. The situation in obstetrics is complicated by increased requirements for the safety of drugs associated with the safety of the fetus and newborn. As a result, most immunomodulators are contraindicated during pregnancy, childbirth and the postpartum period. One of the few immunomodulators not contraindicated in obstetrics is sodium deoxyribonucleate (SD), which has immunomodulatory, anti-inflammatory, regenerating and reparative effects [4, 5].

An experiment on white laboratory rats showed that SD, which is a sodium salt of DNA depolymerized by ultrasound to particles with a molecular weight of 270-500 kDa, activates cellular and humoral immunity, optimizes specific responses against fungal, viral and bacterial infections, stimulates reparative and regenerative processes, normalizes the state of tissues and organs in dystrophies of vascular origin [6].

The effectiveness of SD in viral infections has been clinically confirmed [7]. Thus, in children with frequent acute respiratory viral infections, a 0.25% solution of SD was administered intranasally before their first visit to a kindergarten for prophylactic purposes. There was a normalization of interferon status, activation of the T-cell link of immunity and phagocytosis. For children from 1 to 3 years old with chronic pharyngitis, a 0.25% solution of SD was administered by inhalation through a nebulizer in a 1:1 dilution with saline. After conducting a study of interferon and immune status before and after treatment with the drug, high clinical and laboratory efficacy was stated. Similar results have been obtained with the use of SD spray in adults [8]. The main pharmacological action of the drug was the stimulation of the phagocytic activity of T-helpers and 7-killers, an increase in the functional activity of neutrophils and monocytes / macrophages, which provide regeneration and repair processes in the epithelial component of the body's antiviral defense. In connection with the positive effect of SD on the course of viral processes, it is interesting to observe that the combination of SD and iron oxide chloride (ferrovir) is considered as an antiviral drug effective in the treatment of papillomavirus infection in women [9]. Especially in combination with destructive methods of treating the cervix.

Viral infections are not the only area of application for SD. The drug is effective in the complex therapy of purulent maxillary sinusitis in combination with antibiotic therapy [10]. The main point of application of SD in this pathology is the restoration of the immune status and the normalization of lipid peroxidation processes. In particular, the concentration in the blood of CD_4 and CD_{16} rises to physiological levels, the concentrations in the blood plasma of IL-1α, IL-8, and the C_3 component of the complement system are normalized. Similar results were obtained when using SD in the complex therapy of exacerbation of chronic prostatitis. The high efficiency of combining SD with antibiotics allowed N.V. Maslova

et al. [11] recommend the drug for widespread use in urological and andrological practice.

Treatment of tuberculosis remains a challenge. One of the central places in anti-tuberculosis immunity is occupied by the T-cell link, represented by various subpopulations of T-lymphocytes. Currently, the T-cell link of immunity is considered as the basis for the formation of anti-tuberculosis immunity, while the humoral link is assigned a secondary role [12]. The experimental and clinical studies carried out to date have shown the high efficiency of SD as an immunocorrector and reparant in the complex treatment of patients with tuberculosis, which is expressed in a more favorable clinical course of the disease and normalization of the immune status [13]. This, in particular, applies to tuberculosis of the genitourinary system. The therapeutic possibilities of his chemotherapy are almost exhausted [14]. There is a need to supplement etiotropic treatment with pathogenetic one. Additional pathogenetic therapy through intramuscular administration of 75 mg of SD leads to a statistically significant increase in the effectiveness of treatment and an improvement in the quality of life of patients.

Evaluation of the effectiveness of DN in oncological practice deserves a separate discussion. There is experience of using a 0.25% solution of SD for external use as the main treatment in 14 patients with malignant skin tumors complicated by radiation ulcers. Sterile napkins were moistened with a SD solution, which covered the ulcerative defect of the skin. Full effect was obtained in 9 patients (64%), partial effect in 2 (14%), stabilization of the process in 2 (14%), no effect in 1 (8%) [15]. R.A. Zukova et al. [16, 17] showed that intramuscular administration of SD as a radioprotector during conformal radiation therapy leads to a decrease in the severity of radiation reactions of grades 2 and 3. It was found that SD has an immunomodulatory effect, restores the indicators of cellular immunity, in particular the content of T- and B-lymphocytes, and also stimulates nonspecific immunity due to the activation of its phagocytic and cytotoxic link.

It also finds its application in gynecological oncology. As a TLR 9 agonist, it may play a dual role when used to regenerate damaged bladder tissue, and as an immunoadjuvant capable of activating an antitumor immune response against bladder cancer. It was found that the use of SD statistically significantly reduced the incidence and severity of clinical manifestations of radioinduced cystitis during radiation therapy for cancer of the body or cervix [18]. The combination of radiation therapy and SD administration in the regimen of chemoradiotherapy for cervical cancer has a great potential for stimulating TLR9 expression in immunocompetent cells of the tumor microenvironment [19].

In obstetrics and gynecology, SD is mainly used in gynecological practice [20]. The use of SD to accelerate tissue regeneration after plastic surgery for pelvic organ prolapse can reduce the treatment time for patients [21]. An interesting

observation was presented by S.N. Kazakova et al. [22]. In July 2020, patient N., 78 years old, applied to the Department of Aesthetic Gynecology and Rehabilitation with complaints of vaginal stump prolapse, bloody discharge, and constant urine leakage 2.5 months after laparoscopic hysterectomy. After the prolapse of the vaginal stump, a decubital ulcer formed on it. The therapy tactics included the cubic pessary of Dr. Arabin No. 3 with daily change and sanitation; physiotherapy; sanitation with a cavitation solution of metrogil No. 5, chlorhexidine No. 5 on the Fotek apparatus daily; colegel with SD - vaginally, 10 days, etc. After 14 days, complete epithelialization of the decubital ulcer.

SD has acquired the widest application in gynecology in the treatment of inflammatory diseases of the pelvic organs (IDPO) [23]. The data of numerous studies indicate that the use of SD in the treatment of acute and chronic, recurrent forms of IDPO promotes faster recovery, restoration of local cellular immune responses and reparative properties of damaged tissues [24]. In a prospective study involving 222 patients of reproductive age with gynecological pathology, tubal-peritoneal infertility and 1-2 degree prevalence of adhesions in the small pelvis, diagnosed during laparoscopy (according to the R-AFS classification) in the early postoperative period from 1 days, intramuscular administration of the immunotropic drug SD with an interval of 24 hours for 10 days contributed to the activation of immunoregulatory mechanisms of cellular humoral immunity, a decrease in the frequency of formation (by 4.5 times, $p<0.001$) and the prevalence of adhesions ($p=0.047$), an increase in the frequency of onset pregnancy by 1.6 times ($p=0.013$) and ensured the maximum improvement in the quality of life in the physical and mental aspects [25]. In particular, concentrations of CD20+-, CD4+-, CD8+-, CD56+-lymphocytes in the peripheral blood normalized more quickly.

SD has acquired great importance in the complex treatment of chronic endometritis (CE) in patients of reproductive age [26]. In particular, as a stage of preparation for in vitro fertilization [27, 28]. The inclusion of SD in the complex therapy of CE contributes to the restoration of the main links of immunity, creating the prerequisites for effective in vitro fertilization [29]. The main improvement mechanisms are due to the prevention of the formation of an inflammatory infiltrate in the endometrium, which is confirmed by a decrease in the number of immunocompetent cells in it (CD8, CD56, CD68, CD138) and the level of pro-inflammatory cytokines and growth factors (Il-1, Il-6, IFN-y, TNF, TGF, VEGF, etc.). Regenerative processes in the endometrium are normalized against the background of a decrease in the intensity of cell apoptosis and sclerotic changes in the tissue, as evidenced by the restoration of Ki-67, EGF, Apo-protein, MMPs levels and various types of collagen. In obstetric practice, SD has proven itself well in the rehabilitation of women after medical termination of an undeveloped pregnancy [30].

All this creates the prerequisites for the successful use of SD as an immunomodulator and a drug with anti-inflammatory, regenerating and reparative effects in the complex treatment of postpartum endometritis.

References

1. Samotrueva M.A., Yasenyavskaya A.L., Tsibizova A.A., Bashkina O.A., Galimzyanov Kh.M., Tyurenkov I.N. Neuroimmunoendocrinology: modern concepts of molecular mechanisms. Immunology. 2017; 38(1): 49-59. DOI: 10.18821/0206-4952-2017-38-1-49-59.

2. Lebedinskaya O. V., Garaev A. T. Immunomodulators based on nucleic acids // Fundamental and applied scientific research: current issues, achievements and innovations: collection of articles of the IX International Scientific and Practical Conference, Penza, January 15, 2018. Penza, 2018, vol. 1, pp. 190-199.

3. Novikova I.A. Modern aspects of the clinical use of immunomodulators // International reviews: clinical practice and health. – 2016. – No. 1. – P. 59-67.

4. Zemskov A.M., Zemskov V.M., Zemskova V.A., Vorontsova Z.A., Zoloedov V.I. Innovative analytical technologies based on the results of traditional immunological monitoring of patients // Bulletin of new medical technologies. 2019. №2. pp. 40–43. DOI: 10.24411/1609-2163-2019-16349.

5. Shumsky V.I., Kaplin V.Yu., Gorenkov R.V. Clinical experience with the use of Derinat - a new generation immunomodulator // Almanac of Clinical Medicine. – 1998. – No. 1. – p. 433-444.

6. Bugrimov D.Yu., Tsvetikova L.N., Ostroushko A.P. Evaluation of the level of expression of TLR-9 receptors with the introduction of the drug Derinat // Journal of scientific articles "Health and education in the XXI century" No. 4, 2012 volume 14. – p. 437-438.

7. Isfarilova O.E. Immunomodulators in complex therapy and prevention // Medical Council. – 2012. – No. 12. – p. 104-110.

8. Babkin A. P., Zuikova A. A., Krasnorutskaya O. N., Kotova Yu. A., Bugrimov D. Yu., Kataeva O. V., Sizova N. M. Evaluation of the clinical efficacy of Derinat® in spray form in the practice of a local therapist // Medical Alphabet. 2019. V. 1. No. 9. P. 38-46. URL: https://www.med-alphabet.com/jour/article/download/1078/913

9. Kolesnikova E.V., Penzhoyan G.A., Zharov A.V., Storozhuk S.V. Evaluation of cytokine status indicators in patients with different variants of the course of human papillomavirus infection. Kuban Scientific Medical Bulletin. 2018; 25(4): 43-50. DOI: 10.25207 / 1608-6228-2018-25-4-43-50.

10. Budyakov S.V. Immunocorrective efficacy of Derinat in maxillary sinusitis. // Scientific statements. Series Medicine. Pharmacy. – 2010. V. 93. – No. 22. – Issue 12. – p. 130-136.

11. Maslova N. V., Frol D. A., Kurilovich N. V. Clinical experience in the complex treatment of chronic bacterial prostatitis // Medical-pharmaceutical journal "Pulse". 2020. V. 22. No. 6. P. 51-54. http://dx.doi.org/10.26787/nydha-2686-6838-2020-22-6-51-54.

12. Cooper A. M. Cell-Mediated Immune Responses in Tuberculosis // Annual Review of Immunology. – 2009. – Vol. 27. – P. 393-422. doi: 10.1146/annurev.immunol.021908.132703.

13. Chubaryan V.T., Mitchenko E.I., Milchakov K.S. Derinat for tuberculosis. Analysis of application experience. // Vestnik VolgSMU. – 2016. – Issue 1 (57). – P. 16-21.

14. Shevchenko S. Yu., Kulchavenya E. V. Assistive technologies in the treatment of patients with urogenital tuberculosis // Urology. 2019. No. 3. P. 50-53. DOI: https://dx.doi.org/10.18565/urology.2019.3.50-53.

15. Kulaev M.T., Al'myashev A.Z., Meltsaev G.G., Shchukin S.A. External use of Derinat in the treatment of radiation ulcers and malignant tumors of visible localizations. // Creative surgery and oncology. – 2009. – No. 1. – p. 35-39.

16. Zukov R. A., Kozina Yu. V., Kozin V. A., Slepov E. V. Optimization of radiation therapy in patients with prostate cancer // Siberian Medical Review. 2018. No. 2 (110). pp. 100-105. DOI: 10.20333/2500136-2018-2-100-105

17. Zukov R. A., Slepov E. V., Kozina Yu. V., Kurtasova L. M., Skopin P. I., Ivashin A. A. Possibility of control of parameters of cellular immunity in patients with bladder cancer during radiotherapy // Effective pharmacotherapy. 2021. V. 17. No. 2. P. 44-48. DOI 10.33978/2307-3586-2021-17-2-44-48.

18. Skopin P. I., Ivashin A. A., Gorgan I. V. Sodium deoxyribonucleate limits the development of radioinduced cystitis during radiation therapy for cancer of the body or cervix // XLIX Ogaryovskie readings: materials of a scientific conference, Saransk, December 07–13, 2020 of the year. Saransk, 2021, vol. 2, pp. 158-164.

19. Andreev P. Y., Bugrimov D. Y., Filin A. A., Kashaeva O. V., Korotkikh N. V., Klimovich A. A. Pathomorphological Markers of Overcoming Radioresistance in the Treatment of Cervical Cancer // International Journal of Biomedicine. 2020 Vol. 10. N. 2. P. 120-123. DOI: 10.21103/Article10(2)_OA6

20. Kolesnikova E.V., Zharov A.V., Penzhoyan G.A. The role of cytokines in the pathogenesis, diagnosis and evaluation of the effectiveness of immunotherapy for various variants of the course of lichen sclerosus in women // Medical Immunology, 2021. V. 23, No. 1. P. 63-72. doi: 10.15789/1563-0625-ROC-2085

21. Nechaikin AS Efficiency of reparants after plastic surgery for pelvic organ prolapse // Bulletin of Science and Practice. Electron. magazine 2017. No. 6 (19).

P. 90 94. Access mode: http://www.bulletennauki.com/nechaikin (Date of access 06/15/2017).

22. Kazakova S. N., Apolikhina I. A., Teterina T. A., Bychkova A. E. An integrated approach to the treatment of decubital vaginal ulcer // Obstetrics and Gynecology: News. Opinions. Learning. 2022. Vol. 10. No. 1 (35). pp. 46-50. doi. org/10.33029/2303-9698-2022-10-1-46-50

23. Konoplya A.A., Petrov S.V., Gavrilyuk V.P. Correction of immune, cytokine and antioxidant status disorders in patients with chronic salpingo-oophoritis // Medical Immunology 2006, V. 8, No. 1, p. 97 100.

24. Khashukoeva A. Z., Ilyina I. Yu., Agaeva Z. A., Agaeva M. I., Khlynova S. A. Features of the correction of the immune status in the treatment of infectious and inflammatory diseases of the reproductive system // Obstetrics and Gynecology. 2019. No. 10. P. 188-193. DOI: https://dx.doi.org/10.18565/aig.2019.10.188-193

25. Sulima A. N., Puchkina G. A. Evaluation of the effectiveness of an integrated approach to the prevention of postoperative adhesions in the small pelvis // BC. Mother and child. 2021. V. 4. No. 2. S. 130-136. DOI: 10.32364/2618-8430-2021-4-2-130-136.

26. Litvinenko O. V., Korotkikh I. N. Immune and reparative therapy in the treatment of chronic endometritis in women of reproductive age // Youth Innovation Bulletin. 2019. V. 8. No. 2. P. 140-141.

27. Grigoryan A. N., Kuznetsova I. V., Zemlina N. S., Sizova N. M. The use of sodium deoxyribonucleate in the complex therapy of chronic endometritis in women with reduced fertility // Medical Alphabet. 2019. V. 1. No. 1. P. 70-74. DOI: 10.33667/2078–5631–2019–1–1(376)-70–74

28. Unanyan A. L., Sidorova I. S., Kogan E. A., Belogubova S. Yu., Demura T. A., Elisavetskaya A. M., Sizova N. M. Endometriosis, adenomyosis, chronic endometritis: Clinical and pathogenetic relationships and reproductive failures // Obstetrics and Gynecology. 2018. No. 10. P. 136-140. https://dx.doi.org/10.18565/aig.2018.10.136-140

29. Kosykh E. V., Korotkikh I. N. The role of macrophages in evaluating the effectiveness of immunotherapy for chronic endometritis // Modern Science: Actual Problems of Theory and Practice. Series: Natural and technical sciences. 2020. No. 5. P. 173-178. DOI 10.37882/2223–2966.2020.05.21

30. Yashchuk A.G., Dautova L.A., Popova E.M., Maslennikov A.V., Imelbaeva A.G. Rehabilitation of women after medical termination of non-developing pregnancy // Medical Bulletin of Bashkortostan. – 2017. – Volume 12, No. 5 (71). – P. 75-81.

DOI 10.34660/INF.2023.49.21.056

控制和停止战斗伤口大血管出血的现代方法
MODERN METHODS OF CONTROLLING AND STOPPING BLEEDING FROM LARGE VESSELS IN COMBAT WOUNDS

Reva Ivan Vladimirovich
Candidate of Medical Sciences, Associate Professor,
Federal State Autonomous Educational Institution of
Higher Education Far Eastern Federal University, Russia
PhD, International education and research center, Niigata, Japan

Hua Xiang
Shandong Qingyshan Petrochemical Con, Ltd, China

Yunqiang Zhao
Shandong Qingyshan Petrochemical Con, Ltd, China

Ilinov Alexander Vladimirovich
Assistant of the Department of Surgery
Krasnoyarsk State Medical University, Russia

Gulkov Alexander Nefedovich
Doctor of Technical Sciences, Full Professor
Far Eastern Federal University, Russia

Avtomonov Evgeniy Gennadievich
Candidate of Technical Sciences, Associate Professor
Far Eastern Federal University, Russia

Nikitina Anna Vladimirovna
Candidate of Technical Sciences, Director of the Department
of Oil and Gas Business and Petrochemistry
Far Eastern Federal University, Russia

Tsoy Inna Evgenievna
Student
Far Eastern Federal University, Russia

Reva Galina Vitalievna
Doctor of Medical Sciences, Full Professor
Far Eastern Federal University, Russia

抽象的。 肢体大血管损伤失血多见，占合并伤结构的82%，占死亡病例的17%。对使用众所周知的局部止血剂进行分析，以提高治疗受损大血管的有效性，防止与生命不相容的失血，并提出在敌对行动背景下优化现场治疗措施的建议 . 考虑了各种止血剂的缺点和优点，并提出了使用这些止血剂治疗各种定位、损伤程度、感染和考虑失血的伤口的最佳选择。

关键词：大血管、伤口、出血控制、再生、凝血、止血、伤口敷料、纤维蛋白胶。

Abstract. *Blood loss due to injury of large vessels of the extremities prevails and makes up 82% in the structure of combined injuries with 17% of deaths. An analysis was made of the use of well-known local hemostatic agents in order to increase the effectiveness of the treatment of damaged large vessels with the prevention of blood loss incompatible with life and recommendations for optimizing therapeutic measures in the field against the backdrop of hostilities. The disadvantages and advantages of various hemostatic agents are considered and the best options for the possibility of using these agents for combat wounds of various localization, degree of damage, infection and taking into account blood loss are proposed.*

Keywords: *large vessels, wounds, bleeding control, regeneration, coagulation, hemostasis, wound dressings, fibrin glue.*

Relevance

At the present stage, the number of armed clashes is increasing, accompanied by an increase in the need for high-quality medical treatment of wounds and timely stopping of bleeding from large vessels to prevent deaths. Between 2014 and 2020, more than 15 ended and ongoing armed conflicts took place around the world, with a total number of irretrievable losses in which more than 800,000 people. Despite the accumulated extensive experience in the treatment of surgical wounded, gunshot wounds are one of the most difficult problems in surgery. Not only the effectiveness of further treatment, but also the saving of the lives of fighters depends on the effectiveness of the applied therapeutic agents and methods against the background of battles and in the field. To prevent possible complications and lethality as a result of improper first aid, as well as to reduce the number of deaths in the process of transporting the wounded, it is necessary to analyze modern methods of stopping bleeding and using optimal hemostatic agents, which determined the direction of our research.

Purpose of the study

To increase the effectiveness of stopping bleeding from large vessels and suppuration of wounds with the prevention of scarring on the basis of studying the possibility of using hemostatic preparations from blood components in gunshot wounds.

Research objectives: to consider the characteristics of injuries in modern armed conflicts; identify the main methods of stopping bleeding based on the clas-

sification of antihemorrhagic drugs; consider the possibility of using fibrin glue for wounds in combat conditions.

Material and methods

The material for the study was more than 150 literature sources over the past 5 years and 150 previously published sources with a selection of the most significant works. A comparative analysis of data on outcomes in the use of various antihemorrhagic agents in the field against the background of hostilities was carried out. The results of hemorrhage arrest with the use of the most popular, effective and frequently used hemostatic materials are considered, taking into account the mechanism of their action. Based on the analysis, recommendations were developed on the use of the most effective agents, taking into account the mechanism of their effect on the blood coagulation system. A promising model of a hemostatic substance based on the patient's blood components has been developed.

Results of the study and their discussion. The aggravated situation in the world has led to the emergence of new and aggravation of pre-existing armed conflicts. The permanent production of new types of weapons and the widespread use of sabotage and terrorist activities have dramatically affected the direction and structure of military losses [1, 2].

One of the most important courses in changing the properties of combat injuries in modern warfare is an increase in the number of combined injuries, mainly of the upper and lower extremities, by 80% with damage to large blood vessels, bones and joints. The most important goals of the treatment of gunshot wounds are: reducing the frequency of purulent complications, reducing the duration of treatment and reducing the disability of the wounded. The main ways to solve this problem are to optimize the timing and volume of surgical treatment, reduce necrobiotic processes, enhance the immunological status and regenerative capabilities of local wound tissues [3, 4, 5].

In addition, 10-15% of all battlefield deaths are due to limb hemorrhage [6]. Tourniquets and compression bandages are currently the main methods for stopping bleeding from the extremities [4]. In the modern world, hemostatic implants are the most popular [7]. Since their action is targeted, they can be used for different types of bleeding, and in this regard, they are in increasing demand. Each antihemorrhagic material has both positive and negative sides, but the main role of all used local hemostatic implants is to create and accelerate the artificial stages of the natural formation of a blood clot and, subsequently, a thrombus (hemostasis), as well as to obtain a fibrin clot, bypassing stages of hemostasis [8]. According to the mechanism of action, all antihemorrhagic agents are divided into 3 main classes: clotting factor concentrators (QuikClot, QuikClot ACS +, Hemostop, WoundStat, TraumaDex, Self-expanding haemostatic polymer); mucoadhesive agents (Hemcon, Chitoflex, Celox, Rapid Deployable Hemostat (RDH) dressing, mod-

ified RDH (mRDH), Syvek Patch, Syvek NT, InstaClot, BloodStop, Super Quick Relief (SuperQR), Minisponges Dressing) [7]; procoagulant agents (Dry Fibrin Sealant Dressing (DFSD), FastAct, TachoComb, CombatGauze, X-Sponge).

Hemostatic substances of these groups have some similarities - high porosity and ability to absorb the liquid part of the blood. This contributes to an increase in its viscosity, thereby accelerating the formation of a blood clot [9].

Local mucoadhesive hemostatics (LHAs) act in a directed manner, they are characterized by strong adhesion to tissues, their scope is extensive, they can be used both in damage to large vessels and in diffuse bleeding, mechanically sealing a bleeding wound. Popular today are “mucoadhesive agents”: chitosan, amylopectin, as well as “coagulation factor concentrators” are zeolites and kaolin [10, 11]. MGS based on chitosan and kaolin in the form of dressings treated with a thromboforming agent, for example, artificial platelets or other coagulation factors, are considered to be the most effective. HemCon has long been a pioneer in battlefield and pre-hospital hemostasis medicines. Tricol, Biomedical, HemCon products are composed of biotechnologies that promote rapid adhesion to damaged tissue and provide a snug fit. In 2001, HemCon partnered with the US Army to develop a hemostatic bandage that was designed to save the lives of soldiers with traumatic injuries. HemCon introduced Chito+ deacetylated chitosan placed on a sterile foam pad. Chitosan is more than 75% deacetylated chitin, composed of a biodegradable polymer of N-acetyl glucasamine derived from marine arthropod shells. Chitosan products have a positive molecular charge that attracts negatively charged red blood cells like a magnet. Upon contact with negatively charged erythrocytes, the chitosan salt quickly cross-links. Red blood cells are attracted to the dressing, forming a tight clot over the wound. This process takes place separately from the natural clotting cascade when the body forms its own blood clot due to injury. Chitosan bandages also provide an antibacterial barrier that keeps a wide variety of bacteria out of the tight seal. This explains the main hemostatic effect of HemCon [8].Dry Fibrin Sealant Dressing (DFSD) is a dry fibrin sealing dressing, a two-component material consisting of fibrinogen and thrombin. In the presence of small amounts of calcium and factor XIII, thrombin converts fibrinogen to insoluble fibrin, the final stable form of the agent. Fibrin sealant has been developed and used for more than a hundred years. It is the only commercially available material approved by the FDA for clinical use in all three of these groups: hemostatics, sealants, and adhesives. The sealant creates a sealing barrier that prevents gas or liquid from escaping from the structure. It polymerizes on its own and is often most effective in dry conditions. Both sealants and adhesives, when applied to potentially leaking blood vessels, can have a hemostatic effect by blocking holes in the vessel and preventing bleeding, but they do not necessarily cause blood clotting. This hemostatic was successfully used in Iraq and Afghanistan, however, due

to the high cost, it was replaced by such hemostatics as QuickClot and HemCon (100 and 10 times more expensive and cheaper, respectively) [12].

QuickClot is a comprehensive tool for the control and prevention of bleeding, the main component is a special inert mineral Kaolin, which has a huge hemostatic power. The Quikclot Combat Gauze Z-fold is a fast acting combat bandage designed with the needs of combat and tactical medical personnel in mind. Translated, it means "Quicklot-combat-bandage", or "bandage for use in battle." This hemostatic dressing combines surgical gauze folded with an accordion and impregnated with a proprietary inorganic material to provide three important benefits. It stops blood flow, is inert and does not cause allergies, and is also easily removed after blood clotting. The Tactical Combat Care Committee recently recommended Combat Gauze as a first line hemostatic agent. The first experimental confirmation of its effectiveness led to its adoption for supply in the armed forces.

Vivostat® is an advanced tissue sealant based on autologous coagulation factors that does not require additional thrombin components. Vivostat fibrin sealant is developed from the patient's own blood and therefore offers excellent biocompatibility. Vivostat Fibrin Sealant does not contain exogenous thrombin or bovine components. This system has its own additional set of consumables, as well as a special mixing mode. Before the start of the operation, whole blood is taken from the patient, which is placed in a specially designated sterile container, where a special cartridge with a buffer solution is inserted. The prepared mixture is then loaded into the Vivostat system and fibrin glue production begins. At the end of this step, the adhesive is ready to use with separate nozzles that deliver it as a spray.

The main disadvantages of this method, in our opinion, are the inability to stop bleeding from the larger arteries of the renal parenchyma and the high cost of the drug. In addition, when using fibrin glue in the form of an aerosol, pulmonary embolism may occur. In addition, the autologous nature of Vivostat effectively eliminates the risks of exposure to contaminants carried by cattle or humans. This is the only way to protect the patient from viral diseases that have not yet been identified [10]. Clinical studies and comparative studies have shown that Vivostat ® Fibrin Sealant is superior to conventional fibrin sealants in such important parameters as hemostasis time, elasticity, adhesion to tissue and effect on tissue [13-16].

Conclusion

The problem of stopping extensive bleeding from combat wounds is still relevant. This is associated with wound suppuration, wound infections, as well as hyperregeneration and the formation of keloid scars. The main modern approach to stop bleeding in combat wounds is the imposition of tourniquets and bandages. In addition to mechanical methods of stopping blood, biological hemostatic agents are also used. Despite the fact that today there is a wide range of different hemostatic agents, they have their drawbacks. It is required to create modern,

high-tech and pathogenetically substantiated, more advanced hemostatic agents that do not have serious side effects. Their wide application in practice, of course, will improve the quality of pre-hospital care, reduce the frequency of disability and reduce the number of cases of mortality among the wounded. Given the high efficiency of stopping bleeding with hemostatic agents from blood components already used in surgery, but having a number of drawbacks, there is a need to study and improve them to address the issue of the possibility of using these agents in combat wounds.

References

1. Fox, C. J. Update on Wartime Vascular Injury / C. J. Fox, B. Patel, W. D. Clouse // Perspectives in Vascular Surgery and Endovascular Therapy. – 2011. № 23 (1). – 13-25 p.

2. Smith S., White J., Wanis K.N., Beckett A., McAlister V.C., Hilsden R. The effectiveness of junctional tourniquets: A systematic review and meta-analysis. J Trauma Acute Care Surg. 2019 Mar;86(3):532-539. doi: 10.1097/TA.0000000000002159.

3. Pipinos II., Patel K.P., Wadman M.C., Li Y.L. A comparison of acute mouse hindlimb injuries between tourniquet- and femoral artery ligation-induced ischemia-reperfusion. Injury. 2021 Nov;52(11):3217-3226. doi: 10.1016/j.injury.2021.09.002.

4. Goralnick E, Ezeibe C, Chaudhary MA, McCarty J, Herrera-Escobar JP, Andriotti T, de Jager E, Ospina-Delgado D, Goolsby C, Hunt R, Weissman JS, Haider A, Jacobs L; Stop the Bleed National Research Agenda Consensus Conference Working Group; Andrade E, Brown J, Bulger EM, Butler FK, Callaway D, Caterson EJ, Choudhry NK, Davis MR, Eastman A, Eastridge BJ, Epstein JL, Evans CL, Gausche-Hill M, Gestring ML, Goldberg SA, Hanfling D, Holcomb JB, Jonson CO, King DR, Kivlehan S, Kotwal RS, Krohmer JR, Levy-Carrick N, Levy M, Meléndez Lugo JJ, Mooney DP, Neal MD, Niskanen R, O'Neill P, Park H, Pons PT, Prytz E, Rasmussen TE, Remley MA, Riviello R, Salim A, Shackelfold S, Smith ER, Stewart RM, Swaroop M, Ward K, Uribe-Leitz T, Jarman MP, Ortega G. Defining a Research Agenda for Layperson Prehospital Hemorrhage Control: A Consensus Statement. JAMA Netw Open. 2020 Jul 1;3(7):e209393. doi: 10.1001/jamanetworkopen.2020.9393.

5. Szul, A. C., Davis B.. Emergency war surgery. - 3rd U.S. revision. – Washington: Borden Institute Walter Reed Army Medical Center, 2004. – 488 p.

6. Lawton, G. Novel haemostatic dressings / G. Lawton, J. Granville-Chapman, P. J. Parker // J. R. Army Med. Corps. – 2009. - № 155 (4). - 309-314 p.

7. Mueller, G.R. A novel sponge-based wound stasis dressing to treat lethal noncompressible hemorrhage / G.R. Mueller, T. J. Pineda, H.X. Xie. J. S. Teach, A. D. Barofsky, J. R. Schmid, K. W. Gregory // J. Trauma Acute Care Surg. – 2012. - № 73 (2). – 134-139 p.

8. Pozza, M. Celox (chitosan) for haemostasis in massive traumatic bleeding: experience in Afghanistan / M. Pozza, R. W. J. Millner // Eur. J. Emerg. Med. – 2011. - № 18 (1). - 31-33 p.

9. Spotnitz, W. D. Fibrin sealant: past, present, and future: a brief review / W. D. Spotnitz // World journal of surgery. – 2010. - № 34 (4). – 632-634 p.

10.Jie Li. Topical use of topical fibrin sealant can reduce the need for transfusion, total blood loss and the volume of drainage in total knee and hip arthroplasty: A systematic review and meta-analysis of 1489 patients / Jie Li, Hong-Biao Li, Xi-Cheng Zhai, Qin-Lei, Xin-Qiang, Zhen-Hua Zhang // International journal of surgery. – 2016. - № 36 (Pt A). – 127-137p.

11.Kraus, T. W. Scientific evidence for application of topical hemostats, tissue glues, and sealants in hepatobiliary surgery / T. W. Kraus, A. Mehrabi, P. Schemmer, A. Kashfi, P. Berberat, M. W. Büchler // Journal of the American College of Surgeons. – 2005. - № 200(3). - 418–427 p.

12.Hardean E., Achneck. A comprehensive review of topical hemostatic agents: efficacy and recommendations for use / Hardean E Achneck, Bantayehu Sileshi, Ryan M Jamiolkowski, David M Albala, Mark L Shapiro, Jeffrey H Lawson // Ann Surg . - 2010. - №251 (2). - 217-228 p.

13.Hua Xie. Use of a chitosan-based hemostatic dressing in laparoscopic partial nephrectomy / Hua Xie, Yashodhan S Khajanchee, Jeffrey S Teach, Brian S Shaffer // J Biomed Mater Res B Appl Biomater . - 2008. - №85 (1). - 267-271 p.

14.Hidas, G. Sutureless nephron-sparing surgery: use of albumin glutaraldehyde tissue adhesive (BioGlue) / G Hidas, A Kastin, M Mullerad, J Shental, B Moskovitz, O Nativ // Urology. - 2006. - №67 (4). - 697-700 p.

15.Cox E.D., Schreiber M.A. McManus J., Wade C.E., Holcomb J.B. New hemostatic agents in the combat setting. Transfusion. 2009 Dec;49 Suppl 5:248S-55S. doi: 10.1111/j.1537-2995.2008.01988.x.

16.Wang, J., Zhang H., Wang J., Pan F., Zhang H., Luo J., Guo C., Li K., Li T. Efficacy of New Zeolite-Based Hemostatic Gauze in a Gunshot Model of Junctional Femoral Artery Hemorrhage in Swine. J. Surg Res. 2021 Jul;263:176-185. doi: 10.1016/j.jss.2020.12.040.

DOI 10.34660/INF.2023.86.72.057

视觉分析器神经结构和大脑神经内分泌系统发育的危险因素
RISK FACTORS FOR THE DEVELOPMENT OF NEURAL STRUCTURES OF THE VISUAL ANALYZER AND THE NEUROENDOCRINE SYSTEM OF THE BRAIN

Mogilevskaya Ekaterina Sergeevna
Far Eastern Federal University, Senior Lecturer,
Candidate of Medical Sciences

Zhibanov Pavel Vitalievich
postgraduate
Far Eastern Federal University

Sadovaya Yana Olegovna
postgraduate
Far Eastern Federal University

Shahriar Islam
postgraduate
Far Eastern Federal University

Gorbarenko Rodion Sergeevich
postgraduate
Far Eastern Federal University
Head of the Department of Neurosurgery
Regional Clinical Hospital

Reva Galina Vitalievna
Doctor of Medical Sciences, Professor
Far Eastern Federal University
Chief Researcher
International Medical Research and Educational Center,
(Niigata, Japan).

Introduction Was conducted analysis of the relationship between the pathology of the structures of the neuroendocrine system and the organ of vision, depending on various risk factors. It is indicated that neurodegenerative processes in the brain and visual system are interconnected, dependent on the level of melatonin. This is due not only to the presence of membrane receptors for melatonin in neurons, but also to the common origin of the neuroglia of the brain, retina, trans-

parent media of the eye and epiphysis. A wide range of pharmacological effects of epiphyseal melatonin during neurodegenerative processes indicates its key role in the pathogenesis of multiple sclerosis, Huntington's disease, acute and chronic cerebral ischemia, leading to disability and being socially significant. Data on the important role of melatonin in the development of type I and II diabetes mellitus indicate its inductive role in triggering neovascularization of the transparent media of the human eye, leading to irreversible loss of visual functions. The possible common origin of the transparent structures of the human eye, brain sand and cortical neuroglia secreting crystallins with A-immunoreactivity is considered. It is indicated for the first time that the progenitor pool of stem cells involved in the formation of transparent eye media, epiphysis brain sand and cortical formations can differentiate from neuroglial migrants from the eye glass formation zone who have received a general development program. The development and proof of the concept of sources and mechanisms of development of the neuroendocrine and visual systems will serve as a fundamental platform for obtaining material using a promising inexhaustible source for cell transplantation not only in neurosurgery, ophthalmology, endocrinology, but also oncology. **Key words:** epiphysis, neuroglia, brain sand, ischemia, stem cells, circadian rhythms, adaptation, neurodegeneration, melatonin.

Relevance. According to WHO, one of the main causes of human disability is neurodegenerative processes in the cortical formations of the brain and the organ of vision [1]. Although the death of neurons occurs for various pathogenetic reasons, as a result, progressive neurological symptoms with specific visual impairments develop. There is increasing evidence that glia plays a key role in nerve damage after hypoxia-ischemia [2]. Huntington's disease, multiple sclerosis, and cerebral ischemia are characterized by various changes in melatonin levels [3]. Ritzenthaler T., Nighoghossian N., Berthiller J. et al. (2015) believe that melatonin may have potential neuroprotective properties [4]. One of the risk factors may be shift and night work, which, according to Basler M., Jetter A., Fink D. (2014), is a risk factor for the development of ischemia of brain neurons and cardiomyocytes [5]. In these processes, the epiphysis plays an important role as a source of the hormone melatonin, the physiological significance of which has been intensively studied in recent decades. Morphological changes in the structure of the epiphysis under various external influences and their connection with the pathology of the visual system have been established. Liu X., Niu X, Feng Q., Liu Y. (2014) found that under the influence of night loads and low temperatures in laboratory animals in the experiment, there is a weak development of the Golgi complex in pinealocytes, in whose cytoplasm there are no melatonin granules [6; 7]. It should be noted that the data available in the available literature are fragmentary and do not contain generalizing information about the pathogenetic relationship between the

development of brain and retinal pathology associated with melatonin deficiency. In this regard, for the socio-economic sphere, analytical studies of the developing pathology of the visual and neuroendocrine systems against the background of circadian rhythms disorders in workers associated with shift work are of particular relevance, which determined the direction of our research. The purpose of our work was to analyze and generalize the literature data on the relationship of melatonin production disorders by the epiphysis with neurodegenerative processes in neurons of the central nervous and visual systems. The material for the study was the data available in the available literature on the relationship between the pathology of the brain and the visual system with a violation of the production of melatonin.

Material and methods. The research method consisted in analyzing data on the protective role of melatonin in neurodegenerative processes in the nervous system, endocrine pathology and carcinogenesis, especially in gerontological groups of patients, on the relationship of brain sand and the level of melatonin produced by the epiphysis.

The results of the study. Melatonin synthesized from tryptophan is a hormone secreted not only by pinealocytes, but also by peripheral glandulocytes, has a very wide range of pharmacological activity and is able to participate in the generalized protection of both the central nervous system and internal organs from damage. The epiphysis, involved in the regulation of endocrine functions in mammals, is a rudimentary third eye of lower vertebrates, which in the process of evolution plunged deep into the brain. In the process of evolution, having lost its own photoreceptor cells, the gland still retains close ties with the visual analyzer, both its peripheral and cortical parts. Through its biologically active compounds, and above all the main hormone melatonin, the pineal gland provides control over the transmission of visual potentials and participates in the realization of the physiological effects of light on organ structures. Melatonin, as one of the main hormones of the cerebral gland of the epiphysis, is widely represented not only in all structures of the eye, but mainly in the retina. It is in the retina that a high density of specific melatonin receptors is identified. The change of day and night is an inducer of the launch of many physiological processes. Violation of the light regime in the conditions of shift work is a risk factor for the development of pathology of the visual organ and the neuroendocrine system. However, studies at the present stage have been conducted in terms of studying the risks of malignancy of various parts of the reproductive system of women, the role of continuous illumination in oncogenesis. The importance of melatonin in the mechanism of neurodegeneration indicates the possibility of its use in conservative treatment both for the relief of multiple sclerosis and other pathological conditions associated with acute and chronic circulatory disorders in the central nervous system. The secretion of

melatonin by the epiphysis is carried out in accordance with the circadian rhythm during the day in connection with the temperature regime, through affiliated endogenous circadian rhythms, regulating certain physiological functions. Experimental studies on animals and at the cellular level have revealed one of the key roles of melatonin in the normalization of carbohydrate metabolism through inhibition of glucose release, which is especially important for understanding the pathogenesis of diabetes mellitus, and also confirmed the molecular genetic findings of variants of the MTNR1B melatonin receptor. The pathogenesis of diabetes mellitus is associated with G protein, which mediates the action of melatonin through MT1 receptors (in the MTNR1A format) and MT2 (encoded by MTNR1B) in higher vertebrates [8]. Kor Y., Geyikli I., Keskin M., Akan M. evidence of the main role of melatonin in the development of type I diabetes in children of younger age groups [9]. It follows from this that the low level of melatonin in children can be explained by the fact that the pineal gland in early ontogenesis does not have a level of development of the definitive epiphysis. Some authors claim the maximum level of melatonin secretion in 2-3 years. After ten years, the pineal gland secretes hormones that regulate puberty. One of the significant decreases in the function of the epiphysis occurs with the onset of menopause. This explains the frequency of strokes and cancer in women in this age group. Maślińska D., Laure-Kamionowska M., Deręgowski K., Maśliński S. (2010) adhere to the concept of the formation of brain grains in the epiphysis with secretory activity of mast cells located under the capsule perivasally along the perimeter of crystallizing structures [10]. Bulc M., Lewczuk B., Prusik M. (2010, 2013) associate the formation of sand with pineal gland cells [11; 12]. We identified brain grains of sand both in the pineal gland and in the brain tissue in the region of the bottom of the third ventricle, similar findings were described by Admassie D., Mekonnen A. (2009), who noted an increase in calcifications in the vascular plexuses of the brain with age [13]. Grases F., Costa-Bauzà A., Prieto R.M. (2010) noted a decrease in melatonin synthesis with age in patients with Alzheimer's disease, which confirms the correlation of the hormone with brain sand, as in the risk group with stroke [14]. The authors pointed out that melatonin synthesis decreases with age in all people, but the greatest decrease is observed in patients with Alzheimer's disease. This may be due to the fact that melatonin blocks the formation of beta-amyloid protein. The mechanism responsible for this decrease is not fully understood, although it is known that the pineal gland of a person calcifies with age. Calcification may lead to tissue damage. Therefore, the absence of crystallization inhibitors may be a risk factor for the development of Alzheimer's disease. Turgut A.T., Sönmez I., Cakıt B.D. (2008) found significant correlations of epiphysis calcification and degenerative processes in intervertebral discs, as well as a link with atherosclerosis of the abdominal aorta [15]. It is known that the epiphysis, as the most

important link of the neurohumoral system, participates in ensuring the regulation of the activity of many organs and systems depending on external conditions, and not only annual and daily rhythms, but also temperature indicators, the strength of the electromagnetic field, the effects of radiation. The epiphysis has close connections not only with the visual analyzer, but is also activated depending on the level of illumination. The secretory activity of the gland is associated with an increase in blood flow at night, so the important role of the gland in changing the time of sleep and wakefulness of the body is undeniable. Hormone secretion is associated with programmed death of epiphyseal neuroglyocytes, calcification of the pineal gland, dynamics of structural relations of parenchyma and brain sand. Conceptually, the same nature of the transparency of the cerebral sand of the epiphysis and the refractive media of the eye is not excluded. In lower vertebrates, pinealocytes are identical to photoreceptor cells, on this basis, many authors claim that the human epiphysis is homologous to the posterior pineal body of reptiles [16]. The grains of brain sand primarily fluoresce in ultraviolet rays, which can occur due to the presence of calcium phosphate. Blue chemiluminescence of brain grains of sand is associated with the peculiarities of metabolism, possibly due to the content of compounds of uranium isotopes, creating pathological local foci of X-ray radiation. Irregular multi-layered concentric sand structures contain both inorganic and organic components. Inorganic is mostly represented by calcium salts, including: hydroxyapatite; calcium phosphate (Ca) Ca3(PO4)2; Ca - Ca3(PO4)2 × 3OH hydrophosphate; Ca - Ca3(PO4) phosphate2 carbonatapatite CaCO3ON; calcite CaCO3. The organic component is characterized by the presence of indolamines: melatonin and serotonin, and tryptophan derivatives: 5-hydroxytryptophol, 5-methoxytryptamine, 5-methoxytryptophol, norepinephrine, adrenoglomerulotropin; peptides: arginine, vasotocin, pinoline, thyrotropin releasing factor. Brain sand not only has high strength, but also magnetic properties. According to observations in our research, brain sand is attracted to a needle or metal tools being brought. The results of phase contrast microscopy indicate the neuroglial origin of brain grains due to the blue glow. Indirect confirmation is provided by the blue glow of myelin sheaths associated with neuroglia. The transparency of the lens and the transparency of the crystals of brain sand allow not only to assume the presence of common sources of development, but also further differentiation of cells in the direction of the ability to secrete light-optically transparent tissue. It should also be noted that crystals of brain sand are also found in the brain tissue, in the hypothalamus. Research in this direction is required to find evidence of the involvement of neuroglia in the secretion of brain sand, capable of secreting crystallins and being immunoreactive to vitamin A. Thus, at the present stage, the concept of the origin of brain sand as a result of the metabolic activity of pinealocytes is the most convincing. The issue of the influence of an increase in

the amount and size of brain sand on pathological processes associated with neurodegeneration in cortical formations and the visual system, cataracts and age-related macular degeneration remains unresolved. The pineal gland affects the aging process, participates in the induction of seasonal depression and reproductive functions, has an antioxidant and antiproliferative effect, affects cellular immunity. Intimate connections of the microcirculatory bed of the epiphysis and epiphyseal sand indicate the possibility of influencing the body in a non-humoral way. Concepts based on correct ideas about the sources and mechanisms of the development of nervous and sensory systems constitute the main theoretical basis for the isolation of material with directed differentiation from pluripotent stem cells and the provision of cellular material for conservative treatment in clinical practice.

At the present stage, there is no clear understanding of the mechanisms and sources of the development of neuroendocrine organs and the human visual system, based on common origin of neuroglial migrants. Pathogenetically unjustified treatment of pathological conditions associated with the absence of induced migration of stem neuroglia, or a decrease in its functions due to gerontological problems accompanied by neurodegeneration, and, as a consequence, leading to disability, indicates the importance of research on this problem. At the present level, the issues of the formation of neuroendocrine organs and visual organs by various types of cells, as well as factors coordinating the development of the neuroendocrine and visual systems, have not been resolved. Directed migration and differentiation of neuroglia is of particular interest because of their involvement in the occurrence of associated degenerative diseases of the brain and retina associated with circadian rhythm disorders and adaptation of the body to environmental conditions. Molecular genetic advances in the study of the mechanisms of these pathologies leave unresolved questions about signals affecting the re– and expression of genes, which suggests the need to continue molecular genetic research, which has achieved high results so far only in experiments on lower vertebrates and insects. Scant data on the morphogenesis of the neuroendocrine and visual systems of humans are an obstacle to the implementation of existing results in practical healthcare. Tikhonovich M.V. et al. (2018) include factors inducing aging and pathology of these systems, changes in the secretion of macrophages, hyalocytes, Muller cells, the secretion of cytokines, chemokines and growth factors affecting proliferation [17]. Surgical treatment of cataracts, retinopathy and neovascularization of transparent eye media, age-related macular degeneration and glaucoma, neurodegenerative disorders will be developed on the basis of new data on morphogenesis in the human body. There is a connection between the pathogenesis of glaucoma and changes in neuropsychic parameters in patients, which indicates a common neurodegenerative processes in the retina, epiphysis

and cortical formations of the human brain. Data from Matteucci A. et al. (2013) on the presence of dysbindin in Muller cells, a product of the DTNBP1 gene, confirm the possible involvement of this protein in visual disturbances associated with neuropsychiatric disorders. In the retina, neurons and glia are generated from the same pool of multipotent progenitor cells [18; 19]. According to Sung P.H., Lee F.Y., Lin L.C. et al. (2017) and Liu J.Y., Chen X.X., Chen H.Y. (2018), despite the expression of the genome of stem progenitor retinal cells (RPC), under the influence of internal transcription and external factors, stem cell potencies are nevertheless preserved in Muller cells [20; 21]. Yamagami T. et al. (2014) it has been shown that, although beta-catenin/Pax6 signaling plays a crucial role in the regeneration of neuroglia, and the induction of Wnt signaling in radial glia provides intercellular interactions, it has not been practically studied in humans [22]. Jayaram H. et al. (2014) showed that stem neuroglia (hMSCs) acquires phenotypic and genotypic features of relay photoreceptors in an experiment, for the interpretation of data on the human body, there is still no clear idea of the timing of genomic expressions [23]. The concept of the development of the structures of the neuroendocrine and visual systems requires updating and correction for the correct application of new data in cellular technologies.

Conclusion A new era of treatment of socially significant pathologies of the brain and visual organ is associated with obtaining new data on migrating cambial and stem cells, establishing the nature of the sources of development and mechanisms of induction of their migration and directed differentiation. Solving the issue of the formation of transparent eye media with the identification of the role of the epiphysis in the structure and functions of the visual analyzer system will allow the development of new pathogenetically sound methods for the treatment of neurodegenerative diseases of the central nervous system and retina. Conclusion. The available scientific background of our own research and data from the available literature indicate the connection of disabling socially significant human gerontological pathology (cataracts, AMD, glaucoma, neurodegenerative disorders) with general disorders in the system of neuroendocrine organs and visual analyzer. The expression of neuroglial migrants into the zone of the forming transparent media of the human eye and epiphysis from the ectomesenchyme is accompanied by differentiation in the direction of secretion of protein S100B and crystallins. In addition, neuroglial migrants have the function of inhibiting angiogenesis. At the same time, the role, significance and functions of brain sand in the epiphysis have not been studied, numerous hypotheses about its role in the pathology of neurodegenerative processes are empirical. Nevertheless, the connection of neurodegenerative processes of various localization with a violation of melatonin synthesis by the epiphysis has been established. Methods of treatment of neurodegenerative diseases based on cellular technologies are still at the development stage and re-

quire improvement of neuroprotection based on real pathogenetic mechanisms of interrelated processes in the structures of the epiphysis, the organ of vision and cortical formations of the brain. Conclusions. The analysis of the available data indicates the common origin of the neuroglia of the transparent structures of the peripheral part of the visual analyzer, cortical formations of the human brain and pinealocytes of the epiphysis. The current state of the neuroprotection problem dictates the need to continue a comprehensive study of these issues for a deeper understanding of the cause-and-effect relationships between cellular interactions in the neural structures of the visual analyzer and the neuroendocrine system of the human brain.

Reference

1. Jiang S., Li T., Ji T., Yi W., Yang Z., Wang S., Yang Y., Gu C. AMPK: Potential Therapeutic Target for Ischemic Stroke. Theranostics. 2018 Aug 10. no.8(16). P.4535-4551. DOI: 10.7150/thno.25674.

2. Galinsky R., Davidson J.O., Dean J.M., Green C.R., Bennet L., Gunn A.J. Glia and hemichannels: key mediators of perinatal encephalopathy. Neural Regen Res. 2018 Feb. no.13(2). P. 181-189.

3. Paredes S.D., Rancan L., Kireev R., González A., Louzao P., González P., Rodríguez-Bobada C., García C., Vara E., Tresguerres J.A. Melatonin Counteracts at a Transcriptional Level the Inflammatory and Apoptotic Response Secondary to Ischemic Brain Injury Induced by Middle Cerebral Artery Blockade in Aging Rats. Biores Open Access. 2015 Oct 1. no.4(1). P. 407-416.

4. Ritzenthaler T., Nighoghossian N., Berthiller J., Schott A.M., Cho T.H., Derex L., Brun J., Trouillas P., Claustrat B. Nocturnal urine melatonin and 6-sulphatoxymelatonin excretion at the acute stage of ischaemic stroke. J. Pineal Res. 2009. Apr. no.46(3). P. 349-352.

5. Basler M., Jetter A., Fink D., Seifert B., Kullak-Ublick G.A., Trojan A. Urinary excretion of melatonin and association with breast cancer: meta-analysis and review of the literature. Breast Care (Basel). 2014 Jul. no.9(3). P. 182-187.

6. Liu X., Niu X., Feng Q., Liu Y. Effect of temperature on the pineal gland cell in rats. Chin. Med. J. (Engl). 2014. V.127(17). P.3134.

7. Liu X., Niu X., Feng Q., Liu Y. Effects of five-element music therapy on elderly people with seasonal affective disorder in a Chinese nursing home. J. Tradit. Chin. Med. 2014 Apr. no.34(2). P. 159-161.

8. She M., Laudon M., Yin W. Melatonin receptors in diabetes: a potential new therapeutical target? Eur. J. Pharmacol. 2014. Dec. 5. no.744. P. 220-3. DOI: 10.1016/j.ejphar.2014.08.012.

9. Kor Y., Geyikli I., Keskin M., Akan M. Preliminary study: Evaluation of melatonin secretion in children and adolescents with type 1 diabetes mellitus. Indian J. Endocrinol. Metab. 2014. Jul. no.18(4). P. 565-8.

10. Maślińska D., Laure-Kamionowska M., Deręgowski K., Maśliński S.. Association of mast cells with calcification in the human pineal gland. Folia Neuropathol. 2010. no.48(4). P. 276-82.

11. Bulc M., Lewczuk B., Prusik M., Gugołek A., Przybylska-Gornowicz B. Calcium concrements in the pineal gland of the Arctic fox (Vulpes lagopus) and their relationship to pinealocytes, glial cells and type I and III collagen fibers. Pol. J. Vet. Sci. 2010. no.13(2). P. 269-78.

12. Bulc M., Lewczuk B., Prusik M., Całka J. The foetal pig pineal gland is richly innervated by nerve fibres containing catecholamine-synthesizing enzymes, neuropeptide Y (NPY) and C-terminal flanking peptide of NPY, but it does not secrete melatonin. Histol. Histopathol. 2013. May. no.28(5). P. 633-46. DOI: 10.14670/HH-28.633.

13. Admassie D., Mekonnen A. Incidence of normal pineal and chroids plexus calcification on brain CT (computerized tomography) at Tikur Anbessa Teaching Hospital Addis Ababa, Ethiopia. Ethiop Med. J. 2009. Jan. no.47(1). P. 55-60.

14. Grases F., Costa-Bauzà A., Prieto R.M. A potential role for crystallization inhibitors in treatment of Alzheimer's disease. Med. Hypotheses. 2010. Jan no.74(1). P. 118-9.

15. Turgut A.T., Sönmez I., Cakıt B.D., Koşar P., Koşar U. Pineal gland calcification, lumbar intervertebral disc degeneration and abdominal aorta calcifying atherosclerosis correlate in low back pain subjects: A cross-sectional observational CT study. Pathophysiology. 2008. Jun no.15(1). P.31-9.

16. Santee H. Anatomy of the Brain and Spinal Cord. Philadelphia. P. Blakiston's son & co.2007. P.1-32.

17. Tikhonovich M.V., Erdiakov A.K., Gavrilova S.A. Nonsteroid anti-inflammatory therapy suppresses the development of proliferative vitreoretinopathy more effectively than a steroid one. Int. Ophthalmol. 2018. Aug. no.38(4). P. 1365-1378.

18. Matteucci A., Gaddini L., Villa M., Varano M., Parravano M., Monteleone V., Cavallo F., Leo L., Mallozzi C., Malchiodi-Albedi F., Pricci F. Neuroprotection by rat Müller glia against high glucoseinduced neurodegeneration through a mechanism involving ERK1/2 activation. Exp. Eye Res. 2014. Aug. no.125. P. 20-29.

19. Matteucci A., Gaddini L., Villa M., Varano M., Parravano M., Monteleone V., Cavallo F., Leo L., Mallozzi C., Malchiodi-Albedi F., Pricci F., .Matteucci A., Gaddini L., Macchia G., et al. Developmental expression of dysbindin in Muller cells of rat retina. Exp. Eye Res. 2013. V. 116. P. 1- 8.

20. Liu J.Y., Chen X.X., Chen H.Y., Shi J., Leung G.P., Tang S.C., Lao L.X., Yip H.K., Lee K.F., Sze S.C., Zhang Z.J., Zhang K.Y. Downregulation of Aquaporin 9 Exacerbates Beta-amyloid-induced Neurotoxicity in Alzheimer's Disease Models In vitro and In vivo. Neuroscience. 2018. Sep no.26. pii: S0306-4522(18)30614-6.

21. Sung P.H., Lee F.Y., Lin L.C., Chen K.H., Lin H.S., Shao P.L., Li Y.C., Chen Y.L., Lin K.C., Yuen C.M., Chang H.W., Lee M.S., Yip H.K. Melatonin attenuated brain death tissue extract-induced cardiac damage by suppressing DAMP signaling. Oncotarget. 2017. Dec. 12. no.9(3). P. 3531-3548.

22. Gan Q., Lee A., Suzuki R., Yamagami T., Stokes A., Nguyen B.C., Pleasure D., Wang J., Chen H.W., Zhou C.J. Pax6 mediates ß-catenin signaling for self-renewal and neurogenesis by neocortical radial glial stem cells. Stem Cells. 2014. Vol. 32(1). P. 45-58.

23. Jayaram H., Jones M.F., Eastlake K., Cottrill P.B., Becker S., Wiseman J., Khaw P.T., Limb G.A. Transplantation of photoreceptors derived from human Muller glia restore rod function in the P23H rat. Stem. Cells Transl. Med. 2014. Vol. 3(3). P. 323-333.

DOI 10.34660/INF.2023.79.71.058
UDC 616–03. 612.8.04

基于显性 A.A. 学说的安慰剂的医疗效果机制 乌赫托姆斯基

MECHANISMS OF MEDICAL EFFECTS OF PLACEBO BASED ON THE DOCTRINE OF THE DOMINANT A.A. UKHTOMSKY

Ananiev Vladimir Nikolaevich
Doctor of Medical Sciences, Full Professor
SSC of the Russian Federation "Institute of Biomedical Problems of the RAS", Moscow

Prokopyev Nikolay Yakovlevich
Doctor of Medical Sciences, Full Professor
Tyumen State University, Tyumen

Ananieva Olga Vasilievna
Doctor of Medical Sciences, Full Professor
Tyumen State Medical University, Tyumen

Gurtovoy Elisey Sergeevich
Student
Tyumen State Medical University, Tyumen

抽象的。 从生理学的角度来看，安慰剂效应给现代医学带来了一定的问题，因为在某些情况下，即使是完善的治疗方法也无法解释安慰剂的作用。 我们从主流院士 A.A. 的生理学说的角度分析了安慰剂效应。 乌赫托姆斯基。 结果表明，安慰剂通常代表具有所有特性的主导因素，因此，使用 A.A. 院士的教导。 Ukhtomsky 关于占主导地位，从生理学的角度预测和解释各种安慰剂效应要有效得多。 我们已经证明，安慰剂效应的生理作用机制是通过治疗显性的形成来进行的。 我们首次表明，安慰剂效应的生理机制具有一阶条件反射的特性，并且对应于 I.P. 院士教导的所有参数。 巴甫洛夫关于条件反射和有机结构适合治疗的主导地位。 研究结果表明，安慰剂药物的使用通过院士 P.K. 现实的预期反映功能系统起作用。 Anokhin，它允许主导治疗提前采取行动，提高主导治疗的有效性。

该研究使概括人类疾病中安慰剂效应的各种表现成为可能，并表明安慰剂中优势的形成非常适合各种病理学中正常和病理生理学的经典机制。

关键词：安慰剂，药效，显性 A.A. Ukhtomsky，安慰剂应用的生理机制。

Abstract. *From a physiological point of view, the placebo effect poses a certain problem for modern medicine, since even well-developed methods of treatment, in some cases, due to placebo cannot be explained. We have analyzed the placebo effect from the point of view of the physiological doctrine of the dominant*

academician A.A. Ukhtomsky. It is shown that often the placebo represents the dominant with all its properties, therefore, using the teachings of Academician A.A. Ukhtomsky about the dominant, it is much more effective from the point of view of physiology to predict and explain the various placebo effects. We have proved that the physiological mechanism of action of the placebo effect is carried out through the formation of a treatment dominant. We have shown for the first time that the physiological mechanism of the placebo effect has the property of a conditioned reflex of the first order and corresponds to all the parameters of the teachings of Academician I.P. Pavlov about conditioned reflexes and organically structurally fits into the dominant of treatment. The results of the study showed that the use of placebo drugs acts through the functional system of anticipatory reflection of reality of Academician P.K. Anokhin, which allows the treatment dominant to act ahead of the curve, improving the effectiveness of the treatment dominant.

The study made it possible to generalize the various manifestations of the placebo effect in human diseases and show that the formation of a dominant in placebo fits well into the classical mechanisms of normal and pathological physiology in various pathologies.

Keywords: *placebo, drug effect, dominant A.A. Ukhtomsky, physiological mechanisms of placebo application.*

Relevance. Evaluation of the patient's communication with the doctor should be focused on the patient's opinion, which allows building a harmonious relationship between them [8, 13, 15, 31]. Moreover, focusing on empathic care to enhance physician empathy will make communication with the physician more effective and efficient [12, 18, 28, 33, 56, 68].

Today we note with gratitude that throughout the history of the development of civilization, the great Greek and Byzantine doctors of the past - Hippocrates, Erasistratus, Herophilus, Praxagoras of Kos, Oribasius, Euryphon of Cnidus, Aetius of Amidia, Paul of Aegina and others, made a great contribution to the development of medical science [32]. By today's standards, they used very strange and bizarre methods of treating the sick and injured, because they had very poor knowledge in the field of human anatomy and physiology [25, 50].

As anatomical and physiological descriptions of the human body began to emerge over time, the need for a scientific explanation for many treatments became a pressing concern for physicians and the entire scientific medical community. An important historical period during which scientific skepticism arose about the effectiveness of certain medical remedies dates back to the second half of the 18th century and includes such treatments as mesmerism, Perkinism and homeopathy.

For example, the German physician and Enlightenment astrologer Franz Anton Mesmer (1734-1815) hypothesized that some people have “magical magnetism” and are able to radiate telepathic energy.

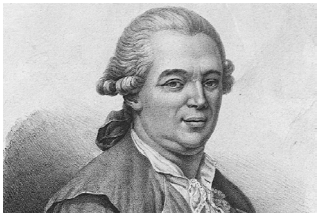

Figure1. *Franz Anton Mesmer.*

F. A. Mesmer believed that there are gravitational waves that emanate from the planets in the form of an invisible and elusive gas and fill the universe. These waves permeate the atmosphere and affect everything on earth. According to his theory, the power of magnetism is inherent in some people who can transmit it not only over distances, but also revive and even kill living beings.

As for homeopathy, the issue of its use in clinical practice, including from a legal point of view, has been causing various disputes and doubts for a long time [10, 11, 34, 44]. It should be noted that in Russia homeopathy has become quite widespread, as evidenced by the opening of the first homeopathic pharmacy on August 23, 1834 in St. The new pharmacy was consecrated by Father John of Kronstadt, who during the opening said: “Your method is the most reasonable and true. Divine wisdom itself has not found a surer means to heal mankind indignant with sin and innumerable diseases, as the healing of like with like.

In 1866 the company Dr. Willmar Schwabe for the production of phytopreparations, and in 1867 his monograph “Guidelines for the manufacture of homeopathic medicines” was published.

Figure 2. *Willmar Schwabe.*

Homeopathy as a medical system of treatment was created by the German professor at the University of Leipzig, Christian Friedrich Samuel Hahnemann (1755-1843) in 1796.

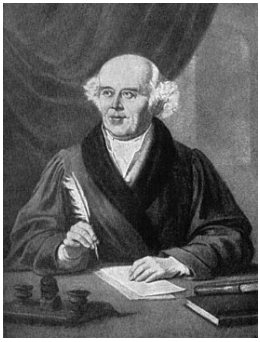

Figure 3. *Christian Friedrich Samuel Hahnemann.*

It should be noted that throughout the development of homeopathy, up to the present day, heated debates between supporters and opponents of this method of treatment have not ceased.

In 1995, the order of the Ministry of Health and Medical Industry of the Russian Federation No. 335 dated November 29, 1995 "On the use of the homeopathic method in practical health care" was issued, allowing the use of the homeopathic method of treatment in practical health care. Thus, federal legislative acts do not interfere with the activities of a doctor using a homeopathic method of treatment.

Concerning the placebo, we note that for the first time in 1955, the placebo effect was described in the article «Powerful Placebo» by the American professor at Harvard Medical School, physician Henry Knowles Beecher (1904 - 1976).

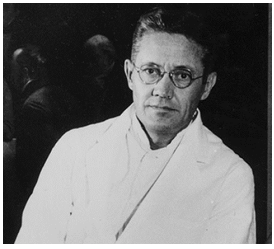

Figure 4. *Henry Beecher.*

During World War II, as an anesthesiologist, Henry Beecher treated American infantrymen who suffered from the bombing of the German army. When the

morphine supply ran out, the patient was given an injection of saline, which relieved the pain. He also found that about a third of patients recover from the use of empty pills that do not contain any active drugs in their composition. Let's note that this article was not the first to introduce the idea of the «placebo effect». The term placebo was first used by T.C. Graves in 1920 in The Lancet. On June 16, 1966, in the New England Journal of Medicine, he published an article «Ethics and Clinical Research» in which he drew attention to 22 examples of unethical clinical research that endangered the lives of patients, thus laying the foundation for human research. Beecher's 1955 article «*The Powerful Placebo*» was not the first to introduce the idea of the placebo effect. In his 1955 article, Beecher speaks of placebo effects only in special cases when he contrasts them with drug effects.

Briefly touching on history, we note that since 1940 in the medical literature it is indicated that the mention of placebo is noted in more than 100 thousand articles. Ignorance of the placebo effect is now no longer acceptable, and that research into the use of placebo in clinical practice should not only continue but be improved [1, 9, 27, 35, 42, 43, 46, 47, 53, 72].

A number of authors believe that the placebo effect goes far beyond the traditionally prescribed therapeutic context, and its study contributes to understanding the nature of mental functions and is useful for specialists in various fields, including psychologists and educators [16].

The use of the word «placebo», which is Latin for «I will be glad» in clinical research, has evolved gradually over time to refer to a control group that receives a sham treatment, as has been done with sham mesmerism, dummy sticks in Perkinism, and sham homeopathy. Therefore, the word «pretense» was gradually replaced by the word «placebo». Another important point that was critical to the modern use of placebos in clinical trials was the growing awareness that even physicians and clinical researchers are subject to imagination and prejudice. This led to the use of a double-blind method in which neither the investigator nor the patient knew the nature of the therapy being tested [50].

Today, the placebo effect, or reaction, is an excellent model for understanding how the brain works. Placebos have been used not only to confirm the effectiveness of therapy, but also traditionally as an example of a powerful interaction between mind and body. For example, in mesmerism and Perkinism, the main conclusion was that the imagination played an important role in the therapeutic outcome, thereby emphasizing the important role of the mind in the modulation of a number of physiological functions. Following this psychological perspective on the placebo phenomenon, the concept of the placebo has made its way into the psychological literature over the years [16, 50].

To date, placebo effects and placebo response data have been obtained, which can be viewed from several internal and external points of view. Internal factors

can influence the patient and the researcher. Patient expectations and previous experience are considered to be the two main intrinsic factors that determine placebo response. Other determinants of a patient include the neural systems under treatment, situational factors and responses to the environment, and personality traits.

Placebo responses include personality factors such as empathy, perceived experience, clinical relationship with the patient, and the physician's belief in the effectiveness of the treatment, as well as the patient's belief in the treating physician. The French philosopher and writer Michel de Montaigne (1533-1592) noted in 1572: «There are people who are affected simply by the look of a doctor.»

Figure 5. *Michel de Montaigne.*

External determinants include the type of study design, advertising or cultural influences. These determinants do not act in isolation, but rather form a complex interaction that ultimately influences the promotion or suppression of the placebo effect in clinical and research settings [49].

Current learning theories suggest that conditioning relies heavily on the processing of prediction errors signaling a discrepancy between expected and observed outcomes. This line of research provides a framework with which to reconcile the classical theories of placebo effects, expectancy, and conditioning. Brain regions associated with prediction error processing (anterior cingulate cortex, orbitofrontal cortex, or nucleus accumbens) overlap with regions involved in placebo effects. The possibility that the magnitude of objective neurochemical responses to placebo administration will depend on individual comparisons of expected efficacy is considered. Comparison of expectations and outcomes emerges as a cognitive mechanism that, in addition to associations with reward, seems to contribute to the formation of the stability of the body's responses to placebo [63]. Thus, in particular, it has been established that patients with rheumatoid osteoarthritis respond better to treatment aimed at both peripheral and central pain disorders [17, 24, 54, 65, 66, 70, 73].

When choosing a treatment, one should not forget that many drugs are expensive [58, 62, 67].

Physicians have received evidence from clinical research in cardiology that the placebo effect is a clinical benefit resulting from interactions with caregivers and the healthcare system in the absence of bioactive intervention, and has been used successfully for millennia. The placebo response is the result of the interplay of psychosocial mechanisms, human attitudes and prejudices operating in certain neuroanatomical locations, with known genes and neurotransmitters. This occurs with or without the administration of an inactive substance. The placebo effect results from the activation of opioid, cannabinoid, and dopaminergic pathways involved in reward, anticipation, conditioning, and pain modulation. Eleven specific anatomical features of the brain identified using positron emission tomography and magnetic resonance imaging are involved. Polymorphisms in the structural genes for catecholamine-O-methyltransferase and fatty acid amide oxidase significantly influence placebo response. The placebo effect may be important for symptom suppression in angina pectoris, paroxysmal atrial fibrillation, and congestive heart failure. In the absence of deliberate deception, there are no ethical issues and, given its effectiveness, it is time to think about how best to use placebo in clinical practice [64].

Physicians' analysis of placebo mechanisms has shown that patients develop expectations as a result of treatment and this has a significant impact on what we actually experience. Anticipation has been identified as a key process underlying the placebo effect. Both laboratory and clinical studies consistently show that when people take a pharmacologically inert substance (placebo) but believe it to be the active substance, they experience both the subjective sensations and the physiological effects expected from that active substance. substances. Expectation also plays an important role in the response to «real» treatment. These data suggest that physicians can not only increase the effectiveness of treatments by promoting positive patient expectations [52], but also their resistance to drug exposure [48, 59, 60, 66, 69, 71].

In a placebo study in psychiatry, there was little effect in studies of psychiatric disorders, both in general and for those who received sham psychotherapy. This effect has been observed in patients with anxiety or depression, but not in the treatment of schizophrenia [14, 22, 45, 61].

An analysis of the literature has shown that the mechanisms of placebo action have not yet been sufficiently studied, although a large practical clinical material has been accumulated, proving that the placebo effect really exists [19, 21, 51, 55, 57].

Since the mechanisms of placebo from the point of view of modern science are multifaceted and have not yet been studied enough, we decided [2, 3, 4, 5, 6, 38, 39, 40, 41] to study the effect of placebo from the point of view of academician A.A. Ukhtomsky [36, 37], which can generalize into one concept all the effects of placebo on the human body.

The purpose of the study: to identify the effect of the placebo effect as a physiological mechanism for the functioning of the dominant Academician A.A. Ukhtomsky.

Research methods. The great Russian physiologist Aleksey Alekseevich Ukhtomsky (1875–1942) entered the history of physiology and psychology as the author of the doctrine of the dominant, the fundamental aspect of human behavior.

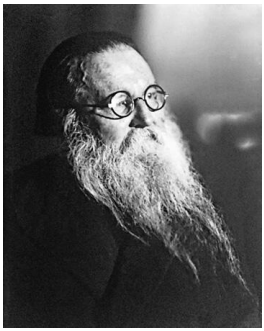

Figure 6. *Alexey Alekseevich Ukhtomsky.*

Let us list the main properties of the dominant focus, established by A.A. Ukhtomsky: increased excitability, inertia in time, the ability to summarize external stimuli, the external expression of the dominant is a stationary work or a working posture of the body.

This article was written by us on the basis of a generalization of the literature on the effects of placebo action and the work of the physiologist Academician A.A. Ukhtomsky about the dominant, as well as the study of the so-called. «food» dominant in male students. The dominant is a huge mobile association of nerve cells, the final activity of which is aimed at achieving some physiological modality (any goal, for example, an unconditioned food reflex) [5, 6]. When the goal is reached, the dominant disappears and makes room for a new dominant, as a result of which a narrowly directed concentrated nervous energy is released for the body to achieve various other goals. The main property of the dominant is the capture of motor pathways to the muscles in its subordination, which is easily explained by the need to move for the implementation of the dominant. In many cases, it is by motor activity that we can determine whether there is a dominant and which one, or not.

In 12 adolescent students, we performed a food dominant, which consisted in the study of Ph saliva before and after eating a slice of lemon. It is well known that the reaction of saliva is slightly alkaline, and its Ph is the most important indicator of oral homeostasis. Due to the fact that pH of saliva during the day ranges from

6.2 to 7.5, we studied the food dominant in the morning in the range from 9 to 11 hours two hours after eating. We took into account that in the morning the pH of saliva is lower than in the evening.

The study complied with the principles of voluntariness, individual rights and freedoms, guaranteed by Articles 21 and 22 of the Constitution of the Russian Federation, as well as the Order of the Ministry of Health and Social Development of Russia No. 774n dated August 31, 2010 «On the Ethics Council». The study was conducted in compliance with the ethical standards set forth in the Declaration of Helsinki and the Directives of the European Community (8/609EC) and the informed oral consent of the students.

Research results and discussion of the obtained data.

It was established that Ph of saliva in the young men we surveyed 19.4 ± 0.7 years old for the period from 9 to 11 hours before eating a lemon slice ranged from 6.4 to 7.7. Ph values of saliva in 2 students were 6.5; 3 - 6.7; 3 - 6.8; 1 - 7.0; 2 - 7.3; in 1 - 7.4 (Fig. 7).

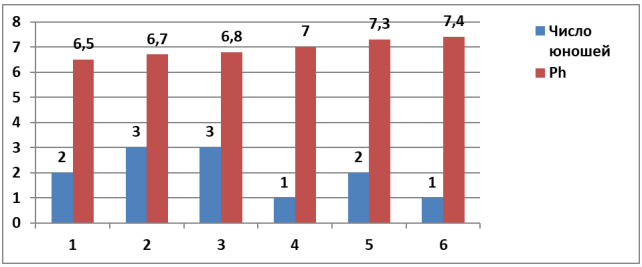

Figure 7. *Ph value of saliva in adolescent students before drinking lemon.*

5 minutes after eating a lemon wedge, saliva pH of all young men changed downward. So, in 4 young men, Ph saliva decreased to 5.8; in 3 - up to 5.6; 3 to 5.5; 1 to 5.4 and 1 to 5.3 (Fig. 8).

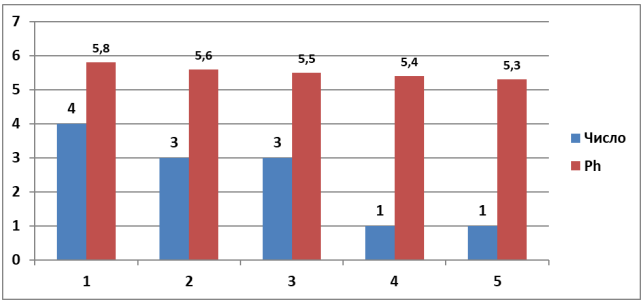

Figure 8. *Ph index of saliva in adolescent students after drinking lemon.*

It can be stated that even a short-term consumption of lemon, which contains acid, causes a sharp decrease in the pH of saliva. We noticed that after 20 minutes from the moment of drinking the lemon, the pH of saliva returned to its original values.

Thus, the «food» dominant, caused by the use of a small proportion of lemon, contributed to the activation of the autonomic nervous system in the form of increased saliva production and a decrease in its Ph, which is important in terms of, for example, the occurrence of dental caries. This is an active state of excitation of a newly formed large group of neurons, which is aimed at achieving a specific goal of the body. The main property of the dominant is the priority control and possession of the efferent pathways of the nervous system, especially the muscular system, due to the possession of muscles, the dominant can achieve the goal and be satisfied. After reaching the goal, the dominant disappears and gives control of the efferent pathways (including muscles) to another dominant so that she can be satisfied. If this is a food dominant, then after receiving food, it fades away, but after a while, hunger excites receptors, the food dominant intensifies and selects efferent pathways for satisfaction (nerve pathways for muscle control are especially important).

We believe that the placebo effect occurs in those people who, when using a placebo, have a dominant in the brain, that is, the goal of the action (I will get better, I will get better from the placebo). These thoughts must be stable, a person must truly believe in it, these thoughts must last a certain time. Then the dominant treatment is formed, which will be strengthened daily by taking a placebo drug. The formation of a placebo treatment dominant will have the same properties as other dominants in the body. With the correct prescription of drugs, the patient in any case forms a dominant for cure, that is, the body receives an order from the dominant cure to include adaptive physiological mechanisms for repairing body cells (especially during sleep), synchronize the rhythms of all organs and systems of the body, as it was in a healthy person. organism before. Here you need to pay attention to the fact that the human body “repairs” its cells every day, and information is taken from DNA about how a healthy cell should work. This does not surprise us. So why, when the body from an external stimulus, like a placebo, begins to carry out a well-known program for repairing its body, a number of doctors sharply criticize the placebo. We believe that not only placebo drugs can trigger the body’s response to recovery, but also other treatments, such as acupuncture. Many methods of forming a recovery dominant can turn on or enhance the body’s natural repair dominant. It can be some kind of stress or strong experience, such as travel, hunting, fishing, fear, great joy, intense sports, etc. There is only one mechanism for this cure, the external influence must be much greater in terms of the strength of excitation of the receptors (reverse afferentation) than that of the dominant disease in the patient.

Academician I.P. wrote about this. Pavlov, pointing out that there is a struggle of dominants for efferent pathways in the body, and that the struggle of dominants is the most difficult process in the body and the most energy-consuming [26].

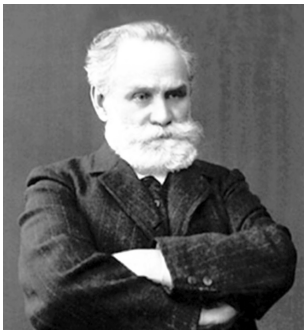

Figure 9. *Ivan Petrovich Pavlov.*

It is also possible to destroy the dominant of the disease and turn on the dominant of recovery by the method of psycho-concentration, which has been well developed over the millennia by Indian yogis. Note that the method of yogis requires long training and a significant concentration of the will of a person. We believe that the placebo effect in the human body arises and is formed to a greater extent on the basis of the fundamental laws of the nervous system. Academician I.P. Pavlov in experiments on animals proved that the main principle of the nervous system is a conditioned reflex [26]. When a light bulb is turned on (a conditioned signal, an informational food substitute) and food is given five minutes later (unconditional reinforcement, receptors in the mouth and stomach are irritated), it is repeated dozens of times, and only the lighting of the light bulb leads to the production of saliva and gastric secretion, as a result of which a conditioned reflex of the first order. Why does a dog produce saliva when a light bulb is lit, it is clear that not for a light bulb, a virtual image of food is formed in the dog's brain, which turns on the light of a light bulb.

Let's give a little historical background. Working in the laboratory of Pavlov I.P., Anokhin P.K. believed that the conditioned reflex has the property of anticipatory reflection of reality [7]. However, Pavlov I.P. [26] stood rigidly on the concept that a conditioned reflex is just a simple response of the nervous system (even the simple reflex theory of how the brain works was already revolutionary at the time).

Figure 10. *Pyotr Kuzmich Anokhin.*

So, for example, an engineer plans to build a bridge, he has a bridge plan in his head, all the parameters, there is no bridge yet, but there is already a virtual model (mental), the bridge is being built, and all the parameters of the bridge correspond to the mental model of the leading reflection. Academician Anokhin P.K. for his work on the theory of functional systems was awarded the Lenin Prize.

In connection with the above, we can also imagine the mechanism of placebo action as the development of a conditioned reflex (it is more difficult, like in I.P. Pavlov's dog, since the human brain is a more perfect mechanism of nature). When a placebo medicine is given (this is like a conditioned signal by Pavlov I.P., when a light bulb was lit) and after that, according to the reflex theory, unconditional reinforcement should follow, it is replaced in a person by psycho-concentration of thoughts and faith in recovery. Such a repetition of events can lead to the development of a conditioned reflex according to Pavlov, a conditioned placebo stimulus, an unconditional reinforcement of this thought and faith in recovery. If thoughts about recovery after a placebo are expressed and have the power of reverse afferentation to suppress other dominants, then the dominant about recovery becomes the strongest in the brain, it begins to own all the resources of the body. Then the placebo cure dominant actually leads to recovery or significant relief of the disease.

The study of the placebo effect required the use of a blind method, when the patient does not know whether he is receiving a real drug or a placebo. However, this was not enough, since the doctor, knowing what the patient was receiving in some unconscious way (look, movements, timbre of speech, behavior, etc.), showed that the patient was receiving a placebo or medicine. Therefore, they began to use a double-blind method to analyze the placebo effect, when neither the patient nor the doctor knows whether the patient is receiving a placebo or a medicine. This double-blind method is used to study new drugs, since in some cases the placebo effect exceeds the effect of the test drug [20, 23, 29, 30].

The proven therapeutic effect of the use of a placebo drug raises the assumption that the real mechanism of action of the drug can be added (or subtracted) and the psychological effect in the form of a placebo stimulation of the therapeutic result. We believe that the use of drugs for treatment causes the formation of a therapeutic dominant (as in placebo therapy), based on the physiological mechanisms of the development of a conditioned reflex according to the teachings of academician I.P. Pavlov.

Let us consider this process of formation of a conditioned reflex during drug therapy and the formation of a treatment dominant. The use of a medicine simulates the process of giving a conditioned signal (according to Pavlov, this is the inclusion of a light bulb). Further, the drug enters the body through the mouth or through injections (and other methods) and causes a change in the activity of a number of functional systems in the body. The body's receptors register these changes and, due to afferent impulses, transmit information along the nerves to the brain (both to the subcortical centers of the subconscious and to the neurons of the cerebral cortex). A permanent focus of excitation of a large group of neurons in the cerebral cortex is formed, which is informationally associated with the intake of the drug. This effect plays the role of unconditioned reinforcement (according to Pavlov, the analogue would be the reinforcement of a conditioned reflex in a dog with food). The focus of excitation in the brain when taking the drug is constantly increasing as a result of impulses from internal receptors. A mentally ill person (unconsciously or with the help of logic) inspires himself and begins to believe in his recovery, which leads to the formation of a recovery dominant. As a result, the dominant gains strength, captures more and more executive mechanisms in its submission, activates the reading of reserve regulatory genes in DNA and the synthesis of regulatory proteins, which was proven in the study of stress, including cold adaptation. The educated dominant of recovery when taking medications begins to have the same properties as the usual dominant.

It should be noted that the doctor can also form a dominant treatment for this patient. Then the patient at the subconscious level reads information from the doctor (voice tone, look, etc.) and, as it were, fulfills and realizes the doctor's subconscious will to improve his condition by strengthening the dominant of recovery. This mechanism is confirmed by the fact that they began to use a double-blind method of efficacy analysis for evaluating drugs, since it was noticed that if the doctor knows where the drug is used and where the placebo is used, then the placebo results are significantly improved.

We believe that the patient's recovery dominant (if formed) and the doctor's treatment dominant (if formed) begin to interact, reinforcing each other. From this we can conclude that the doctor's psyche plays a significant role in the recovery of the patient due to the subconscious interaction of the dominant of the patient's

recovery and the dominant of the doctor's treatment. It should be remembered that such interactions of dominants with a heavy workload in the work of a doctor often lead to the effect of "burnout" of the doctor. This is due to the fact that Academician I.P. Pavlov proved in experiments that the formation of dominants and their change is the most energy-consuming process in the central nervous system. Proceeding from this, it turns out that the doctor for each patient forms the dominant of treatment, which should be of such strength as to strengthen the dominant of recovery in the patient. For example, in a year of work, a doctor will experience a large number of changes in dominants (different patients), which significantly depletes the tone of his central nervous system. The dominant of treatment and the desire to treat increase in the doctor when he uses new drugs, new methods of treatment, undergoes advanced training, that is, for any reason for stimulating mental processes in the brain, when he wants to prove to everyone that he can solve the most complex problems. The greater the doctor's desire to cure the patient, the more the placebo effect can manifest itself due to the interaction of the treatment dominants in the doctor and the patient.

Conclusion. Academician Ukhtomsky A.A. created the doctrine of the dominant as a newly formed in the brain center of the association of neurons, whose work is aimed at achieving any goal that the body needs. After reaching the goal, the dominant is satisfied and gradually fades away. Analysis of the placebo effect of a drug from the point of view of the dominant makes it possible to streamline this knowledge, create a model for predicting placebo effects, and provide a scientific fundamental basis for the theory of placebo use.

Works of Academician I.P. Pavlov about conditioned reflexes fit well into the doctrine of the dominant. Analyzing the sources of special medical and pedagogical literature available to us, we have shown that the action of the placebo effect has the property of a first-order conditioned reflex.

Further development of the reflex theory of the brain in the works of Academician Anokhin P.K. highlighted the anticipatory action (virtual reality) of the work of the functional system of the body. Anokhin P.K. proved that the conditioned reflex has the property of anticipatory reflection of reality (with a conditioned reflex, when the light bulb is turned on, gastric juice is released after 5 minutes, but not on the light bulb, but on the food that was given 5 minutes after the light bulb was turned on). Analysis of the placebo effect from the point of view of the works of Anokhin P.K. showed that the use of a placebo drug, in some cases, forms a functional system of placebo action, which fits into a broader dominant of the patient's treatment, retaining all the properties of the functional system of Academician P.K. Anokhin.

Conclusions.

1. The physiological mechanism of the placebo effect is carried out through the formation of a treatment dominant, which was first introduced by Academi-

cian A.A. Ukhtomsky. We have shown for the first time that the mechanism of the placebo effect has the property of a conditioned reflex of the first order and corresponds to all the parameters of the teachings of Academician I.P. Pavlov about conditioned reflexes and organically structurally fits into the dominant of treatment.

2. The results of our work showed that the use of placebo drugs acts through the functional system of anticipatory reflection of reality of academician P.K. Anokhin and allow the treatment dominant to act ahead of the curve, improving the effectiveness of the treatment dominant.

References

1. Azizova E.R. Philosophical understanding of the placebo effect / E.R. Azizova //Ceteris Paribus. 2022. – No. 1. – P. 46–49.

2. Ananiev V.N. Analysis of the mechanisms of hypnosis from the standpoint of the doctrine of the dominant Academician Ukhtomsky / V.N. Ananiev, V.I. Torshin // Natural and technical sciences. 2020. – No. 9 (147). – P. 69–72.

3. Ananiev V.N. The value of the Ukhtomsky muscle dominant for increasing muscle strength / V.N. Ananiev, E.A. Semizorov, N.Ya. Prokopiev // Physical culture in the system of vocational education: ideas, technologies and prospects: Materials of the VI All-Russian Scientific and Practical Conference. – Omsk, 2021. – P. 64–68.

4. Ananiev V.N. The value of the doctrine of the dominant academician Ukhtomsky in explaining the mechanisms of hypnosis / V.N. Ananiev // Trends in the development of science and education. 2020. - No. 64-2. – P. 19–23.

5. Ananiev V.N. Pedagogical physiology of the dominant A.A. Ukhtomsky during the functioning of brain mirror neurons / V.N. Ananiev, O.V. Anan'eva, E.A. Semizorov // Trends in the development of science and education. 2021. - No. 70-4. – P. 12–18.

6. Ananiev V.N. Pedagogical methods K.D. Ushinsky from the point of view of academician A.A. Ukhtomsky / V.N. Ananiev, E.A. Semizorov //Modern science-intensive technologies. 2022. – No. 3. – P. 97–103.

7. Anokhin P.K. Biology and neurophysiology of the conditioned reflex /P.K. Anokhin - M.: Medicine, 1968. - 546 p.

8. Vinogradova K.S. Empathy as a basis for doctor-patient communication / K.S. Vinogradova, Yu.S. Borodova, V.P. Tsyganov // Innovations. The science. Education. 2020. – No. 19. – P. 725-730.

9. Gasparyan N. The origin of the term «placebo», the mechanisms of the «placebo effect» / N. Gasparyan // Medico-ecological information technologies

- 2020: Collection of scientific articles based on the materials of the XXIII International Scientific and Technical Conference: in 2 hours - Kursk, 20 – May 22, 2020. – S. 107–110.

10. Gotovsky M.Yu. Theory of functional systems P.K. Anokhin - the language of informational medicine and homeopathy / M.Yu. Gotovsky, K.N. Mkhitaryan // Homeopathic Yearbook - 2019. Collection of materials of the XXIX Scientific and Practical Conference. – Moscow, January 25–26, 2019. – S. 231–238.

11. Zarina N.N. Legal issues of homeopathy. New aspects in teaching homeopathy / N.N. Zarina // Topical issues of medical rehabilitation and adaptive physical culture. Conference materials. – St. Petersburg, November 21–22, 2017. – P. 43–44.

12. Zarina N.N. Legal issues of homeopathy. New aspects in teaching homeopathy / N.N. Zarina // Topical issues of medical rehabilitation and adaptive physical culture. Conference materials. – St. Petersburg, November 21–22, 2017. – P. 43–44.

13. Zakharova E.A. Empathy as a basis for doctor-patient communication: the current state of the problem / E.A. Zakharova, Yu.M. Ezhova, N.A. Rakov // Psychology. Historical and critical reviews and modern research. 2019. – V. 8. – No. 3-1. – P. 119–138.

14. Zashikhina I.G. Distrust of Russian citizens to doctors, conflict «doctor - patient» - one of the key problems of health care in the Russian Federation / I.G. Zashikhina // Medical Law. 2021. – No. 2. – P. 52–56.

15. Karaschuk L.N. Problems of trust in doctor-patient relationships / L.N. Karashchuk // Personality in a changing world: health, adaptation, development. 2020. – V. 8. – No. 1 (28). – P. 17–24.

16. Kashtanova A.I. Evolution of the doctor-patient relationship model / A.I. Kashtanova // Scientific Review. Medical Sciences. 2016. – No. 6. – P. 50–53.

17. Kenunen O.G. The placebo phenomenon as a promising direction of psychological and psychophysiological research / O. G. Kenunen, N. P. Rebrova // Bulletin of the Irkutsk State University. Series Psychology. 2020. – V.31. – P. 30–42. https://doi.org/10.26516/2304–1226.2020.31.30

18. Konorev M.R. Modern approaches to the pharmacotherapy of rheumatoid arthritis / M.R. Konorev // Bulletin of Pharmacy. 2020. – No. 1 (87). – P. 6–18.

19. Laius E.A. Transition to a new model of relationship between a doctor and a patient under the influence of a pandemic / E.A. Laius, E.G. Pozdeeva // Technologies of PR and advertising in modern society. Meaning Engineers: Transformation of Competences and Global Challenges of the Communications Industry: Proceedings of a Scientific and Practical Conference with International Participation. – St. Petersburg, November 25, 2020. – P. 237–241.

20.Lapin I.P. Personality and medicine. Introduction to the psychology of pharmacotherapy. / I.P. Lapin - St. Petersburg Dean 2001 – 416 p. (ISBN: 5–93630–001–3/5936300013).

21.Treatment of acute respiratory viral infections in adults: results of a randomized, double-blind, placebo-controlled clinical trial / E.P. Selkova, M.P. Kostinov, B.Ya. Bart, A.V. Averyanov, D.V. Petrov // Pulmonology. 2019. – V. 29. – No. 3. – P. 302-310.

22.Malkov A.V. Possibilities of using the placebo effect in the physical training of military personnel / A.V. Malkov, V.A. Egorov, A.V. Glushkov // Perspective directions of scientific research in the field of physical culture and sports (theory and practice): Collection of articles of the final scientific and practical conference for 2018, dedicated to the 65th anniversary of the founding of the Research Center (for physical training and military applied types sports in the Armed Forces of the Russian Federation. In 2 parts. – St. Petersburg, February 26-27, 2019. – P. 299-304.

23.Markelicheva E.V. Reflexivity of the patient's thinking as an effective therapeutic agent on the example of placebo action / E.V. Markelycheva, M.V. Rumyantseva, A.G. Kraeva // Innovative potential of youth - 2021: Collection of works based on the results of the All-Russian Festival of Scientific Creativity. Compiled and Executive Editor Associate Professor Mikhailova I.V. – Ulyanovsk, June 27–28, 2021. – P. 134-139.

24.Multicenter, randomized, double-blind study of the efficacy and safety of sustained-release tolperisone hydrochloride 450 mg (mydocalm® long, once a day) and tolperisone hydrochloride 150 mg (three times a day) in acute nonspecific pain in the lower back / V. A. Parfenov, E.I. Bogdanov, V.B. Laskov, N.S. Makarov, N.V. Pizova, E.A. Salina, J.Yu. Chefranova, L.V. Chichanovskaya. //Neurology, neuropsychiatry, psychosomatics. 2021. – V. 13. – No. 6. – P. 14-22.

25.Myasoedova S.E. Pain syndrome in rheumatoid arthritis: features and mechanisms of pain, modern approaches to diagnosis and treatment / S.E. Myasoedova // Neurology and rheumatology. Supplement to Consilium Medicum. 2019. – No. 1. – P. 32–36.

26.Oparin A.A. Medicine in the Byzantine Empire / A.A. Oparin // Skhidnoevropeisky journal of internal and family medicine. 2016. – No. 2. – P. 77-95.

27.Pavlov I.P. Twenty years of experience in the objective study of the higher nervous activity (behavior) of animals. / I.P. Pavlov – M.: Nauka, 1973. – 661 p.

28.Petrosyan G.R. What is the placebo effect? / G.R. Petrosyan // Reference book of a general practitioner. 2021. – No. 8. – P. 64–67.

29.Povalyukhina D.A. Problems of relationship between a doctor and a patient in Russia and Germany / D.A. Povaliukhina, A.D. Glukhova //International Journal of the Humanities and Natural Sciences. 2020. – No. 7-3 (46). – P. 143–147.

30.Results of a multicenter, double-blind, randomized, placebo-controlled clinical trial to evaluate the efficacy and safety of mexidol in the treatment of attention deficit hyperactivity disorder in children (mega) / N.N. Zavadenko, N.Yu. Suvorinova, T.T. Batysheva, O.V. Bykova, A.N. Platonova, D.D. Gainetdinova, E.V. Levitina, V.V. Mashin, I.N. Vakula, N.E. Maksimova // Journal of Neurology and Psychiatry. C.C. Korsakov. 2022. – V. 122. – No. 4. – P. 75-86.

31.Results of a randomized double-blind parallel study of the efficacy and safety of tolperisone in patients with acute nonspecific pain in the lower back / M.L. Kukushkin, L.V. Brylev, V.B. Laskov, N.S. Makarov, N.V. Pizova, E.L. Sokov, Zh.Yu. Chefranova, I.I. Sholomov, A.B. Hecht // Journal of Neurology and Psychiatry. C.C. Korsakov. 2017. – –. 117. - No. 11. – P. 69-78.

32.Sidorovich I.A. On the issue of optimal solutions in the event of conflicts in the triad «doctor-patient-society» / I.A. Sidorovich //ORGZDRAV: news, opinions, training. Vestnik VSHOUZ. 2020. - Vol. 6. - No. 3 (21). – P. 82–84.

33.Simonyan R.Z. Social conflict «doctor - patient» in modern Russian society: objective reasons and subjective factors / R.Z. Simonyan, E.S. Osipenkova // Trends in the development of science and education. 2021. - No. 74-6. – P. 158–164.

34.Tikhonovich I.I. Psychological features of communication between a doctor and a patient / I.I. Tikhonovich, I.Yu. Abedkovskaya / Medical discourse: questions of theory and practice. collection of articles based on the materials of the 9th International Scientific, Practical and Educational Conference. – Tver, April 08–09, 2021. – P. 123–127.

35.Turenko A.D. Homeopathy: a historical review / A.D. Turenko, E.E. Safronova // Problems of modern integration processes and ways to solve them: collection of articles on the results of the International Scientific and Practical Conference. 2017. – P. 59–62.

36.Umurzakova N.S. Placebo in clinical practice and when testing new drugs / N.S. Umurzakova, M.A. Turgunov, O.O. Eshonhuzhaev //Pharmaceutical business and drug technology. 2022. – No. 4. – P. 39-40.

37.Ukhtomsky A. Dominant: physiology of behavior. Series: Medical bestseller. / A. Ukhtomsky – M .: AST, 2020 – 320 p.

38.Ukhtomsky A.A. Dominant. / A.A. Ukhtomsky – St. Petersburg. Peter 2020. – 512p.

39. Academician A.A. Ukhtomsky in the pedagogical practice of the sphere of physical culture and sports / N.Ya. Prokopiev, V.N. Ananiev, E.A. Semizorov, E.S. Gurtova, S.I. Khromina // Scientific and sports bulletin of the Urals and Siberia. 2020. - No. 4 (28). – P. 71–75.

40.Academician A.A. Ukhtomsky and his role in modern medicine and biology / V.N. Ananiev, N.Ya. Prokopiev, L.A. Boyarskaya, O.V. Anan'eva, E.A. Semizorov // Natural and technical sciences. 2022. – No. 5 (168). – P. 93–102.

41. Physiological mechanisms of medical placebo effects, based on the doctrine of the dominant academician A.A. Ukhtomsky / V.N. Ananiev, N.Ya. Prokopiev, O.V. Ananyeva, E.S. Gurtova // International Journal of Applied and Fundamental Research. 2022. – No. 10. – P. 22–27.

42. Physiological mechanisms of functioning of the dominant Academician A.A. Ukhtomsky when analyzing the works of K.D. Ushinsky / V.N. Ananiev, N.Ya., Prokopiev E.A. Semizorov, O.V. Ananyeva, E.S. Gurtova // Natural and technical sciences. 2022. – No. 2 (165). – P. 134-139.

43. Khaikin A.V. On the study of the triggering mechanism of the placebo effect: placebo and self-hypnosis / A.V. Khaikin // Personality in a changing world: health, adaptation, development. 2021. – Vol. 9. – No. 3 (34). – P. 221–228.

44. Shakhmatova N.I. Study of aspects of the effectiveness of the placebo effect and its physiological properties / N.I. Shakhmatova, Ya.V. Abramochkina, Yu.P. Galyamova //Psychology of Development and Education: (Russian Journal of Applied Research). 2021. – No. 1. – P. 16–18.

45. 4Shvygina N.V. Comparative analysis of the use of homeopathy in Russia and Europe / N.V. Shvygina, V.S. Sedenkov // Theory and practice of project education. 2018. – No. 1 (5). – P. 40–43.

46. Placebo effect in the treatment of asthenic disorders in patients with schizophrenia in remission / S.A. Zozulya, A.V. Yakimets, I.V. Oleichik, T.P. Klyushnik // Russian Psychiatric Journal. 2019. – No. 1. – P. 38–46.

47. Yurov A.Yu. Placebo effect, pros and cons / A.Yu. Yurov, V.V. Vostrikov, S.N. Proshin // VI Baltic Congress on Child Neurology: collection of abstracts of the Congress. – St. Petersburg, June 09–11, 2016. – P. 411-412.

48. Yanovsky T.S. Placebo effect in medical practice / T.S. Yanovsky //Modern issues of biomedicine. 2020. – Vol. 4. – No. 2 (11). – P. 19–28.

49. Aletaha D. Optimisation of a treat–to–target approach in rheumatoid arthritis: strategies for the 3–month time point / D. Aletaha, F. Alasti, J. S. Smolen // Ann. Rheum. Dis. – 2016. – Vol.75. – P.1479–1485.

50. Anderson S. Determinants of placebo. / S. Anderson, G.T. Stebbins //Int Rev Neurobiol.2020;153:27–47. doi: 10.1016/bs.irn.2020.03.029. Epub 2020 Jun 9.PMID:32563291.

51. Benedetti F. Placebo and the new physiology of the doctor–patient relationship. / F. Benedetti //Physiol Rev. 2013 Jul;93(3):1207–46. Doi: 10.1152/physrev.00043.2012.

52. Branthwaite A. Analgesic effects of branding in treatment of headaches / A. Branthwaite, P. Cooper // Br Med J (Clin Res Ed). – 1981. – P. 1576–1578.

53. Brown W.A. Expectation, the placebo effect and the response to treatment. / W.A. Brown //R I Med J. 2015 May 1;98(5):19–21.PMID: 25938400

54.Enck P. Placebos and the Placebo Effect in Drug Trials. / P. Enck, S. Klosterhalfen //Handb Exp Pharmacol. 2019;260:399–431. doi: 10.1007/164.2019.269

55.EULAR recommendations for the management of rheumatoid arthritis with synthetic and biological disease–modifying antirheumatic drugs: 2016 update / J. S. Smolen [et al.] //Ann. Rheum. Dis. – 2017. – Vol. 76. – P. 960–977.

56.Fuente–Fernandez R. Expectation and dopamine release: mechanism of the placebo effect in Parkinson's disease / R. Fuente–Fernandez // Science. – 2001. – P. 1164–1166.

57.Gupta R. Rebuilding Trust and Relationships in Medical Centers / Reshma Gupta, Leah Binder, Christopher Moriates // JAMA.2020; 324 (23): 2361–2362.

58.Hauser W. Nocebo phenomena in medicine. Their relevance in everyday clinical practice / W. Hauser // Dtsch Arztebl Int. – 2012. – 459–465.

59.Holloway K. The world medicines situation 2011. Rational use of medicines. WHO/EMP/MIE/2011.2.2. / K. Holloway, L. van Dijk. – Geneva: World Health Organization, 2011.

60.How much does Disease Activity Score in 28 joints ESR and CRP calculations underestimate disease activity compared with the Simplified Disease Activity Index? / R. Fleischmann [et al.] // Ann. Rheum. Dis. – 2015. – Vol. 74. – P. 1132–1137.

61.In patients with early rheumatoid arthritis, the new ACR/EULAR definition of remission identifies patients with persistent absence of functional disability and suppression of ultrasonographic synovitis / G. Sakellariou [et al.] // Ann. Rheum. Dis. – 2013. – Vol. 72. – P. 245–249.

62.Influence of placebo effect in mental disorders research: A systematic review and meta–analysis. / R. Fernández–López, B. Riquelme–Gallego, A. Bueno–Cavanillas, K.S. Khan //Eur J Clin Invest. 2022 Jul;52(7):e13762. doi: 10.1111/eci.13762.

63.Nasonov E.L. Does Russia need a treat–to–target initiative? / E. L. Nasonov, D.E.Karateev // Rheumatology (Oxford). – 2015. – Vol. 54. – P. 381–382.

64.Peciña M. Neurobiology of placebo effects: expectations or learning? / M. Peciña, C.S. Stohler, J.K. Zubieta //Soc Cogn Affect Neurosci. 2014 Jul;9(7):1013–21. doi: 10.1093/scan/nst079.

65.Sheldon R. The Placebo Effect in Cardiology: Understanding and Using / R. Sheldon, M. Opie–Moran //It. Can J Cardiol. 2017 Dec;33(12):1535–1542. doi: 10.1016/j.cjca.2017.09.017. Epub 2017 Oct 6.PMID: 29173596.

66.Smolen J. S. Interleukin–6 receptor inhibition with tocilizumab and attainment of disease remission in rheumatoid arthritis: the role of acute–phase reactants / J. S. Smolen, D. Aletaha // Arthritis Rheum. – 2011. – Vol. 63. – P. 43–52.

67. Smolen J.S. Rheumatoid arthritis therapy reappraisal: strategies, opportunities and challenges / J. S. Smolen, D. Aletaha // Nat. Rev. Rheumatol. – 2015. – Vol. 11. – P. 276–289.

68. The changing landscape of biosimilars in rheumatology / T. Dörner [et al.] // Ann. Rheum. Dis. – 2016. – Vol. 75. – P. 974–982. EDN: WVSRUV

69. The Effects of Physicians' Communication and Empathy Ability on Physician–Patient Relationship from Physicians' and Patients' Perspectives. / Y. Wang, Q. Wu, Y. Wang, P. Wang //J in Psychol Med Settings. 2022 Jan 28:1–12. doi: 10.1007/s10880–022–09844–1. Online ahead of print.PMID: 35089529

70. Time to achieve remission determines time to be in remission / L. G. Schipper [et al.] // Arthritis Res. Ther. – 2010. – Vol. 12. – P. R97.

71. Treating rheumatoid arthritis to target: recommendations of an international task force /J.S. Smolen [et al.] // Ann. Rheum. Dis. – 2010. – Vol. 69. – P. 631–637.

72. Ultrasound in management of rheumatoid arthritis: ARCTIC randomised controlled strategy trial / E. A. Haavardsholm [et al.] // BMJ. – 2016. – Vol. 354. – P. i4205.

73. Waber R. L. Commercial features of placebo and therapeutic efficacy / R. L. Waber et al. // JAMA. – 2008. – № 299(9). – P. 1016–1017.

74. Zhang W. The powerful placebo effect in osteoarthritis. / W. Zhang //Clin Exp Rheumatol. 2019 Sep–Oct; 37 Suppl 120(5):118–123. Epub 2019 Oct 15.PMID: 31621561.

DOI 10.34660/INF.2023.61.96.059

使用 3D 模型选择用于修复 MUSTERING 组断裂牙齿的最佳根嵌体设计

USING 3D MODELS TO SELECT THE OPTIMUM DESIGN OF THE ROOT INLAY FOR RESTORATION OF DISRUPTED TEETH OF THE MUSTERING GROUP

Ertuvkhanov Marat Zainulabidovich
Postgraduate
Central Research Institute of Dental and Maxillofacial Surgery, Moscow, Russia

Andreeva Svetlana Nikolaevna
Doctor of Medical Sciences, Full Professor
Moscow State University of Medicine and Dentistry named after A.I. Evdokimov, Moscow c., Russia

Smerdov Alexey Andreevich
Candidate of Technical Sciences, тестировщик
Fidesis LLC, Moscow, Russia

抽象的。 在研究过程中，创建了上颌和下颌咀嚼组牙齿的 3D 模型，其中牙根结构的各种变体通过带有一个、两个和三个销的根销标签修复，以确定应力- 在咀嚼负荷的作用下牙齿组织中发生的应变情况。 对获得的数据进行分析，可以确定最合适的根销片类型，从而实现最佳的咀嚼压力分布。

关键词：牙根针片，在 3D 模型上研究牙齿的应力-应变状态。

Abstract. *In the course of the study, 3D models of the teeth of the masticatory group of the upper jaw and lower jaw were created with various variants of the structure of the roots restored by root pin tabs with one, two and three pins to determine stress-strain conditions that occur in the tissues of the teeth under the action of chewing load. The analysis of the data obtained made it possible to determine the most appropriate types of root pin tabs that allow optimal distribution of chewing pressure.*

Keywords: *root pin tabs, studying the stress-strain state of teeth on 3D models.*

Dental implantation has become the leading method of replacing dentition defects, however, in clinical practice, it is far from always possible to use this method due to difficult clinical conditions or for economic reasons. In addition, undoubtedly, the preservation of the natural root of the tooth and periodontium

is beneficial for maintaining physiological processes in the jaws. Therefore, the method of restoring destroyed teeth of the chewing group with root pin tabs remains very relevant today.

However, it should be noted that with a thorough study of the issues of modeling root inlays, all studies on the distribution of stress and masticatory pressure, fixation of structures, etc., were carried out on single-rooted teeth [1,2]. Multi-rooted teeth have a fundamentally different root structure and the chewing load is transmitted in a completely different way. Clinical guidelines that govern the manufacture of root post inlays contain a limited number of criteria for multi-rooted teeth [3].

The analysis of the scientific literature did not allow finding data on how the shape of the root pin inlay changes depending on the structure of the tooth root, in which clinical cases it is preferable to model one pin, and when it is necessary to make a root inlay with two or three pin parts. All this causes difficulties for practicing dentists when planning the restoration of destroyed teeth of the chewing group. According to the frequency of occurrence in court complaints of patients about the quality of fixed orthopedic structures, root pin tabs are in 3rd place (after metal-ceramic crowns and implant-supported crowns) and the number of claims has not decreased over the past 10 years [4.5].

The purpose of this study was to compile and study 3D models of multi-rooted teeth with different root shapes to study the nature of the distribution of physiological load when modeling root inlays of various designs (with one, two and three cores).

Materials and methods:

Using the Ansys SpaceClaim software, 3D models of chewing teeth were made with various, the most typical, variants of the root structure: with parallel roots (P-shaped), with a significant root divergence of more than 35º (L-shaped), with roots that have a bend on the border of the middle and upper thirds is more than 30º (L-shaped) and with O-shaped roots (Figure 1).

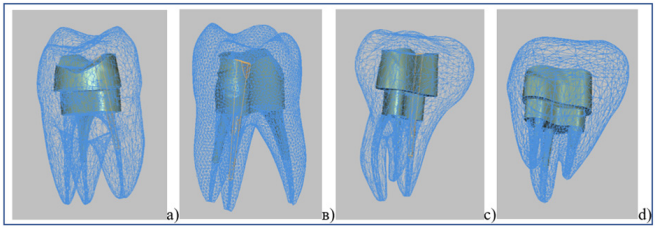

Figure 1. *3D models of teeth with different root structure: a) parallel arrangement of roots (U-shaped); b) divergence of roots more than 35º (V-shaped roots); c) with a bend in the area of the middle apical third more than 30º (L-shaped roots); d) roots in the form of the letter O (O-shaped roots)*

Using the Ansys Workbench software, for each model of teeth, calculations were made for the distribution of the physiological (chewing) load of 100N for cases where the root post core had only one core, as well as two and three cores (Figure 2).

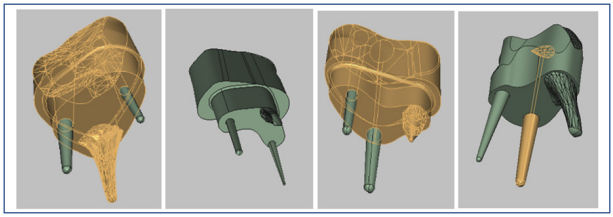

Figure 2. *Models of root post cores with different number of core parts*

When modeling root inlays, the requirements of the Clinical recommendations (treatment protocols) for the diagnosis of periapical tissue disease, approved by Resolution No. 18 of the Council of the Association of Public Associations "Star" dated September 30, 2014, Appendix No. 4, were observed. Chewing load was modeled along the axis of the tooth and at angles of 15º, 30º and 45º to the axis of the tooth for all variants of the structure of the teeth and the number of pin parts of the root inlays. Calculations of the distribution of principal stresses were carried out for the options for manufacturing root inlays from the CCA and from zirconium dioxide. Thus, the total number of models for which calculations were carried out was 84 units (48 models for CCA inlays and 36 models for zirconium dioxide inlays).

Research results:

In the course of research and calculations of stress-strain states under load, it was determined that the greatest stresses are concentrated on the outer side of the tooth in the area of contact with the cortical layer of the bone. The stresses inside the tooth, when using several long core parts, were distributed along the length of the pin, in the absence of pins, they were concentrated in the zone of the furcation of the roots of the teeth. With an increase in the angle of application of the load from 0º to 45º, the maximum stresses in the zone of furcation of the roots of the teeth increase with an increase in the number of pin parts at the root insert for teeth with L-shaped and O-shaped roots and decrease for teeth with parallel roots (U-shaped) and L-shaped roots. However, the differences in voltage values are rather insignificant.

For example, Figures 3 and 4 show the distributions of the third principal stresses in a tooth model with parallel roots for different directions of load application.

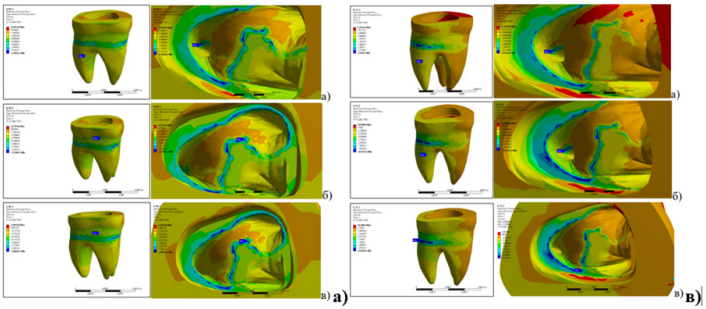

Figure 3. *The third main stresses in the tooth with one, two, three cores at the root tab in the case of a force acting at an angle of a) 0º; c) 15º*

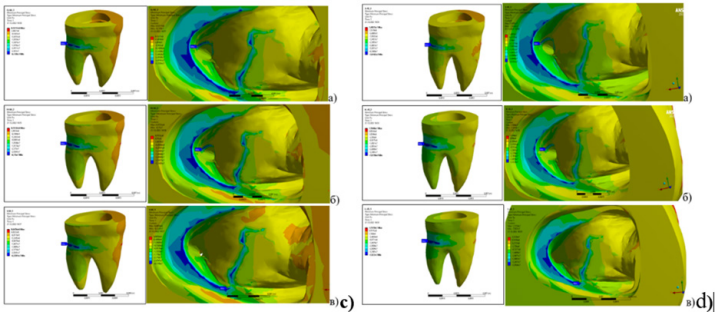

Figure 4. *The third main stresses in the tooth with one, two, three cores at the root tab in the case of a force acting at an angle of a) 30º; c) 45º*

When using zirconium dioxide root pin inserts, in all comparable cases, the stresses are lower than when using the CCA due to the lower elasticity of the material.

Conclusions:

In the course of studying the distribution of the physiological (chewing) load acting on a multi-rooted tooth restored with a root pin tab, it was determined that the leading factor that increases stress in the zone of chewing teeth furcation is not the shape of the root structure, but the presence or absence of an unloading area in the bottom of the cavity tooth, perpendicular to the axis of the tooth and the main vector of the application of the load on the tooth. In the absence of an unloading platform, the load is distributed along the length of the pin part of the root insert and is concentrated in the pin end zone. In this regard, when modeling root inlays in multi-rooted teeth, several pin parts should be made only if it is possible to model extended pins. If it is not possible to model long core parts for

2/3 of the root length, for example, with curved canals, the presence of impassable canals, etc., one pin should be modeled at the root insert and an unloading platform perpendicular to the tooth axis. With proper preparation of the tooth root, taking into account the preservation of retention zones, the fixation of the root core tab will not suffer. The manufacture of several short core parts of the root inlays of chewing teeth sharply increases the stress in the zone of root furcation, which can lead to the appearance of microcracks and the development of inflammatory and destructive phenomena in this zone.

References

1. Ohanyan A.I., Apresyan S.V., Akulovich A.V. Pin structures made of zirconium dioxide used in various areas of the dentition. Russian Dental Journal. 2017;21(3):135-137.]

2. Markov B.P., Tsalikova N.A., Krikheli N.I., Markova G.B. Prevention of errors and complications in planning and conducting orthopedic treatment. Dental Forum. 2017; 4:55-56.

3. Andreeva S.N., Ertuvkhanov M.Z., Andreev M.M. Errors and complications in prosthetics with cast root tabs according to forensic medical examinations 2013-2022. Medico-pharmaceutical Journal Pulse. 2022. Vol.24(10):12-20.

4. Andreeva S.N., Gusarov A.A., Fetisov V.A. Analysis of judicial practice in civil cases related to defects in the provision of dental care to the population of the Russian Federation for the period from 1993 to 2017. Forensic medical examination. 2018.V.61(3):44-48.

5. Andreeva S.N. Salagay O.O. Analysis of the features of forensic medical examinations in dentistry based on the study of judicial practice for 2013-2022. Forensic medical examination. 2023;V66(1):5-8.]

DOI 10.34660/INF.2023.82.79.060

动态电神经刺激对实验性 1 型糖尿病骨组织胶原代谢的合成代谢作用
ANABOLIC EFFECT OF DYNAMIC ELECTRONEUROSTIMULATION IN BONE TISSUE COLLAGEN METABOLISM IN EXPERIMENTAL TYPE 1 DIABETES MELLITUS

Bulanova Olga Ivanovna
State Autonomous Healthcare Institution of the Republic of Tatarstan "Regional Energency Medical Center", Department of traumatological and orthopedic, Naberezhnye Chelny

Yegorkina Svetlana Borisovna
Doctor of Medical Sciences, Professor
Department of Hominal Physiology Federal State Budgetary Educational Institution of Higher Professional Education "Izhevsk State Medical Academy" of the Ministry of Healthcare of Russia

Kutyavin Albert Leonidovich
State Autonomous Healthcare Institution of the Republic of Tatarstan "Regional Energency Medical Center", Department of traumatological and orthopedic, Naberezhnye Chelny

注解。 这项工作的目的是评估动态神经电刺激对四氧嘧啶诱导的高血糖大鼠骨组织胶原交换的影响。 实验是在性成熟的杂种雌性大鼠上进行的。 通过以 170 mg/kg 体重的剂量腹膜内施用一次四氧嘧啶来模拟高血糖症。 对照组动物四氧嘧啶引起的高血糖伴随着骨组织中胶原代谢参数的变化，从而增加了胶原溶解活性。 在这些条件下对实验组动物使用动态神经电刺激降低了分解代谢的严重程度。 因此，动态电子神经适应性刺激的作用可以被认为是一种防止结缔组织中胶原蛋白分解的方法。

关键词：四氧嘧啶诱导的高血糖症，动态电神经刺激，胶原蛋白。

Annotation. *The aim of the work was to evaluate the effect of dynamic electroneurostimulation on the collagen exchange of bone tissue of rats with alloxan-induced hyperglycemia. The experiments were carried out on sexually mature mongrel female rats. Hyperglycemia was modeled by intraperitoneal administration of alloxan at a dose of 170 mg/kg of body weight once. Alloxan-induced hyperglycemia in animals of the control group was accompanied by changes in the parameters of collagen metabolism in bone tissue, thereby increasing collagenolytic activity. The use of dynamic electroneurostimulation in*

animals of the experimental group under these conditions reduced the severity of catabolism. Thus, the effect of dynamic electroneuroadaptive stimulation can be considered as a method that prevents the breakdown of collagen in connective tissue.

Keywords: *alloxan-induced hyperglycemia, dynamic electroneurostimulation, collagen.*

Diabetes mellitus remains one of the serious problems, the scale of which continues to increase. Diabetes mellitus is characterized by a syndrome of chronic hyperglycemia, which leads to a violation of all types of metabolism and is accompanied by damage, dysfunction and disruption of various organs, especially the eyes, kidneys, nerves, heart and blood vessels, as well as a violation of bone remodeling processes and bone fragility. Currently, one of the most common experimental models of diabetes is the model in which DM is induced by the administration of alloxan mono- or tetrahydrate. The defeat of β-cells of the pancreas after the introduction of alloxan leads to metabolic consequences.

Currently, one of the most common experimental models of diabetes is the model in which DM is induced by the administration of alloxan mono- or tetrahydrate [3]. The defeat of β-cells of the pancreas after the introduction of alloxan leads to metabolic consequences. The products resulting from such destruction are widely used as markers of oxidative stress activity both at the level of the whole organism and in in vitro experiments [4, 5]. It is known that the dynamic stability of bone tissue, its resistance and adaptation to the impact of various extreme factors depend on the functional state of collagen.

To date, it is of interest to search for affordable and effective medical technologies that increase the adaptive potential of the body, the use of which helps to significantly optimize the results of ongoing therapy. Such methods include dynamic electrical neuroadaptive stimulation (DENAS). The method of dynamic electrical neuroadaptive stimulation (DENAS) is a method of percutaneous influence on certain areas of the body. DENAS-therapy is a method of treatment and prevention officially approved by the Russian Ministry of Health. The equipment has a registration certificate of the Federal Service for Supervision of Health and Social Development of the Russian Federation (No. FS-2005/004 dated March 04, 2005) and a certificate of the European Union dated 03.03.2004 No. RQ0406623 EUROCAT.

Purpose of the study: to evaluate the effect of dynamic electrical nerve stimulation on the metabolism of bone tissue collagen in rats with alloxan-induced hyperglycemia (type 1 diabetes).

Materials and methods of research: Maintenance, care of animals and their removal from the experiment was carried out in accordance with the “Rules for

carrying out work using experimental animals" (Appendix to the order of the Ministry of Health of the USSR dated 12.08.1977 No. 755). The study was carried out in compliance with the ethical standards and principles set forth in the World Medical Association Declaration of Helsinki (1964, 2000 ed.). The legitimacy of the research work was confirmed by the Biomedical Ethics Committee of the Izhevsk State Medical Academy, application number 732 dated 08.02.2022 d. The model of hyperglycemia was reproduced by intraperitoneal administration of alloxan at a dose of 170 mg per 100 g of animal body weight, the validity of the model was confirmed by changes in the blood carbohydrate profile (an increase in fasting glucose levels by 30 days of the study by 156% ($p = 0.0002$), the content of glycated hemoglobin by 287.5% ($p = 0.0004$) compared with the data of intact animals). The exchange of collagen in the bone tissue (homogenate of the femoral shaft) was assessed by the amount of: total collagen (SC), neutral salt-soluble (NSC) and citrate-soluble fractions of collagen (CRK), as well as free hydroxyproline (CO) and collagenolytic activity (KA). Prior to the start of the experiments, rats were divided into experimental and control groups of 10 animals each. The experimental group of animals was subjected to daily dynamic electrical neurostimulation (DiaDENS-PKM device), applying the electrodes of the device to the tail of the rat for 10 minutes for 30 days. The control group of animals was subjected to an unplugged device under similar conditions.

The results obtained and their discussion: As a result of the study, it was found that intraperitoneal administration of alloxan led to the development of hyperglycemia. Already on the 2nd day after the administration of alloxan, the animals showed polydipsia, polyuria, and a decrease in body weight was noted. During the control weighing of rats on the 30th day, the weight of the animals decreased by 11.3% in the experimental group and by 17.5% in the control group. Violation of the insulin-producing function of the pancreas and the occurrence of a diabetogenic state in rats that were injected with alloxan was confirmed by a significant increase in the concentration of glucose in the blood of animals compared to intact animals. Alloxan-induced hyperglycemia in animals of the control group was accompanied by changes in the parameters of collagen metabolism in bone tissue: an increase in CA, CO, CRK and a decrease in SC, NRK, which is consistent with the data in the works of E.G. Butolina et al. (2005) and indicates an increase in collagenolytic activity [1].

The use of dynamic electrical nerve stimulation in animals of the experimental group under these conditions reduced the severity of CA in the bone tissue by 52.6%, SO by 62%, CRK by 52.9%, and also increased the level of NRK by 70.9% and SC by 48.7 % compared with the control group of animals. Thus, alloxan-induced hyperglycemia causes changes in bone tissue collagen metabolism, manifested by inhibition of synthetic processes and activation of catabolic pro-

cesses[2]. Under the influence of dynamic electrical nerve stimulation, there was an increase in the synthesis processes in the metabolism of collagen in compact bone tissue. Taking into account the hypoglycemic and anabolic effects of dynamic electrical nerve stimulation, this method can be recommended as a non-drug correction method in the complex therapy of diabetes mellitus, as well as as a prevention of disease progression and the development

References

1. Butolin E.G., Mosyagin I.I., Savinova N.V., Petrov Yu.L. Modern ideas about collagen metabolism and its regulation: a review // Biochemistry of connective tissue (norm and pathology): Collection of scientific articles , dedicated to the 70th anniversary of the Department of Biochemistry, IGMA. - Izhevsk, 2005. - P. 25-36

2. Rozhinskaya, L.Ya. Systemic osteoporosis / L.Ya. Rozhinskaya. - M.: Publisher Mokeev, 2000. - 196 p.

3. Reshetnyak V.K., Kukushkin M.L., Meyzerov E.E. Neurophysiological substantiation of the parameters of electroacupuncture, electropuncture and transcutaneous electrical stimulation in the treatment of pain syndromes of various origins / Sat. mat-s scientific conf. TsNIIR "Results and prospects for the development of traditional medicine in Russia" / / M .: Ministry of Health of the Russian Federation, Federal Scientific Clinical and Experimental Center for Traditional Methods of Diagnosis and Treatment. -2002. - P.122-125.

4. Terzi M.S., Nikitina V.I. Dynamic Electro-Neurostimulating Therapy for Sports Injuries: Educational Method. allowance. - Chelyabinsk: Harmony LLC, 2009. - 10 p.

5. Walsh R.N., Cummim R. The open-field test: a critical review // Psychological Bulletin. 1976 Vol. 83. R. 482-504.

DOI 10.34660/INF.2023.66.16.064
UDC 664.681

纸杯蛋糕生产中的蔬菜泥
VEGETABLE PUREE IN CUPCAKE PRODUCTION

Tumanova Alla Evgenievna
Doctor of Technical Sciences, Full Professor
Russian Biotechnological University

Dzanagova Dana Alanovna
Student
Russian Biotechnological University

Goloeva Yana Alanovna
Student
Russian Biotechnological University

抽象的。 维护人民健康是最重要的国家任务之一。 营养是健康生活方式的主要组成部分。 尽管近年来观察到积极的动态，但俄罗斯人口的营养结构并不符合现代关于健康营养的观念。

由于俄罗斯人口的饮食失衡，富含最重要功能性营养素的食品的问题很严重。创造营养价值更高的糖果产品的一个有前途的方向是用加工过的水果和蔬菜来丰富它们。

关键词：蛋糕，胡萝卜泥，面粉糖果的浓缩，化学成分，营养价值，研究。

Abstract. *Preserving the health of the population is one of the most important state tasks. Nutrition is the main component of a healthy lifestyle. Despite the positive dynamics observed in recent years, the nutrition structure of the Russian population does not correspond to modern ideas about healthy nutrition.*

Due to the imbalance in the diet of the population of Russia, the issue of enrichment of food products with the most important functional nutrients is acute. A promising direction in the creation of confectionery products of increased nutritional value is their enrichment with processed fruits and vegetables.

Keywords: *cake, carrot puree, enrichment of flour confectionery, chemical composition, nutritional value, research.*

Flour confectionery products are a traditional product for the Russian market and today occupy one of the first places in terms of production in the confectionery industry [1]. They have an attractive appearance, pleasant taste and aroma. Cupcakes rightfully occupy a worthy place among flour confectionery products. Cakes

baked from rich dough are high in calories and sugar content due to the high content of egg products, butter and sugar and the low content of functional nutrients. Research is aimed at minimizing the above drawbacks [2].

Based on the foregoing, it seems relevant to create a cake with a lower calorie content, reduced sugar content, enriched with healthy substances.

The purpose of the work is to improve the technology and develop a recipe for cakes with increased nutritional value, enriched with functional nutrients - dietary fiber, minerals, based on the use of inexpensive local raw materials - carrot puree.

Carrots are a real pantry of vital natural substances that are in an easily digestible form and in optimal ratios for the human body. The therapeutic effect of carrots and products based on it is due to the rich composition of this vegetable, the beneficial properties of which can be preserved during production [3].

Carrot puree contains beta-carotene, vitamins (A, C, PP, B1, B2, E), minerals (potassium, calcium, sodium, magnesium, iron, phosphorus), flavonoids, enzymes, phytoncides, organic acids, dietary fiber, which predetermines its useful properties. Puree improves immunity, has antibacterial and antiseptic properties, promotes digestion, improves eyesight, and is a complete source of vitamin C.

The goal was achieved by solving the following tasks:

- study of the properties of carrot puree;
- study of the effect of different dosages of carrot puree on the organoleptic, physico-chemical, rheological properties of dough and finished products, determination of the optimal dosage of puree, which allows to obtain high quality products;
- development of a new cake recipe using carrot puree and adaptation of technology to the use of non-traditional raw materials for this production;
- confirmation of the increase in the functional status of the developed product based on the calculation of the nutritional value of the new cake in comparison with the traditional one.

The following materials were used in the work: baking wheat flour of the highest grade (GOST 26574-2017); white sugar (GOST 33222-2015 «White sugar. Specifications»); butter (GOST 32261-2013 «Butter. Specifications»); melange (GOST 30363-2013 «Egg liquid and dry food products»; salt (GOST 13830-97 «Edible salt. General specifications»; baking powder - ammonium carbonate (GOST R 55580-2013 «Food additives. General specifications»); vanilla essence (GOST 32049-2013 «Food flavors. General specifications»; carrot puree (GOST 32742-2014 «Fruit and vegetable puree»).

As a control, a product was produced according to the recipe of the «Student» cake [4].

The dough for cupcakes in accordance with the basic recipe was prepared as follows: plasticized butter was churned with sugar in a kneader for 7-10 minutes,

then melange was gradually added, and continued to churn for another 5-7 minutes. Separately, wheat flour of the highest grade with baking powder was sifted and added to the butter-egg mixture, thoroughly mixed for 5-8 minutes until a homogeneous mass was formed. The moisture content of the finished dough was 18 + 2%. The dough weighing 50 g was laid out in silicone baking molds. Cupcakes were baked in a baking chamber for 20 minutes at a temperature of 180ºC [5].

In the manufacture of developed cupcakes, carrot puree was added at the stage of dough kneading, 3 minutes before it was finished.

The work used generally accepted methods for the study of raw materials, semi-finished products and finished products (GOST 15052-2019 Cupcakes. General specifications).

Research results

When preparing samples and conducting the first series of experiments, carrot puree in cake recipes varied from 5% to 20% by weight of all product components on a dry basis, with an interval of 5%. In addition, samples of cakes were made with the addition of carrot puree and a partial reduction in white sugar by 5, 10, 15% of the prescription.

Analysis of the results showed that cupcakes with the addition of carrot puree in an amount of 5% to 20% of the total mass of raw materials, similarly to the control, had a smooth surface, regular shape, small gaps on the top crust. Products prepared with 5-15% puree differed from the control in pronounced pleasant (reminiscent of nutty) taste and aroma, attractive orange crumb of different intensity, uniform and developed porosity. In cupcakes with 10 and 15% puree, an increase in the specific volume of products by 6-4% compared to the control was noted. In a cake with 20% carrot puree, an increase in density and a slight decrease in the specific volume of the product by 1-3% were recorded compared to the control sample. The mass fraction of moisture and alkalinity in the studied samples remained within the requirements of GOST.

In samples of cupcakes with the addition of 10-15% carrot puree, it was possible to reduce the amount of white sugar in the recipe by 5-10% without compromising the quality of products.

Findings

1. The possibility of using carrot puree in the production of cakes has been established in order to enrich the composition of the product, when making puree at the dough kneading stage;

2. The influence of different dosages of carrot puree on the properties of the product was studied. The optimal dosage of puree in the recipe of cupcakes was established i.e. 10-15% by weight of all components of the product on a dry basis.

3. The possibility of reducing white sugar in the cake recipe by 5-10% of the recipe value, when using carrot puree, without reducing the quality of products, was revealed.

4. A recipe has been developed for a cake enriched with a wide range of functional nutrients through the use of carrot puree and a 10% reduced sugar content.

References

1. Grigorieva V.E. Analysis of the confectionery market / V.E. Grigoriev // NOVAINFO.RU. Agricultural sciences. - 2015. - No. 33-1. pp.14-18.

2. Vaskina V. A., Novozhilova E. S., Geller B. E., Chirtulov V. G. A method of cake production. Patent 4912 RB dated 17.03.98.

3. Vaskina V. A., Goryacheva G. E., Kuznetsova L. V., Novozhilova E. S. A method of obtaining puree from vegetables. Patent 1075 RB dated 14.

4. Lapshina, V. T., Fonareva, G. S., & Ahiba, S. L. (2000). A collection of recipes for cakes, pastries, muffins, rolls, cookies, gingerbread, gingerbread and fancy bakery products (part 3). Moscow: Khlebproinform.

5. Technological instructions for the development of flour confectionery products. /CRIIFS food industry. // 1992. – 240 p..

DOI 10.34660/INF.2023.88.18.062

碳化硅和二硼化锆联合机械活化结果

RESULTS OF SILICON CARBIDE AND ZIRCONIUM DIBORIDE JOINT MECHANICAL ACTIVATION

Gladkov Dmitry Sergeevich
Postgraduate
D. I. Mendeleev University of Chemical Technology of Russia

Lukin Evgeny Stepanovich
Doctor of Technical Sciences, Full Professor
D. I. Mendeleev University of Chemical Technology of Russia

Popova Nelly Aleksandrovna
Senior Lecturer
D. I. Mendeleev University of Chemical Technology of Russia

抽象的。 本文讨论了碳化硅和二硼化锆接头机械活化过程中发生的过程。分析了研磨时间对粒度和相组成的影响。 比较了各种组合物的混合物的机械活化动力学。 研究了机械活化影响 SiC-ZrB2 体系中所得材料的可烧结性和性能的方式。

关键词：碳化硅，二硼化锆，机械活化，烧结，超高温陶瓷材料。

Abstract. *The article discusses processes that take place during silicon carbide and zirconium diboride joint mechanical activation. The influence of milling time on granulometric and phase composition was analyzed. Kinetics of mechanical activation of mixtures of various compositions was compared. The way mechanical activation influences sinterability and properties of resulting materials in SiC-ZrB_2 system was studied.*

Keywords: *silicon carbide, zirconium diboride, mechanical activation, sintering, ultra-high- temperature ceramic materials.*

Ultra-high temperature ceramics (UHTC) are widely used in the aerospace industry, especially as thermal protection and in heat-loaded propulsion systems. This work is devoted to methods for obtaining UHTC in the ZrB_2-SiC system, namely, methods for preparing the charge by mechanical activation and the subsequent effect of mechanical activation on the properties of the material. Mechanoactivation, as a method of preparing a charge for sintering, has been used for a long time in the technology of high-temperature ceramic materials. Mechani-

cal activation is the mechanical treatment of solid mixtures, as a result of which plastic deformation of substances occurs, mass transfer is accelerated, mixture components are mixed at the atomic level, and the chemical interaction of solid reagents is activated [1]. Mechanical milling reduces the diffusion paths of mass transfer and accelerates the interaction of particles. This is especially important for systems with refractory covalent compounds, where not only physical interactions but also chemical transformations are possible in the zone of contact between particles of different substances.

The mechanical activation of pure powders of silicon carbide and zirconium diboride has been studied in sufficient detail. The presence of polytype transitions determines the features of high-energy grinding of SiC, in which there is not only the accumulation of defects on the surface and the destruction of grains, but also transitions from one polytype to another [2–4]. According to XRF data, there are no lattice microstresses in the ZrB_2 particles obtained after mechanical activation, which means that the decrease in grain size occurs according to the brittle fracture mechanism [5]. Taking into account the different hardness of these powders, it is possible to assume several processes occurring during the joint mechanical activation of SiC and ZrB_2: mutual attrition of particles, aggregation of smaller particles on the surface of large ones, formation of near-boundary transition phases and solid solutions in near-surface regions.

The purpose of mechanical activation is mainly to reduce the sintering temperature and increase the density of the final materials, however, taking into account that the formation of new phases is possible in the MA process, its influence can be much wider. Materials based on mechanically activated powders can have greater strength, chemical resistance, and melting point, which makes it possible to expand their fields of application.

The purpose of this work was to study the processes occurring during the joint mechanical activation of SiC and ZrB_2, to study the properties of the obtained mechanically activated powders and to identify the relationship between the mechanical activation processes and the properties of the sintered material.

Experimental part

Commercial powders of grade silicon carbide and zirconium diboride were used as starting materials in the work. As an additive, a nanopowder of the β-phase SiC was introduced experimentally. The properties of the initial powders are presented in Table 1.

Table 1.
Properties of initial powders

Combination	Phases, %	Lattice parameters, Å		Crystallite size, nm
		a	b	
α-SiC	SiC-6h (85,6%)	3,0819	15,1208	65
	SiC-15r (11,6%)	3,0827	37,7924	64
	Si (0,8%)	5,4310	-	154
	Quartz (1,6%)	4,9286	5,4499	51
	Cristobalite (0,5%)	4,9547	7,0345	43
β-SiC	SiC-6h (70,5%)	3,0827	15,1272	43
	SiC-4h (22,2%)	3,0820	10,0850	60
	SiC-15r (6,6%)	3,0819	37,8006	60
	Quartz (0,7%)	4,9350	5,4999	31
ZrB_2	ZrB_2	3,1699	3,5313	103

Mechanical activation was carried out on a Fritsch planetary mill, Pulverisette 5 model. For grinding, carbide grinding bodies Ø 8 mm and drums with carbide inserts with a volume of 250 ml were used. The ratio of the mass of the crushed material to the mass of the balls was 1:10; the duration of mechanical treatment varied from 15 to 90 min.

The microstructure of powder particles was studied using a JEOL JSM-6610 scanning electron microscope with an X-ray fluorescence energy-dispersive spectrometer BRA-135F. The phase composition of the samples was determined using a D2 PHASER X-ray diffractometer (Bruker AXS). Phase identification was performed using the JCPDS-PDF2 database. The lattice parameters and phase crystallite sizes were estimated using the DIFFRAC.EVA and TOPAS 5 software.

To study the processes occurring during the joint mechanical activation of silicon carbide and zirconium diboride, the following compositions (% wt.) were chosen: 70% SiC-30% ZrB_2, 50% SiC-50% ZrB_2, 30% SiC-70% ZrB_2. The content of the β-phase of SiC varied from 5 to 10%, however, according to the results of the studies, it was found that the presence of this additive did not have any significant effect on mechanical activation.

Based on the results of the analysis of the granulometric (Fig. 1) and phase (Fig. 2) compositions of the obtained mechanically activated mixtures, the optimal time for grinding the charge was chosen, which was 60 min. With a shorter time of mechanical activation, large crystallite sizes are observed, and with a longer time, the process of particle agglomeration begins, which, although it indicates their higher specific surface area, entails difficulties due to the need for disaggregation of adhered particles during further preparation for material sintering. According to XRF data, the phase composition of mixtures mechanically activated for 15 min.

significantly different from mixtures exposed for 60 min. There is a pronounced polytype transition of silicon carbide 15r → 6h, the intensity of the peaks of the compounds decreases, which indicates the amorphization of the mixture. At the same time, there are no significant changes in the transition from 60 min. of mechanical activation by 90 min. are not found on diffractograms.

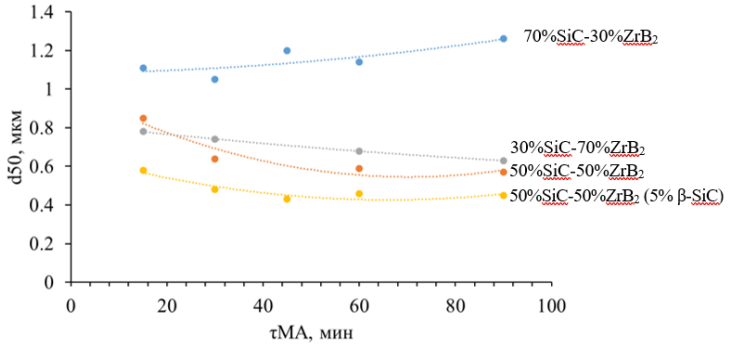

Figure 1. *Effect of MA duration on the average particle size of mechanically activated mixtures*

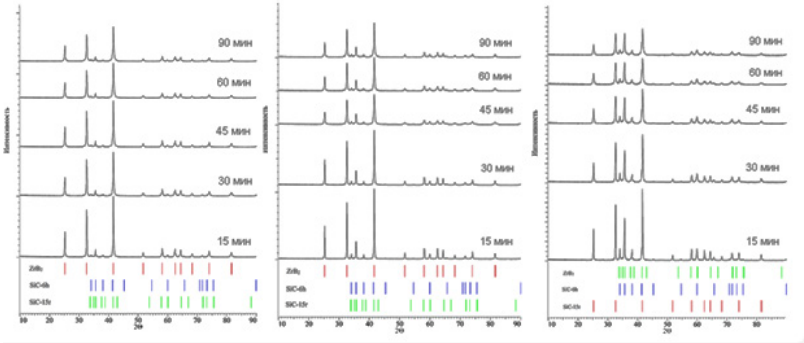

Figure 2. *Effect of MA duration on the phase composition of mixtures: a) 70% SiC-30% ZrB_2, b) 50% SiC-50% ZrB_2, c) 30% SiC-70% ZrB_2*

Based on the results of X-ray phase analysis, the lattice parameters of the main phases were calculated by the Rietveld method. It has been established that at 60 minutes of mechanical activation, the lattice parameters of silicon carbide and zirconium diboride undergo significant changes. For ZrB_2 composition, 50%SiC-50%ZrB_2, there is an increase in the parameters “a” and “c” by 0.06% and 0.04%, respectively, for the composition 70%SiC-30%ZrB_2 - the parameter

"c" of the lattice decreases by 0.03%, the parameter "a" remains unchanged, for the composition 30% SiC-70% ZrB_2 - the parameter "c" of the lattice decreases by 0.01%, the parameter "a" increases by 0.04%. The lattice parameters "a" and "c" of the SiC-6h phase for the composition 50% SiC-50% ZrB_2 increase by 0.07% and 0.1%, respectively, for the composition 70% SiC-30% ZrB_2 the parameter "c" increases by 0.07%, while "a" decreases by 0.03%, for the composition 30% SiC-70% ZrB_2 the parameter "c" increases by 0.08%, and the parameter "a" remains unchanged.

The sintering of the samples was carried out by hot pressing in molds 40 × 40 mm on hot pressing presses of the PGP-2200-70 and HVHP-446S brands at a maximum temperature of 1850 ℃.

Table 2.

Properties of sintered material

Composition, % wt.	**ρ, g/cm^3**	**ρ_{rel}, %**	**Porous, %**	**Water absorption, %**	**Hardness, GPa**	**Modulus of elasticity, GPa**	**K_{1C}, MPa·m$^{1/2}$**
30%SiC-70%ZrB_2	4,54	94,68	1,51	0,33	24,7 ± 5,3	214 ± 27	4,18 ± 1,99
50%SiC-50%ZrB_2	3,88	92,38	5,94	1,53	26,7 ± 8,8	301 ± 59	4,28 ± 1,99
70%SiC-50%ZrB_2	3,21	85,92	11,96	3,72	19,7 ± 5,3	112 ± 27	3,25 ± 0,88
50%SiC(5%β-SiC)-50%Zr_B2	4,01	95,48	1,36	0,34	27,7 ± 8,8	311 ± 59	4,70 ± 1,09
50%SiC(7,5%β-SiC)-50%ZrB_2	**4,13**	**98,33**	**1,01**	**0,25**	**35,2 ± 5,5**	**531 ± 81**	**5,92 ± 1,43**
50%SiC(10%β-SiC)-50%ZrB_2	4,06	96,67	1,11	0,27	28,8 ± 8,4	168 ± 46	4,48 ± 0,99

Based on the results of sintering, the properties of the obtained materials, mechanically activated for 60 min, were studied. (Table 3). It has been established that the addition of a nanosized fraction of the β-phase SiC has a significant effect on both the sintering of the material and the mechanical properties. The optimal content of the additive from the selected values was 7.5% wt.

The high-temperature strength of covalent refractory materials, in particular SiC, tends to increase with increasing temperature, so strength studies were carried out in the temperature range of 25-1400 ℃ (Fig. 3). It has been found that the material reaches its maximum compressive strength at 1200 ℃.

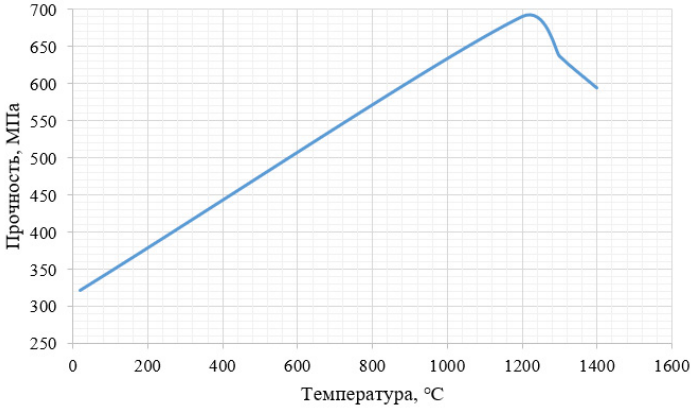

Figure 3. *Dependence of material strength on temperature*

Samples from a charge mechanically activated for 60 min. They were subjected to high-temperature tests in a high-enthalpy gas oxidizing flow on a plasma torch. The test mode, Figure 4, consisted in the fastest possible heating to a temperature of 2000-2200 °C in 20-30 seconds and holding the sample at this temperature. The exposure time was limited to 180 seconds.

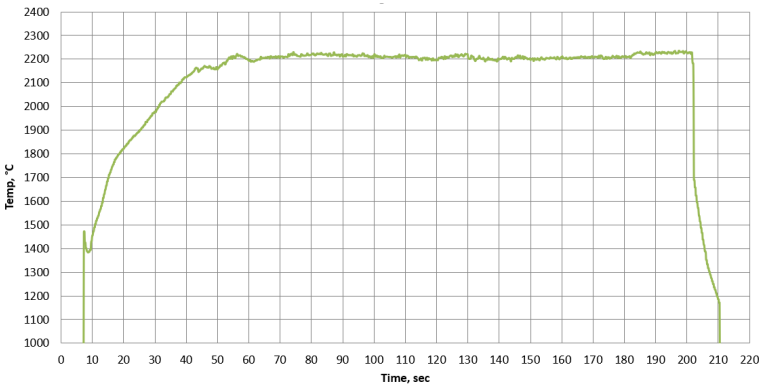

Figure 4. *Typical graph of sample surface heating during testing.*

Figure 5 shows photographs of samples from a thermal imager during testing and samples after testing.

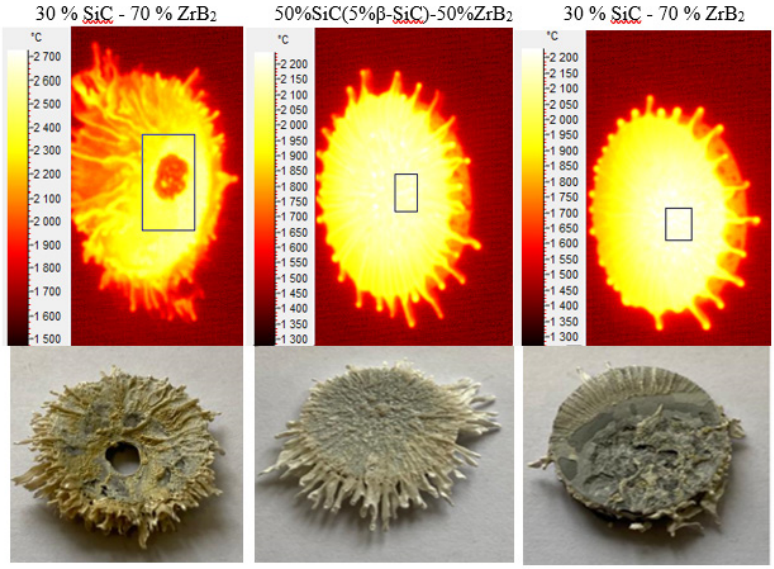

Figure 5.*Photos from the thermal imager during testing and samples after testing*

Conclusion

Joint mechanical activation of silicon carbide and zirconium diboride powders makes it possible to obtain submicron powders with a developed amorphous surface, which makes it possible to sinter them at relatively low temperatures. Intense mechanical abrasion, heating, and collisions of particles against each other and against the material of grinding media lead to a distortion of the crystal lattice of both the zirconium diboride phase and silicon carbide, which indicates their transition to a metastable state. For the selected powders and compositions, the optimal time of mechanical activation is 60 min.

Hot pressing of mechanically activated mixtures at a temperature of 1850 ℃ makes it possible to obtain a material with a density of up to 98% of the theoretical one, which indicates a high sintering activity of the powders. The introduction of β-SiC nanopowder enhances the physico-mechanical properties of the material. The most optimal composition of 50%SiC(7.5%β-SiC)-50%ZrB_2 has been tested to have a compressive strength at 20℃ 394MPa, which increases with temperature and reaches a maximum at 1200℃ 690MPa. This composition has a high hardness of 35.2 GPa, an elastic modulus of 531 GPa and a crack resistance coefficient K_{1C} of 5.92 MPa $m^{1/2}$.

Heating the material in a high-enthalpy oxidizing gas flow made it possible to establish that the sample of the composition demonstrated the highest oxidative resistance.

30% SiC - 70% ZrB_2. This is due to the higher viscosity of the melt formed during oxidation on the surface of the material. Further X-ray studies will make it possible to establish the phase composition of the resulting melt and modify the composition of the material to make it even more oxidatively stable.

References

1. Gusev AI Nanomaterials, nanostructures, nanotechnologies. - M.: Fizmatlit, 2007. - 416 p.

2. Garshin, A. P. Materials science in 3 volumes. Volume 1. Abrasive materials: a textbook for academic undergraduate studies / A. P. Garshin, S. M. Fedotova; under the general editorship of A.P. Garshin. - 2nd ed., revis. and correct. - M.: Ed. Yurayt, 2018. — 214 p.

3. Zhao Q.-Q. The mechanism and Grinding Limit of Planetary Ball Milling / Zhao Q.-Q., Yamada S., Jimbo G. // KONA. - 1989. - №7. - P. 26-36.

4. HREM observations of kinking in sic induced by ball milling // X. Y. Yang, Y. K. Wu, and H. Q. Ye // Materials Characterization. - 2000. - Vol. 44, Is. 4–5. - PP. 403-406.

5. Crystallite size refinement of ZrB2 by high-energy ball milling // Carlos A. Gala´n. // J. Am. Ceram. Soc. - 2009. - № 92(12). - PP. 3114-3117.

DOI 10.34660/INF.2023.95.67.063

同位素质谱法作为验证西红柿（SOLANUM LYCOPERSICUM）真伪的工具
ISOTOPE MASS SPECTROMETRY AS A TOOL FOR VERIFYING THE AUTHENTICITY OF TOMATOES (SOLANUM LYCOPERSICUM)

Panasyuk Alexand Lvovich
Doctor of Technical Sciences, Full Professor, corresponding member of the RAS

Ganin Mikhail Yurevich
Research Assistant
All-Russian Research Institute of the Brewing, Non-Alcoholic and Wine Industry - Branch of the Federal State Budgetary Scientific Institution "Federal Scientific Center for Food Systems named after V.M. Gorbatov RAS, Moscow, Russia

抽象的。 西红柿（Solanum lycopersicum）是世界上最受欢迎和无处不在的蔬菜作物。 与此同时，越来越多的制造商开始在其产品（包括西红柿）上贴上"有机"标签。 然而，这种产品的高质量和天然性声明必须得到使用可靠仪器方法进行的分析结果的支持。 为此，同位素质谱法是最有前途的。 研究对象是来自俄罗斯超市或在莫斯科地区种植的西红柿样品。 确定了商业生产的有机和常规西红柿以及该过程中使用的肥料的 δ15N 同位素特征参数。 同时，应注意所获得的同位素比率的重要性，这与文献数据基本一致。 结果表明，所开发的方法可以在未来用作验证各种商业种植的绿色产品（包括有机产品和常规产品）的农业实践的可靠工具。

关键词：西红柿，同位素质谱法，碳同位素，氮同位素，鉴定，起源，伪造。

Abstract. *Tomatoes (Solanum lycopersicum) are the most popular and ubiquitous vegetable crops in the world. At the same time, more and more manufacturers began to label their products, including tomatoes, under the term "organic". However, such a declaration of high quality and naturalness of products must be supported by the results of an analysis carried out using a reliable instrumental method. For this purpose, isotope mass spectrometry is the most promising. The objects of the study were samples of tomatoes from Russian supermarkets or grown in the ground in the Moscow region. The parameters of $\delta^{15}N$ isotopic characteristics were determined for commercially produced organic and conventional tomatoes, as well as for the fertilizers used in this process.*

At the same time, the significance of the obtained isotope ratios, which largely coincided with the literature data, should be noted. The results show that the developed approach can be used in the future as a reliable tool in the verification of agricultural practices for various commercially grown green products, both organic and conventional.

Keywords: *tomatoes, isotope mass spectrometry, carbon isotopes, nitrogen isotopes, identification, origin, falsification.*

1. Introduction

Tomatoes (Solanum lycopersicum) are one of the most popular and ubiquitous vegetable crops in the world. The volumes of their production and consumption are gradually growing, so over the past 30 years the world market of tomatoes has increased 3 times. At the same time, more and more manufacturers began to label their products, including tomatoes, under the term "organic". Organically grown products are becoming more and more popular every day, including among the Russian population, due to their usefulness and safety, thanks to new farming methods that are cleaner and more environmentally friendly.

However, the declaration of high quality and naturalness of products must be supported by the results of an analysis carried out using a reliable instrumental method. One of the promising directions in solving this problem is isotope mass spectrometry. Previously published scientific results [1-6] show that the developed approach using isotope mass spectrometry can be used as a reliable tool in testing agricultural practices for various types of commercially grown vegetable and green products, both organic and conventional, including tomatoes. In addition, the buyer is faced with the fact that under the guise of organic products, hydroponic grown tomatoes are exhibited. Moreover, this type of mass spectrometry also allows you to find out the nature of the fertilizers used, which is an important point, since chemical fertilizers are prohibited in the use of organic products.

2. Materials and methods

The objects of the study were samples of tomatoes purchased in Russian supermarkets or grown in the traditional conditions of the Moscow region.

The composition of stable carbon isotopes in the samples was determined using an analytical complex consisting of: a Flash EAIsolink two-reactor elemental analyzer of organic and inorganic objects equipped with a MAS200 autosampler for working with solid samples; universal interface ConfloIV; a mass spectrometer for the analysis of stable isotopes of light elements IRMS Delta V Advantage; high-purity gas supply systems; a specialized workstation for managing isotope research; registration and processing of measurement results using the high-level software package Isodat 3.0. (Thermo Fisher Scientific, USA – Germany). The $\delta^{15}N$ values were measured using a redox reactor. Sample preparation consisted

in crushing the sample in a blender to a puree state and then removing moisture using Zirbus Vaco 2 Germany freeze drying during the day. Next, the dried sample was ground in a mortar to a powdery state, after which a sample portion of 0.4-0.6 mg of the test sample was introduced into a tin capsule. The capsule was hermetically sealed with tweezers. At least 3 capsules were prepared for each sample, after which they were placed in an autosampler for solid samples and sequential determinations were performed. The encapsulated samples were burned in a redox reactor at a temperature of 1000 °C in a flow of oxygen and a carrier gas (helium) to nitrogen and carbon dioxide. Chemically pure compounds Cr_2O_3 and CuO were used as oxidizing agents, and metallic copper (Cu) was used as a reducing agent. Next, the resulting N_2 gas passed through a packed column and a Conflow IV interface and entered the ion source of the isotope mass spectrometer, where the isotope ratios were analyzed. The ion current and peak intensity data were processed using the ISODAT software package.

The isotope ratio values were expressed in δ‰ using the formula:

$$\delta‰ = [(Rsample - Rstandard)/Rstandard] \times 1000$$

where R - $^{15}N/^{14}N$ for values $\delta^{15}N$. In accordance with the international convention, the ratio of nitrogen isotopes relative to air was used as standards, and to normalize the scale of the device, the international caffeine standard IAEA-600 with passport values $\delta^{15}N_{air} = +1{,}00 \pm 0{,}2$ ‰, was used, as well as atmospheric air values $\delta^{15}N_{Air} = 0{,}0$ ‰.

3. Results and discussion

Based on a number of scientific papers [7,8], as well as our own accumulated data, there are the following differences in vegetables, including tomatoes, grown using chemical and organic fertilizers. Isotopic mass spectrometry can be used to determine the nature of the fertilizers used. According to the European standard (EC Council Regulation No. 834/2007) [9], organic production excludes the use of chemical fertilizers to improve plant growth. One of the approaches to the determination is presented in [4], where the products are analyzed for the isotope characteristics of nitrogen $\delta^{15}N$. The type of nitrogen compound and the timing of fertilization affect volatilization and leaching losses. Previous studies [6] have shown that stable nitrogen isotopes can form the basis of an identification system for determining whether a crop has been grown using chemical or organic fertilizers containing nitrogen [10,11]. Tomatoes grown with such fertilizers as peat, sewage sludge, manure, compost, as a rule, have isotope characteristics from + 8 ‰ до + 20 ‰ [1,10]. Tomatoes grown using chemical fertilizers, such as nitrate, ammonia and amide, usually have values from 0 ‰ до + 6 ‰ [1-3]. This pro-

vides a basis for comparing vegetables grown with organic or chemical fertilizers (Figure 1). This difference in terms of nitrogen isotope characteristics occurs as a result of ammonia volatilization, denitrification, nitrification, and other processes of transformation of nitrogen-containing compounds before absorption by plants [11, 12]. At the same time, it should be understood that these ranges apply mainly to tomatoes, since in other vegetables these ranges may differ and more data and experiments are needed, including with the use of Russian vegetables.

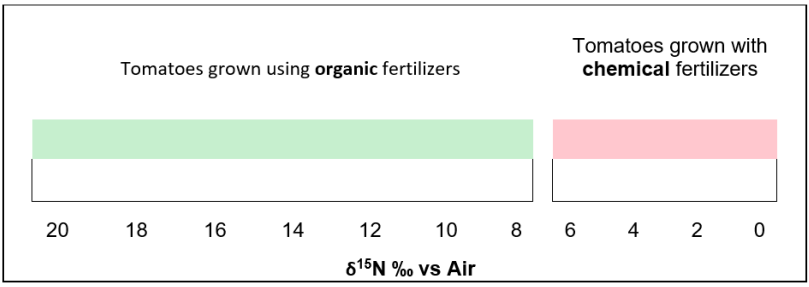

Figure 1. *Measuring ranges $\delta^{15}N$ ‰ tomatoes grown with organic and chemical fertilizers.*

During the research, we selected and analyzed 16 samples of tomatoes purchased in Russian supermarkets or grown in the outer Moscow. The results of $\delta^{15}N$ studies are shown in Table 1.

Table 1

Values of nitrogen isotope characteristics in tomatoes

№	Name	$\delta^{15}N$ ‰ vs Air	Type of fertilizer used, based on the results obtained
1	Cherry tomatoes, declared as hothouse. Bought in a supermarket	11,55±0,19	organic
2	Tomatoes are pink, withered as greenhouse. Bought in a supermarket	2,22±0,3	chemical
3	Tomatoes. Bought from a supermarket.	2,4±0,57	chemical
4	Pink tomatoes Uzbekistan. Bought in a supermarket	5,01±0,21	chemical
5	Pink tomatoes. Bought in a supermarket.	5,52±0,1	chemical
6	Pink cream tomatoes. Bought in a supermarket	2,72±0,26	chemical
7	Tomatoes Pink Paradise Uzbekistan. Bought in a supermarket.	-17,46±0,2	uncertainty

8	Tomatoes ordinary Krasnodar. Bought in a supermarket.	3,84±0,14	chemical
9	Tomatoes. Kostroma district. Bought in a supermarket.	6,8±0,57	uncertainty
10	Tomatoes variety Pink first). Azerbaijan. Bought in a supermarket.	11,57±0,79	organic
11	Red tomatoes, Leningrad Oblast, Pikalevo c. Bought in a supermarket.	6,28±0,93	uncertainty
12	Tomatoes in Kashira c. Bought in a supermarket.	8,63±1,16	organic
13	Tomatoes Baku cherry. Bought in a supermarket.	9,42±0,4	organic
14	Tomatoes Uzbekistan pink. Bought in a supermarket.	2,83±0,15	mineral
15	Tomatoes from the dacha, Dubrovo, Moscow region, without chemicals	7,67±0,31	organic
16	Tomatoes from the dacha, Semenovskoe, Moscow oblast, without chemicals	10,73±0,25	organic

4. Conclusion

The indicators of isotope characteristics of total $\delta^{15}N$ for commercially produced organic and traditionally grown tomatoes, as well as the fertilizers used in this, were determined. At the same time, the significance of the obtained 15N/14N isotopic ratios, which largely coincided with the literature data [1–8, 10–14], should be noted.

Organically grown tomatoes, both in greenhouses and outdoors, tended to have higher nitrogen isotopic characteristics than conventionally grown tomatoes. Various greenhouse tomato growers use various soil substitutes, although compost and aged manure appear to be very common additions to peat-based organic mixes. To avoid complications such as blockage of droppers, growers of greenhouse tomatoes quite often prefer to use extracts from organic nitrogen fertilizers of plant origin: alfalfa flour, $\delta^{15}N = - 0.06 \pm 0.53$ ‰, molasses, $\delta^{15}N = 4.32 \pm 2.01$ ‰ and others [13]. As a result, according to [14], the nitrogen isotopic composition of organic tomatoes is a higher average value than those grown using mineral fertilizers. Also in the future it is necessary to study the water used in cultivation. Thus, according to [15], the $\delta^{15}N$ values of total nitrogen in water samples provided by greenhouse and field producers varied slightly depending on the growing conditions. The mean value of $\delta^{15}N$ in water samples taken from greenhouse producers was 6.66 ± 0.12‰, while it was 7.44 ± 0.18‰ from field producers.

As a result, we can say that according to the data obtained, 6 tomato samples (No. 8.14) refer to tomatoes grown using mineral fertilizers. There are also a number of samples (No. 7,9,11) whose isotopic composition does not fit into the ranges according to [1,2], that is, they fall under some uncertainty, in which

accurate identification is impossible and additional studies are needed, including using indicators of the isotopic characteristics of sulfur and carbon [16, 17]. The results show that the developed approach can be used in the future as a reliable tool in testing agricultural practices for commercially grown vegetable and green products, both organic and traditional. Knowledge and understanding of these interactions provides a powerful tool for the reconstruction of physiological phenomena in plants and animals, their geographical origin, makes it possible to use the isotope characteristics of the product under study to elucidate the biochemical pathways and mechanisms of reactions, as well as to reconstruct climatic, physiological and environmental conditions in the process of biosynthesis.

Credibly labeling horticultural products as «organic» affects the health and financial costs of consumers. It is important to correctly identify the nature of the products sold on the shelves and counters of the store. Now, in the context of the law on organic products, this is becoming extremely important and relevant.

References

1. Christopher Brodie and Oliver Kracht, Thermo Fisher Scientific, Bremen, Germany, detect organic grown vegetables using nitrogen isotopes. https://tools.thermofisher.com/content/sfs/brochures/AB-30399-IRMS-Organic-Vegetables-AB30399-EN.pdf

2. Laursen, K. H., Mihailova, A., Kelly, S. D., Epov, V. N., Bérail, S., Schjoerring, J. K., Husted, S. (2013). Is it really organic? – Multi-isotopic analysis as a tool to discriminate between organic and conventional plants. Food Chemistry, 141(3), 2812–2820. doi: 10.1016/j.foodchem.2013.05.068

3. Schmidt, H.-L., Robins, R. J., & Werner, R. A. (2015). Multi-factorialin vivostable isotope fractionation: causes, correlations, consequences and applications. Isotopes in Environmental and Health Studies, 51(1), 155–199. doi: 10.1080/10256016.2015.1014355

4. Bateman, A. S., Kelly, S. D., & Woolfe, M. (2007). Nitrogen Isotope Composition of Organically and Conventionally Grown Crops. Journal of Agricultural and Food Chemistry, 55(7), 2664–2670. doi:10.1021/jf0627726

5. Oganesyants L.A., Panasyuk A.L., Kuzmina E.I., Ganin M.Yu. Isotopes of Carbon, Oxygen, and Hydrogen Ethanol in Fruit Wines. Food Processing: Techniques and Technology. 2020;50(4):717–725. (In Russ.). https://doi.org/10.21603/2074-9414-2020-4-717-725

6. Kuzmina, E. I., Ganin, M. Yu., Sviridov, D. A., Egorova, O. S., Shilkin, A. A., Akbulatova, D. R. (2022). Using modern instrumental methods for coffee identification. Food systems, 5(1), 30-40. https://doi.org/10.21323/2618-9771-2022-5-1-30-40

7. Verenitch, S., & Mazumder, A. (2015). Isotopic characterization as a screening tool in authentication of organic produce commercially available in western North America. Isotopes in Environmental and Health Studies, 51(2), 332–343. doi:10.1080/10256016.2015.997723

8. Verenitch, S., & Mazumder, A. (2012). Carbon and Nitrogen Isotopic Signatures and Nitrogen Profile to Identify Adulteration in Organic Fertilizers. Journal of Agricultural and Food Chemistry, 60(34), 8278–8285. doi:10.1021/jf302938s

9. Council Regulation (EC) No 834/2007 of 28 June 2007 on Organic Production and Labelling of Organic Products and Repealing Regulation (EEC) No 2092/91. Off. J. Eur. Union L 189/1, 1–23 (2007).

10. Trandel MA, Vigardt A, Walters SA, Lefticariu M, Kinsel M. Nitrogen Isotope Composition, Nitrogen Amount, and Fruit Yield of Tomato Plants Affected by the Soil-Fertilizer Types. ACS Omega. 2018 Jun 30;3(6):6419-6426. doi: 10.1021/acsomega.8b00296

11. Ehleringer, J. R., Chesson, L. A., Valenzuela, L. O., Tipple, B. J., & Martinelli, L. A. (2015). Stable Isotopes Trace the Truth: From Adulterated Foods to Crime Scenes. Elements, 11(4), 259–264. doi:10.2113/gselements.11.4.259

12. Calderone, G., Reniero, F., Guillou, C. Rapid Communication Mass-Spectrometria. 20. (2006), 937-940

13. Trandel, M. A., Vigardt, A., Walters, S. A., Lefticariu, M., & Kinsel, M. (2018). Nitrogen Isotope Composition, Nitrogen Amount, and Fruit Yield of Tomato Plants Affected by the Soil–Fertilizer Types. ACS Omega, 3(6), 6419–6426. doi:10.1021/acsomega.8b0029

14. Verenitch, S., & Mazumder, A. (2012). Carbon and Nitrogen Isotopic Signatures and Nitrogen Profile to Identify Adulteration in Organic Fertilizers. Journal of Agricultural and Food Chemistry, 60(34), 8278– 8285. doi:10.1021/jf302938s

15. Curt, M. D.; Aguado, P.; Sanchez, G.; Bigeriego, M.; Fernandez, J. Nitrogen isotope ratios of synthetic and organic sources of nitrate water contamination in Spain. Water, Air Soil Pollut. 2004, 151, 135−142.

16. Afanasev R.A., Nosikov V.V., Litvinskiy V.A., Voronchiihina I.N. Spectrometric support of nitrogen gas diagnostics plant nutrition and organic nitrogen identification and mineral fertilizers. « Fertility », №4, 26-29, (2019). DOI: 10.25680/S19948603.2019.109.09

17. Litvinskiy V.A., Nosikov V.V., Sushkova L.O., Grishina E.A. The possibility of using of the stable isotopes of Sulphur and nitrogen as a criterion allowing to identify the nutrients at organic farming. Agrochemical Bulletin, No. 6, 79-82, (2019)

DOI 10.34660/INF.2023.97.76.061
UDC 664.782.86

菊苣糖浆在全价饲料生产中的应用

APPLICATION OF CHICORY SYRUP IN THE PRODUCTION OF COMPLETE FEED

Tumanova Alla Evgenievna
Doctor of Technical Sciences, Full Professor
Russian Biotechnological University

Sveshnikova Inga Eduardovna
Master's degree Student
Russian Biotechnological University

抽象的。 本文讨论了谷物棒的有益特性和缺点，例如含糖量高、卡路里含量高、矿物质成分差、可能存在非天然和有害成分，以及几乎完全不含抗坏血酸。研究致力于谷物棒的开发，其中所有上述缺点被最小化。 制定了研究的目的和目标，给出了工作中使用的材料和方法，并描述了制作酒吧的过程。 在谷物棒的配方中，使用了裸露的大米，糖浆完全被菊苣糖浆取代，芝麻和冻干覆盆子的比例在干原料总质量的 5% 到 15% 之间变化 基础。 作为这项研究的结果，已经确定了在巧克力棒的生产中使用菊苣糖浆作为粘合剂和甜味剂完全替代糖浆的可能性。 确定了芝麻和升华覆盆子的最佳含量 - 10%。 已经开发出一种不含白糖和麸质的环保专业全价饲料配方，富含多种功能性营养素，尤其是维生素 C。

关键字。 全价饲料、裸米、菊苣糖浆、芝麻、覆盆子、无糖、无麸质。

Abstract. *This article discusses both the beneficial properties of cereal bars and the disadvantages, such as high sugar content, high calorie content, poor mineral composition, the possible presence of unnatural and harmful components, as well as the almost complete absence of ascorbic acid. Research is devoted to the development of cereal bars, in which all of the above disadvantages are minimized. The purpose and objectives of the study are formulated, materials, methods used in the work are given, as well as a description of the process of making bars. In the recipe of cereal bars, exposed rice was used, sugar syrup was completely replaced with chicory syrup, and the proportion of sesame seeds and freeze-dried raspberries was varied from 5% to 15% of the total mass of raw materials on a dry basis. As a result of the study, the possibility of using chicory syrup in the production of bars as a complete replacement for sugar syrup, as a binder and sweetener, has been established. The optimal content of sesame seeds and sublimated raspberries was determined - 10%. A recipe has been developed*

for eco-friendly, specialized complete feed without white sugar and without gluten, enriched with a wide range of functional nutrients, in particular vitamin C.

Keywords: *Complete feed, exposed rice, chicory syrup, sesame seeds, raspberries, sugar free, gluten free.*

Complete feed (snacks) are food concentrates that are very popular among the population, they satisfy the feeling of hunger, are indispensable on the road, do not require special storage conditions, and energize for a long time.

Complete feed are the result of pressing cereals, usually oats, but often bars are prepared on the basis of or with the addition of other grains: rye, wheat, barley. Pieces of dried fruits and berries, nuts and seeds are also added to the bars. The bars may also contain yogurt, milk, chocolate, cocoa and other ingredients. Distinguish between raw and baked bars. The former are considered more useful, since the crushed grain is treated with ultraviolet light without the addition of oil. Due to the oil, baked, as a rule, have more calories than dry ones. But grains and seeds after heat treatment are easier to digest, do not overload the gastrointestinal tract.

Feeds have been popular for over 100 years as they have a lot of advantages: do not require special storage conditions, have a high nutritional value, energize for a long time. All the useful properties of cereals are preserved in the feeds. Because the bars contain both fast and slow carbs, they fill you up quickly without spikes in blood sugar.

The composition of the bars contains the main set of proteins, fats and carbohydrates, as well as dietary fiber and other useful substances.

Most often, complete feeds contain cereals such as wheat, rye, barley, and oats that contain gluten, so they are not indicated for consumption by patients with celiac disease (gluten intolerance).

To bind the components, honey, molasses, white sugar, maltose and glucose syrups, chocolate are used in the production of bars, so this product is contraindicated for diabetics. To obtain a brighter aroma, chemical flavors are used, as well as other chemical auxiliary substances are used.

The main claims to the bars from nutritionists: high sugar content, high calorie content - 400 kcal and more (many bars are filled with chocolate or chocolate icing, which greatly increases the calorie content), poor mineral composition, the presence of unnatural and harmful components is possible, as well as the almost complete absence ascorbic acid [1]. In connection with the foregoing, the development of cereal bars, in which all the above disadvantages are absent, is relevant.

The purpose of our research was to develop a technology and recipe for an ecological, enriched with a wide range of functional ingredients, specialized sugar-free cereal bar, using natural raw materials produced in Russia, intended both for healthy people - adherents of a healthy diet, and for people with certain health problems (diabetes, celiac disease).

The materials used were: exposed rice, chicory syrup, sesame seeds and freeze-dried raspberries.

Rice does not contain gluten, so it is indicated for celiac patients. Exposed (exploded, loosened) rice is easier to digest. It is a source of energy, a source of protein, removes toxins and toxins, promotes weight loss, improves immunity, supports the health of the nervous system, reduces the risk of diabetes, improves heart function, and lowers bad cholesterol [2].

Chicory syrup (TU 11.07.19-157-54904577-2020) is a natural sweetener that has a relatively low calorie content - 167 kcal per 100 g of product. It is a rich source of dietary fiber, including inulin, a soluble fructooligosaccharide (FOS), whose content in the finished product reaches 85%. Upon receipt of the syrup, most of the inulin is stored as dietary fiber, without forming carbohydrates. Chicory syrup has a low glycemic index, no more than 10. Syrup is a natural prebiotic, restores intestinal microflora, improves immunity, reduces allergic reactions, lowers blood cholesterol, helps normalize blood pressure (BP), has anti-inflammatory properties, is allowed for people with diabetes - reduces blood glucose levels, does not contain gluten [3].

Sesame seeds (GOST 12095-76) contain 18 g of high-quality protein per 100 g of product, they are rich in B vitamins, vitamin E, tocopherols, they contain a wide range of minerals, a source of poly- and monounsaturated fatty acids. Also contain sesamin, which is an antioxidant, trace elements - zinc, iron, magnesium, phosphorus, calcium, potassium. Sesame seed perfectly strengthens the immune system, speeds up metabolism, has a beneficial effect on digestion and metabolic processes in the body.[4].

Freeze-dried raspberries (TU 10.39.21-089-35749547-2020) - stands out from other berry crops with a high concentration of antioxidants (flavonoids, phenols, anthocyanins, carotenoids) that prevent cell damage in the body, which stops the aging process. Incredibly rich in vitamins and microelements, it contains a large amount of B vitamins, C (26 mg per 100 g), A, silicon, molybdenum, magnesium, manganese, calcium, iron, phosphorus, sodium, chromium, zinc. In combination, such a rich composition contributes to: improving the state of the cardiovascular and nervous system; strengthening immunity; normalization of metabolism; improving collagen production and eliminating the effects of free radicals; due to the content of ellagic acid, it contributes to the prevention of oncology; has an anti-inflammatory effect. [5].

To achieve this goal, the following tasks were solved:

- to study the effect of different dosages of chicory syrup on the quality of finished complete feeds;
- to study the effect of sesame seeds, freeze-dried raspberries on the quality indicators of finished products;

- to determine the rational dosages of chicory syrup, sesame seeds and freeze-dried raspberries in the production of complete feeds;

- to develop a recipe for eco-friendly specialized cereal bars using natural raw materials, high nutritional value, no white sugar, gluten free.

As a control, traditional bars were made using sugar-treacle syrup.

In bars, according to TU 10.89.19-004-41986941-2020, organoleptic and textural indicators (appearance, aroma, hardness, chewiness, friability, stickiness), physicochemical properties - moisture content of the finished product were determined.

Feeds were made as follows: chicory syrup was boiled down to 118°C to a light straw color. The dry components of the mixture were cleaned of impurities, weighed in accordance with the recipe, and then mixed with a mixer. The resulting mixture was poured with hot syrup and stirred for 1 min. Next, the bars were molded and baked for 12 minutes in a convection oven.

Complete feeds based on exposed rice with a complete replacement of sugar-treacle syrup with chicory syrup, in comparison with the control sample, had a more even surface, a pronounced aroma, were less hard and crumbly, retained their shape better, did not stick to hands and equipment, chewed well.

5, 10, 15% of freeze-dried raspberries and 5,10,15% of sesame seeds were added to the recipe of the bars to the total mass of raw materials. It was noted that when adding a maximum of 10% of these components did not lead to a deterioration in their quality, organoleptic indicators - chewability, hardness, friability, stickiness of bars, were at the level of the control sample.

The moisture content of the developed cereal bars practically did not differ from the control sample and was within 15%.

The study found:

1. Chicory syrup can be used in the production of complete feeds as a complete replacement for sugar syrup, as a binder and sweetener.

2. The influence of sublimated raspberries and sesame seeds on the organoleptic and textural properties of the product. A rational dosage of these components in the recipe of cereal bars has been established i.e. 10% by weight of all components of the product.

3. The ratio of the studied components is determined. A recipe for eco-friendly, specialized cereal bars enriched with a wide range of functional ingredients without added sugar has been developed.

References

1. Poznyakovsky V. M., Reznichenko I. Yu., Popov A. M. Examination of food concentrates. Teaching guide. – Novosibirsk: Siberian Univ. Publishing House, 2004.

2. Olsen, K. M., Purugganan, M. D. Molecular Evidence on the Origin and Evolution of Glutinous Rice. // Genetics. – 2002 – Vol. 162 - P.941 - 950.

3. Tarasenko N.A. Inulin and oligofructose: effectiveness as a prebiotic fiber for the confectionery industry // Fundamental research. 2014. No. 9-6. P. 1216-1219.

4. Alvan Amin, Minakova A.D., Shcherbakov V.G. Features of the protein complex of sesame seeds – News of higher educational institutions. Food Technology 1998, 4, 92-93

5. Ed. Borisova M. I. Medicinal properties of agricultural plants. – Mn.: Harvest, 1974. – P. 236. - 336 p.

DOI 10.34660/INF.2023.70.40.066

库页岛西南部（Chekhovskiy 地区）中新世 Kurasiyskaya 组的双壳类软体动物
BIVALVE MOLLUSKS FROM THE MIOCENE KURASIYSKAYA FORMATION IN SOUTHWESTERN SAKHALIN (CHEKHOVSKIY REGION)

Khudik Vladimir Dmitrievich
Candidate of Geologo-Mineralogical Sciences, Senior Research Officer
Far Eastern Geological Institute of the Far Eastern Branch of the Russian Academy of Sciences, Vladivostok, Russia

抽象的。 介绍了库页岛西南部（Chekhovskiy 地区）Kurasiyskaya 组岩石中新世双壳类动物遗骸的研究结果，以及地层识别和研究的历史。 在萨哈林岛西南部的 Novoselovo 定居点附近发现了一个与 Kurasiyskaya 地层有关的具有重要地层学意义的沉积层序列，并追踪了与下方 Sertunaiskaya 地层的接触。对该序列的双壳类化石分析得出了年龄：中中新世至 下伏的 Sertunaiskaya 和重叠的 Kurasiyskaya 组的中新世中晚期。 已经确定，尽管生态学相似，但双壳类动物群的分类组成和古生物地理结构之间存在差异。 显然，这反映了中新世中晚期（恰好是萨哈林岛 Sertunaiskaya 和 Kurasiyskaya 矿床形成时期）远东地区气候变冷的趋势。

关键词：双壳类软体动物，中新世，库页岛西南部。

Abstract. *The results of the study of Miocene bivalve fauna remains from rocks of the Kurasiyskaya Formation of southwestern Sakhalin (Chekhovskiy region) as well as the history of formation identification and research are presented. A stratigraphically important sequence of sedimentary deposits related to the Kurasiyskaya Formation was found nearly Novoselovo settlement in the southwest of Sakhalin Island and the contact with the subjacent Sertunaiskaya Formation was traced.The analysis of bivalve fossils from the sequence has yielded ages: the middle Miocene for the underlying Sertunaiskaya and the middle-late Miocene for the overlapping Kurasiyskaya Formation. It is established that in spite of similar ecology there is a difference between taxonomic compositions and paleobiogeographic structures of the formations bivalve faunas. Apparently this reflects a tendency of climate cooling on the Far East during the middle-late Miocene (just the time of formation of the Sertunaiskaya and Kurasiyskaya deposits on Sakhalin).*

Keywords: *Bivalve mollusks, Miocene, Southwestern Sakhalin.*

In southwestern Sakhalin, the sedimentary strata of the Kurasi Formation in the volume of the Kurasian horizon of South Sakhalin [13] extend along the western slope of the West Sakhalin Mountains in the form of coastal outcrops from the area of the village of Shebunino in the south, reaching approximately the latitude of the city of Uglegorsk in the north (Fig. 1).

Figure 1. *Overview scheme of the study area.*

Until now, the priority of allocation of the Kurasi Formation is not quite clear. From the earliest works it is known that in 1932 the Japanese researchers Junji Nagumo and Minakumo Atsushimi in their works in southwestern Sakhalin, north of the city of Noda (Chekhov), in the area of the village. Kurashi (Novosibirskoye Settlement) have already mentioned the Kurashi sandshale formation, which was later repeatedly cited in various Japanese geological sources [20–23]. As most of them make clear, under the Kurashi Formation (Kurasi Formation), Japanese geologists understood coastal outcrops developed on the coast of the Tatar Strait in the area of the village. Kurasi and are represented by "a monotonous stratum of light opoka-like siltstones with concretions according to the Ausi Formation" [21]. Later, these ideas were accepted by Soviet geologists when compiling the first national stratigraphy scheme for the Tertiary deposits of South Sakhalin [18], and in 1959 the Kurasi Formation in South Sakhalin received the status of a stratigraphic unit at the Interdepartmental stratigraphic division [12]. For the stratotype of the formation, a section of coastal outcrops developed in the area of the Novosibirskoye settlement was taken. (1 in Fig. 2). According to available information [19], here the Kurasi Formation consists of light gray siltstones, siltstone mudstones with rare interlayers of sandstones and marl nodules with a total thickness of up to 600 m. According to our studies and literature data [3], in this section, the Kurasi Formation overlies the sandstones of the Sertunai (= Ausinskaya) Formation and

is represented by a relatively uniform sequence of light opokas and clay-siliceous rocks with a visible thickness of up to 300 m. The flasks are thin-platy, bleached from the surface with a yellow-green coating of jarosite and Liesegang rings. The upper part of the section is represented by more massive, gravel deposits. Large (0.1-0.3 m) carbonate ellipsoid nodules are characteristic. The contact of the Kurasi Formation with the underlying Sertunai Formation is transgressive. Glauconite sandstones with visible thickness from 1 to 5 meters lie at the base of the suite.

Over the years, a number of prominent Soviet geologists, stratigraphers, and paleontologists have been studying the Kurasi Formation to one degree or another. These studies are associated with the names of such of them as E.M. Smekhov, G.K. Nevsky, V.N. Kirkinskaya, L.M. Sayapina, P.D. Shklyaev, I.G. Grinberg, A.A. Kapitsa, L.V. Krishtofovich, A.P. Ilyina, I.I. Ratnovsky, I.A. Teplov, V.I. Bogidaeva, V.K. Ternikov, L.S. Zhidkova, I.N. Kuzina, R.R. Atlasov, G.N. Novikov, L.A. Pavlov, L.S. Margulis, V.O. Savitsky, G.N. Sheremetiev and many others.

There is an opinion [3] that in southwestern Sakhalin, many suites, as lithological bodies, in some cases have diachronic boundaries, which creates certain difficulties in tracing them as stratigraphic units. For this reason, the volumes of suites are sometimes understood by different geologists ambiguously. In particular, facies changes within individual formations, for example, on the flanks of the basin, are sometimes taken as manifestations of underlying or overlying formations of the section [1, 10, 16].

Figure 2. *Places of fauna collection in the south of Sakhalin: 1 - area of the Novosibirskoye settlement, 2 - r. Novoselka, 3 - coast north of Novoselovo settlement, 4 - r. Lesnaya, 5 - r. Gar, 6 - r. Gornaya*

According to literature data [3, 10, 13-15], in southwestern Sakhalin, the thickness of the Kurasi Formation increases from south to north from 200–250 m in the Chekhov region and up to 2300 m in the Uglegorsk region. In different areas, the stratigraphic volume of the formation and its relationship with the higher-lower strata differ. In the region, in most of the sections, the deposits of the formation with erosion lie on the underlying formations (often of different ages) and do not have an upper boundary, which significantly complicates the correlation constructions.

An analysis of the studies carried out indicates that certain successes have been achieved in the study of the Kurasi Formation, a huge amount of factual material has been collected, however, some issues remain unresolved, in some places being the subject of lengthy discussions. Among them are correlation constructions, in some cases the contact of the suite with underlying deposits is not always clear, it is necessary to clarify the taxonomic composition and paleobiogeographical structure of the Kurasian bivalve fauna, to clarify the nature and tendency of the change of mollusk faunas at the turn of the Sertunai-Kurasian time of South Sakhalin, and a number of other points. The study of the Miocene bivalves of South Sakhalin, as well as the analysis of the malacofaunal complexes, taking into account the general climate change in the Miocene of the Northwestern Pacific, allows us to express our opinions on a number of these issues.

According to our observations in the Chekhov region, the deposits of the Kurasi Formation in the stratotype are very poorly characterized by organic remains, which has been repeatedly pointed out by researchers. Here, in different years, we found rare remains of bivalves of the genera *Nuculana, Crassoleda, Malletia, Delectopecten*, which characterize quite significant depths of the marine basin within the lower horizons of the middle–lower sublittoral (50–200 m). It is noteworthy that the material composition of the deposits of the suite in the stratotype, as well as the nature of the mollusk fauna, can be traced almost unchanged in spatial terms with the strike of the suite in coastal outcrops from the village. Novosibirsk in the south to the Novoselovo settlement in the north.

In contrast to the deposits of the Kurasi Formation, developed on the coast of the area of the Novoselovo settlement, outcrops of the suite, discovered by us upstream of the river Novoselka (2 in Fig. 2), in our opinion, are undoubtedly of greater interest. However, it should be noted that due to the complex geology of the area [3] and its strong turf cover, they also appear here locally and quite isolated, mainly upstream of the river for almost 3 km. So, 200 m above the mouth of the river Novoselka, there is a section of deposits of the Kurasi and Sertunai formations with an apparent thickness of about 30 m.

The history of the study of this section is interesting. In the post-war period, geological research in South Sakhalin was carried out mainly by specialists from

VNIGRI, A.P. Karpinsky Russian Geological Research Institute and FENU. This section was originally identified, described and mapped by G.K. Nevsky [11] as the Lower Nevelsk and Upper Nevelsk subformations of the Nevelsk Formation of South Sakhalin, and the mollusk fauna collected by him was studied to one extent or another mainly by VNIGRI malacologists A.P. Ilina [6] and L.V. Krishtofovich [7]. This point of view existed for quite a long time and was accepted by the majority of geologists. In the early periods of studies of the Miocene malacofauna of Sakhalin, when studying the Miocene bivalves of the genera Mya and Thyasira, the author also adhered to this point of view [27, 30] . However, over time, with the receipt of new data on the fauna and stratigraphy of the Miocene deposits in South Sakhalin, it became clear to us that the nature of the mollusk fauna established here does not correspond to the composition of the fauna of the Nevelskaya Formation in different regions of South Sakhalin. We believe that in this section, the bivalve fauna of the Lower Nevelsk Subformation, as well as the composition of the host deposits, fully correspond to the nature of the deposits of the Ausinskaya (= Sertunaiskaya) Formation of South Sakhalin, while the fauna of the Upper Nevelsk Subformation is Kurasian. In the 1970s, in personal correspondence with the author A.P. Ilyina fully allowed this state of affairs, subject to additional research in this direction.

We believe that the above section exposes the upper part of the deposits of the Sertunai Formation of the region, represented by silicified gray, reddish-brown sandstones and siltstones with calcareous nodules (5–10 cm), rounded by pebbles of effusive and sedimentary rocks with a visible thickness of about 15 m. Sandstones and concretions contain a large number of traces of small charred plant detritus, a species-diverse fauna of bivalves and gastropods, among them are *Acila sp., Nuculana cf. tatarica* Kogan, *Yoldia sp, Glycymeris yessoensis* Sower., *G.* sp., *Anadara watanabei* (Kanehara), *Mizuhopecten* subyessoensis (Yok.), *Chlamys cf. otukae* Masuda et Sawada, *Lucinoma acutilineata* (Conrad), *Taras goldi forma sertunayensis* (Kogan), *Thyasira bisecta* (Conrad), *Th.* (*Conhocele) disjuncta forma alta* (L. Krisht.), *Th. sp., Ciliatocardium shijuense* (Khram.), *Clinocarium sp., Tellina cf. emacerata* Conrad, *Peronidia cf. pulchra* (Slod.), *Macoma nasuta* (Conrad), *M. optiva* (Conrad), *M. incongrua* (Mart.), *M. cf, albaria* (Conrad), *M. loveni* (Steenstrup), *Dosinia ausiensis* Ilyina, *D. cf. tugaruana* Nomura, *Mactra sp., Cultellus izumoensis* Yok., *Mercenaria yiizukai* (Kanehara), *Hiatella? sp., Solemya tokunagai* (Yok.), *Mya cuneiformis* (Boehm), *M. sertunayensis* (Laut.), *Periploma besshoensis* (Yok.), *Thracia pertrapezoidea* Nomura, *Turritella sp., Polinices sp., Euspira meisensis* (Mak,), *Tateiwaia sp.*

Further up the section, a monotonous sequence of opoka-like bluish-gray sandstones, silty sandstones, and siltstones occurs transgressively with inclusions of marl nodules (10–20 cm) from the lower part of the Kurasi Formation, with an

apparent thickness of about 12 m. At the base of the sequence lies a member of glauconite sandstone 3 m thick. Sandstones and concretions contain a numerous and species-diverse fauna of bivalves and gastropods, among them are *Acila conradi* (Dall), *Ovaleda iturupensis* Sav., *Yoldia caudata* Khom., *Megayoldia thracieformis* (Stor.), Chlamys sp, *Mizuhopecten subyessoensis* (Yok.), *Delectopecten sp., Musculus krishtofovitschi* (Sim.), *Taras goldi forma sertunayensis* (Kogan), *Thyasira (Conhocele) disjuncta forma alta* (L. Krisht.), *Th. (Conhocele) disjuncta forma ochotica* L. Krisht., *Ciliatocardium kurasiensis* Kafanov et Savitsky, *C. sakhalinense* (Khram.), *Clinocardium sp., Serripes groenlandicus* (Brug.), *Liocyma fluctuosa* (Gould), *Tellina cf. bodegensis* Hinds, *Macoma salcarea* (Gmel.), *M. nasuta* (Conr.), *M. optiva* (Yok.), *M. baltica* Linne, *M. gracilis* Khudik, *M. sp., Hiatella sakhalinensis* (Tak.), *Solemya tokunagai* Yok., *Panomya simotomensis* Otuka, *P. ampla* Dall, *Mya cf. japonica* Jay, *M. pseudoarenaria* Schlesch, *M. cuneiformis* (Boehm), *Periploma besshoensis* (Yok.), *Pandora sp*., *Thracia sp., Neptunea sp., Turritella sp., Natica sp*., *Polinices sp*., *Buccinum sp.,*). Many bivalves and gastropods are of different growth stages, bivalves have closed valves, often with traces of life-time shell color [28] and traces of drilling by gastropods. In addition, numerous remains of shells and claws of crabs, fragments of seaweed and grasses are observed in the concretions.

It should be noted that the lithological composition of the Sertunai and Kurasi formations is quite similar in this section. Earlier, L.S. Margulis and V.O. Savitsky, who conducted research in this area in the 1970s. According to these researchers (oral communication), the main lithological difference between the formations here is the presence of glauconite grains at the base of the Kurasi Formation. At the same time, the taxonomic composition and paleobiogeographical structure of the mollusk fauna of both formations in the section mentioned above differ significantly. According to our data, here the Sertunai mollusk fauna is represented by boreal (48%), boreal-Arctic (28%), and subtropical-low-boreal (24%) mollusk genera. So, along with *Anadara watanabei, the Sertunai fauna* also contains other subtropical-low-bore species (*Glycymeris yessoensis*, *Lucinoma acutilineata*, *Taras goldi forma sertunayensis, Cultellus isumoensis*, *Mercenaria yiizukai, Periploma besshoensis* – up to 35 %), boreal (*Yoldia sp., Tellina emacerata, Macoma nasuta, M. optiva, Mactra sp*., – 25 %), and boreal-arctic (*Thyasia bisecta, Th. disjuncta forma alta, Ciliatocardium shijuense*, *Mya cuneiformis, M. sertunayensis* – about 40 %).

Despite the noticeable presence of inhabitants of tropical and temperate waters, boreal and boreal-arctic taxa dominate among them, accounting for about three-quarters of the generic composition of the Sertunai fauna.

The Kurasian fauna is also distinguished by a large variety of bivalve molluscs. Boreal and boreal-arctic genera of bivalves in it account for up to 84%.

From boreal mollusks, they are *Yoldia caudata, Mizuhopecten subyessoensis, Musculus krishtofovitschi, Clinocardium sp*., *Mya japonica* (25% of species composition), and from the boreal-arctic – *Thyasira disjuncta forma alta, Th. disjuncta forma ochotica, Ciliatocardium sakchalinense, C. kurasiensis, Serripes groenlandicus, Liocyma fluctuosa, Macoma calcarea, M. baltica, Hiatella sachalinensis*, *Panomya simotomensis, P. ampla, Mya pseudoarenaria, M. cuneiformis* (70–75% of species). Relatively heat-loving subtropical-low-bore taxa are represented by single *Taras, Periploma, Pandora*, although they make up about 16% of the total generic composition of the fauna.

Many bivalves (*Serripes groenlandicus, Liocyma fluctuosa, Macoma calcarea, M. baltica, Mya pseudoarenaria*, etc.) still exist, being common inhabitants of marine communities of the upper–middle sublittoral of the Northwestern Pacific [17] and Arctic seas of the Northern Hemisphere [5, 8, 30, 31].

Building the successional series of the Sertunai and Kurasian faunas, one cannot but pay attention to the emerging trend towards an increase in the content of North Pacific boreal and boreal-arctic taxa in them. If in the Sertunai community they make up 76% of the generic composition, or 60–65% of the species, then in the Kurasian community they already account for 84% of the genera, or 95–100% of all species. At the same time, along with an increase in the percentage of cold-water genera, the diversity of their species composition increases. Thus, in the Sertunai paleocenosis, makoms are represented by five species (*M. nasuta*, *M. optiva*, *M. incongrua*, *M. cf. albaria*, *M. loveni*), and Mya - by two (*M. cuneiformis*, *M. sertunayensis*), Kurasian paleocenosis contains six species of poppies (*M. salcarea*, *M. nasuta, M. optiva*, *M. baltica*, *M. gracilis*, *M. sp.*) and three Mya species (*M. cf. japonica*, *M. pseudoarenaria*, *M. cuneiformis*). The increase in the content of boreal and boreal-arctic bivalves is parallel to the decrease in the content of subtropical-low-bore genera from 24% in the Sertunai fauna to 16% in the Kurasian fauna, and in the latter representatives of the warm-water fauna are quite rare.

Most likely, the qualitative and quantitative change in the composition of the Sertunai and Kurasian paleocenoses towards the predominance of boreal and boreal-Arctic forms in them fixes the beginning of a gradual cooling of the climate on Sakhalin Island in the Miocene during the Sertunai-Kurasian time, which we indicated earlier [29] .

In recent years, there have been no broad discussions regarding the age of the Sertunai Formation and the overlying Kurasi Formation of South Sakhalin. Today, the vast majority of researchers date the age of the Sertunai Formation to the Middle, and the Kurasian Formation to the Middle–Late Miocene [3], based on data on mollusks, diatoms, and other groups of the animal and plant kingdom. Our observations also support this. Thus, in the composition of the faunas of the

Sertunai Formation of the Tomarinsky region of the western (3 in Fig. 2) and Makarov region of the eastern (4-6 in Fig. 2) coasts of South Sakhalin, we distinguish the cardioid mollusk Ciliatocardium shijuense (Khram.). According to the literature data [6, 7, 32, 34, 35], the participation of this species in the Early and Middle Miocene faunas of Sakhalin and Japan was established. We have not noted its presence in faunas younger than the Sertunai age on Sakhalin.

We found bivalve mollusks of the genus Mya in the Sertunai and Kurasian faunas. If in the Sertunai fauna these are *M. cuneiformis* (Boehm) and *M. sertunayensis* (Laut.), then in the Kurasian fauna, in addition to *M. japonica*, there are *M. cuneiformis* and *M. pseudoarenaria* Schlesch. Our special study of representatives of the genus Mya from the Neogene of the northwestern Pacific [25, 26] showed the significant participation of two species of myas, *M. cuneiformis* and *M. pseudoarenaria*, in the Miocene faunas of Sakhalin and their definite stratigraphic significance. In our opinion, *M. cuneiformis* is undoubtedly the oldest species on Sakhalin, characterizing the sequences in the Early–Late Miocene age interval. In the late Miocene, it was replaced by the species *M. pseudoarenaria*, which exists from the end of the Miocene to the present day and constitutes a significant part of the boreal malacofauna in many areas of the northwestern Pacific (northern Japan, Sakhalin, Kamchatka, and Koryakia). The presence of *M. pseudoarenaria* on Sakhalin in faunas older than the Upper Miocene was not noted by us and, apparently, is unlikely.

In our opinion, the above information can serve as an additional justification for the accepted point of view regarding the Middle Miocene age established in South Sakhalin for the fauna and host strata of the Sertunai Formation and the Middle-Late Miocene age for the Kurasi Formation. Obviously, these data, taking into account the change in the paleobiogeographical structure of bivalve mollusk communities indicated by us at the turn of the Sertunai–Kurasian time of South Sakhalin, reflect the beginning of the Middle-Late Miocene epoch of global climate cooling in the Miocene of the North Pacific, which occurred after the climatic optimum at the turn of the Early and Middle Miocene (Upper Duya time of Sakhalin) and noted in different years by many researchers [2, 4, 35, 36].

References

1. Alekseychik S.N., Kuzina I.N., Ratnovsky I.I. Stratigraphy of the Tertiary deposits of Sakhalin // Bull. MSN. Dep. of Geol. 1954. V. 29, No. 5. P. 37-51.

2. Baranova Yu.P., Biske S. Yu. Tertiary climates of northeast Asia // XIV Pacific Scientific Congress. Stratigraphy and paleobiogeography of the Cenozoic of the Pacific Rim. Thes. of report M., 1979. V. 2. P. 18-19.

3. Gladenkov Yu.B., Bazhenova O.K., Grechin V.I., Margulis L.S., Salnikov B.A. Cenozoic of Sakhalin and its oil and gas content. M., Geos, 2002. 224 p.

4. Gladenkov Yu.B. Climatic fluctuations in the Neogene of the northern part of Kamchatka // Report of Academy of Sciences of the USSR. Ser.geol. 1982. V.265, No. 2. P. 407-409.

5. Golikov A.N., Scarlato O.A. Composition, distribution and ecology of gastropods and bivalves in the archipelago of Franz Josef Land // Studies of the fauna of the seas. L.: Nauka, 1977. P. 313-189.

6. Ilyina A.P. Mollusks of Neogene deposits of South Sakhalin // Mollusks of Tertiary deposits of South Sakhalin. L.: Gostoptekhizdat, 1954. P. 188-316. (Tr. VNIGRI; Issue 10).

7. Krishtofovich L.V. Mollusks of Tertiary deposits of South Sakhalin (lower formations) // Mollusks of Tertiary deposits of South Sakhalin. L.: Gostoptekhizdat, 1954. P. 5-186. (Tr. VNIGRI; Issue 10).

8. Kuznetsov A.P. Fauna of bottom invertebrates of the Kamchatka waters of the Pacific Ocean and the Northern Kuril Islands, Moscow: AN SSR. 1963. 268 p.

9. Margulis L.S., Savitsky V.O. On the Marking Horizons of the Arakay Formation in the Bolshoy Kholmskaya Anticline Region. In: Biostratigraphy, fauna and flora of the Cenozoic of the northwestern part of the Pacific Mobile Belt. M., 1969. P. 66-73.

10. Margulis L.S., Savitsky V.O. The problem of the boundary of the Paleogene and Neogene in South Sakhalin. In: Geology and Mineral Resources of Sakhalin and the Kuril Islands. Yuzhno-Sakhalinsk. 1974. P. 8-14.

11. Nevsky G.K. Geological survey on the western coast of South Sakhalin (Kholmsky and Uglegorsky districts). Yuzhno-Sakhalinsk. 1949. 58 p. (Funds of the Far East. Phil. Federal State Institution "Rosgeolfond").

12. Decisions of the Interdepartmental Conference on the development of unified stratigraphic schemes for Sakhalin, Kamchatka, the Kuril and Commander Islands. Leningrad: Gostoptekhizdat, 1961. 338 p.

13. Decisions of working interdepartmental regional stratigraphic meetings on the Paleogene and Neogene of the eastern regions of Russia - Kamchatka, the Koryak Highlands, Sakhalin and the Kuril Islands. Explanatory note to stratigraphic schemes M.: GEOS, 1998. 147 p.

14. Savitsky V.O., Migdisov S.A. Stratigraphy of the Mesozoic and Cenozoic deposits of the western coast of Sakhalin. Yuzhno-Sakhalinsk. 1969. 307 p. (Funds of the Far East branch of the Federal State Institution NPP "Rosgeolfond").

15. Savitsky V.O., Sycheva O.A. Paleontological substantiation of the detailed stratigraphy of the Cenozoic deposits of the Uglegorsk region. Yuzhno-Sakhalinsk. 1971. 307 p. (Funds of the Far East. fil. FSU NPP "Rosgeolfond").

16.Serova M.Ya. Marine Oligocene in the reference section of the Paleogene of Western Sakhalin. Bull. of Academy of Sciences of the USSR. Ser. geol. 1985. No. 11. P. 86-89.

17.Scarlato O.A. Bivalve mollusks of temperate latitudes of the western part of the Pacific Ocean. L.: Nauka, 1981. 480 p.

18.Smekhov E.M. Tertiary deposits of South Sakhalin // Izv. Academy of Sciences of the USSR. Ser. geol. 1948. No. 6. P. 125-130.

19.Stratigraphic Dictionary of the USSR. State Scientific and Technical Literature on Geology and Subsoil Protection. M. 1956. 1281 p.

20.Takama M. Report on the geological study of the Maoko-Honto (Kholmsk-Nevelsk) area / transl. from Japanese lang. I. A. Ivanova // Collection No. 4 of reports on the geological study of oil for 1935. Okha, 1937. 48 p. (Funds SakhNIINneftegazprom).

21.Uwatoko K., Takeda H. Report on the geological study of the Kusyunai-Oite area (Ilyinsk - Novoselovo) / transl. from Japanese lang. I. A. Ivanova // Collection No. 5 of reports on the study of the oil fields of Sakhalin in 1936. Okha, 1938. 46 p. (Funds of SakhNIINeftegazprom).

22.Uwatoko K. Explanatory note to the geological map of South Sakhalin (scale 1: 500000). Okha, 1939. 47 p. (Funds of SakhNIINeftegazprom).

23.Uwatoko K. Stratigraphy of South Sakhalin / per. from Japanese lang. Z.P. Nikolaeva // Bull. of Sakh. mining industry companies. 1938. Vol. 9, no. 29. 29 p. (Funds of the Far Eastern Branch of the Federal State Institution NPP Rosgeolfond).

24.Fotyanova L.I. Cenozoic floras and climate of the North Pacific // Fossil fora and fauna of the Far East and issues of Phanerozoic stratigraphy. Vladivostok: FESC AN USSR, 1977, pp. 65-82.

25.Khudik V.D., Zakharov Yu.D. Analysis and revision of the Miocene boreal faunas of bivalves in South Sakhalin Vestn. FEB RAS. 2020. No. 5. P. 68-80.

26.Khudik V.D., Amano K., Nakashima R., Tuzov V.P. On the problem of studying bivalves of the genus Mya from the Neogene of the northwestern part of the Pacific // Vestn. FEB RASN. 2004. No. 2. P. 79-84.

27.Khudik V.D. On representatives of the species Thyasira disjuncta (Gabb) from the Nevelskaya Formation of southwestern Sakhalin // Fossil flora and fauna of the Far East and issues of Phanerozoic stratigraphy. Vladivostok, 1977, pp. 94-97.

28.Khudik V.D. Traces of in vivo coloration of some bivalve mollusks from the Miocene of South Sakhalin. // All-Union meeting on the topic "Morphology, systematics, phylogeny and ecogenesis of bivalves". Thes. of report M., 1984. P. 109-110.

29.Khudik V.D. Communities of bivalves and climate change in the Miocene of southwestern Sakhalin // All-Union conf. on sea biology. Thes. of report Vladivostok. 1982. P. 48-50.

30.Khudik V.D. Mollusk Communities and Species Composition of the Mii Nevel Formation (Miocene) of Southwestern Sakhalin // Paleoecology of Marine Invertebrate Communities. Vladivostok, 1979. P. 90-99.Bernard F.R. Identification of the Living Mya (Bivalvia: Myaida) // Venus (Jap. J. Malac.) 1979. V. 38. N 3. P. 185-204.

31.Kamada Y. Tertiary marine Mollusca from the Joban coal-field, Japan // Paleont. Soc. Japan, Spec. Papers. 1962. N. 8. P. 1-187.

32.MacNeil F. S. Evolution and distribution of the genus Mya, and Tertiary migrations of Molluscs. // U.S. Geol. Surv. Prof. Pap. 1965. N 483-G. P. 1-51.

33.Noda Y. Neogene molluscan faunas from the Haboro Coal-field, Hokkaido, Japan // Sci. Rep. Tohoku Univ. Ser. 2. 1992. Vol. 62, N.1-2.140 p.

34.Suehiro M. Upper Miocene Molluscan fauna of the Fujima formation, Shimane prefecture, West Japan // Bull. Mizunami Fossil Mus. 1979. N. 6. P. 65-100 (in Japanese).

35.Tanai T. Miocene floras and climate in East Asia // Abh. Zentr. Geol. Inst. 1967. N 10. P. 195-205.

DOI 10.34660/INF.2023.39.90.067

描述多相制冷剂换热器中多相流的现象学等效模型
A PHENOMENOLOGICAL EQUIVALENT MODEL FOR DESCRIBING MULTIPHASE FLOWS IN HEAT EXCHANGERS WITH A MULTIPHASE REFRIGERANT

Zhigalov Vladimir Ivanovich
Doctor of Economic Sciences, Chief Researcher
All-Russian Research Institute of Experimental Physics

抽象的。 本文讨论了建立物理模型的问题，这些模型可以描述在许多热交换设备中发生的管道和通道中的复杂多相流，特别是在天然气液化过程中。 由于在冷却混合物系统和制冷剂系统中多相流的运动过程中，相以不同的速度运动并发生相变，因此解释困难。 该论文提出了构建具有热交换的等效双管回路的原理，该回路由分离冷却混合物和多组分制冷剂的壁之间的有效导热系数控制。 作为计算冷却混合物通道和制冷剂通道中流动行为的工具，使用了封闭管道系统中的多相流模拟器。

关键词：具有相变的多相混合物，多组分制冷剂，气体液化，高效传热，双流多组分系统。

Abstract. *The paper discusses the issues of building physical models that could describe complex multi-phase flows in pipes and channels that occur in a number of heat exchange devices, in particular, during the liquefaction of natural gas. Difficulty in interpretation arises due to the fact that during the movement of a multiphase flow both in the system of the cooled mixture and in the refrigerant, the phases move at different velocities and phase transitions occur. The paper proposes the principle of constructing an equivalent two-pipe circuit with heat exchange, which is controlled by the effective coefficient of thermal conductivity between the walls separating the cooled mixture and the multicomponent refrigerant. As a tool for calculating the behavior of flows in the channel of the cooled mixture and the channel of the refrigerant, a multi-phase flow simulator in a closed pipe system is used.*

Keywords: *Multiphase mixtures with phase transitions, multicomponent refrigerant, gas liquefaction, efficient heat transfer, two-stream multicomponent systems.*

Introduction

Recently, in connection with the development of numerical simulation, an important feature in the creation of modern systems in various branches of science

and technology is the simulation of the behavior of the flow of multiphase mixtures with phase transitions. Examples of such problems are processes in the production of hydrocarbons, liquefaction of gases, filtration and separation in chemical processes, and even problems in medicine in the simulation of inhalation of the respiratory tract. Approaches to the description of physical models of the behavior of multiphase flows are known from the literature, and a number of software products (simulators) for certain processes have been developed [1,2,5,6.7, 10,11,12]. A team of researchers with the participation of the author of the article developed a simulator that describes the behavior of a multiphase flow, taking into account the difference in phase velocities, as well as surface phenomena in pipes [3,4].

Of particular interest is the use of these products for modeling cooling devices, in which, in particular, natural gas is liquefied in the presence of a multicomponent refrigerant, which, in turn, heats up and undergoes phase transitions while moving along the structure. In this case, during the flow in the tube space, the mixture is cooled, and in the outside of the tube space, in which the refrigerant is located, a multiphase flow with phase transitions also occurs, which is initiated by the heat that is taken from the cooled mixture. Thus, two types of multiphase flows are realized with a certain heat exchange between these two flows. In this paper, we propose a physical model for calculating such multiphase two-flow systems based on the developed simulator for a single-flow branched system [3] with the construction of an equivalent system of equations in which the mutual influence of one flow on another is due to heat transfer with an effective thermal conductivity.

Main results and discussions

In the simulator of a single-stream multiphase flow, implemented as part of the development [3], the following assumptions were made, which determine the main properties of the mixture flow model. The presence of two-phase and multicomponent. And at the same time, the mixture can be in two states: liquid and gaseous. Each phase may include several components. It is also assumed that there is heterogeneity, velocity and temperature non-equilibrium, and each phase has its own volume, velocity and temperature. Interfacial interactions (heat and mass transfer, friction) depend on the flow regime (bubble, dispersed-annular, stratified, etc.). Heat exchange with the wall depends on the heat transfer mode (convection, nucleate boiling, heat transfer crisis, transition boiling, film boiling, condensation). Such approaches are usually considered when developing this type of simulators [8,9,13,14,15,16]. Heat transfer in the structural elements of systems can be modeled at the user's choice, both in one-dimensional and two-dimensional approximations. The equation of state, taking into account phase transitions, was developed within the framework of software codes [4], which work in conjunction with a pipe simulator. The system of equations characterizing this type of flow has exchange terms. In particular:

Gas phase continuity equation

$$\frac{\partial}{\partial t}(\alpha_g \rho_g) + \frac{1}{A}\frac{\partial}{\partial z}(A\alpha_g \rho_g V_g) = \Gamma_{iv} + \sum_{n=1}^{Nn} S_n + S_v.$$

Liquid Phase Continuity Equation

$$\frac{\partial}{\partial t}(\alpha_f \rho_f) + \frac{1}{A}\frac{\partial}{\partial z}(A\alpha_f \rho_f V_f) = -\Gamma_{iv}.$$

List of symbols and parameters used in equations:

A – channel flow area, m^2

S – the specific intensity of the "source-drain" phase, non-condensable gases or liquid impurities, $kg \cdot m^{-3} \cdot s^{-1}$

t – time, sec

V_k - speed of phase k, $m \cdot sec^{-1}$

V_{ik} – phase velocity at the interface, $m \cdot s^{-1}$

α_k – the volume concentration of the phase

Γ_{ik} – the specific intensity of mass transfer between the phase and the interface, $kg \cdot m^{-3} \cdot s^{-1}$

$\rho = \alpha_g \rho_g + \alpha_f \rho_f$ – coolant density, $kg \cdot m^{-3}$

ρ_k – phase density, $kg \cdot m^{-3}$

θ -angle of inclination of the channel to the horizontal

τ – the time step, s

Subscripts

f are liquid phase parameters, g are gas phase parameters

i – parameters at the interface, k – phase identifier (f, g)

n - parameters of non-condensable gases, s - parameters in saturation state

To close the entire system of equations, the equations of the laws of conservation of momentum and energy are used. Let's note that when calculating two-phase flows, it is necessary to correctly describe the interfacial friction. Since interfacial friction is described by correlation relations, it is necessary to verify the implemented friction model. Verification of interfacial friction models was carried out by comparison with experimental data published in [11,12,13,14]. In particular, the article [12] presents the data of two series of experiments on a straight horizontal pipe:

In a problem with two multiphase flows that do not mix, but exchange heat flows, which significantly affects the mutual transformation of multiphase flows. For the first stream, which is cooled by the influence of the second, this process leads to a gradual transition to the liquid phase, while the second stream heats up and vice versa, it undergoes a transition to the gas phase.

The figure shows a radial section of a real cooling system and its equivalent two-pipe version. In this case, the calculated heat flow occurs using the effective thermal conductivity coefficient, which takes into account the effective increase in

the contact surface. There is a variant of calculating two flows using a multiphase simulator and the formation of conditions at the boundaries, taking into account heat transfer with an increased thermal conductivity.

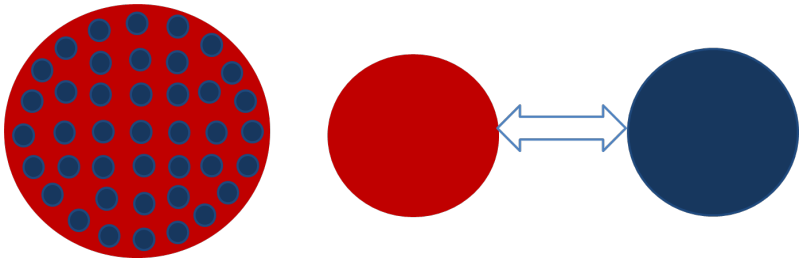

Figure 1. *Radial Section of a Dual Flow Cooler and an Equivalent Heat Exchange Two Pipe System*

With this approach, it is possible to correctly calculate all the mass and energy characteristics of the two flows, and the thermal interaction is modeled both by correctly taking into account the temperature difference in the flows and the effective thermal conductivity of the walls. Such a calculation system makes it possible to model such a rather complex structure within the framework of an engineering methodology.

Conclusion

Modeling of two-stream multiphase systems with phase transitions, in which the flows do not mix, but are in a state of heat exchange, is a complex physical and mathematical problem. The paper proposes an engineering method for calculating such systems using a pipe simulator of a multiphase flow, which is used to calculate each flow with the presence of a thermal calculation for the exchange of thermal energy using an effective thermal conductivity coefficient that takes into account the developed heat exchange surface.

References

1. Nigmatulin R.I. Dynamics of multiphase media. M.: Nauka, 1987.

2.V. DE HENAUT , G. D. RAITHBY. A STUDY OF TERRAIN-INDUCED SLUGGING IN TWO-PHASE FLOW PIPELINES. Department of Mechanical Engineering, University of Waterloo, Waterloo, Ontario, Canada N2L 3GI (Received 28 April 1994; in revised form 4 November 1994).

3. Kibkalo A.A., Bashurin V.P., Kibkalo A.A., Myshkin A.S., Degtyarenko N.N., Vankov A.V., Ktitorov A.L., Danilov A.G., Zhigalov V.I. TUBE YYDRO

SIMULATION 2.0, Computer program registration certificate 2021616704, 04/26/2021

4. Zhigalov V.I., Kibkalo A.A., Baturin V.P., Vankov A.V., Danilov A.G., Degtyarenko N.N., Ktitorov L.V., Kibkalo A.A., Myshkin A.S., Pletenev F.A., Rogozhkin I.G., Ukhanov O.S., Khabibulin M.M., Shvedov A.V. The concept of end-to-end hydrodynamic modeling "well-reservoir" system Oil. Gas. Innovations. 2019. No. 12 (229). pp. 38-43.

5.D. Bestion. The Physical Closure Laws in CATHARE code. Nuclear Engineering and Design, 124, 1990.

6. V. I. Zhigalov, A. A. Kibkalo, V. P. Bashurin, A. Kibkalo, A. S. Myshkin, N. N. Degtyarenko, A. V. Van'kov, and L. V. Ktitorov, Russ. Fluid PVT TCC 2.0. Certificate of state registration of the computer program No. 2020615213 dated May 19, 2020

7. Kostyukov V. E., Zhigalov V. I., Kibkalo A. A., Bashurin V. P., Danilov A. G. Model of transport of a multiphase fluid with nonequilibrium interfacial exchange, Scientific and technical collection of Vesti gazovoy nauki, 2020. No. 2(44). From 175-180.

7. Okava T., Yoneda K., Znou S., Tabata H. New Interfacial Drag Force Model Including Effect of Bubble Wake. Nucl. Sci. Tech. Vol. 36, No. 11, p.1030-1040, 1999

8. I. Kataoka, M. Ishii. Drift flux model for large diameter pipe and new correlation for pool void fraction Int. J. Heat Tranafer 30, (9), 1987.

9. D. Bestion. The Physical Closure Laws in CATHARE code. Nuclear Engineering and Design, 124, 1990.

10. Wallis G.B. Annular two-phase flow—Part 1: a simple theory // ASME J. Basic Eng. - 1970 – Pp.59- 72.

11. Ottens M., Hoefsloot H. C. J., Hamersma P. J. Correlations Predicting Liquid Holdup and Pressure Gradient in Steady State Nearly Horizontal Cocurrent Gas-Liquid Pipe Flow // Institution of Chemical Engineers, Trans. of IchemE – 2001. - vol. 79 - pp. 581-592.

12. Hart J., Hamersma P .J., Fortuin J.M.H. Correlations predicting frictional pressure drop and liquid hold-up during horizontal gas-liquid pipe flow with a small liquid hold-up // Int. J. Multiphase Flow - 1989 - 15(6): 947- 864.

13. Badie S., Hale C.P., Lawrence C.J., Hewitt G.F. Pressure gradient and holdup in horizontal two-phase gas–liquid flows with low liquid loading. // Int. J. Multiphase Flow 2000. - 26, 1525–1543.

14. Thomas J. Danielson .Transient Multiphase Flow: Past, Present, and Future with Flow Assurance Perspective Thomas J. Danielson ConocoPhillips, 600 North Dairy Ashford, Houston, Texas 77079, United States*

15. Mack Shippen. William J. Bailey. Steady-State Multiphase Flow□Past, Present, and Future, with a Perspective on Flow Assurance Schlumberger SIS, Houston, Texas 77056, United States Schlumberger−Doll Research, Cambridge, Massachusetts 02139, United States

16.Richard Saurel Rémi Abgrall.A Multiphase Godunov Method for Compressible Multifluid and Multiphase Flows Computational Physics · April 1999 DOI: 10.1006/jcph.1999.6187 Polytech Marseille University of Zurich

DOI 10.34660/INF.2023.48.97.068

无核原子内部结构的证据
EVIDENCE OF THE INTERNAL STRUCTURE OF A NUCLEAR-FREE ATOM

Belashov Alexey Nikolaevich
Theoretical Physicist
ORCID 0000-0002-4821-8004

抽象的。 这篇文章致力于证明无核原子的内部结构，它基于德国实验物理学家 Philipp Eduard Anton von Lenard 于 1903 年开发的原子动力学模型。这种无核原子模型部分类似于太阳系行星结构的行星模型，其中将太阳系行星保持在其轨道上的主要功能是由外层空间物质或 旧名称“宇宙以太”。 在无核原子中，这种功能是由所研究物质体的物质执行的，它具有自己的密度和不同数量的中性粒子“dynamide”，在现代解释中，这种表达可以定义为“电子偶极子” ”。

关键词：原子内部结构，原子非核结构，反驳原子结构核模型，原子电子。

Abstract. *The article is devoted to the proof of the internal structure of a nuclear-free atom, which is based on the dynamic model of the atom developed in 1903 by the German experimental physicist Philipp Eduard Anton von Lenard. This model of a nuclear-free atom partially resembles the planetary model of the structure of the planets of the solar system, where the main function of keeping the planets of the solar system in their orbits is performed by the substance of outer space, or by the old name “cosmic ether”. In a nuclear-free atom, this function is performed by the substance of the studied material body, which has its own density and a different number of neutral particles “dynamide”, in the modern interpretation, this expression can be defined as “electronic dipoles”.*

Keywords: *internal structure of the atom, non-nuclear structure of the atom, refutation of the nuclear model of the structure of the atom, electrons of the atom.*

Mankind has been trying for many centuries to understand how our world works. In the beginning, all the knowledge acquired by man formed the ancient science of astronomy. With the development of knowledge, humanity began to learn what our inner world consists of, forming the natural and physical sciences. The science of the knowledge of our microworld has gathered many founders and followers. It is very difficult to note all the scientists who have dealt with and are now dealing with these problems taking place on our planet, so we will highlight some of the works of scientists that relate to this scientific article.

At the end of the 19th and the beginning of the 20th centuries, many new scientific discoveries occurred, which forced to reconsider a number of basic provisions of Newton's classical physics, who was far ahead of several generations of his followers in his scientific insights, and established a new view of this world. An opponent of the theory of relativity and changes in the direction in the study of physics was the winner of the Nobel Prize in Physics in 1905, for research work on cathode rays, Philipp Eduard Anton von Lenard, a German experimental physicist, author of many works in the field of solid state physics and atomic physics. In 1936, Lenard's textbook German Physics in Four Volumes was published. He described only areas of classical physics and did not deal with either quantum mechanics or the theory of relativity. The discoveries of modern physics were explained using the theory of the ether and the atomic model of Johann Stark.

It should be noted that Lenard, based on the measurement of the absorption of cathode rays, developed in 1903 his dynamid model of the atom, according to which the atom was, in general terms, "empty", and in this atom there were identical neutral particles "dynamides" of small volume, consisting of an electron and a strongly bound positively charged particle. With this model, Lenard for the first time refuted the then dominant idea of the atom as a massive homogeneous object. Leonard's model was the forerunner of Rutherford's 1910 and 1911 planetary model of the atom, which he developed from his experiments on alpha particle scattering.

It must be emphasized that an atom cannot be empty, where there are identical neutral particles "dynamides" of small volume, consisting of electrons and positively charged particles strongly connected with them, which are in the substance of a material body having a different number and different power, which can be proved by specific examples based on the laws of physics.

The first models of the structure of the atom appear at the very beginning of the 20th century. The French physicist Jean Baptiste Perrin in 1901 suggested a nuclear-planetary structure of the atom. The model of the structure of the atom was widely used in 1902 by the cake model of the atom by the British physicist, mechanic and engineer William Thomson, who suggested that the atom is a bunch of positively charged matter, inside which electrons are evenly distributed. A similar model was proposed in 1904 by the Japanese physicist Hantaro Nagaoka. A detailed model of the structure of the atom was developed by the English physicist Joseph John Thomson, who believed that the electrons inside a positively charged substance are located in the same plane and form concentric rings and proposed a method for determining the number of electrons in an atom, based on the scattering of X-rays, based on the assumption that electrons should be scattering centers. Experiments have shown that the number of electrons in the atoms of elements is approximately half the size of the atomic mass. Joseph John Thomson suggested

that the number of electrons in an atom continuously increases when moving from element to element, for the first time he tried to connect the structure of atoms with the periodicity of the properties of elements.

The basis of the modern theory of the structure of the atom is the planetary model, supplemented and improved. According to this theory, the nucleus of an atom consists of protons (positively charged particles) and neurons (uncharged particles). And around the nucleus, electrons (negatively charged particles) move along indefinite trajectories.

Scientists who adhere to these views on the given structure of the atom need to answer one elementary question who inside each atomic nucleus determines the chemical composition and properties of the material under study, the number of rotating electrons and distributes them over different levels, for example, during the melting of copper and zinc in various proportions.

For convincing evidence of the internal structure of the structure of the atom, we will use a visual device depicted in figure 1 having a tank 1 with a base 2 filled with liquid 3, where the liquid of the tank can contain different densities.

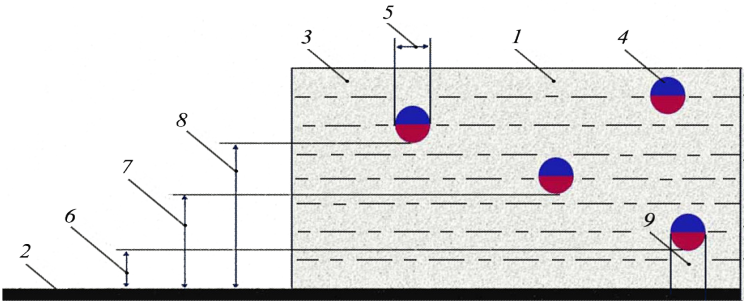

Figure 1.

Inside the liquid 3, at different levels, there are a different number of semi-submerged floats 4. Composite semi-submerged floats 4 have a different diameter 5 and consist of cork and lead. At the first level 6 inside the tank 1 there are a different number of semi-submerged floats 4. At the second level 7 inside the tank 1 there are a different number of semi-submerged floats 4. At the third level 8 inside the tank 1 there are a different number of semi-submerged floats 4. The mass and volume of the composite semi-submerged floats 4 are at different levels inside the tank 1 is equal to the mass and volume 9 of the liquid 3 located between the lower base of the semi-submerged float 4 and the base 2. Moreover, it should be noted that when replacing the liquid 3 in the tank 1 having a different density, the levels between the composite semi-submerged floats 4 and the base 2 will change tank 1.

This circumstance, in which composite semi-submerged floats can be compared with the location of the “electronic dipoles” of the atom at different levels and the location of the planets of the solar system in their orbits.

Indeed, the model of the atom in some way corresponds to the planetary structure of the planets of the solar system. The planets of the solar system are kept in their orbits with the help of the substance of outer space “cosmic ether” emanating from the surface of the Sun. The matter of the substance of outer space emanating from our star has its own composition, mass, density and energy, which is distributed throughout the solar system, holding and connecting all cosmic bodies in their orbits. Inside the atom, “electronic dipoles” interact with each other using the forces of gravitational attraction, counter forces and interaction forces that can be determined according to the new laws of physics discovered by A.N. Belashov.

However, the atom has a great difference from the planetary system, since the atom does not have a nucleus. The main function of keeping the planets of the solar system in their orbits is the substance of outer space or, according to the old name, “cosmic ether” emanating from our star. In the atom of figure 2, this function is performed by the substance of the investigated material body 1 given by the chemical and physical properties of the investigated material having its own density and a different number of neutral particles 2 “dynamide”. As mentioned earlier in the modern interpretation, this expression can be defined as “electronic dipoles”, as pointed out by the German experimental physicist Philipp Eduard Anton von Lenard.

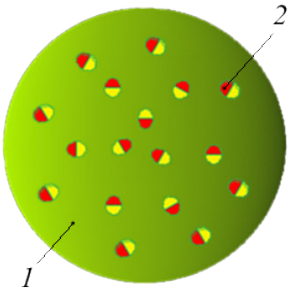

Figure 2.

It should be emphasized that after a detailed study of new discoveries explaining the mechanism of formation of the Sun’s magnetic field, the mechanism of formation of the substance of outer space, the mechanism of movement of the planets of the Solar System around the Sun and the law of determining the distance from the surface of the Sun to any planet of the Solar System, it becomes clear

that the previously approved model of the structure atom is not consistent. In fact, the model of the atom, which was proposed by the German experimental physicist Philipp Eduard Anton von Lenard, is the most relevant. An atom, according to the Lenard model, consists of neutral particles "dynamide" in the translation into modern language "electronic dipoles" located in the substance of various materials having different physical and chemical properties, having different properties and different density of the substance of the material under study. According to this model of the structure of the atom, it is easy to explain the electrical, electromagnetic and dielectric properties of any material. According to the new laws of forces of gravitational attraction, forces of reaction and interaction, it is possible to determine the different forces that arise between "electronic dipoles", as well as to understand the mechanism of movement of electric charges through a conductor or semiconductor, it is easy to explain the mechanism of diffusion between different metals during their long contact, and so on...

The most important thing in the structure of such an atom is that the studied materials, different in physical properties, having different densities, when they are fused, a new material is formed with different physical and chemical properties of the material. It must be remembered that in any atom there is no nucleus, which, as it were, should be responsible for the chemical and physical properties of this material, and even in their percentage and a different number of "electronic dipoles" that are distributed over different levels.

In my opinion, the atomic model proposed by the German experimental physicist Philip Eduard Anton von Lenard is closer to reality. The atom, according to Lenard's model, consists of neutral particles "dynamide", each of which is an electric doublet. The calculations performed by Lenard showed that these particles must have extremely small dimensions, and, consequently, most of the volume of the atom is a void. The concentration of the mass of an atom in a small part of its volume was partly confirmed by the experiments carried out by Leonard in 1903, in which a beam of fast electrons easily passed through a thin metal foil.

Another important discovery capable of proving the mechanism of rotation of the planets of the Solar System around the Sun was the discovery of the constant of the substance of outer space or the density of the outer space medium = 0.3 126005345650193429716951029921 5 kg/m^3, which was popularly presented in the scientific journal Higher School in September 2017. However, many cannot understand what physical quantities the "ether" or the substance of outer space consists of, although many physical quantities and components have been known since ancient times.

The existence of the ether located in outer space for many centuries excited the minds of scientists and thinkers of antiquity. This phenomenon of nature remains relevant at the present time, as there are fierce disputes between modern scientists

who adhere to different scientific concepts. In the scientific community, there are many disputes not only about the existence of the ether, but also about the exact definition of the name of this natural phenomenon, since each scientist puts a different concept into this word. This phenomenon of nature has many interpretations and is not fully known, and no one can give clear and affirmative mathematical evidence for the existence of the ether in outer space.

In the old theories, physicists called the substance of outer space "ether", which expresses a special continuous medium that fills the entire world space. Now many scientists call it "cosmic ether" as the basic physical matter of the Universe, which fills the entire physical space and is the medium of all physical phenomena. In my opinion, this phenomenon of nature must be called the substance of outer space expressing matter, which has its own composition, its mass, density and energy in the unity of the forms of its movement as the carrier of this phenomenon. Moreover, the substance of outer space is not homogeneous and consists of many different physical quantities and components that interact with each other, creating an environment in which not only the solar system, but the entire universe is located.

It is necessary to emphasize that inside the "ether" or the substance of outer space, electrically charged particles are interconnected by the forces of interaction of two point charges located in vacuum. Now the word corpuscle, which was proposed by Isaac Newton, can be supplemented with modern words. Such elements as molecule, atom, photon, electron, neutrino, meson, quark, antiquark, pion, kaon, tetraquark, hadron, proton, neutron. However, the percentage ratio of all substances, their number and combination, which are part of the substance of outer space or "ether", which are constantly transforming during their movement, no one will ever know, since we still do not know well how our microworld is arranged and interacts with each other.

Scientists who do not recognize this natural phenomenon will have to agree or answer one elementary question about how about 5,200 tons of cosmic dust are deposited on the surface of our planet every year from the cosmic vacuum and why they are looking for them in the depths of our planet behind ancient artifacts of human activity.

The matter of the substance of outer space has its own composition, mass, density and energy, which is evenly distributed throughout the Universe, holding and connecting all cosmic bodies in their orbits. The substance of outer space of different systems of the Universe has a different physical value, which smoothly passes from one medium to another. After the discovery of the constant of the substance of outer space, it became clear that the substance of the outer space of the solar system can unite material bodies of different groups in one medium. The material bodies of the solar system include not only terrestrial, but also space objects. From the new laws of physics, it is possible to determine and prove the

physical composition of the substance of outer space. These mathematical proofs are needed for a better understanding of the development of all processes taking place in the Solar System of our Galaxy, which is an integral part of our Universe.

It is necessary to emphasize the basic laws, mechanisms and forces that contribute to the movement of the planets of the solar system strictly along their orbits in the substance of outer space.

It should also be noted that the discovery of the reciprocal speed constant of light became possible after the discovery of a new law of the force of interaction of two point charges located in a vacuum, a new law of the force of the source of an electric charge passing through a conductor, and a new law that determines the speed of movement of an electric charge at a given point of the trajectory.

Mathematical evidence for the existence of "cosmic ether" or the substance of the outer space of the solar system is popularly presented in the scientific information and analytical journal "Actual problems of modern science", No. 1 for 2021, "Sputnik" + publishing house, Moscow city.

The magnetic field of the Sun, its rotation and the formation around it of the acceleration of free fall of bodies in space are popularly described in the scientific information and analytical journal "Actual problems of modern science", No. 6 for 2022, "Sputnik" + publishing house, Moscow city.

According to the new law, we have established that the new physical quantity that determines the acceleration of free fall of bodies in the space of the solar system = 0.000836759790836120401337792642140 48 m/s².

The new law for determining the distance from the surface of the Sun to any surface of the planets of the solar system is presented in a popular form in the scientific and practical journal Higher School No. 17 for 2018, "Infiniti" Publishing House, Ufa.

The mechanism of formation of gravitational forces and the new law of acceleration of free fall of bodies in space was presented in the international research journal, No. 2-9, 2013. "Impeks" Publishing house, the city of Yekaterinburg. The article describes the mechanism of the origin of the resulting force, which is directed to the center of the Belashov intermediate layer at a small angle.

The new law of gravitation of one material body located in the space of the solar system to the central star of the Sun was outlined in the scientific and analytical journal "Scientific Perspective", No. 1-35 for 2013. "Infiniti" Publishing house, Ufa.

The new law of gravity between two material bodies located in the space of the solar system was presented in the scientific and methodological journal "Problems of Modern Science and Education", No. 1-15 for 2013. "PresSto" Publishing house, the city of Ivanovo.

The new law for determining the acceleration of free fall of bodies in space on the planets of the solar system was popularly presented in the scientific journal

“Postgraduate Student and Competitor” No. 5 for 2018. “Sputnik +” Publishing house, Moscow.

The new law for determining the distance from the surface of the Sun to any surface of the planets of the solar system is presented in a popular form in the scientific and practical journal Higher School No. 17 for 2018, “Infiniti” Publishing House, Ufa.

The reciprocal speed constant of light was presented in a popular form in the scientific and analytical journal “Scientific Observer”, No. 1-25 for 2013. “Infiniti” Publishing house, Ufa.

Additions that refute the law of universal gravitation and the gravitational constant are set out in the scientific information and analytical journal “Actual Problems of Modern Science” No. 2 for 2019. “Sputnik +” Publishing house, Moscow

The mechanism of formation of gravitational gravitational forces, cosmic counteraction forces and cosmic interaction forces are set out in the scientific journal “Postgraduate Student and Competitor” No. 1 for 2019. Publishing house “Sputnik +”, Moscow.

The forces of gravitational attraction between two material bodies located in the space of the solar system were presented in the scientific and practical journal “Higher School” No. 12 for 2018. “Infiniti” Publishing house, Ufa.

Additions to the discovery of the reciprocal speed of light constant and the refutation of the postulates and Einstein’s law are presented in the scientific journal “Postgraduate Student and Competitor” No. 1 for 2019. Publishing house “Sputnik +”, Moscow.

It should be emphasized that after a detailed study of new discoveries explaining the mechanism of formation of the Sun’s magnetic field, the mechanism of formation of the substance of outer space, the mechanism of movement of the planets of the Solar System around the Sun and the law of determining the distance from the surface of the Sun to any planet of the Solar System, it becomes clear that the previously approved model of the structure atom is not consistent. In fact, the model of the atom, which was proposed by the German experimental physicist Philipp Eduard Anton von Lenard, is the most relevant. An atom, according to the Lenard model, consists of neutral particles “dynamide” in the translation into modern language “electronic dipoles” located in the substance of various materials having different physical and chemical properties, having different properties and different density of the substance of the material under study. According to this model of the structure of the atom, it is easy to explain the electrical, electromagnetic and dielectric properties of any material. According to the new laws of forces of interaction, counteraction and interaction, it is possible to determine the different forces that arise between “electronic dipoles”, as well as to understand the mechanism of movement of electric charges through a conductor or semicon-

ductor, it is easy to explain the mechanism of diffusion between different metals during their long contact, and so on...

The most important thing in the structure of such an atom is that the materials under study, different in physical properties, having different densities, when they are fused, a new material is formed with different physical and chemical properties of the material. It must be remembered that in any atom there is no nucleus, which, as it were, should be responsible for the chemical and physical properties of the material under study, and even for the number of electrons that must be distributed to different levels. The substance of the studied material is responsible for the chemical and physical forces of the material under study, which distributes "electronic dipoles" depending on their volume, density and energy status at different levels. When changing the density of the substance of the material under study, the number of "electronic dipoles" changes depending on their volume, density and energy status, which occupy their position at different levels, which is popularly shown in Fig.1.

As a result, the essential unity between the planets of the solar system and atoms is that the density of the substance of outer space "cosmic ether", together with the forces of gravitational attraction, forces of interaction and forces of opposition, keeps the planets of the solar system in their orbits, where each planet has its own volume and density. In an atom of any material body, "electronic dipoles" are distributed over their levels depending on the density, volume and their energy state with the help of the density of the substance of the studied material body and the force of gravitational attraction, the interaction force and the counteraction force. Moreover, in a structured atom, the first level can contain an even or odd number of "electronic dipoles" interconnected.

In conclusion, we can say that our material world is very diverse and all the processes performed in it from random circumstances that occur in time affect one another to a different extent, therefore a new theory of multifaceted dependence is put forward. In this world, everything is intertwined, and one natural phenomenon is dependent on another to a different extent. More active material bodies dominate less active material bodies, therefore there cannot be independent and constant constants, laws or physical quantities. For example, the new law of gravitational attraction and cosmic interaction between two material bodies located in the space of the Solar System or another system is closely related to the new law of gravitational attraction of one material body located in the space of the Solar System to the central star of the Sun. At the same time, the laws of gravitational attraction and cosmic interaction are in constant dependence on the new law of activity of a material body located in space and the new law of free fall acceleration of bodies in space. And the listed laws are closely connected with the new law of energy between two material bodies that are in the space of the solar system and

the new law of energy of one material body located in the space of the solar system, to the central star the Sun and many others...

References

1. Belashov A.N. "New views on the model of the internal structure and structure of the atom". Information and analytical journal "Actual problems of modern science", No. 1 for 2023, page 7. "Sputnik +" Publishing house, Moscow. Registration certificate PI No. FS 77-39976 ISSN 1680-2721.

2. Belashov A.N. "Discovery of the mechanism of rotation of the planets of the solar system around the sun". Journal of relevant scientific information "Postgraduate student and competitor", No. 6 for 2022. "Sputnik +" Publishing house, Moscow. Registration certificate PI No. FS 77-39976 ISSN 1608-9014.

3. Belashov A.N. "Reverse speed constant of light". Scientific and analytical journal "Scientific Observer", No. 1-25 for 2013, page 64. "Infiniti" Publishing House, Ufa. Certificate of state registration PI No. FS 77-42040 ISSN 2220-329X.

4. Belashov A.N. "Mechanism of formation of gravitational forces and a new law of acceleration of free fall of bodies in space". International Research Journal, No. 2-9 for 2013, page 7. "Impex" Publishing House, Yekaterinburg. Certificate of state registration PI No. FS 77 - 51217 ISSN 2303-9868.

5. Belashov A.N. "New energy laws of material bodies located in the space of the solar (or other) system". International Research Journal, No. 3-10 for 2013, part 1 page 12. "Impex" Publishing House, Yekaterinburg. Certificate of state registration PI No. FS 77 - 51217 ISSN 2303-9868.

6. Belashov A.N. "A new law of gravitation between two material bodies located in the space of the solar system". International Research Journal, No. 4-11 for 2013, part 1 page 9. "Impex" Publishing House, Yekaterinburg. Certificate of state registration PI No. FS 77 - 51217 ISSN 2303-9868.

7. Belashov A.N. "A new law of gravitation of one material body located in the space of the solar system to the central star". International Research Journal, No. 4-11 for 2013, part 1 page 12. "Impex" Publishing House, Yekaterinburg. Certificate of state registration PI No. FS 77 - 51217 ISSN 2303-9868.

8. Belashov A.N. "The evolutionary development of the planets of the solar system". International Research Journal, No. 7-14 for 2013, part 1 page 14. "Impex" Publishing House, Yekaterinburg. Certificate of state registration PI No. FS 77 - 51217 ISSN 2303-9868.

9. Belashov A.N. "New Views on the Law of Conservation of Energy". Scientific and analytical journal "Scientific Perspective", No. 11-45 for 2013, page 94. Infiniti Publishing House, Ufa. State registration certificate PI No. FS 77-38591 ISSN 2077-3153.

10. Belashov A.N. "Mechanisms for the formation of planets in the solar system". Scientific and analytical journal "Scientific Perspective", No. 9-43 for 2013, page 45. "Impex" Publishing House, Ufa. State registration certificate PI No. FS 77-38591 ISSN 2077-3153.

11. Belashov A.N. "Refutation of the fundamental law of conservation of energy in mechanics and hydrodynamics". International Research Journal, No. 9-16 for 2013, part 1 page 7. "Impex" Publishing House, Yekaterinburg. Certificate of state registration PI No. FS 77 - 51217 ISSN 2303-9868.

12. Belashov A.N. "An explanation of the laws of motion and mutual dependence of the planets of the solar system". Scientific and practical journal "Journal of Scientific and Applied Research", No. 11 for 2015, page 139. "Infiniti" Publishing House, Ufa. State registration certificate PI No. FS 77-38591 ISSN 2306-9147.

13. Belashov A.N. "The law of gravitational attraction between two material bodies". Scientific and practical journal "Journal of Scientific and Applied Research", No. 05 for 2016, page 145. "Infiniti" Publishing House, Ufa. State registration certificate PI No. FS 77-38591 ISSN 2306-9147.

14. Belashov A.N. "The Refutation of the Theory of the Slow Approach of the Planet Earth to the Sun". Scientific and practical journal "Journal of Scientific and Applied Research", No. 07 for 2016, page 106. "Infiniti" Publishing House, Ufa. State registration certificate PI No. FS 77-38591 ISSN 2306-9147.

15. Belashov A.N. "Refutation of the Law of Conservation of Energy and the Gravitational Constant". Scientific and practical journal "Journal of Scientific and Applied Research", No. 08 for 2016, page 72. "Infiniti" Publishing House, Ufa. State registration certificate PI No. FS 77-38591 ISSN 2306-9147.

16. Belashov A.N. "Constant of the substance of outer space". Scientific and practical journal "Higher School", No. 17 for 2017, page 39. "Infiniti" Publishing House, Ufa. Certificate of state registration PI No. FS 77-42040 ISSN 2409-1677.

17. Belashov A.N. "A new value that determines the substance of outer space". Scientific and practical journal "Higher School", No. 18 for 2017, page 27. "Infiniti" Publishing House, Ufa. Certificate of state registration PI No. FS 77-42040 ISSN 2409-1677.

18. Belashov A.N. "A new physical quantity that determines the acceleration of free fall of bodies in the space of the solar system." Scientific and practical journal "Higher School", No. 19 for 2017, page 33. "Infiniti" Publishing House, Ufa. Certificate of state registration PI No. FS 77-42040 ISSN 2409-1677.

19. Belashov A.N. "Mechanism of gravitational attraction of the planets of the solar system". Scientific and practical journal "Higher School", No. 12 for 2018, page 5. "Infiniti" Publishing House, Ufa. Certificate of state registration PI No. FS 77-42040 ISSN 2409-1677.

20. Belashov A.N. "Laws of the energy of the planets of the solar system". Scientific and practical journal "Higher School", No. 14 for 2018, page 88.

"Infiniti" Publishing House, Ufa. Certificate of state registration PI No. FS 77-42040 ISSN 2409-1677.

21. Belashov A.N. "A new law for determining the distance from the surface of the Sun to the surface of the planets of the solar system". Scientific and practical journal "Higher School", No. 17 for 2018, page 49. "Infiniti" Publishing House, Ufa. Certificate of state registration PI No. FS 77-42040 ISSN 2409-1677.

22. Belashov A.N. "New Laws of the Forces of Gravitational Gravitation". Journal of relevant scientific information "Postgraduate student and competitor", No. 4 for 2018, page 48. "Sputnik +" Publishing house, Moscow. Registration certificate PI No. FS 77-39976 ISSN 1608-9014.

23. Belashov A.N. "A new law for determining the acceleration of free fall of bodies in space on the planets of the solar system". Journal of relevant scientific information "Postgraduate student and competitor", No. 5 for 2018, page 48. "Sputnik +" Publishing house, Moscow. Registration certificate PI No. FS 77-39976 ISSN 1608-9014.

24. Belashov A.N. "Discovery of new parameters of planet Earth". Journal of relevant scientific information "Postgraduate student and competitor", No. 6 for 2018, page 48. "Sputnik +" Publishing house, Moscow. Registration certificate PI No. FS 77-39976 ISSN 1608-9014.

25. Belashov A.N. "Discovery of the mechanism of the forces of gravitational attraction, the forces of cosmic counteraction and the forces of cosmic interaction". Journal of relevant scientific information "Postgraduate student and competitor", No. 1 for 2019, page 65. "Sputnik +" Publishing house, Moscow. Registration certificate PI No. FS 77-39976 ISSN 1608-9014.

26. Belashov A.N. "Additions to the refutation of Newton's law of universal gravitation". Information and analytical journal "Actual problems of modern science", No. 2 for 2019, page 106. "Sputnik +" Publishing house, Moscow. Registration certificate PI No. FS 77-39976 ISSN 1680-2721.

27. Belashov A.N. "A Complement to the Discovery of the Inverse Speed Constant of Light and the Refutation of Einstein's Postulates". Journal of relevant scientific information "Postgraduate student and competitor", No. 1 for 2019, page 38. "Sputnik +" Publishing house, Moscow. Registration certificate PI No. FS 77-39976 ISSN 1608-9014.

28. Belashov A.N. "Mathematical evidence for the existence of the cosmic ether or substance of outer space". Information and analytical journal "Actual problems of modern science", No. 1 for 2021, page 33. "Sputnik +" Publishing house, Moscow. Registration certificate PI No. FS 77-39976 ISSN 1680-2721.

29. Belashov A.N. "The law of determining energy within diverse spaces and additions refuting the law of conservation of energy" was discovered. Information and analytical journal "Actual problems of modern science", No. 4 for 2022, page

92. "Sputnik +" Publishing house, Moscow. Registration certificate PI No. FS 77-39976 ISSN 1680-2721.

30. Belashov A.N. "The magnetic field of the Sun, its rotation and the formation around it of the acceleration of free fall of bodies in space." Information and analytical journal "Actual problems of modern science", No. 6 for 2022. "Sputnik +" Publishing house, Moscow. Registration certificate PI No. FS 77-39976 ISSN 1680-2721.

31. A.N. Belashov "Device of rotation of magnetic systems". Description of the application for the invention No. 2005129781 dated September 28, 2005.

32. A.N. Belashov "A new theory of multifaceted dependence", which was formulated as a result of a comprehensive scientific and analytical method of studying the description of the application for invention No. 2005129781 dated September 28, 2005 and the description of the application for invention No. 2012142735 dated October 09, 2012 URL: http://www. belashov.info/LAWS/theory.htm

33. A.N. Belashov "Discoveries, inventions, new technical developments". URL: http://www.belashov.info

34. L.A. Seine. "Units of physical quantities and their dimensions", Ch. ed. of Phys.-Math. lit., for 1988.

35. Yu.A. Khramov "Physicists" biographical guide, Kyiv "Naukova Dumka" 1977.

DOI 10.34660/INF.2023.43.68.069

太阳辐射接收器斯特林发动机参数研究
INVESTIGATION OF THE PARAMETERS OF THE SOLAR RADIATION RECEIVER STIRLING ENGINE

Tursunbaev Zhanbolot Janyshevich
Candidate of Technical Sciences, Associate Professor, Rector
Osh Technological University named after acad. M.M. Adyshev

摘要：对圆柱形空腔散热器给定参数的比较分析表明，尺寸 d = 0.27 和 l = 0.35 m 的空腔散热器对于功率为 3 kW 的 SE 的 SPP 是最佳的。 过大，有效吸收系数达到最高值。 当使用真正的抛物面聚光器和 SE 作为发电厂的一部分时，有必要对聚光器-受热器系统的参数进行相互优化。 为此，需要采取额外的措施来增加调整系数的值。 使用简单形状的圆柱形空腔散热器可以实现调整系数值的增加。 当使用简单形状的散热器时，可以引入额外的装置来协调集中器-散热器系统。

Abstract. *A comparative analysis of the given parameters of a cylindrical cavity heat sink shows that cavity heat sinks with dimensions d = 0.27 and l = 0.35 m are the most optimal for SPP with a SE with a power of 3 kW. are too large, and the effective absorption coefficient reaches the highest value. When using a real paraboloid concentrator and SE as part of a power plant, it is necessary to carry out mutual optimization of the parameters of the concentrator-heat receiver system. For this, it is necessary to take additional measures to increase the value of the adjustment coefficient. An increase in the value of the adjustment coefficient can be achieved using cylindrical cavity heat sinks of simple shapes. When using heat sinks of simple shapes, additional devices can be introduced to coordinate the concentrator-heat sink system.*

An important element of a solar power plant with a Stirling engine (SE) is a solar radiation receiver. It is designed to receive solar radiation, convert it into thermal energy, and then transfer the latter to the working fluid of the Stirling engine. Therefore, the parameters of the receiver of solar radiation, on the one hand, are related to the parameters of the dynamic transducer, and, on the other hand, to the quality of the concentrator. The efficiency of converting concentrated solar radiation into thermal energy transmitted to the working fluid of the engine depends on the design and characteristics of the solar radiation receiver. To determine these

characteristics, it is necessary to analyze the thermal processes occurring in the receiver, taking into account the requirements of the engine and the capabilities of the concentrator.

Receivers that convert the energy of solar radiation into thermal energy (hereinafter referred to as heat receivers), depending on the method of heating the working fluid of the engine, can be volumetric and surface [1]. Usually, heat sinks for volumetric absorption of solar radiation are made of glass. In this case, the flux of solar radiation, passing through a transparent window, enters a closed cavity, where the working fluid is heated. The main advantage of volumetric type heat receivers is a high degree of absorption of solar radiation. However, they are difficult to manufacture and unreliable in operation. Therefore, the use of these heat receivers in power plants with SE is impractical from a practical point of view.

Surface heat receivers are of open and closed types. Open-type heat sinks have high heat losses even with a small working surface. More rational for use in power plants with SE are heat sinks of a closed type, commonly called “cavity” heat sinks [2,3]. In cavity heat receivers, various ratios of the sizes of the holes through which the radiation flux enters, and various configurations of the surface of the cavity for absorbing solar radiation are possible.

The geometrical parameters of the heat receiver, in turn, determine the obtaining of its various optical and thermal characteristics.

The most suitable for a power plant with SE and simple in terms of manufacturing technology are cylindrical cavity. In cylindrical cavity heat receivers of surface absorption, solar radiation is absorbed by the inner surface of the cylinder. At the same time, the temperature of the heat receiver wall can reach up to 600-700 ^{0}C. Heat is transferred to the working fluid by heat transfer between the inner wall of the cylinder and the wall of the heater channel, then by convective heat transfer between the wall of the heater channel and the working fluid. For the operation of the SE, it is necessary that the operating temperatures of the heater and heat sink be within 600-625 ^{0}C. Experience with cavity heat sinks has shown that the most technologically suitable material for its manufacture is I2XI8HIOT GOST 5632-72 stainless steel. Therefore, in our further calculations, we used tabular data on the thermophysical properties of this material.

The sequence of calculating the parameters of cavity heat receivers is conditionally divided by us into two stages. In the first stage, we reveal the mechanism of heat transfer from the heat sink to the working fluid, and in the second stage, by analyzing the heat balance of the system, the heat sink concentrator determines the value of the main parameters of the heat sink.

The first stage of calculating the heat sink is carried out according to the value of the useful heat flux $Q_{p.t.}$, supplied to the working fluid of the engine.

The area of the internal heat transfer surface of the cavity heat sink F_n (м^2), can be calculated from the relation [4]:

$$F_n = \frac{Q_{p.т.}}{K \cdot \Delta T}, \quad (1)$$

where K - heat transfer coefficient;

ΔT - average temperature difference, (W/m2).

The heat transfer coefficient K is determined from the equation

$$K = \left(\frac{1}{\alpha} + \frac{S_1}{\lambda_{м.ст.}} \right)^{-1} \quad (2)$$

where α - heat transfer coefficient of the heat receiver wall (W/m2deg);

S_1 - heat sink wall thickness (m);

$\lambda_{M.CT}$ - thermal conductivity of the heat receiver wall (kJ·s).

The heat transfer coefficient of the heat receiver wall α, included in equation (2) is calculated from the relation:

$$\alpha = \frac{N_u \cdot \lambda}{d_r}, \quad (3)$$

where λ - thermal conductivity of the working fluid (helium) (kJ·s);

$d_г$ - hydraulic diameter of the heater channel (m);

Nu - Nusselt criterion.

The Nusselt criterion, depending on the mode of convective heat transfer from the surface of the heat sink, is determined based on the tabular data of the Reynolds and Prandtl criteria [5] according to the equations:

for free convection

$$Nu = 0{,}17 \cdot \mathrm{Re}^{0{,}33} \cdot \mathrm{Pr}^{0{,}43} \cdot (\mathrm{Pr}_{Ж} \cdot \mathrm{Pr}_{CT.})^{0{,}25} \cdot Gr^{0{,}1} \quad (4)$$

for forced convection

$$Nu = 0{,}021 \cdot \mathrm{Re}^{0{,}8} \cdot \mathrm{Pr}^{0{,}43} \cdot (\mathrm{Pr}_{Ж} \cdot \mathrm{Pr}_{CT.})^{0{,}25}, \quad (5)$$

The value of the average temperature difference ΔT, included in equation (1), is determined from the expression:

$$\Delta T = \psi \frac{(T'_{ст.} - \mathrm{Tmin}) - (T''_{ст.} - \mathrm{Tmax})}{\mathrm{Lg}\frac{T'_{ст.} - \mathrm{Tmin}}{T''_{ст.} - \mathrm{Tmax}}}, \quad (6)$$

where ψ - a dimensionless coefficient depending on the temperature distribution over the internal heat transfer surface of the heat sink F_n;

Тст.' and Тст." - respectively, the temperature of the wall of the heat receiver in the places of supply and removal of heat, ^{0}C;

T_{min} and T_{max} – respectively, the minimum and maximum temperature of the heat receiver wall, ^{0}C.

Calculation formulas for determining the heat supplied to the working fluid and the thermal power supplied to the heat sink are given below.

Calculating the values of the parameters included in equation (1-4), we can determine the approximate value of the heat sink area. Taking the value of the heat transfer surface of the heat sink determined in this way and taking into account the temperatures of the heat sink wall in the places of heat supply and removal, it is possible to perform an optimization calculation of the entire engine to refine its parameters.

The second stage of the calculation includes determining the parameters of the heat sink based on the analysis of the heat balance of the concentrator-heat sink system and heat losses in the heat sink.

The heat balance in the heat sink can be written as follows:

$$Q_{вход} = Q_{р.т.} + Q_{пот.} + \rho_{эф} Q_{вход}, \quad (7)$$

where $Q_{вход}$ - summed up by the concentrator to the heat sink, the focused energy of solar radiation (W);

$Q_{р.т.}$ - thermal energy transferred to the working fluid SE (W);

$Q_{пот.}$ - heat loss from the surface of the heat sink (W);

$\rho_{эф}$ - reflection coefficient of the surface of the heat sink.

The focused energy of solar radiation entering the pupil of the heat sink, supplied by the concentrator, can be determined from the expression

$$Q_{вход} = S_3 \cdot E_{ср} \cdot \eta_{юс}, \quad (8)$$

where S_3 - the area of the entrance pupil of the heat receiver solar radiation (m²);

Ecp. - energy density of focused solar radiation (W/m²·s);

R_3 - reflection coefficient of the concentrator mirrors;

$\eta_{юс}$ - adjustment coefficient showing the proportion of solar radiation flux entering the heat sink opening in the dynamic mode of tracking the Sun.

The heat transferred to the working fluid of the SE can be calculated, in contrast to formula (2), according to the formula obtained on the basis of the Fourier law:

$$Q_{P.T.} = \lambda \cdot \frac{t_{вн} - t_н}{d_н - d_{вн}} \cdot \pi \cdot d_{вн} \cdot h, \quad (9)$$

where λ - coefficient of thermal conductivity;

$d_н$ – the outer diameter of the heat receiver (m);

$d_{вн}$ – the inner diameter of the heat receiver (m);

$t_{вн}$ – temperature of the inner wall of the heat receiver (^{O}C);

$t_н$ – temperature of the outer wall of the heat receiver (^oC);

h – height of the heat sink.

$Q_{пот.}$ - is defined as the sum of heat losses by radiation from the heat receiver cavity and convective losses from the heat receiver cavity and from the outer wall of the thermal insulation determined from the formulas [6,7].

The heat balance component included in equation (7) $\rho_{эф} \cdot Q_{вход}$ determines the loss of initial radiation due to reflection by the cavity.

The reflection coefficient of the surface of the heat sink $\rho_{эф}$ is related to the effective absorption coefficient of the heat sink $\alpha_{эф}$ addiction:

$$\rho_{эф} = 1 - \alpha_{эф}, \quad (10)$$

the effective absorption coefficient of the heat sink is determined from the equation:

$$\alpha_{эф} = \frac{\alpha_\omega}{1-(1-\alpha_\omega)\cdot(1-\varphi)}, \quad (11)$$

where α_ω - coefficient of absorption of the wall material of the heat sink.

To determine the components of the heat balance and the parameters of the heat sink of solar radiation using the above calculation method, an experimental sample of a cylindrical cavity heat sink with d=0,20 m and l =0,27 m (fig.1.) was created for use in the SPP with SE α - modifications with a power of 3 kW. Heat sink absorption surface Fп=0,0792 m^2.

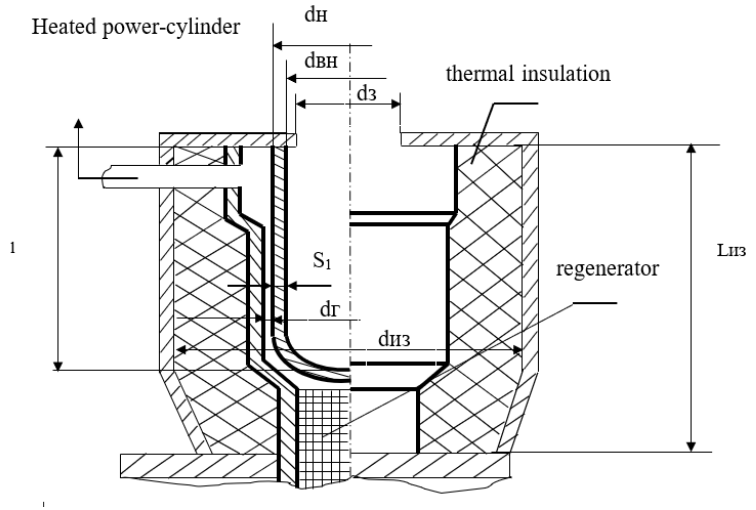

Figure 1. *Calculation scheme of an experimental sample of a cavity receiver of solar radiation*

The heat receiver was heated by an electric heater, and the convective losses were determined experimentally. The convective losses were 460 W with natural convection. At the same time, the following were recorded: temperature in the heat receiver cavity - 625 ^{0}C; the inclination of the axis of the heat receiver cavity to the horizon is 450. The main part of the thermal losses of the heat receiver associated with convection are convective losses from the absorbing surface of the heat receiver. According to our estimates, the losses from the outer wall of the thermal insulation of the heat sink are no more than 20%. For all other values of l and d given in the table, the value of convective losses was approximately expropolated according to the obtained experimental data, for d=0,27 m, l=0,35 m and $Q_{конв} \approx 613\ Bm$.

Knowing the value of the heat supplied to the working fluid of the SE and the efficiency of absorption of solar radiation by the heat receiver, it is possible to calculate the value of the required power of solar radiation, which should enter the entrance pupil of the heat receiver

$$Q_{вход} = \frac{Q_{погл.}}{\alpha_{эф.}}, \qquad (12)$$

Table 1 shows the calculation results φ, $\varepsilon_{эф}$, $\alpha_{эф}$ и $Q_{изл.}$ for various ratios *l/d* of a cylindrical cavity heat sink (T=650 ^{0}C).

Table 1

$\frac{l}{d}$	Sз [$m^2 \cdot 10^{-3}$]	Fп [$m^2 \cdot 10^{-3}$]	φ	$\varepsilon_{эф}$	$\alpha_{эф}$	$Q_{изл.}$ [KW]	$Q_{погл}$ [KW]	$Q_{вход}$ [KW]	$Q_{р.т}$ [KW]	$\eta=Q_{р.т.}/Q_{вход}$
d=0,20 m										
1,27	192,2	769,06	0,25	0,63	0,786	0,428	8,029	8,806	5,250	0,594
1,7	192,2	961,33	0,20	0,68	0,820	0,481	8,064	9,227	5,615	0,608
2,12	192,2	1153,58	0,17	0,72	0,847	0,51	8,092	9,255	5,911	0,639
2,55	192,2	1345,85	0,14	0,75	0,870	0,532	8,114	9,277	6,333	0,682
2,97	192,2	1538,12	0,13	0,77	0,885	0,545	8,127	9,298	6,732	0,724
3,4	192,2	1730,39	0,11	0,80	0,900	0,566	8,149	9,312	6,998	0,751
4,25	192,2	2114,91	0,09	0,83	0,910	0,588	8,170	9,333	7,213	0,772
d=0,27 m										
1,27	341,8	1366,6	0,25	0,63	0,786	0,796	8,634	9,814	6,202	0,631
1,7	341,8	1709,02	0,20	0,68	0,820	0,856	8,688	9,851	6,452	0,654
2,55	341,8	2392,63	0,14	0,75	0,870	0,943	8,787	9,954	6,852	0,688
2,4	341,8	3076,25	0,11	0,80	0,900	1,008	8,850	10,013	7,141	0,713
4,25	341,8	3416,32	0,09	0,83	0,910	1,045	8,887	10,053	7,352	0,731

Table 1 also shows, determined by calculations using formula (13), the values of the average heat load per unit of the absorbing surface of a cylindrical cavity heat sink.

$$K \cdot \Delta T = \frac{Q_{\text{P.T.}}}{F_{\text{п.}}}, \tag{13}$$

Based on the numerical values of the efficiency of a cylindrical cavity heat sink given in Table 1, a curve was constructed depending on the efficiency of the heat sink on the ratio $\frac{l}{d}$ (fig. 2).

The efficiency of the heat sink is calculated from the ratio:

$$\eta = \frac{Q_{\text{р.т.}}}{Q_{\text{вход}}}, \tag{14}$$

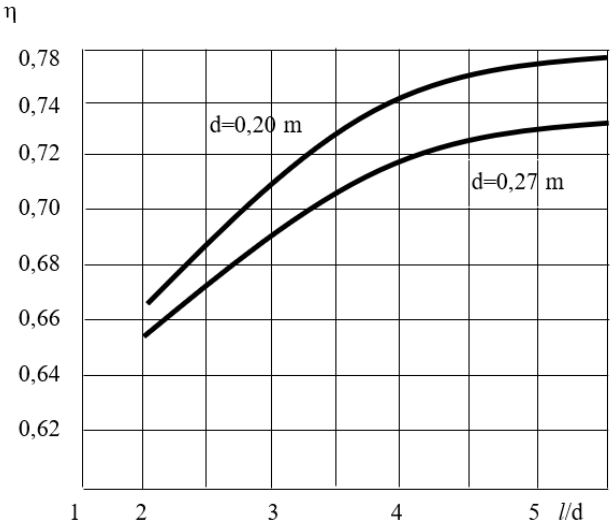

Figure 2. *Changes in efficiency cylindrical cavity heat sink on the l/d ratio.*

A comparative analysis of the parameters of a cylindrical cavity heat sink given in Table 1 shows that cavity heat sinks with dimensions d = 0,27 and *l*=0,35 m. are the most optimal for SPP with a SE with a power of 3 kW. For this case, radiation losses from the absorbing surface of the heat sink are not too large, and the effective absorption coefficient reaches the highest value.

Conclusions: Based on our studies of the concentrator and receiver of solar radiation [6,7], as well as on the basis of the analysis of the numerical values of the

parameters given in Table 1 and the analysis of the dependence of the efficiency of the heat sink on the l/d ratio (Fig. 2.), the following were established:

- The increase $\frac{l}{d}$ is not advisable, because it does not lead to a significant increase in the efficiency of the heat sink, and an increase in the diameter of the cavity significantly increases the energy loss from the cavity and, accordingly, reduces the efficiency of the heat sink;
- The deterioration of the quality of the concentrator and the accuracy of the tracking system leads to the forced need to increase the entrance pupil of the heat sink. The increase in the entrance pupil of the heat sink is one of the main factors that reduce the efficiency of the concentrator-heat sink system. The diameter of the entrance pupil of the cavity heat sink should be selected based on the assessment of the quality of the concentrator and taking into account the performed computational and experimental analysis.
- When using a real paraboloid concentrator and SE as part of a power plant, it is necessary to carry out mutual optimization of the parameters of the concentrator-heat receiver system. For this, it is necessary to take additional measures to increase the value of the adjustment coefficient $\eta_{\text{тос}}$. An increase in the value of the adjustment coefficient can be achieved using cylindrical cavity heat sinks of simple shapes. When using heat sinks of simple shapes, additional devices can be introduced to coordinate the concentrator-heat sink system.

References

1. Putilov K.N. Thermodynamics [Text] / K.N. Putilov. – M.: "Nauka", 1971.– 374 p.

2. Stirling engines / Col. articles under. ed. Brodyansky V.M. - M., 1975. - 253 p.

3. Trukhov V.S. Calculation of the parameters of the internal heat exchange circuit of the Stirling engine [Text] /V.S.Trukhov, I.A.Tursunbaev, G.Ya.Umarov. – Tashkent: "Fan", 1975. - 77 p.

4. Grilikhes V.A. Solar high-temperature heat sources for spacecraft [Text] / V.A. Grikhiles, V.M. Matveev, V.P. Poluektov. - M.: Mashinostroenie, 1975. – 434 p.

5.Leach C.E., Fryer B.C., A7, 3 kW (e) radioisotope energized udder sea Stirling engine // IECES.- 1968 - p. 927. - p. 830-844.

6.Tursunbaev Zh.Zh. Analysis of the energy balance of an autonomous solar power plant [Text] / I.G. Kenzhaev, Zh.Zh. Tursunbaev, B.E. Kuzhaiberdiev. – Bishkek: // Problems of management and informatics: Proceedings of the international conference. - 2000. – 505 p., (p. 454-458).

7.Tursunbaev Zh.Zh. Use of a parabolic trough heliocollector in the heat supply system of a biogas reactor [Text] / [O.M.Osmonov, I.G. Kenzhaev, Zh.Zh. Tuprsunbaev and others]. – Bishkek. // Scientific works of the South Ossetian Academy of Sciences of the Kyrgyz Republic. – 2003. - No. 3. – 296 p., p. 102-116.

DOI 10.34660/INF.2023.77.37.070

技术装置“蒸汽喷头”的有效性研究
RESEARCH ON THE EFFECTIVENESS OF THE TECHNICAL DEVICE «STEAM SPRINKLER»

Mamatalieva Flora Turkmenovna
Candidate of Biological Sciences

Kamilova Lola Toktamuratovna
Candidate of Geographic Sciences
Kyrgyz-Uzbek International University named after B. Sydykov

Samieva Zhyrgal Toktogulovna
Doctor of Biological Sciences, Associate Professor, Director
Institute of Innovative Technologies,
Kyrgyz-Uzbek International University named after B. Sydykov

Smailov Eltar Ablametovich
Doctor of Agricultural Sciences, Full Professor
Kyrgyz-Uzbek International University named after B. Sydykov

抽象的。 为检验“蒸汽喷头”在生产条件下的效果，对某砖厂烘房污染物排放进行了专项对比试验。 来自干燥室和窑炉的废气没有得到足够的清洁，从而导致烟雾和煤烟。 污染物排放总量中：20%来自窑炉，55.5%来自隧道窑和烘干机，20%来自窑炉，还有1000台。 砖释放高达 750 公斤的蒸汽水分。 为了清除有害排放的烟气，我们开发并实施了一种安装在污染源上的新技术装置“蒸汽喷头”。 采用新开发的技术装置“蒸汽喷头”去除废气，污染物净化率可达80%，即污染物浓度从4.97 mg/m3降至1.11 mg/m3。

关键词：蒸汽喷头、污染物、煤固体、硫氧化物、一氧化碳、氮氧化物、砖窑、窑炉、效率。

Abstract. *To test the effectiveness of the “Steam Sprinkler” under production conditions, special comparative tests were carried out on the emission of pollutants from the drying chambers of a brick factory. Exhaust gases from drying chambers and kilns are not cleaned enough, which leads to smoke and gas sooting. Of the total amount of pollutants emitted: 20% from kilns, 55.5% from tunnel kilns and dryers, 20% from kilns, and also from 1000 pcs. of bricks is released up to 750 kg of vaporous moisture. To clean flue gases from harmful emissions, we have developed and implemented a new technical device “Steam Sprinkler” installed*

on pollutant sources. The use of the newly developed technical device "Steam Sprinkler" on the way of exhaust gases removal contributes to the purification of pollutants up to 80%, or the concentration of pollutants decreases from 4.97 mg/m3 to 1.11 mg/m³.

Keywords: *steam sprinkler, pollutants, coal solids, sulfur oxide, carbon monoxide, nitrogen oxide, brick kilns, kilns, efficiency.*

Introduction

To test the effectiveness of the "Steam Sprinkler" under production conditions, special comparative tests were carried out on the release of pollutants from the drying chambers of a brick factory firing and the amount of pollutants emitted from the drying chambers of the brick factory No. 1, while taking into account the following types of pollutants. Below are well-known brief characteristics of the main types of pollutants we studied:

Solid particles of coal are black brittle solids (ash, soot), with a molecular weight of 48.0634 g/mol active carbon, in the form of particles of a fraction of 1-2 mm [2].

Sulfur oxide (sulfur dioxide, sulfur dioxide, SO_2) is a combination of sulfur and oxygen, which in normal conditions has a depressing effect on human health. Plants near sources of sulfur oxide are usually densely dotted with small necrotic spots formed at the sites of sedimentation of sulfuric acid droplets, which proves its presence in the environment in significant quantities [3].

Carbon monoxide (CO) - binary chemical compounds of carbon with oxygen or carbon monoxide, colorless, slightly sour in taste, which reduces hemoglobin to carry and supply oxygen. Extremely toxic, the degree of impact on the human body depends not only on its concentration, but also on the time spent by a person in charged air. Carbon monoxide can be poisonous and is the single most common cause of poisoning in both industrial and domestic settings. Thousands of people die every year as a result of CO intoxication [4].

Nitrogen oxides (NO_2) is a binary inorganic compound of nitrogen and oxygen, molecular weight 30.0061 g/mol, density 1.3402 kg/m³. It is a poisonous gas with a sharp unpleasant suffocating odor. It leads to a drop in blood pressure and the development of disgust characteristic of household waste [5].

Research results

To test the effectiveness of the "Steam Sprinkler" under production conditions, special comparative tests were carried out on the emission of pollutants in the brick firing zone, the results of which are presented in tables 1-3. (Table 1 - the amount of pollutants emitted from the kiln of the brick plant No. 1, before the installation of the Steam Sprinkler, Table 2 - the amount of pollutants emitted from the kiln of the brick plant No. 1, after the installation of the Steam Sprinkler, Table 3 – summary before and after the installation of the "Steam Sprinkler" [6].

Table 1 shows that the amount of pollutants emitted only from the kiln of brick factory No. 1, on average for one year, is 51.09 tons, including solid particles of coal - 13.96 tons, which is 27.32% of the total emitted pollutants in one year, and, accordingly, sulfur oxide (SO_2) - 21.83 tons or 42.73%, carbon oxides (CO) - 12.45 tons or 24.37%, and nitrogen oxides (NO_2) - 2.85 t/year or 2.85%. After the installation and operation under production conditions of the new technical device "Steam Sprinkler", the amount of pollutants emitted only from the kiln of brick factory No. 1 decreased to 11.32 t/year - including solid particles of coal - 3.85 t or 34.01% of the total pollutant emissions for one year after the installation of a new technical device "Steam sprinkler", respectively, sulfur oxide (SO_2) - 4.35 tons or 38.42%, carbon oxides (CO) - 2.56 tons or 22.62%, and nitrogen oxides (NO_2) – 0.56 t/year or 4.95%.

Table 1.

The amount of pollutants emitted from the kiln of the brick plant No. 1, before the installation of the "Steam Sprinkler"

Name of pollutants	**Quantity, t/year**								
	2016			**2017**			**2018**		
	I	**II**	**III**	**I**	**II**	**III**	**I**	**II**	**III**
Solid particles of coal	13,8	13,76	13,75	13,89	13,9	13,91	15,11	15.10	15,12
Sulfur oxides (SO_2)	20,66	20,67	20,65	23,15	23,13	23,17	25,01	25,0	25,02
Oxides of carbon (CO)	12,28	12,32	12,3	12,39	12,41	12,4	12,65	12,64	12,66
Nitrogen oxides (NO_2)	2,82	2,83	2,81	2,88	2,89	2,87	2,90	2,89	2.91
							2012	2013	2014
Assessment of the significance of the main effects:						HCP_{05}	0,31	0,66	0,95
						$HCP_{\%}$	2,54	5,21	7,28

Table 2.

The amount of pollutants emitted from the kiln of the brick plant No. 1, after the installation of the "Steam Sprinkler"

Name of pollutants	**Quantity, t/year**								
	2016			**2017**			**2018**		
	I	**II**	**III**	**I**	**II**	**III**	**I**	**II**	**III**
Solid particles of coal	3,93	3,94	3,92	3,8	3,79	3,81	3,83	3,82	3,84
Sulfur oxides (SO_2)	4,61	4,6	4,62	4,1	4,11	4,09	4,35	4,34	4,36
Oxides of carbon (CO)	2,9	2,91	2,89	2,23	2,25	2,24	2,56	2,57	2,58
Nitrogen oxides (NO_2)	0,56	0,58	0,57	0,55	0,56	0,54	0,57	0,55	0,56
							2015	2016	2017
Assessment of the significance of the main effects:						HCP_{05}	0,15	0,12	0,10
						$HCP_{\%}$	5,49	4,33	3,52

Table 3.

The amount of pollutants emitted from the kiln of the brick factory No. 1, before and after the installation of the "Steam Sprinkler"

Name of pollutants	Quantity, t/year							
	before installation				after installation			
	2016	2017	2018	average	2019	20120	20121	average
Solid particles of coal	13,74	13,84	14,31	13,96	3,87	3,83	3,85	3,85
Sulfur oxides (SO_2)	20,68	21,90	22,91	21,83	4,39	4,26	4,39	4,35
Oxides of carbon (CO)	12,39	12,35	12,46	12,45	2,61	2,45	2,61	2,56
Nitrogen oxides (NO_2)	2,84	2,85	2,87	2,85	0,56	0,56	0,56	0,56
Total	49,65	50,94	52,55	51,05	11,43	11,1	11,41	11,32
			2016	2017	2018	2019	2020	2021
Assessment of the significance of the main effects:		HCP_{05}	0,31	0,66	0,95	0,15	0,12	0,10
		$HCP_{\%}$	2,54	5,21	7,28	5,49	4,33	3,52

These data (Table 3) confirm the effectiveness of using the "Steam Sprinkler" under production conditions in the brick firing zone, the total capture (reduction) of pollutant emissions is 77.84%, incl. solid particles of coal decreased by - 72.42%, respectively, sulfur oxides (SO_2) are retained by 80.08%, carbon oxides (CO) by 79.44%, nitrogen oxides (NO_2) by 80.35%. In general, the capture of pollutants in the brick firing zone, as noted above, is 77.84%, which is 2.23% lower than the results obtained in the experimental study. Despite this, these data indicate the high efficiency of the use of the new technical device "Steam Sprinkler" in the brick firing zone. It should also be noted that this technical device, when operating in the brick firing zone, showed high efficiency in capturing solid particles of coal of 72.42%, although it is slightly inferior in comparison with capturing other components of pollutants.

To test the effectiveness of the "Steam Sprinkler" under production conditions, special comparative tests were carried out on the emission of pollutants from the drying chambers of the brick plant No. 1, the results of which are presented in tables 4 - 6 Table 1, before the installation of the "Steam Sprinkler", Table 5 - the amount of pollutants emitted from the drying chambers of the brick plant No. 1, after the installation of the "Steam Sprinkler", Table 6 - summary before and after the installation of the "Steam Sprinkler". emitted from the drying chambers of brick factory No. 1, before and after the installation of the "Steam Sprinkler" are presented in Tables 4 - 6. From the data of Table 6 it can be seen that the amount of pollutants emitted from the drying chambers of brick factory No. 1 (Table 4) is 59.45 t/year, including respectively: solid particles of coal - 14.1 t, sulfur oxides (SO_2) - 29.92 t, carbon oxides (CO) - 12.65 t, and nitrogen oxides (NO_2) – 2.89 t/year. After the installation and operation under production conditions of the new

technical device “Steam Sprinkler”, the amount of pollutants emitted only from the drying chambers of brick plant No. 1 decreased to 17.21 t/year - including solid particles of coal to - 8.31 t , sulfur oxides (SO_2) - 5.56 tons, carbon oxides (CO) - 2.77 tons, and nitrogen oxides (NO_2) - 0.57 tons/year.

Table 4.

The amount of pollutants emitted from the drying chambers of the brick factory No. 1, before the installation of the “Steam Sprinkler”

Name of pollutants	**Quantity, t/year**								
	2016			**2017**			**2018**		
	I	**II**	**III**	**I**	**II**	**III**	**I**	**II**	**III**
Solid particles of coal	12,1	12,2	12,0	15,2	15,1	15,3	15,0	15,1	14,9
Sulfur oxides (SO_2)	25,5	25,48	25,52	29,1	29,11	29,09	35,1	35,13	35,07
Oxides of carbon (CO)	12,0	12,1	11,9	12,1	12,2	12,0	13,85	13,83	13,87
Nitrogen oxides (NO_2)	2,4	2,38	2,42	2,85	2,83	2,87	3,42	3,40	3,44
							2016	2017	2018
Assessment of the significance of the main effects:						HCP_{05}	0,51	0,49	0,74
						$HCP_{\%}$	3,87	3,32	4,56

Table 5.

The amount of pollutants emitted from the drying chambers of the brick factory No. 1, after the installation of the “Steam Sprinkler”

Name of pollutants	**Quantity, t/year**								
	2019			**20120**			**2021**		
	I	**II**	**III**	**I**	**II**	**III**	**I**	**II**	**III**
Solid particles of coal	6,4	6,35	6,45	10,1	10,2	10,0	8,35	8,25	8,15
Sulfur oxides (SO_2)	6,6	6,5	6,7	5,5	5,55	5,45	4,5	4,4	4,3
Oxides of carbon (CO)	3,65	3,6	3,55	2,9	2,85	2,8	2,15	2,1	2,05
Nitrogen oxides (NO_2)	0,67	0,65	0,63	0,6	0,58	0,56	0,52	0,5	0,48
							2019	2020	2021
Assessment of the significance of the main effects:						HCP_{05}	0,23	0,30	0,23
						$HCP_{\%}$	5,50	6,52	5,83

The data in tables 4 and 5 confirm the results of the research and the effectiveness of the new technical device “Steam Sprinkler”. This is confirmed by the results of mathematical processing using the applied computer program for processing data from field experience Field Expert vl.3Pro (Tables 1-6) [7].

These data (Table 6) confirm the effectiveness of using the “Steam Sprinkler” under production conditions, the total capture (reduction) of pollutant emissions in the area of the drying chambers is 71.27%, incl. solid particles of coal decreased by - 41.89%, respectively, sulfur oxides (SO_2) are retained by 81.23%, carbon ox-

ides (CO) by 78.07%, nitrogen oxides (NO_2) by 80.42%. In general, the trapping of pollutants in the area of the drying chambers is 71.27%, these data indicate the high efficiency of the use of the new technical device "Steam Sprinkler" in the area of the drying chambers of a brick factory.

Table 6.

The amount of pollutants emitted from the drying chambers of the brick factory No. 1, before and after the installation of the "Steam Sprinkler"

Name of pollutants	**Quantity, t/year**										
	before installation					**after installation**					
	2016	**2017**	**2018**	**average**		**2019**	**2020**	**2021**	**average**		**% reduction in pollutants**
				t/year	**% of everything**				**t/ year**	**% of everything**	
Solid particles of coal	12,37	15,47	15,02	14,3	23,67	6,46	9,91	8,56	8,31	48,6	41,89
Sulfur oxides (SO_2)	25,29	29,47	34,09	29,61	50,25	6,52	5,35	4,81	5,56	32,5	81,23
Oxides of carbon (CO)	12,73	12,16	13,01	12,63	21,23	3,35	2,58	2,38	2,77	16,19	78,07
Nitrogen oxides (NO_2)	2,83	2,84	3,06	2,91	4,85	0,62	0,55	0,53	0,57	3,33	80,42
Total	53,22	59,94	65,18	59,45	100	16,95	18,39	15,97	17,21	100	71,27
The results of mathematical processing, according to Field Expert vl.3Pro. [5]:											

Assessment of the significance of the main effects:		2016	2017	2018	2019	2020	2021
	HCP_{05}	0,51	0,49	0,74	0,23	0,30	0,23
	$HCP_{\%}$	3,87	3,32	4,56	5,50	6,52	5,83

Table 7 shows the results of the study (average over 3 years) of the amount of pollutants emitted per year from the kiln and drying chambers of brick factory No. 1, before and after the installation of the "Steam Sprinkler", which clearly show the effectiveness of the new installation for capturing pollutants substances.

From the data in Table. Table 7 shows that the average amount of pollutants emitted from the kiln and drying chambers of brick factory No. 1, before the installation of the new "Steam Sprinkler" device, was 110.65 t/g, (including solid particles of coal amounted to 28.06 t/g or 25.36%, sulfur oxides (SO_2) – 51.75 t/g or 46.77%, carbon oxides (CO) – 25.10 t/g or 22.68%, nitrogen oxides (NO_2) - 5.74 t/year or 5.19%). After the installation of the new technical device "Steam Sprinkler", the average amount of pollutants emitted from the kiln and drying

chambers of brick plant No. 1 per year amounted to 28.43 tons/year, or a decrease of 74.31% (including solid particles of coal 12.06 t/g, which is 42.42% of the volume of pollutants after the installation of the "Steam Sprinkler"; and, accordingly, sulfur oxides (SO_2) - 9.91 t/g or 34.86%; carbon oxides (CO) - 5.33 t/g or 18.75%, nitrogen oxides (NO_2) – 1.13 t/g or 3.97%).

Table 7.

The average amount of pollutants emitted from the brick kiln and drying chambers of brick plant No. 1, before and after the installation of the "Steam Sprinkler"

Name of pollutants	Quantity, t/year								
	before installation				after installation				
	Total	including		% of total pollutant volume	Total	including		% of total pollutant volume	% reduction in pollutants
		from kiln	from drying chambers			from kiln	% of total pollutant volume		
Solid particles of coal	28,06	13,96	14,1	25,36	12,06	3,85	8,21	42,42	57,02
Sulfur oxides (SO2)	51,75	21,83	29,92	46,77	9,91	4,35	5,56	34,86	80,75
Oxides of carbon (CO)	25,10	12,45	12,65	22,68	5,33	2,56	2,77	18,75	78,76
Nitrogen oxides (NO2)	5,74	2,85	2,89	5,19	1,13	0,56	0,57	3,97	80,31
Total	110,65	51,09	59,56	100	28,43	11,32	17,11	100	74,31

Also, the data in Table 7 show that, in general, the efficiency of the new technical device "Steam Sprinkler" is 74.31%. Out of 110.65 t/g of pollutants (Fig. 1), when using this device, 28.43 t/year remain uncaptured.

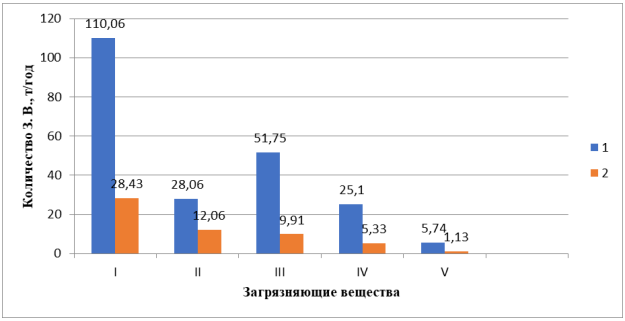

Figure 1. *Diagram of pollutants before and after installation of a new Steam Sprinkler device: 1-before installation; 2-after installation. I - only 3V; II - solid particles; III - sulfur oxides (SO_2); IV - carbon oxides (CO); V - nitrogen oxides (NO_2).*

But at the same time, its efficiency, when capturing solid particles of coal, is 57.02%, the highest efficiency is achieved when capturing sulfur oxide (SO_2) - 80.75%, carbon monoxide (CO) - 78.76%, and nitrogen oxide (NO_2) - 80.31% (Fig. 2).

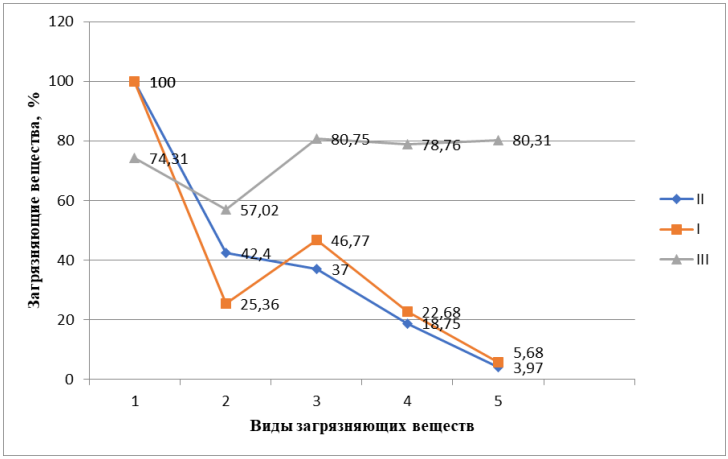

Figure 2. *Quantity of pollutant from the total volume before and after the installation of the "Steam Sprinkler" and its efficiency: 1 - pollutant; 2 - solid particles of coal; 3 – sulfur oxides (SO_2); 4 - carbon oxides (CO); 5 - nitrogen oxides (NO_2). I -% of the total volume before the installation of the "Steam Sprinkler"; II - % of the total volume after the installation of the "Steam Sprinkler"; III- efficiency of the "Steam Sprinkler", in %.*

The production tests of the new technical device "Steam Sprinkler" showed a rather high efficiency of its operation in production conditions, in connection with which a patent was obtained for this device [1].

Conclusions: 1. It is recommended to install a new technical device "Steam sprinkler" at pollutant sources to clean flue gases from harmful emissions. When installing the technical means "Steam sprinkler", the amount of emissions into the atmosphere is reduced to 80%.

References

1. Patent KG No. 325 dated 10/15/2021. "Device for cleaning exhaust gases "Steam sprinkler" from brick and gypsum kilns" [Text] / [E.A. Smailov, F.T.

Mamatalieva, I.J. Osmonov and others] - Osh. OshTU. – 20200025.2; statement. 09/04/2020; publ. 10/15/2021, bul. No. 10/1. – 7p.

2. Avdokhin V.M. Enrichment of coal [Text] / V.M. Avdokhin. – M.: "Mining Book", vol. 1, 2012. – 424 p.

3. WWW. jrg. en.wikipedia Sulfur oxides. 01/19/2020.

4. WWW. chelpogoda.ru. Pollutants.

5. Kuznetsova V.L. Nitrogen oxides: properties, biological role, mechanisms of action [Text] / V.L. Kuznetsova, A.G. Solovieva. – M.: Modern problems of science and education, No. 4, 2015.

6. Smailov E.A. The results of production testing of the new device "Steam Sprinkler" [Text] / E.A. Smailov, F.T. Mamatalieva, M.T. Atamkulova. – Bishkek: Internet Journal of the Higher Attestation Commission of the Kyrgyz Republic, No. 3, part 2, 2020.

7. D. N. Akimov, FieldExpert vl.3Pro data processing program. – [Electronic resource]. – An example. program (728 Kb)/D.N. Akimov//Federal State Scientific Institution "State Coordination Center for Information Technologies", Industry Fund of Algorithms and Programs, FAP number 9455 dated 11/14/2007.

DOI 10.34660/INF.2023.64.77.071

为建筑物的热和空气状态寻找合理的工程支持
SEARCH FOR RATIONAL ENGINEERING SUPPORT FOR THE THERMAL AND AIR REGIME OF THE BUILDING

Vyalkova Nataliia Sergeevna
Candidate of Technical Sciences, Associate Professor
Tula State University, Tula c., Russia

抽象的。　寻求建筑热空气系统的合理工程支持的考虑是改善整个建筑场所的空气分布，通过创建联合供暖系统减少通风设备占用的建筑体积。

关键词：节能技术，联合供暖系统，小气候参数，合理运行方式。

Abstract. *The search for a rational engineering support of the building's heat-air regime is considered in terms of improving the distribution of air throughout the premises of the building, reducing the volume of the building occupied by ventilation equipment by creating a combined heating system.*

Keywords: *energy-saving technologies, combined heating system, microclimate parameters, rational mode of operation.*

The main goal in the design of energy-efficient systems for regulating the internal microclimate of buildings is to provide visual and thermal comfort for people with a minimum amount of energy consumed [1].

Alternative measures such as intermittent heating during the day and seasonal regulation of comfort limits can have a significant effect on reducing energy consumption. Priority in the adopted energy-saving technologies should be given to technical solutions that will simultaneously improve the microclimate of the premises and have a beneficial effect on the environment.

Relevant is the search for rational engineering support of the building's heat-air regime in terms of improving the distribution of air throughout the premises of the building, reducing the volume of the building occupied by ventilation equipment by creating a combined heating system. There is a problem of the correct choice of modes of its operation.

The effective functioning of the system is achieved by determining its rational mode of operation based on mathematical modeling, which provides prediction of the main parameters of the microclimate and improvement of air distribution, reduction of capital and operating costs, energy and environmental safety. Standard

methods of mathematical modeling were used, as well as experimental studies with models and full-scale installations. The reliability of the results obtained was evaluated using mathematical methods for processing experiments, confirmed by practical implementation and economic efficiency assessments [2].

The use of a combined heating system that provides for the heating mode; operating mode; pass mode; the mode of reduced heat supply allows to reduce energy consumption, create the necessary microclimate in the premises of buildings with a periodic operation mode.

To obtain the whole complex of information about the dynamic state of the system, provided for by the objectives of the study, an experimental setup was developed and assembled to ensure the operation of the system in real conditions.

The rational mode of operation of the combined heating system was determined using a computational experiment and refined in the course of an experimental study.

The combined heating system works as follows. During the cold period of the year, the air heating system is used as a reheating part of the combined water-air intermittent heating system. In this case, the air heating system operates in three main modes: in the supply mode, in the recirculation mode and in the pass mode. In the boost mode, with daily periodic operation of air heating and a one-day or two-day break, the system operates as a fully recirculating system. Air is taken from the corridor through the grate, through the recirculation channel it enters the water-moderated heater and the electric heater, from where it is fed through the check valve through the main supply air duct through the supply grilles to the premises of the basement floor. During the working period, the air heating system operates as a supply, with the possibility of using air heating as a heating system in case of failure of the water system. The outside air is taken in through the shaft and, having heated up in the heaters, enters the serviced premises through the supply grilles. The fan operates in a cyclic mode, being switched on by the control unit according to the signals from the temperature and carbon dioxide sensors. In case of exceeding the permissible concentration of carbon dioxide or exceeding the temperature of the internal air, the system operates as an exhaust system (air is removed through the exhaust duct). Supply air is distributed by electric control valves [3].

The description of the object (combined heating system) was taken as the basis for a computer program that calculated the characteristics of the system under study based on the given initial data.

As a result of comparing the data of the computational experiment with the experimental data, the adequacy of the model is checked.

To check the adequacy of the model, an analysis of the experimental data was carried out using the method of mathematical statistics. The resulting value Y in

our case is the temperature of the indoor air in the room.

Having the results of (Xi,Yi) n observations of the value (X, Y) and using the least squares method, a linear regression equation is obtained

$$\hat{Y} = \overline{Y} + \hat{r}_{xy}\frac{\hat{\sigma}_y}{\hat{\sigma}_x}(x - \overline{X}). \quad (1)$$

Equating $x = X_i$, we find

$$\hat{Y}_i = \overline{Y} + \hat{r}_{xy}\frac{\hat{\sigma}_y}{\hat{\sigma}_x}(X_i - \overline{X}). \quad (2)$$

The average square of deviations of observed "Ys" (Y_i) from "Ys" ($\hat{Y}_i$) was calculated using the regression equation:

$$\hat{\sigma}_0^{2\,лин} = \overline{(Y - \hat{Y})^2} = \frac{1}{n}\sum_{i=1}^{n}(Y_i - \hat{Y}_i)^2. \quad (3)$$

We introduce the mean square error (the error of the regression equation)

$$\hat{\sigma}_0^{лин} = +\sqrt{\sum_{i=1}^{n}(Y_i - \hat{Y}_i)^2}/n. \quad (4)$$

and the sample variance of "Ys" calculated using the regression equation (1).

$$\hat{\sigma}_{\hat{y}}^{2\,лин} = \overline{(Y - \hat{Y})^2} = \sum_{i=1}^{n}(\hat{Y}_i - \overline{\hat{Y}_i})^2/n. \quad (5)$$

The following equivalence is true:

$$\hat{\sigma}_y^2 = \hat{\sigma}_{\hat{y}}^{2\,лин} + \hat{\sigma}_0^{2\,лин}. \quad (6)$$

Let's find a simpler equation for $\hat{\sigma}_{\hat{y}}^{2\,лин} = \overline{(Y - \hat{Y})^2}$, for which it is necessary to make sure that $\overline{\hat{Y}} = \overline{Y}$. Really,

$$\overline{\hat{Y}} = \frac{1}{n}\sum_{i=1}^{n}\hat{Y}_i = \frac{1}{n}\sum_{i=1}^{n}\left[\overline{Y} + \hat{r}_{xy}\frac{\hat{\sigma}_y}{\hat{\sigma}_x}(X_i - \overline{X})\right] = \frac{1}{n}\sum_{i=1}^{n}\overline{Y} + \hat{r}_{xy}\frac{\hat{\sigma}_y}{\hat{\sigma}_x}\left(\underbrace{\frac{1}{n}\sum_{i=1}^{n}X_i}_{\overline{X}} - \underbrace{\frac{1}{n}\sum_{i=1}^{n}\overline{X}}_{n\overline{X}}\right) = n\overline{Y} + \hat{r}_{xy}\frac{\hat{\sigma}_y}{\hat{\sigma}_x}(\overline{X} - n\overline{X}) = \overline{Y}$$

so

$$\hat{\sigma}_{\hat{y}}^{2\,лин} = \overline{(Y - \hat{Y})^2},$$

or

$$\hat{\sigma}_{\hat{y}}^{2\,лин} = \frac{1}{n}\sum_{i=1}^{n}(\hat{Y}_i - \overline{Y})^2 = \frac{1}{n}\sum_{i=1}^{n}\left[\overline{Y} + \hat{r}_{xy}\frac{\hat{\sigma}_y}{\hat{\sigma}_x}(X_i - \overline{X}) - \overline{Y}^2\right] = \hat{r}^2\underbrace{\frac{\hat{\sigma}_y^2}{\hat{\sigma}_x^2}\frac{1}{n}\sum_{i=1}^{n}(X_i - \overline{X})^2}_{\hat{\sigma}_x^2} = \hat{r}^2\sigma_y^2.$$

Consequently,

$$\hat{\sigma}_{\hat{y}}^{2\,лин} = \hat{r}_{xy}^2\sigma_y^2 \quad (7)$$

I find a simpler expression for $\hat{\sigma}_o^{2\,лин}$. We have

$$\hat{\sigma}_o^{2\,лин} = \sum_{i=1}^{n} \frac{(Y_i-\hat{Y}_i)^2}{n} = \frac{1}{n}\sum_{i=1}^{n}\left[Y_i - \left(\bar{Y} + \hat{r}_{xy}\frac{\hat{\sigma}_y}{\hat{\sigma}_x}(X_i - \bar{X})\right)\right]^2 = \frac{1}{n}\sum_{i=1}^{n}\left[(Y_i - \hat{Y}_i) - \hat{r}\,\frac{\hat{\sigma}_y}{\hat{\sigma}_x}(X_i - \bar{X})\right]^2 = \underbrace{\frac{1}{n}\sum_{i=1}^{n}(Y_i - \bar{Y})^2}_{\hat{\sigma}_{\hat{y}}^2} + \hat{r}^2\frac{\hat{\sigma}_y^2}{\hat{\sigma}_x^2}\underbrace{\frac{1}{n}\sum_{i=1}^{n}(X_i - \bar{X})^2}_{\hat{\sigma}_x^2} - 2\hat{r}\,\frac{\hat{\sigma}_y}{\hat{\sigma}_x}\frac{1}{n}\sum_{i=1}^{n}(Y_i - \bar{Y})(X_i - \bar{X}) =$$

$$\hat{\sigma}_{\hat{y}}^2 + \hat{r}^2\hat{\sigma}_{\hat{y}}^2 - 2\hat{r}\,\frac{\hat{\sigma}_y}{\hat{\sigma}_x}\underbrace{\overline{(Y-\bar{Y})(X-\bar{X})}}_{\hat{r}\hat{\sigma}_x\hat{\sigma}_y} = \hat{\sigma}_{\hat{y}}^2 + \hat{r}^2\hat{\sigma}_{\hat{y}}^2 - 2\hat{r}^2\hat{\sigma}_{\hat{y}}^2 = \hat{\sigma}_{\hat{y}}^2(1-\hat{r}^2).$$

So,

$$\hat{\sigma}_{\hat{y}}^{2\,лин} = \overline{(\hat{Y}-Y)^2} = (1-\hat{r}_{xy}^2)\hat{\sigma}_{\hat{y}}^2. \qquad (8)$$

Adding (7) and (8) we get

$$\hat{\sigma}_{\hat{y}}^{2\,лин} + \hat{\sigma}_o^{2\,лин} = \hat{r}_{xy}^2\hat{\sigma}_{\hat{y}}^2 + (1-\hat{r}_{xy}^2)\hat{\sigma}_{\hat{y}}^2 = \hat{\sigma}_{\hat{y}}^2.$$

From relation (7) we have

$$\hat{r}_{xy}^2 = \frac{\hat{\sigma}_{\hat{y}}^{2\,лин}}{\hat{\sigma}_{\hat{y}}^2} = \frac{\overline{(\hat{Y}-\bar{Y})^2}}{\overline{(Y-\bar{Y})^2}} \qquad (9)$$

(as $\hat{\sigma}_{\hat{y}}^{2\,лин} \le \hat{\sigma}_{\hat{y}}^2$, то $\hat{r}_{xy}^2 \le 1$).

Thus, $\hat{r}_{xy}^2$ shows what proportion of the sample variance $\hat{\sigma}_{\hat{y}}^2$ of "Ys" is the sample variance $\hat{\sigma}_{\hat{y}}^{2\,лин}$ of "Ys" calculated by the linear regression equation, or, in other words, what the proportion of the sample variance $\hat{\sigma}_{\hat{y}}^2$ is explained by the average linear dependence of "Ys" on "Xs".

Identity (6) is the main one in testing the hypothesis

$$H_o: r_{xy} = 0. \qquad (10)$$

that the general correlation coefficient is zero.

Hypothesis (10) is tested by a one-way analysis of variance, in which the factor is a regression function.

Let us assume that the conditions necessary for conducting the analysis of variance are met:

- for each observed value x_i of the X value, the observations of the Y value must be independent and carried out under the same conditions; observations must be independent even with different "Xs";

- for each value of x_i the value of Y д must have a normal law with a constant general variance for different “Xs”.

If hypothesis (10) is true, then the value

$$F = s_{\phi}^2 / s_o^2 \tag{11}$$

has an F-distribution with $l = 2 - 1$ and $k = n - 2$ degrees of freedom, where

$\widehat{\sigma}_{\phi}^2$ - is the variance of group means. It is calculated as follows:

We find

$$S_{\phi}^2 = (\overline{Y}^1 - \overline{Y})^2 n_1 + (\overline{Y}^2 - \overline{Y})^2 n_2 + \cdots (\overline{Y}^v - \overline{Y})^2 n_v = \sum_{i=1}^{v} (\overline{Y}^i - \overline{Y})^2 n_i. \tag{12}$$

Then

$$\widehat{\sigma}_{\phi}^2 = \frac{S_{\phi}^2}{n} = \sum_{i=1}^{v} (\overline{Y}^i - \overline{Y})^2 n_i / n. \tag{12}$$

Mean variance of group variances $\widehat{\sigma}_{\text{^}}^2$:

$$\widehat{\sigma}_o^2 = \frac{S_o^2}{n} \tag{13}$$

$$S_o^2 = (Y_1^{(1)} - \overline{Y}^{(1)})^2 + \left(Y_2^{(1)} - \overline{Y}^{(1)}\right)^2 + \cdots + (Y_{n_1}^{(1)} - \overline{Y}^{(1)})^2 + (Y_1^{(2)} - \overline{Y}^{(2)})^2 + \left(Y_2^{(2)} - \overline{Y}^{(2)}\right)^2 + (Y_{n_2}^{(2)} - \overline{Y}^{(2)})^2 + \cdots + (Y_1^{(v)} - \overline{Y}^{(v)})^2 + \left(Y_2^{(v)} - \overline{Y}^{(v)}\right)^2 + (Y_{n_v}^{(v)} - \overline{Y}^{(v)})^2 = \sum_{i=1}^{v} \sum_{j=1}^{n_i} (Y_j^{(i)} - \overline{Y}^{(i)})^2$$

(14)

Using the above, for a given significance level α we find the right-hand critical point $x_{\text{прα}}^{\text{кр}}$ according to the following scheme:

$$\begin{cases} \alpha \rightarrow \gamma = 1 - \alpha \\ l = 2 - 1 \\ n \rightarrow k = n - 2 \end{cases} \rightarrow f_{\gamma} \rightarrow x_{\text{пр},\alpha}^{\text{кр}} = f_{\gamma}. \tag{15}$$

If the value $F_{\text{чис}}$ of the criterion (10) is more than $x_{\text{прα}}^{\text{кр}}$, then the hypothesis H_o (10) is not rejected; in this case, the correlation coefficient is said to be insignificant.

The resultant feature y in our case is the air temperature in the room.

The correlation coefficient was $R_{xy} = 0{,}822503$, the determination coefficient was R — square= 0,704353321, Fisher’s criterion F=24,14332505, which is

more than the critical value Fкр=3,842866883, which confirms the significance of the correlation coefficient (R≠0). There is a linear relationship between the values (Table 1).

Table 1

One-way analysis of variance. Results

Groups	**Calculation**	**Sum**	**Mean**	**Variance**		
Column 1	3303	60255,2403	18,24258	1,935037		
Column 2	3304	60759,6825	18,38973	1,028064		
Analysis of variance						
Source of variation	SS	df	MS	F	P- Value	F Critical
Between groups	35,76790136	1	35,7679	24,14333	9,15799E-07	3,842866883
Within groups	9785,188577	6605	1,481482	-	-	-
Total	9820,956479	6606	-	-	-	-
Rxy=	0,822503		-	-	-	-
F	*P-Value*	*F Critical*	-	-	-	-
24,14332505	9,15799E-07	3,842866883	-	-	-	-
Total output						
Regression statistics						
R	0,839257601	-	-	-	-	-
R^2	0,704353321	-	-	-	-	-
Normalized R^2	0,704070676	-	-	-	-	-
Standard error	0,557758488	-	-	-	-	-
Observations	1048	-	-	-	-	-

The results of theoretical calculations were compared with experimental data at various outdoor temperatures. For the same operating conditions, a comparison was made of the graphs of changes in the temperature of the internal air, the concentration of carbon dioxide (Fig. 1-2).

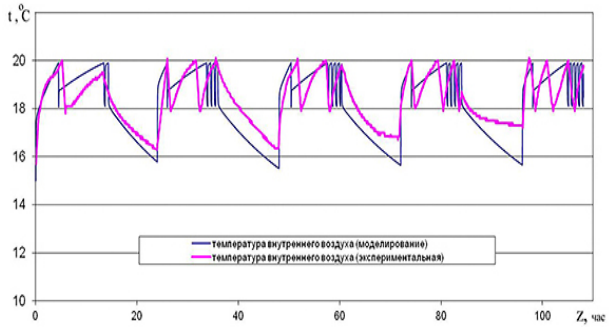

Figure 1. *Change in indoor air temperature in the weekly cycle of the combined heating system*

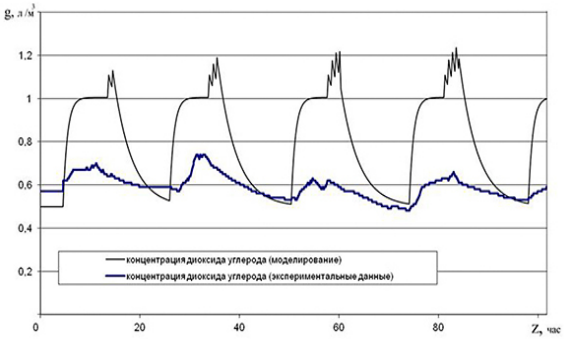

Figure 2. *Change in the concentration of carbon dioxide in the weekly cycle of the combined heating system*

Thus, the statistical analysis confirms the adequacy of the mathematical model to the experimental data. The indicated evaluation of the mathematical model was carried out for the existing experimental combined heating system.

References

1. Automated systems of heat supply and heating / S.A. Chistovich, V.K. Averyanov, Yu.V. Tempel, S.I. Bykov. L.: Stroyizdat, 1987. – 247p.

2. Yeremkin A.I., Vyalkova N.S. Automated combined system of water and air heating // Regional architecture and construction. Penza: Penza GUAS. 2011. No. 2(11). pp. 106-112.

3. Ventilation and heating system: Pat. 36042 Rus. Federation. No. 2003124889; bid.19.08.03; publ. 20.02.04. Bull. No. 5. 3 p.

DOI 10.34660/INF.2023.93.40.072

减少污染物排放的煤炭研究成果

RESULTS OF COAL RESEARCH TO REDUCE POLLUTANT EMISSIONS

Mamatalieva Flora Turkmenovna
Candidate of Biological Sciences

Kamilova Lola Toktamuratovna
Candidate of Geographic Sciences
Kyrgyz-Uzbek International university named after Batyraly Sydykov

Samieva Zhyrgal Toktogulovna
Candidate of Biological Sciences, Associate Professor, Director
Institute of Innovative Technologies,
Kyrgyz-Uzbek International university named after Batyraly Sydykov

Smailov Eltar Ablametovich
Candidate of Agricultural Sciences, Full Professor
Kyrgyz-Uzbek International university named after Batyraly Sydykov

抽象的。 燃烧固体燃料时，污染性有毒化学物质会作为烟道气的一部分释放到环境中。 最常见的污染大气的有毒物质是一氧化碳CO、二氧化硫SO2、氮氧化物NO2、碳氢化合物CnHm和灰尘。 研究了吉尔吉斯斯坦奥什地区阿莱“Sary Monol”矿床和乌兹根地区“Muz-bulak”矿床固体燃料的热值和化学成分。 目前，奥什“Ak-Tash”OJSC 企业使用来自阿莱地区“Sary Monol”矿床的煤炭烧制砖块。 推荐使用乌兹根地区的“木兹布拉克”煤烧砖（工况灰分7.37%，干燥灰分7.52%，低热值30860齐尔， kJ/kg 7370 kcal/kg， 硫含量 S - 0%）。 当改用乌兹根地区“穆兹布拉克”矿床的煤炭时，由于乌兹根“穆兹布拉克”矿床的煤炭热值高，企业将节省热量使用 区 30860 Qir，kJ/kg kcal/kg，灰分含量低，约为 7.37%。

关键词：蒸汽喷头、污染物、煤固体、硫氧化物、一氧化碳、氮氧化物、砖窑、窑炉、效率。

Abstract. *When solid fuels are burned, polluting toxic chemicals are released into the environment as part of the flue gases. The most common toxic substances polluting the atmosphere are carbon monoxide CO, sulfur dioxide SO_2, nitrogen oxides NO_2, hydrocarbons CnHm and dust. The calorific value and chemical composition of solid fuels of the “Sary Monol” deposit of Alai and “Muz-bulak” deposits of Uzgen districts, Osh region of Kyrgyzstan were studied. Currently, the*

Osh "Ak-Tash" OJSC enterprise uses coal from the "Sary Monol" deposit in the Alai region for brick firing. It is recommended to use "Muz-Bulak" coal from the Uzgen region for firing bricks (which has an ash content in working condition of 7.37%, an ash content in a dry state of 7.52%, a lower calorific value of 30860 Qir, kJ/kg 7370 kcal/kg, sulfur content S - 0%). When switching to the use of coal from the "Muz-Bulak" deposit in the Uzgen district, the enterprise will receive savings in the use of heat due to the high calorific value of the coal from the "Muz-Bulak" deposit in the Uzgen district 30860 Qir, kJ/kg kcal/kg and low ash content of about 7.37 %.

Keywords: *steam sprinkler, pollutants, coal solids, sulfur oxide, carbon monoxide, nitrogen oxide, brick kilns, kilns, efficiency.*

Introduction. Over large cities, the atmosphere contains 10 times more aerosols and 25 times more gases. At the same time, 60-70% of gas pollution comes from road transport. More active moisture condensation leads to an increase in precipitation by 5-20%. Self-purification of the atmosphere is prevented by a 10-20% reduction in solar radiation and wind speed. With low air mobility, thermal anomalies over the city cover atmospheric layers of 250-4000 m; in contrasts, temperatures can reach 5-6oC. Temperature inversions are associated with them, leading to increased pollution, fog and smog.

The territory of Osh is characterized by a high level of air pollution. The main sources of pollutant emissions are industrial enterprises in Osh city, Osh TPP (200 tons of solid fuel are burned per day to produce heat), the production enterprise of Osh "Ak-Tash" OJSC (20 tons of solid fuel are burned per day in kilns). It is well known that the composition of solid fuels and the pollutants released during combustion of various deposits differ significantly from each other. Therefore, it is important and necessary to know for each enterprise what kind of fuel is used, and, if necessary, to recommend the safest solid fuel deposits that cause less damage to the environmental situation in the region.

Important principles of environmental protection are prevention, i.e. focus on preventing negative consequences from various impacts during human activities; complexity, ubiquity, territorial differentiation and scientific environmental validity.

It should also be noted that there is little information in the literature about the impact of the activities of enterprises producing building materials using solid fuels on the environment, about the causes and sources of air pollution, about the degree of influence of pollutants on human health. Therefore, there is a need for a deep study of the causes and sources that pollute the natural environment, causing irreversible harm to human ecology, to investigate and find measures to prevent air pollution.

Due to the fact that the enterprise manufactures products under high-temperature conditions using solid fuel - coal - in the form of fuel, in such a situation, pollutants (P) enter the atmosphere from the kilns, dryer and gypsum production workshop.

The entry of pollutants into the atmospheric air depends mainly on the economic state of industries that have the greatest impact on the environment, the state of public utilities in cities. In addition, the lack of own natural gas reserves in Kyrgyzstan forces private houses to use solid fuel for heating, which has a relatively low calorific value and high ash content. The following permissible concentrations of pollutants are established [1] in the atmospheric air of populated areas (Table 1.).

Table 1.

Permissible concentrations of pollutants in the atmospheric air of populated areas [1]

Pollutants	MAC mg/m^3 maximum	MAC mg/m^3 average daily	Hazard Class
nitrogen dioxide	0,85	0,04	2
Sulfur dioxide	0,5	0,005	3
Carbon monoxide	5	3,0	4
Dust (suspended particles)	0,5	0,15	3
Ammonia	0,2	0,04	4
Sulfuric acid	0,3	0,1	2
Phenol	0,01	0,003	2
Mercury metal	-	0,0003	1
Benzene	1.5	0,1	2
Dichloroethane	3.	1.	2
carbon disulfide	0,03	0,005	3
Benzene	1,5	0,1	2
Benzo(a)pyrene	-	1мг/л	3
Styrene	0,04	0,002	4
Soot	0,15	0,05	3

When studying and researching the issues of a possible connection between the impact of pollutant emissions by the industrial enterprise Osh “Ak-Tash” OJSC on the health of the population living in the nearby area, it cannot be categorically and with certainty that all diseases of the population are associated only with the work of this plant, although the impact exists. This is evidenced by the studies of many authors [2–9]. There are a lot of factors here, ranging from the social status of the family to emissions of pollutants not only by industrial enterprises, but also

many other things, therefore, to study this issue, special studies are needed that can be planned in the future, but the collection of information on diseases for our general awareness spent.

Research methodology.

To select coal with a lower ash content, the solid fuel of the "Muz-Bulak" deposit in the Uzgen region was investigated. (Sampling site "Muz-Bulak" site. Methods of analysis GOST 27314-91, GOST 8606-93) and "Sary-Monol" of Alai districts. Sampling site site "Sary-Monol". Methods of analysis GOST 27314-91, GOST 8606-93).

Research results. We have carried out a number of studies and calculations on the following issues:

1. Determining the trend of air pollution, determining the dispersion of the pollutant (we determine the dispersion, according to the calculation it is equal to 5, the standard deviation y= ± 2.24. The coefficient of variation X = 1.8. This means that the fluctuation of air pollution varies from the average level by X = ± 1.8%);

2. Calculation of dynamics and standard deviation. **Out of 1,775 requests from brick factory workers for medical assistance, 455 were respiratory diseases.** There is a moderate relationship between air pollution and morbidity, which is confirmed by the results of correlation analysis (correlation coefficient, g=0.32).

To select coal with a lower ash content, the solid fuel of the "Muz-Bulak" deposit in the Uzgen region was investigated (test report No. 53A dated September 19, 2020). Sampling date 09/15/20, test date 09/18/20. Sampling site - "Muz-Bulak" site. Methods of analysis GOST 27314-91, GOST 8606-93) and "Sary-Monol" Alai districts (test report No. 52 A dated September 19, 2020. Sampling date 09.15.20. Testing date 09.18.20. Location sampling site "Sary-Monol. Methods of analysis GOST 27314-91, GOST 8606-93)

The characteristics of coal "Muz-Bulak" of the Uzgen region are given in Table. 2.

Table 2.

Characteristics of the coal deposit "Muz-Bulak"

№	The name of indicators	Analysis Methods	Designation and unit of measurements of indicators	Analysis results
1	*Mass fraction of moisture in working condition*	*GOST 27314-91*	*Wt, %*	*2,09*
2.	*Analytical sample moisture*	*GOST 27314 - 91*	*Wa, %*	*1,11*
3	*Ash content in working condition*	*GOST 11022 - 95, GOST 27313 - 95*	*Ar, %*	*7,37*
4.	*Dry ash content*	*GOST 11022 - 95, GOST 27313 - 95*	*Ad, %*	*7,52*

5.	*Yield of volatile substances*	*GOST 6382 - 01*	*Vdaf, %*	*9,97*
6.	*Lower calorific value of working fuel*	*GOST 147 - 95,*	*Qir, kJ/kg kKal/kg*	*30860 7370*
7.	*Sulfur content*	*GOST 8606 - 93*	*Sоб., %*	*-*

At present, the brick factory No. 1 of Osh "Ak-Tash" JSC uses coal from the "Sary-Mogol" site of the Alai deposit as fuel for firing. The characteristic of coal is given in table 3.

Table 3.

Characteristics of coal from the "Sary-Monol" site of the Alai deposit

№ п/п	The name of indicators	Analysis Methods	Designation and unit of measurements of indicators	Analysis results
1	*Mass fraction of moisture in working condition*	*GOST 27314-91*	*Wt%*	*5,89*
2.	*Analytical sample moisture*	*GOST 27314-91*	*Wa, %*	*4,38*
3	*Ash content in working condition*	*GOST 11022 - 95, GOST 27313 - 95*	*Ar,%*	*20,07*
4.	*Dry ash content*	*GOST 11022 - 95, GOST 27313 - 95*	*Ad,%*	*21,32*
5.	*Yield of volatile substances*	*GOST 6382 - 01*	*Vdaf,%*	*39,0*
6.	*Lower calorific value of working fuel*	*GOST 147-95*	*Qir,кДж/кг. kKal/кг.*	*21880 5230*
7.	*Sulfur content*	*GOST 8606 - 93*	*Sоб.,%*	*-*

Coal from the "Muz-Bulak" deposit in the Uzgen region has a higher net calorific value of the working fuel.

The coal of the "Sary-Monol" deposit of the Alay region has a lower calorific value of working fuel 21880 Qir, kJ/kg and 5230 kKal/kg.

To preserve the purity of the surrounding air, it is more profitable to work on the coal of the "Muz-Bulak" deposit in the Uzgen region. It should be taken into account that the ash content of the coal of the "Sary-Monol" deposit of the Alai region in working condition is 20.07% and the ash content in the dry state is higher 21.32%; the ash content of coal from the "Muz-Bulak" deposit in the Uzgen district in working condition is 7.37%, and in dry condition 7.52%, which is much lower, almost 2.6 times. And the yield of volatile substances of coal from the "Sary-Monol" site of the Alai deposit is 39%, and

the "Muz-Bulak" coal from the Uzgen district is only 9.97%. Therefore, in the production of building materials, it is more efficient to use, from the point of view of reducing the emission of pollutants, coal from the "Muz-Bulak" deposit in the Uzgen region, in which all harmful polluting indicators are 2 or more times lower, and the calorific value (kcal/kg) is almost 1.5 times higher.

We also believe that it would be economically feasible to use the heat of flue gases from the brick kiln and brick drying to heat tap water to a temperature of 70 °C, for use for industrial and domestic needs.

Conclusions: When solid fuels are burned, polluting toxic chemicals are released into the environment as part of flue gases. The most common toxic substances polluting the atmosphere are carbon monoxide CO, sulfur dioxide SO_2, nitrogen oxides NO_2, hydrocarbons CnHm and dust.

2. In the production of building materials, it is more efficient to use, from the point of view of reducing the emission of pollutants, coal from the "Muz-Bulak" deposit in the Uzgen region, in which all harmful polluting indicators are 2 or more times lower, and the calorific value (kcal/kg) is almost 1.5 times higher.

References

1. Tetior A.N. Urban ecology [Text]: textbook for students. higher educational institutions / A.N. Tethior. – M.: Publishing Center "Academy" 2008 – 336p.

2. Bezuglaya E.Yu. What the industrial city breathes [Text] / E.Yu. Bezuglaya, G.P. Rastorgueva, I.V. Smirnova. - L.: Gidrometeoizdat, 1991. – 143 p.

3. Girusov, E.V. Fundamentals of social ecology [Text] / E.V. Girusov. - M.: Nauka, 1998. - 248p.

4. Davydova, S.L. Environmental problems of industry and monitoring [Text] / S.L. Davydova, S.I. Petrov. – M.: "GUNG" Publishing house, 2006. – 162p.

5. Mamatalieva, F.T. The problem of the negative impact of the activities of the brick factory of JSC "Osh Ak-Tash" on the environment and health of the population of the city of Osh and residents of nearby areas of the Osh region of Kyrgyzstan. [Text] / F.T. Mamatalieva. New word in science: prospects for development. Volume 1. Collection of materials of the VII International Scientific and Practical Conference. Cheboksary: No. 1 (7), 2016. - P.19 – 24.

6. Mamatalieva, F.T. The impact of the activities of industrial enterprises on the health of mother and child (on the example of the enterprise OJSC "Osh Ak-Tash"). [Text] / F.T. Mamatalieva. New word in science: prospects for development. Volume 1. Sat. Materials VII Int. scientific - practical conference. – Cheboksary: No. 1 (7), 2016. - P. 29 – 35.

7. Mamatalieva, F.T. Problems of the impact of the activities of auxiliary, shops of JSC "Osh Ak-Tash" [Text] / F.T. Mamatalieva. Actual problems of the humanities and natural sciences. - M.: 2017. - P.124-127.

8. Smailov E.A. Exhaust gas purification technology using a new device "Steam Sprinkler" [Text] / E.A. Smailov, F.T. Mamataliyeva. – B.: / Science, new technologies and Innovations of Kyrgyzstan, No. 7,2020. – P.17-44.

9. Stepanovskikh, A.S. Applied ecology: Environmental protection [Text]: Textbook for universities / A.S. Stepanovskikh, – M.: UNITI–DANA, 2003. – 751 p.

DOI 10.34660/INF.2023.10.94.073

钻井现场无线传感器网络的路由算法
ROUTING ALGORITHM FOR THE WIRELESS SENSOR NETWORK OF THE DRILLING SITE

Krasnov Andrey Nikolaevich
Candidate of Technical Sciences, Associate Professor
Ufa State Petroleum Technological University

Prakhova Marina Yurievna
Associate Professor
Ufa State Petroleum Technological University

Kalashnik Yulia Viktorovna
Senior Lecturer
Ufa State Petroleum Technological University

抽象的。 大多数油田采用集群法进行油气生产钻探，其中定向井口在一个共同的有限区域中彼此相距很近，钻井平台本身和大量其他物体在该区域上 位于。为了钻机的高效和安全运行，分布式系统的所有组件之间必须保持持续可靠的通信。 建议使用自组织无线传感器网络 (WSN)。 此类网络中数据传输的效率取决于它们的结构和各个节点之间的通信算法。 文章提出了一种寻找最小路径的主动算法，可以让你在节点之间铺设最短路线。

关键词：钻井现场，通信信道，无线传感器网络，路由，算法。

Abstract. Production drilling for hydrocarbons is carried out at most fields by the cluster method, in which the mouths of directional wells are grouped at a close distance from each other from a common limited area, on which the drilling rig itself and a large number of additional objects are located. For the efficient and safe operation of the drilling rig, there must be constant reliable communication between all components of a distributed system. It is proposed to use self-organizing wireless sensor networks (WSNs). The efficiency of data transmission in such networks is determined by their structure and communication algorithms between individual nodes. The article proposes a proactive algorithm for finding the minimum route, which allows you to lay the shortest route between nodes.

Keywords: drilling site, communication channel, wireless sensor network, routing, algorithm.

Introduction

Drilling wells for hydrocarbons is a complex technological process characterized by a large number of different technological parameters and indicators. On the drilling site, in addition to the drilling rig itself, there are a number of other technological and auxiliary facilities (Fig. 1), such as an operator room, a drilling fluid preparation unit, a sludge pit, a reagent facility, a laboratory, a well cementing control station, etc., between which a reliable connection must be provided. The drilling technologies used are constantly evolving to improve the quality of the wells being constructed and the efficiency of the drilling process itself, which leads to the complication of both the control of the drilling process and its management. For example, the use of cluster drilling, in which the wellheads are grouped on a common site, and the end faces are located at points corresponding to reservoir or field development projects. In Western Siberia, more than 90% of drilling is currently performed from well pads.

Simultaneously with the development of cluster drilling, there is a tightening of requirements for the accuracy of hitting the bottom of wells at a given point and for compliance with the design profile of the well, and effective control of the spatial position of the wellbore, in turn, requires constant updating of downhole telemetry data [1]. To change the trajectory of the wells, a rotary steerable system (RSS) is used, the operation of which also requires the prompt transmission of information obtained at the bottomhole by inclinometers and logging tools. This is necessary to control the spatial position of the well relative to geological objects during the drilling process, to justify decisions to change the well trajectory depending on the changing geological conditions of the well right in the process of drilling, and to quickly obtain data for a quantitative assessment of the formation parameters and its reservoir properties [2].

Figure 1. *Drilling site*

The communication systems used at drilling rigs can be conditionally divided into two components: the bottom-hole system, which provides transmission of downhole telemetry data, and the surface system, which provides transmission of downhole telemetry data to the operator and operator control commands to the drilling rig. Both systems must work in real time.

Both the downhole and surface systems used at drilling sites use different communication channels. So, for example, both wired and wireless communication channels (hydraulic, acoustic, electromagnetic) are used to exchange information between the bottomhole and the wellhead [3]. Both types of communication channels, both wired and wireless, are also found in terrestrial systems. This article considers the problem of increasing the efficiency of a wireless sensor network (WSN) for communication of ground facilities at a drilling site by minimizing the message transit time.

Review and analysis of known solutions

Choosing the type of network - wired or wireless - for a particular drilling site turns into a choice of the “lesser evil”, because each type has its own set of advantages and disadvantages.

In [4], a complex is described for ground transmission within the drilling site of information received from downhole equipment and from various ground sensors installed at the drilling site, and for real-time monitoring and control of the drilling process. Data transmission is carried out over the wires of the power grid that feeds the recording devices of consumers of information and ground sensors installed at the drilling site and pumping equipment, that is, the telecommunications technology for data transmission over the power lines of the PLC (Power Line Communication) power grid is used, which provides for connecting any information measuring device using a PLC modem and allowing the use of the already existing infrastructure of the laid power grids. Unlike wireless methods, PLC technology has no limitations related to line-of-sight and transmission range. Another advantage is the absence of special connecting wires between measuring sensors and recording devices, which makes it possible to simplify the complex of ground information transmission during drilling, increase its reliability and ensure prompt relocation.

However, the complexity of organizing communication over power lines lies in the fact that they were not originally intended for data transmission, therefore they are characterized by a high level of interference and high attenuation of the high-frequency signal, and also by the fact that the line parameters, often constant for traditional physical data transmission media, in this case change significantly in time depending on the current load. Unshielded power lines of the electrical network, separated by transformers, are critical to large noise resulting from the operation of numerous energy consumers, especially to impulse noise that occurs during the operation of electric motors [5].

The classic wireless communication channel is used in the station "LEUZA-2" [6], designed for continuous monitoring and recording of the main technological parameters of the drilling process in the remote well monitoring mode. For wireless data transmission from the driller's console to the computer, a wireless data transmission/reception device (complex: radio modem-antenna-cable) with a line-of-sight range of 1.5 km is used. There are several communication channels for transmitting information from the rig to the upper level: existing telephone lines using a conventional modem; radio channel (distance 10-20 km) using a radio modem; cellular communication using a GSM modem; satellite connection. However, a prerequisite for reliable radio communication between the transmitting and receiving antennas is the absence of metal barriers between them, which limits the coverage area of the radio channel.

The radio channel is also used in the DEL-140 control and measuring complex for measuring and visualizing the main technological parameters during drilling and well workover [7]. All data on the magnitude and dynamics of controlled parameters are recorded in a removable module and transmitted online via GPRS (GSM) channel to the dispatcher's computer. In parallel, data from the DEL-140 can be transmitted via radio to the automated workstation (AWS) of the foreman, where visual control is exercised over the value of the controlled parameters on the AWS display in online mode. The disadvantage of this system is the impossibility of operation in areas where there is no GSM connection. For such cases, the DEL-140 provides a removable memory module up to 1GB in which data is accumulated and then transferred via a special interface to the dispatcher's PC, but real-time use is not available.

The most promising direction for creating a communication network for a drilling site is wireless sensor networks (WSN). They represent a distributed self-organizing network consisting of many sensors and actuators, interconnected via a radio channel [8]. The coverage area of such a network can range from several meters to several kilometers due to the ability to relay messages from one node to another. It is integrated into the industrial monitoring system in the area between the SCADA control system and the process to be monitored. Each network node includes a sensor to control any physical process, an autonomous power source (battery), a microcontroller, a transceiver, memory and, if necessary, actuators. The data received by the sensor nodes in such a WSN is usually sent to the base station, which connects the sensor network to other networks (including the Internet), where the data is collected, analyzed, and then control actions are formed on their basis.

Statement of the research problem. The purpose of this study is to improve the efficiency of the WSN for drilling sites represented as cluster zones by developing an algorithm for finding the minimum route both between these zones and between nodes within the cluster.

Theoretical foundations of the study. The organization of a radio channel at the drilling site is a separate problem, because signal transmission occurs in the presence of a large number of man-made interference, for example, interference from various electric motors, in particular, the electric motor of the top drive of the drilling rig, telemetry and control systems operating in the same radio frequency range, etc. In addition, if there are any obstacles in the signal path that do not transmit radio waves, it may be completely lost.

In very small sensor networks, the base station and sensor nodes are so close that they can communicate with each other directly. However, with an increase in the coverage area and the number of nodes, a situation arises in which, due to the large distance between the sensor nodes and the receiver node (gateway), it is not possible to directly communicate with the base station [9, 10]. The same problem arises in networks with a small distance between nodes, if between them there are materials that are impervious to the radio signal. In this case, the sensor nodes not only produce and deliver their data, but also serve as a path for other sensor nodes to reach the base station. The process of finding the best path from a source node to a destination node is called routing, and this function is the primary responsibility of the network layer.

The purpose of routing is the efficient transmission of information, while the efficiency depends on the scope and purpose of the wireless sensor network. The distribution of nodes in a real network can be uneven, the network can have a sufficiently large number of areas with different node densities. The shape and size of these areas can also be different. The criteria for choosing the optimal route can be the path length (number of hops), reliability, network delay, network bandwidth, channel congestion, etc. The most common metric is the path length - the sum of the distances between the sensor nodes through which the path from the sender to the recipient runs.

To develop a shortest path search algorithm (SPSA) for wireless data transmission between WSN nodes, first of all, it is necessary to describe the distribution of nodes over the service area.

To simplify modeling, it is usually assumed that the infrastructure served by the network has a finite number of objects that can have arbitrary coordinates within the service area. Network nodes can be unevenly distributed within each of the serviced objects, and the objects themselves can have a different shape.

The concept of the proposed BSS drilling site is shown in fig. 2.

As can be seen from the figure, the conceptual model has two distribution modes: the drilling control center and the process information collection points. To describe such a structure on a plane, a multimodal two-dimensional distribution for independent random variables can be used, which is determined by the formula [11]:

$$f_M(x_1,x_2) = \sum_{i=1}^{K} f(x_1,x_2,\mu_{1i},\mu_{2i},\sigma_{1i},\sigma_{2i},\rho_i),$$

where f (x_1, x_2) – independent random coordinates; σ_1 and σ_2 are standard deviations; ρ is the correlation coefficient of random variables; μ_1 and μ_2 are mathematical expectations; K is the number of distribution modes.

The values of n (the number of nodes) are given as simulation parameters; R is the node radius; w, h are the dimensions of the service area; σ is the standard deviation; ρ is the correlation coefficient; μ are scattering centers.

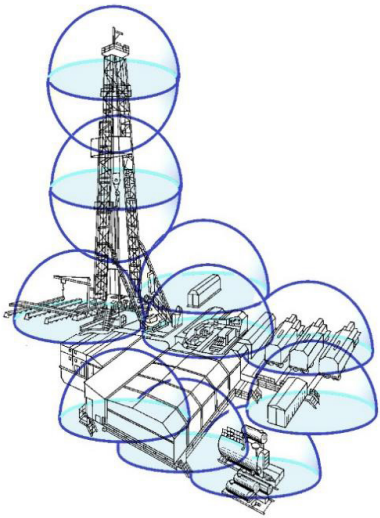

Figure 2. *Conceptual model of the WSN drilling site*

Results and discussion

The network model is considered for a limited service area (200 × 200) m in size, the node radius is assumed to be 45 m. The number of rows and columns of the routing tables corresponds to the number of nodes.

The algorithm for finding the minimum route consists of several stages.

At the first stage, a matrix of coordinates N is formed. With the help of the random number generator function rnd (1), sets of random coordinates from 1 to 100 are generated, taking into account the simulation parameters, and written into the previously created matrix.

The resulting model of the drilling site WSN in the form of cluster zones is shown in Fig. 3.

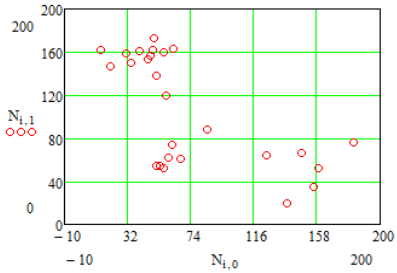

Figure 3. *Model of the WSN of the drilling site*

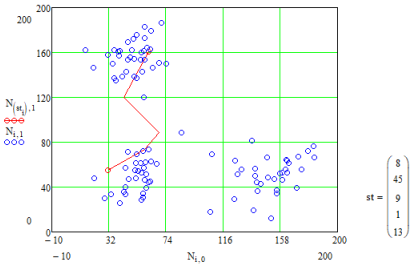

Figure 5. *Shortest route from node 8 to node 13*

At the second stage, the distance between all 100 nodes in the network is calculated and formed into a matrix D:

$$D_{i,j} = \sqrt{(N_{i,0} - N_{j,0})^2 + (N_{i,1} - N_{j,1})^2},$$

where j – matrix rows.

A fragment of the matrix D is shown in fig. 4.

D =

	0	1	2	3	4	5
0	0	42.21	77.69	$1.09 \cdot 10^2$	89.65	$1.02 \cdot 10^2$
1	42.21	0	$1.18 \cdot 10^2$	$1.48 \cdot 10^2$	$1.23 \cdot 10^2$	$1.23 \cdot 10^2$
2	77.69	$1.18 \cdot 10^2$	0	33.43	37.95	$1.29 \cdot 10^2$
3	$1.09 \cdot 10^2$	$1.48 \cdot 10^2$	33.43	0	36.59	$1.59 \cdot 10^2$
4	89.65	$1.23 \cdot 10^2$	37.95	36.59	0	...

Figure 4. *Fragment of the matrix of distances between network nodes*

The generated matrix D is checked for the presence or absence of connections between the nodes, for which each matrix variable is compared with the radius of the node. If the matrix element is greater than the radius of the node, then this means that there is no connection between the nodes, otherwise there is a connection.

Based on the identified links between the nodes, the Floyd-Warshall algorithm [12], which is implemented by the function F(d), searches for the lengths of all shortest paths between the nodes of the network (in this case, the nodes are considered as stationary).

Then the routing table SP = $F(D)_1$ and the table of the number of hops (the number of vertices in the path) SD = $F(D)_2$ are formed. The number of hops in a path is the number of final actuators, sensors, and equipment that help send data from one node to another.

Fragments of the obtained results are given in Table. 1 and 2.

Table 1. *Routing table*

	0	1	2
0	0	1	8
1	0	1	0
2	44	44	2
3	2	2	2
4	2	2	2
5	11	11	...

Table 2. *Table of the number of hops*

	0	1	2
0	1	1	3
1	1	1	4
2	3	4	1
3	4	5	1
4	4	5	...

The resulting algorithm allows you to search for the minimum route between nodes within the cluster zone and between cluster zones. For example, the sender is node 8, and the recipient is node 13, the range is 45 m. The shortest route st = p (SP, 8, 13) determined by the algorithm consists of three intermediary nodes (8, 45, 9, 1, 13) (Fig. 5).

Checking the obtained WSN for connectivity showed that it is connected, since there is at least one connection between all nodes (vertices).

The generalized operation of the minimum route search algorithm is shown in fig. 6.

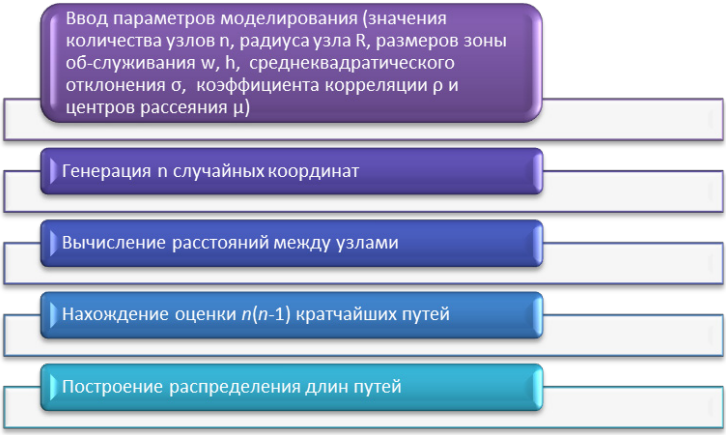

Figure 6. *Algorithm for finding the minimum route*

Conclusions

At drilling sites, it is advisable to use a self-organizing WSN for communication between individual objects. Compared to traditional wired communication, WSN provides a more flexible network configuration, faster installation at the drilling site, and higher reliability in the face of man-made interference.

The location of nodes in such networks is determined using the clustering algorithm proposed in earlier studies, but this algorithm does not allow optimizing the data transmission process according to any criterion.

The proposed algorithm for finding the minimum route between nodes refers to proactive protocols and provides efficient data transfer to the WSN by choosing the minimum route between nodes within the cluster zone and between cluster zones. Using this algorithm, it is possible to lay the shortest route between nodes and optimize the operation of WSN.

The work was carried out at FSBEI Ufa State Petroleum Technological University, a co-executor of the Research and Development Institute «Set of wellhead equipment modules for a high-speed data transmission channel complex during drilling» with financial support from the Ministry of Science and Higher Education of the Russian Federation in accordance with the Decree of the Government of the Russian Federation dated April 9, 2010 No. 218.

References

1. *Arkhipov I. S. Organization of the collection of technological data from the drilling rig and data transfer to a centralized storage, Young scientist, 2018, No. 15, p. 99-102*
2. *Stukach O.V. Development of a new telesystem for data transmission over a radio channel during well drilling / O.V. Stukach, A.B. Mirmanov, A.S. Goponenko, V.A. Kochumeev // Bulletin of Science of Siberia. 2014. No. 1 (11). pp. 76-83.*
3. *Yemets S.V., Krasnov A.N., Prakhova M.Yu., Kalashnik Yu.V. Transmission of information in control systems and drilling process control / Norwegian Journal of development of the International Science, No. 73, 2021, p. 56-64.*
4. *Shaikhutdinov R. A., Belkov A. V., Shibanov S. N., Khasanov K. R. A method of ground data transmission and reception during drilling and a device for its implementation / Patent RU 2 527 962, E21V 47/12 , 09/10/2014.*
5. *Okhrimenko V. PLC-technologies / Electronic components. 2009. No. 10. P. 58-62.*
6. *Station for monitoring the drilling process «LEUZA-2». Electronic resource. https://leuza.ru/produkcziya/stanczii/leuza-2*

7. Lagutkin O.K. Well drilling control / Neftegaz.RU, 2013, No. 6. (No. 6, 2013) https://magazine.neftegaz.ru/articles/tekhnologii/619041-kontrol-bureniya-skvazhin/

8. G. Wu, S. Talwar, K. Johnsson, N. Himayat. M2M: from mobile to embedded Internet // IEEE Commun Mag 49. – 2011. – P. 36–43.

9. Al-Kadami N.A. Estimation and comparative analysis of routing algorithms for homogeneous and heterogeneous wireless sensor networks // Information technologies and telecommunications. 2014. No. 4 (8). pp. 14–22.

10.Al-Kadami N. A. Estimation and comparative analysis of routing algorithms for homogeneous and heterogeneous wireless sensor networks // Information technologies and telecommunications. 2014. No. 4 (8). pp. 14–22.

11. Krasnov A.N., Prakhova M. Yu., Novikova Yu. V. Mathematical Simulating Qualitative Parameters of Routing and Clustering Protocols in Wireless Data Gathering Networks /FarEastCon 2020: international Multi-Conference on Industrial Engineering and Modern Technologies, 6-9 Oct. 2020, Vladivostok, Russia. 2020. Cm. 9271165. - DOI 10.1109/FarEastCon50210.2020.9271165

12.Buzyukov L.B., Okuneva D.V. Analysis of the sensor network model with uneven distribution of devices / Actual problems of infotelecommunications in science and education. III International scientific-technical and scientific-methodical conference. SPb., 2014. P. 200–203.

13.Paramonov A.I., Buzyukov L.B., Okuneva D.V. Analysis of WSN connectivity with different distributions of nodes / 71st All-Russian scientific and technical conference dedicated to Radio Day: Proceedings of the conference. SPb., 2016. P. 179–180.

DOI 10.34660/INF.2023.20.26.074

考虑地域特征的局部大地水准面模型参数确定
DETERMINING PARAMETERS OF THE LOCAL GEOID MODEL CONSIDERING TERRITORY FEATURES

Safari Mohammad Amin
PhD student
State University of Land Use Planning (Moscow, Russia)

Nilipovskiy Vasily Ivanovich
Candidate of Economic Sciences, Associate Professor
State University of Land Use Planning (Moscow, Russia)

抽象的。 目前，在创建高精度和空间分辨率的地球引力场（EGF）全球模型方面取得了进展。 该技术基于卫星观测，卫星方法的性能远高于地面方法，但同时需要知道EGF的参数，这些参数包括：大地水准面和铅垂斜率。

本研究的目的是确定局部大地水准面模型的参数和进行大地测量的领土的特征，开发和改进使用最小二乘法（LS）评估模型的准确性 ） 和全球大地水准面模型。

根据所使用的人造地球卫星（AES）技术，确定EGF参数的精度，特别是大地水准面高度，必须满足工作精度的要求。 进行1：500-1：2000比例尺的地形测量时，其精度必须与大地对正精度相对应，测量精度与标桩精度应为同一量级。 在制定使用 GNSS 技术实施工程的项目时，我们必须坚持这种精度水平。 从研究的数据来看，获取阿富汗共和国境内大地水准面模型的局部参数肯定是使用最小二乘法和全球大地水准面模型。 结果表明，得到的线性矛状大地水准面局部几何模型精度为±0.010 m，方形±0.009 m，立方±0.008 m，XGM2019全球大地水准面模型精度为 ±0.015 米。 在阿富汗境内建立局部大地水准面模型，在不超过1.3平方公里的区域，不需要几何水准测量，GNSS测量和重力测量可以从XGM2019全球模型计算出大地水准面高度，精度估计为± 0.015 米。

关键词：地形测量，最小二乘法，计算精度，局部大地水准面模型，全球大地水准面模型。

Abstract. *Currently, there is a remarkable progress in creation of global models of the Earth's gravitational field (EGF) with high accuracy and spatial resolution. This technology works based on satellite observation; the performance of satellite methods is much higher than terrestrial methods. But at the same time, it is necessary to know the parameters of the EGF, including geoid height and vertical deflection. The purpose of this study is to determine the parameters of the*

local geoid model and the features of the territory on which the geodetic survey is carried out, and to develop and improve the assessment of the accuracy of the model using the least squares method (LS) and the global geoid model.

Based on applied artificial Earth satellite (AES) technology, the accuracy of the EGF parameters, in particular the geoid heights, must be met the requirements for the accuracy of the work. During performing a topographic survey of 1:500-1:2000 scale, the accuracy must correspond to the accuracy of the geodetic justification and the accuracy of the determination and the picket should be the same. We must adhere to this level of accuracy when drawing up projects for the implementation of works using global navigation satellite systems (GNSS) technologies. In this study, to obtain local parameters of geoid model in the territory of the Afghanistan, least square method and global geoid model were used. As a result, the study indicates that the accuracy of the obtained local geometric model of the linear lance geoid is ±0.010 m, and the square ±0.009 m, cubic ±0.008m. The accuracy of the XGM2019 global geoid model for these territories is ±0.015m. Developing a local geoid model on the territory of Afghanistan, for an area of no more than 1.3 km2, geometric leveling is not required. The GNSS and gravity measurements are able to calculate the geoid height from the XGM2019 global model with an accuracy approximately of ±0.015m.

Keywords: *topographic survey, least squares method, calculation accuracy, local geoid model, global geoid model.*

Introduction

Presently the method of satellite leveling, based on the joint use of GNSS measurements and geoid models, is receiving much attention [1]. The study of the accuracy characteristics of global geoid models and the determine of high precision local geoid models, both gravity and derived from GNSS measurements and high-precision leveling, are of particular importance. Local geoid models, which are built for a limited area, have a higher accuracy than global models. The resolution of the global models do not allow one to see the local characteristics of the Earth's gravitational field [2]. Due to the high (centimeter) positioning accuracy achieved to date, the final accuracy of satellite leveling is largely determined by the accuracy characteristics of the geoid model used [3]. There are many techniques for determining surface models of the geoid. Some of these methods use direct observation values, while others can be used after adjustment and filtering. Modules using the definition of the geoid surface must be realistic and well adapted to the structure of the surface. At the same time, surface models must correspond to the surface structure and filtration conditions, and also be suitable for extrapolation and interpolation. Several techniques are employed to determine the surface of the geoid, which can be listed as follows; interpolation; finite elements; collocation;

numerical differential solution; transformation of one-dimensional data, etc. [4]. The choice of this method for constructing a model geoid depends on the type of materials used and the scale of the territory. To apply any of these models in a particular area, it is necessary to determine the parameters of the model, as well as its accuracy using the least squares method. Determining the accuracy of the model makes it possible to ensure the reliability of the model [5]. This study obtained local parameters of geoid models fora small part of the Afghanistan and their accuracy is determined using the least squares method and using the global geoid model XGM2019. of the objective of this study is to determine the parameters of the geoid model, taking into account the territorial features of Afghanistan, on the basis of GNSS leveling with the involvement of the global geoid model.

Materials and methods

Исследуемая территория (рисунок 1) включает в себя области Газни и Султан плотина в Афганистане (N33°45’24» и E68°22’47”).

The study area (Figure 1) includes the areas of Ghazni and the Sultan Dam in Afghanistan (N33°45’24” and E68°22’47”).

The area of the territory is 1.5 km^2 and includes 29 GNSS leveling stations. GNSS measurements were carried out by the relative method, the root-mean-square errors

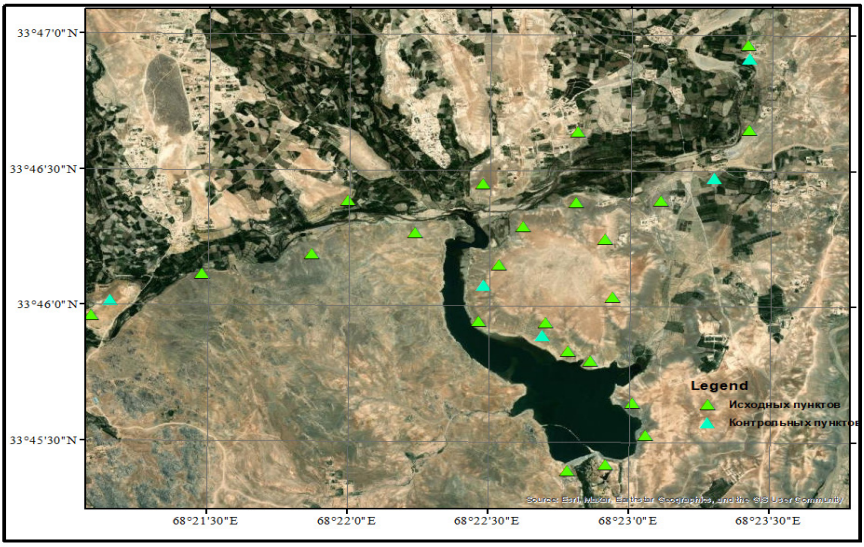

Figure 1. *Study area*

in plan and height were 1-1.5 cm. The orthometric height was determined with a grade III leveling accuracy. The parameters of the local model are determined by the least squares method.

The resulting model is used to perform topographic surveys and geodetic works of medium accuracy. When solving the height anomaly problem (ζ) the following types of equations were used:

$$\zeta = \zeta_0 + a_0 + a_1 x + a_2 y + a_3 x^2 + a_4 y^2 + a_5 xy + a_6 x^2 y + a_7 xy^2 + a_8 x^3 + a_9 y^3 \quad (1)$$

where $y = (Y - Y_0)$, $x = (X - X_0)$, X, Y- coordinates of the observed station,

X_0, Y_0- the average value of the coordinates of the given position of the points

$$X_0 = \frac{\sum X}{n}, Y_0 = \frac{\sum Y}{n}, \zeta_0 = \frac{\sum \zeta}{n} \quad (2)$$

where ζ —geoid height, ζ_0 mean geoid height, a_i - unknown coefficient, and n-number of observation points

Linear, quadratic and cubic equations (1) were used to determine the parameters of the local model. The values of the unknown coefficient were compared with the original data. The resulting equations were written for 24 points evenly distributed over the territory, the remaining 5 points were used as control points to assess the accuracy of the proposed methodology. Table 1 shows the initial data - rectangular coordinates, orthometric heights, geodetic heights and geoid heights; stations BM9, BM16, BM18, CP7 and BM11 are control points.

Table 1

Coordinates and heights of control points

Stantion	Coordinates		H^g (m) Orthometric height	H (m) Geodetic height	ζ (m)
	Y (m)	X (m)			
BM1	3735379.940	442759.973	2379.187	2353.823	-25.364
BM5	3735579.550	442979.575	2400.079	2374.688	-25.391
BM6	3735800.602	442910.114	2404.941	2379.556	-25.385
BM7	3736086.537	442681.817	2392.035	2366.66	-25.374
BM8	3736152.396	442556.39	2394.822	2369.451	-25.371
BM9	3736260.439	442420.996	2403.797	2378.426	-25.371
CP10	3736349.853	442435.078	2412.237	2386.872	-25.364

CP11	3736520.530	442801.601	2414.981	2389.605	-25.376
CP12	3736915.259	442764.053	2421.277	2395.909	-25.368
BM15	3737178.263	443067.762	2411.245	2385.881	-25.364
BM16	3737327.418	443367.108	2399.915	2374.526	-25.389
BM17	3737654.297	443555.476	2409.071	2383.687	-25.384
BM18	3738144.423	443560.217	2405.738	2380.355	-25.382
CPM1	3738233.167	443548.776	2405.537	2380.148	-25.388
BM19	3737648.445	442614.947	2401.179	2375.831	-25.349
BM14	3737165.681	442602.876	2407.673	2382.312	-25.361
CP2	3737292.496	442094.251	2412.122	2386.775	-25.3471
CP3	3736962.516	441718.594	2420.455	2395.123	-25.332
BM21	3737182.333	441350.308	2400.89	2375.538	-25.353
CP4	3736820.662	441151.728	2424.879	2399.576	-25.303
CP5	3736684.888	440550.531	2403.682	2378.377	-25.305
CP6	3736405.117	439941.807	2426.32	2401.045	-25.275
CP7	3736507.868	440049.143	2424.496	2399.219	-25.278
CP8	3735617.265	439590.741	2413.333	2388.068	-25.265
CP1	3737001.470	442314.532	2414.879	2389.528	-25.351
CP9	3736744.068	442179.263	2413.134	2387.77	-25.364
BM11	3736601.768	442097.444	2407.093	2381.719	-25.373
BM10	3736360.310	442065.231	2385.811	2360.448	-25.363
BM4	3735339.459	442552.597	2381.843	2356.469	-25.374

Values $X_o = 442199.501$м, $Y_o = 3736628.129$ м and $\zeta_0 = -25.353$м *(calculations obtained using Equation 2).*

Calculation order ζ.

The initial equation (1) was processed in three versions using terms of the first, second and third degrees x and y:

Linear equations:

$$\zeta_i = \zeta_0 + a_0 + a_1 x_i + a_2 y_i \ ,$$

where $i = 1,2,3 \ldots .24$

The normal equation is:

$$L = AX \qquad (3)$$

where A - the matrix of coefficients, X – the matrix of unknowns and L- matrix of observations.

$$A = \begin{bmatrix} 1 & x_1 & y_1 \\ 1 & x_2 & y_2 \\ 1 & x_3 & y_3 \\ . & . & . \\ 1 & x_{24} & y_{24} \end{bmatrix}, \quad L = \begin{bmatrix} \zeta_1 \\ \zeta_2 \\ \zeta_3 \\ . \\ \zeta_{24} \end{bmatrix}, X = \begin{bmatrix} a_0 \\ a_1 \\ a_2 \end{bmatrix}$$

Given the above (3), the matrices have the form:

$$\begin{bmatrix}\zeta_1\\ \zeta_2\\ \zeta_3\\ .\\ \zeta_{24}\end{bmatrix}=\begin{bmatrix}1 & x_1 & y_1\\ 1 & x_2 & y_2\\ 1 & x_3 & y_3\\ . & . & .\\ 1 & x_{24} & y_{24}\end{bmatrix}*\begin{bmatrix}a_0\\ a_1\\ a_2\end{bmatrix}$$

Quadratic equations:

$$\zeta_i=\zeta_0+\ a_0\ +\ a_1\,x_i+a_2y_i+\ a_3\,x_i^2+\ a_4y_i^2+\ a_5\,x_iy_i$$

According to (3), A, X, L:

$$A=\begin{bmatrix}1 & x_1 & y_1 & x_1^2 & y_1^2 & x_1y_1\\ 1 & x_2 & y_2 & x_2^2 & y_2^2 & x_2y_2\\ 1 & x_3 & y_3 & x_3^2 & y_3^2 & x_3y_3\\ . & . & . & . & . & .\\ 1 & x_{24} & y_{24} & x_{24}^2 & y_{24}^2 & x_{24}y_{24}\end{bmatrix},\ L=\begin{bmatrix}\zeta_1\\ \zeta_2\\ \zeta_3\\ .\\ \zeta_{24}\end{bmatrix},X=\begin{bmatrix}a_0\\ a_1\\ a_2\\ .\\ a_5\end{bmatrix}$$

Cubic Equations:

$$\zeta_i=\zeta_0+\ a_0\ +\ a_1\,x_i+a_2y_i+\ a_3\,{x_i}^2+\ a_4{y_i}^2+\ a_5\,x_iy_i+\ a_6\,{x_i}^2\,y_i+a_7\,x_i{y_i}^2+a_8\,{x_i}^3+\ a_9\,{y_i}^3$$

According to (3):

$$\mathrm{A}=\begin{bmatrix}1 & x_1 & y_1 & x_1^2 & y_1^2 & x_1y_1 & x^2\,y_1 & x_1y_1^2 & x_1^3 & y_1^3\\ 1 & x_2 & y_2 & x_2^2 & y_2^2 & x_2y_2 & x^2\,y_2 & x_2y_2^2 & x_2^3 & y_2^3\\ 1 & x_3 & y_3 & x_3^2 & y_3^2 & x_3y_3 & x^2\,y_3 & x_3y_3^2 & x_3^3 & y_3^3\\ . & . & . & . & . & . & . & . & . & .\\ 1 & x_{24} & y_{24} & x_{24}^2 & y_{24}^2 & x_{24}y_{24} & x^2\,y_{24} & x_{24}y_{24}^2 & x_{24}^3 & y_{24}^3\end{bmatrix},\ L=\begin{bmatrix}\zeta_1\\ \zeta_2\\ \zeta_3\\ .\\ \zeta_{24}\end{bmatrix},\ X=\begin{bmatrix}a_0\\ a_1\\ a_2\\ .\\ a_9\end{bmatrix}$$

Table 2 gives the elements of matrix A.

The calculation of the unknown coefficient is performed according to the formula [8]:

$$X=(A^TA)^{-1}A^TL \qquad (4)$$

Using, A and L, for the resulting linear form:

$$X=\begin{bmatrix}a_0\\ a_1\\ a_2\end{bmatrix}=\begin{bmatrix}-0.000\\ 0.032\\ -0.006\end{bmatrix}$$

Thus, for the linear form, the equation has the following form:

$$\zeta_i=-25.353+0.00+0.032\,x_i-0.006y_i$$

Table 1

Elements of matrix A

S/N	a_0									
		x (km)	y (km)	x^2	y^2	xy	x^3	y^3	x^2y	y^2x
1	1	-0.560	1.248	0.314	1.558	-0.700	-0.176	1.945	0.392	-0.873
2	1	-0.780	1.049	0.609	1.100	-0.818	-0.475	1.153	0.638	-0.858
3	1	-0.711	0.828	0.505	0.685	-0.588	-0.359	0.567	0.418	-0.487
4	1	-0.482	0.542	0.233	0.293	-0.261	-0.112	0.159	0.126	-0.141
5	1	-0.357	0.476	0.127	0.226	-0.170	-0.045	0.108	0.061	-0.081
6	1	-0.236	0.278	0.055	0.077	-0.066	-0.013	0.022	0.015	-0.018
7	1	-0.602	0.108	0.363	0.012	-0.065	-0.218	0.001	0.039	-0.007
8	1	-0.565	-0.287	0.319	0.082	0.162	-0.180	-0.024	-0.092	-0.047
9	1	-0.868	-0.550	0.754	0.303	0.478	-0.655	-0.166	-0.415	-0.263
10	1	-1.356	-1.026	1.839	1.053	1.391	-2.493	-1.081	-1.887	-1.428
11	1	-1.349	-1.605	1.821	2.576	2.166	-2.456	-4.135	-2.922	-3.476
12	1	-0.415	-1.020	0.173	1.041	0.424	-0.072	-1.062	-0.176	-0.432
13	1	-0.403	-0.538	0.163	0.289	0.217	-0.066	-0.155	-0.087	-0.117
14	1	0.105	-0.664	0.011	0.441	-0.070	0.001	-0.293	-0.007	0.046
15	1	0.481	-0.334	0.231	0.112	-0.161	0.111	-0.037	-0.077	0.054
16	1	0.849	-0.554	0.721	0.307	-0.471	0.612	-0.170	-0.400	0.261
17	1	1.048	-0.193	1.098	0.037	-0.202	1.150	-0.007	-0.211	0.039
18	1	1.649	-0.057	2.719	0.003	-0.094	4.484	0.000	-0.154	0.005
19	1	2.258	0.223	5.097	0.050	0.503	11.508	0.011	1.137	0.112
20	1	2.609	1.011	6.806	1.022	2.637	17.754	1.033	6.880	2.666
21	1	-0.115	-0.373	0.013	0.139	0.043	-0.002	-0.052	-0.005	-0.016
22	1	0.020	-0.116	0.000	0.013	-0.002	0.000	-0.002	0.000	0.000
23	1	0.134	0.268	0.018	0.072	0.036	0.002	0.019	0.005	0.010
24	1	-0.353	1.289	0.125	1.661	-0.455	-0.044	2.140	0.161	-0.586

Similar transformations are performed for the square and cubic forms of the equation:

$$X = \begin{bmatrix} a_0 \\ a_1 \\ a_2 \\ a_3 \\ a_4 \\ a_5 \end{bmatrix} = \begin{bmatrix} -0.002 \\ 0.029 \\ -0.005 \\ 0.002 \\ 0.000 \\ 0.002 \end{bmatrix}$$

$$\zeta_i = -25.353 - 0.002 + 0.029\, x_i - 0.005 y_i + 0.002 x_i^2 + 0.002 x_i y_i$$

$$X = \begin{bmatrix} a_0 \\ a_1 \\ a_2 \\ a_3 \\ a_4 \\ a_5 \\ a_6 \\ a_7 \\ a_8 \\ a_9 \end{bmatrix} = \begin{bmatrix} 0.001 \\ 0.032 \\ -0.023 \\ -0.004 \\ -0.014 \\ 0.010 \\ 0.002 \\ 0.016 \\ 0.010 \\ -0.027 \end{bmatrix}$$

$$\zeta_i = -25.353 + 0.001 + 0.032\ x_i - 0.023 y_i - 0.004 x_i^2 - 0.014 y_i^2 + 0.010\ x_i y_i + +0.002 x_i^3 + +0.016 y_i^3 + 0.01 x_i^2 y_i - 0.027 y_i^2 x_i$$

Results and discussion

The results of calculating the geoid height in three forms, the original and global XGM2019 models and their differences, are shown in Table 2.

Table 2 uses the following designations: ζлин - height anomalies obtained from the linear equation; ζква - height anomalies obtained from the quadratic equation; ζкуб - height anomalies obtained from the cubic equation.

Estimating the accuracy of the model using the equation [9],

$$СКП_{лин} = \pm\sqrt{\frac{V^T V}{n}} = \sqrt{\frac{0.0024}{24}} = \pm 0.010m$$

$$СКП_{ква} = \pm\sqrt{\frac{V^T V}{n}} = \sqrt{\frac{0.0020}{24}} = \pm 0.009m$$

$$СКП_{куб} = \pm\sqrt{\frac{V^T V}{n}} = \sqrt{\frac{0.0010}{24}} = \pm 0.008m$$

$$СКП_{XGM2019} = \pm\sqrt{\frac{V^T V}{n}} = \sqrt{\frac{0.0056}{24}} = \pm 0.015m$$

Table 2

Measurements, model and global models of XGM2019 and their differences

Code	Geoid heights (m)					Geoid height differences (m)			
	$\zeta_{\text{гнсс/нев}}$	$\zeta_{\text{лин}}$	$\zeta_{\text{ква}}$	$\zeta_{\text{куб}}$	$\zeta_{XGM2019}$	$\zeta_{\text{гнсс/нев}} - \zeta_{\text{лин}}$	$\zeta_{\text{гнсс/нев}} - \zeta_{\text{ква}}$	$\zeta_{\text{гнсс/нев}} - \zeta_{\text{куб}}$	$\zeta_{\text{гнсс/нев}} - \zeta_{XGM2019}$
BM1	-25.364	-25.379	-25.379	-25.372	-25.364	0.015	0.016	0.008	0.000
BM5	-25.391	-25.385	-25.384	-25.381	-25.369	-0.006	-0.007	-0.010	-0.022
BM6	-25.385	-25.381	-25.380	-25.387	-25.366	-0.004	-0.004	0.002	-0.019
BM7	-25.374	-25.372	-25.372	-25.381	-25.359	-0.002	-0.002	0.007	-0.015
BM8	-25.371	-25.367	-25.368	-25.376	-25.355	-0.004	-0.003	0.005	-0.016
CP10	-25.365	-25.362	-25.363	-25.367	-25.351	-0.003	-0.001	0.003	-0.014
CP11	-25.376	-25.373	-25.373	-25.376	-25.361	-0.003	-0.003	0.000	-0.015
CP12	-25.368	-25.369	-25.369	-25.365	-25.359	0.001	0.001	-0.003	-0.009
BM15	-25.364	-25.378	-25.375	-25.371	-25.367	0.013	0.011	0.007	0.003
BM17	-25.384	-25.390	-25.383	-25.382	-25.381	0.006	-0.001	-0.002	-0.004
CPM1	-25.388	-25.387	-25.379	-25.386	-25.379	-0.002	-0.009	-0.003	-0.009
BM19	-25.348	-25.360	-25.361	-25.360	-25.351	0.012	0.014	0.012	0.004
BM14	-25.361	-25.363	-25.364	-25.356	-25.353	0.002	0.003	-0.005	-0.008
CP2	-25.347	-25.345	-25.349	-25.346	-25.336	-0.002	0.002	-0.001	-0.011
CP3	-25.332	-25.335	-25.339	-25.336	-25.326	0.003	0.007	0.004	-0.007
BM21	-25.353	-25.322	-25.327	-25.337	-25.312	-0.031	-0.026	-0.016	-0.041
CP4	-25.303	-25.318	-25.322	-25.323	-25.307	0.015	0.019	0.020	0.004
CP5	-25.305	-25.299	-25.301	-25.305	-25.288	-0.005	-0.003	0.000	-0.017
CP6	-25.275	-25.281	-25.279	-25.274	-25.268	0.006	0.003	-0.001	-0.007
CP8	-25.265	-25.275	-25.265	-25.264	-25.262	0.010	0.000	0.000	-0.003
CP1	-25.351	-25.354	-25.357	-25.349	-25.344	0.004	0.006	-0.001	-0.006
CP9	-25.363	-25.352	-25.354	-25.349	-25.341	-0.012	-0.009	-0.014	-0.022
BM10	-25.363	-25.350	-25.352	-25.355	-25.339	-0.013	-0.011	-0.008	-0.024
BM4	-25.374	-25.372	-25.373	-25.371	-25.358	-0.002	-0.001	-0.003	-0.016

The accuracy of the obtained local geometric model of the geoid using the three shapes (linear, square, and cubic) is the same. This means that the geoid height can be interpolated within the area into linear, square and cubic with an accuracy of approximately ±0.01 m. The accuracy of the XGM2019 global geoid model in this area will examine the accuracy of the generated geoid model in the study area, the geoid heights of the 5 GNSS/leveling (ζГНСС/нив), points that were not included in the geoid modeling process were compared with the corresponding geoid heights of those points from the ζкуб model. The results are presented in Table 3. The outputs exhibit that the external accuracy of the geoid model, compared with independent GNSS/levelling measurements in Afghanistan, characterized by the

ERMS at 5 control points does not exceed 0.008 m. Figure 2 shows the measured, computed, and global heights of the geoid model

Table 3

Statistics of predicted and observed geoid heights at external control points

	BM9	BM16	BM18	CP7	BM11
Observations (m)	-25.371	-25.389	-25.382	-25.278	-25.373
Forecasts (m)	-25.369	-25.377	-25.385	-25.281	-25.360
Difference (m)	-0.002	-0.012	0.003	0.003	-0.013

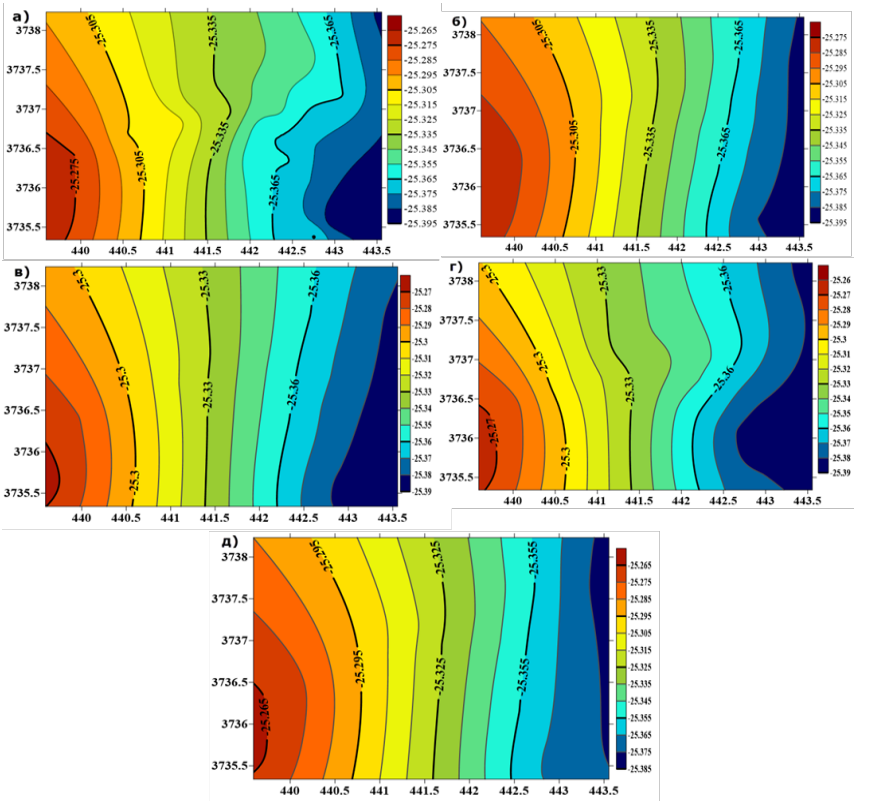

Figure 2. *Height anomalies at 24 points: a) during GNSS leveling; b) when calculating the model with the first degree; c) when calculating the model with the second degree; d) when calculating a model with a third degree; d) with the global model XGM2019*

Results

This manuscript presents a solution to the problem of determining the parameters of the local geoid model, taking into account the characteristics of the territory on which the geodetic survey is carried out. Based on the comparison of the geoid height obtained both with the least squares method and with the help of the global model, it can be stated that the cubic way of calculating the model has a good similarity with the results of the measured data. In addition, in a small area of the surface, the XGM2019 geoid models have acceptable accuracy. The assessment of the accuracy of obtaining normal heights using XGM2019 geoid models showed that the use of these geoid height models in a given area to determine normal heights is possible only when topographic surveys are performed at a scale of 1:500-1:2000. According to the findings of this study, building a local geoid model on the territory of Afghanistan, for an area of no more than 2 km2, does not require geometric leveling, GNSS and gravimetric measurements. It is possible to calculate the geoid height from the XGM2019 global model with an accuracy approximately 0.015 m.

References

1. Solodovnik A.I., Shurygin D.N., Litovchenko T.V. High-precision satellite leveling and study of the local model of quasi-geoid heights on the territory of Russia // Mining Information and Analytical Bulletin, 2017. – No. 12. – P. 109–114.

2. Gienko E.G., Elagin A.V. The results of building a local quasi-geoid model on the territory of the geodetic training ground sgugit // SGUGiT, 2021: No. 10-P. 252-260

3. Ulfred A.B. Development of a preliminary geoid model for the territory of the country based on satellite data // Dissertation for the degree of candidate of technical sciences. (MIIGAiK), 2019-202s.

4. Soycan M.D., Soycan A.M. Parameters of interpolation methods of creation of digital model of landscape.Academia.2017.vol.8.no.14.p.41-51

5. Okiemute E.S., Olujimi O.F. Local Geometric Geoid Models Parameters and Accuracy Determination Using Least Squares Technique. International journal of innovative research & development.2018. Vol 7 Issue 7.P. 251-257.

6. GCINR (GNTA) -03-010-02. Instructions for leveling I, II, III and IV classes. Moscow TSNIIGAiK .2003 .113p.

7. Yehia H. M., Reda Y., Ahmed E. S. Study of the Potential of a Local Geoid Model for Extracting the Orthometric Heights from GPS Measurements in Topographic Works.IISTE.2017.vol.9.no.7. p.16-28.

8. Kolomiets L.V., Ponikarova N.Yu. Least squares: method. instructions // Publishing House of Samara University, 2017 No. 12 (1). – 32-64 p.

9. Nilipovskiy, V.I., Elshewy, M.A., Hamdy, A.M. A Local Geoid for Egypt's Mediterranean Coast: A Model Based on Artificial Neural Networks // International Journal of Geoinformaticsthis link is disabled, 2022, 18(3), pp. 1–11

10. Thanh F.Ch. Development of a technique for improving the accuracy and degree of detail of a local quasi-geoid for the territory of northern Vietnam // Thesis for the degree of candidate of technical sciences. Moscow. 2022-114.

科学出版物

上合组织国家的科学研究：协同和一体化

国际科学大会的材料

2023 年 2 月 10 日，中国北京

编辑A.A.Siliverstova
校正A.I.尼古拉耶夫

2023 年 2 月 10 日，中国北京
USL。沸点：98.7。 订单253.流通500份。

在编辑和出版中心印制
无限出版社